Doctoral   Science

2005-05-01

Cardiac Relaxation Dynamics Investigated by Doppler Tissue Imaging (DTI)

Gerard J. King
Technological University Dublin

Cardiac Relaxation Dynamics

investigated by

Doppler Tissue Imaging (DTI)

Gerard J King, MSc

School of Physics
Faculty of Science
Dublin Institute of Technology

Submitted for the award of PhD of the Dublin Institute of Technology

Supervisors
Dr Matthew Hussey
    Faculty of Science, Dublin Institute of Technology
Dr Pat Goodman
    School of Physics, Dublin Institute of Technology
Prof W Norman McDicken
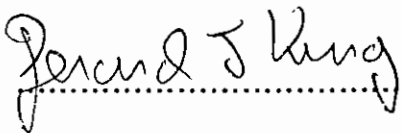   University of Edinburgh

May 2005
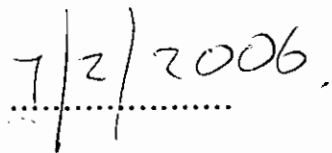
Declaration

I certify that this thesis which I now submit for examination for the award of PhD, is entirely my own work and has not been taken from the work of others save and to the extent that such work has been cited and acknowledged within the text of my work.

This thesis was prepared according to the regulations for postgraduate study by research of the Dublin Institute of Technology and has not been submitted in whole or in part for an award in any other Institute or University.

The Institute has permission to keep, lend or copy this thesis in whole or in part, on condition that any such use of the material be duly acknowledged.

Signature ....   Date 7/2/2006

Gerard King

Dedicated to my wife Jackie, mother Annie, son David and daughters Anna and Claire

Acknowledgements

Abstract

Following an initial pilot study to explore the usefulness of Doppler tissue imaging (DTI) for the assessment of regional systolic dysfunction in the ischaemic heart, new techniques for the diagnosis of diastolic dysfunction have been developed.

In the refinement of the techniques further evidence to support the existence of the early diastolic mechanism was obtained prior to assessing its clinical utility. For this the relationship between peak early diastolic mitral ring tissue velocity (Ea) as a surrogate for recoil, and the acceleration of early transmitral flow (ventricular filling), was investigated in patients with diastolic dysfunction and in normal subjects. This study supported the existence of recoil as the release mechanism for restoring forces (the early diastolic mechanism) in the normal and its delay or absence in patients with diastolic dysfunction.

To confirm the presence, absence or reversal of this early diastolic mechanism two echocardiographic waveforms need to be analysed on the same heart beat. The technique examines the diagnostic utility of the time to peak diastolic tissue velocity (Ea) of the mitral ring measured by DTI compared with the time to peak mitral opening measured by M-mode, for the assessment of left ventricular relaxation in subjects with pathological and physiological athletic hypertrophy, and distinguishing these from normals. We postulate that a slack myocardial state occurs within a period between the peak myocardial tissue velocity measured at the mitral valve ring and the peak of the E-wave (M-mode velocity) through the mitral valve. This slack myocardial state constitutes the early diastolic mechanism and allows for proper filling. This mechanism is absent in stiffer hearts.

As well as the early diastolic mechanism a further novel index of left ventricular performance based on the pressure volume relationship, (E/Ea)/LVIDd, was shown to be a promising index for distinguishing the three groups.

Using two ultrasound systems and optimum operating conditions the characteristics of the technique were examined.

Finally, further developments of the technique are discussed along with possible future clinical applications, particularly to understanding and preventing sudden death in the young athlete.

CONTENTS

Chapter 3
Cardiac anatomy: theories of left ventricular function to provide theoretical and conceptual underpinning of the diagnosis of cardiac diseases

Chapter 4
The developing clinical applications of DTI

Chapter 5
Systolic dysfunction: DTI, 2-D imaging and transmitral blood flow measurement by Doppler ultrasound for assessing infarction arising from ischaemic heart disease

Chapter 6
Diastolic dysfunction: DTI, 2-D imaging and transmitral blood flow measurement by Doppler ultrasound for assessing early filling dynamics in normal controls and patients with diastolic dysfunction

Chapter 7
The potential of DTI in distinguishing pathological from physiological LVH 124

Glossary of Terms and Abbreviations

Θ (°)	angle of incidence in degrees
λ (m)	the wavelength or distance travelled by the wave in one period, T, in metres
Δt (s, ms or µs)	time taken for an echo to return from a reflector in seconds or milliseconds or microseconds
(E/Ea)/LVIDd	proposed new index of myocardial stiffness
2D	two-dimensional echocardiography
3D	three-dimensional echocardiography
A (cm/s)	peak late diastolic blood flow velocity in centimetres per second
ANOVA	analysis of variance
Ao size (mm)	ascending aortic diameter in millimetres
ARVD	arrythmogenic right ventricular dysplasia
At VI (cm)	time velocity integral of late diastole in centimetres
BMI (kg/m²)	body mass index in kilograms per square metre
B-Mode	brightness mode
c (m/s)	speed of propagation in metres per second
cm/s	centimetres per second
cm/s²	centimetres per second per second
CW	continuous wave Doppler
dB	decibel, the logarithmic unit of ultrasound intensity
DTI	Doppler tissue imaging
E (cm/s)	peak early diastolic blood flow velocity in centimetres per second
E Acc (cm/s²)	acceleration of blood across the mitral valve in early diastole in centimetres per second squared

E/A	ratio of peak early diastolic flow to peak late diastolic flow
E/Ea	ratio of early peak diastolic blood velocity to early diastolic tissue velocity Ea
E+E-No1	measurement by observer 1 of mitral opening to peak tissue early relaxation velocity
E+E-No2	measurement by observer 2 of mitral opening to peak tissue early relaxation velocity
Ea (cm/s)	peak early mitral ring tissue velocity recorded by DTI in centimetres per second
Ea avg (cm/s)	average Ea peak early diastolic tissue velocity in centimetres per second
Ea/Aa	ratio of early diastolic tissue E velocity to early diastolic tissue velocity A
ECG	the electrocardiogram
EDV (ml)	end diastolic volume in millilitres
EF (%)	ejection fraction as a percentage of blood ejected per cardiac cycle
ESV (ml)	end systolic volume in millilitres
Et Vl (cm)	time velocity integral of early diastole in centimetres
Frequency (Hz)	the number of cycles occurring each second, in hertz
HCM	hypertrophic cardiomyopathy
Heart Rate (ms)	R to R interval on the ECG in milliseconds, in fact the inverse of the heart rate
Height (cm)	patient's height in centimetres
Hz (cycles/s)	Hertz, the unit of frequency
IQR	inter-quartile range
IVRT (ms)	isovolumic relaxation time in milliseconds
L (m)	depth of the boundary producing the echo in metres
LA (mm)	left atrial size in millimetres

LV	left ventricle
LVIDd (mm)	left ventricular internal diameter in diastole in millimetres
LVIDs (mm)	left ventricular internal diameter in systole in millimetres
LVH	left ventricular hypertrophy
LVMI (kg/m²)	left ventricular mass index in kilograms per square metre
m/s	meters per second
MHz	Megahertz, million hertz
M-Mode	motion mode
MRM	mitral ring movement
NYHA	New York Heart Association
P wave	portion of the ECG that correlates with atrial depolarisation
Period (s)	time for one complete cycle of the pressure fluctuation (in an ultrasound wave) in seconds
PW	pulsed wave Doppler
Q	Q wave on the ECG trace
Q –ME (ms)	time interval from the Q wave of the ECG to mitral valve opening in milliseconds
Q- Tea (ms)	time interval from the Q wave of the ECG to tissue peak early diastolic tissue velocity (Ea) in milliseconds
QRS wave	portion of the ECG that correlates with ventricular depolarisation
Q-Sw (ms)	time interval from the Q Wave on the ECG to peak systolic shortening velocity, in milliseconds
SD	standard deviation
SEM	systolic shortening of left ventricle

Sw (cm/s)	peak systolic shortening velocity of the left ventricle in centimetres per second
T (s)	time interval for one period of a wave in seconds
tau	index of myocardial relaxation
T wave	portion of the ECG that correlates with ventricular repolarisation
TGC	time gain compensation
Time to Acc (ms)	time interval to peak acceleration of early diastole in milliseconds
wall stiffness	the mechanical property of ventricular muscle indicated by the slope of its stress (pressure in the ventricle)/ strain (lengthening of the fibres) characteristic
WHO	World Health Organisation
WT (kg)	patient's mass in kilograms

List of Figures

List of Tables

Chapter 1

Introduction

Cardiac diseases, leading to impairment of cardiac function, account for well over 25% of all deaths in the western world. Therefore cardiology, the diagnosis and treatment of cardiac diseases, constitutes a major strand of medical practice. Research into cardiac diseases, the characterisation of their anatomical, physiological and functional features at the earliest stage of their development, leading to the design and implementation of effective therapeutic strategies, is a key strand within cardiology.

Electrocardiography, which yields insights into the fundamental bioelectrical activity of the myocardial tissues, and echocardiography, which uses ultrasound techniques to study the mechanical functioning of the heart, are among the most significant non-invasive research and diagnostic tools in cardiology. Successive historical developments in echocardiography over the past forty years have provided invaluable advances in the study and understanding of the dynamic functioning of the heart *in vivo* and they continue to provide elucidation of underlying changes in cardiac anatomy and functioning caused by different disease processes.

1.1   Basic physical/technical aspects of echocardiography

The physical and technical fundamentals of the different ultrasound diagnostic

modalities and the scanners used to apply them to diagnosis in human patients are

given in some detail in Chapter 2 of this thesis. The aims there are to outline the key

ways in which ultrasound interacts with tissues in the body and describe the

technologies of the different echocardiography modalities, as they are used to non-

invasively obtain and display information about these tissues.

The modality first used in echocardiography was the M-mode system, used to study

the movement of the leaflets of the mitral valve and later the other cardiac valves and

other movements of myocardial tissues (Edler *et al*, 1954; Edler, 1991). Later

continuous wave Doppler systems were developed to study blood flow in the heart

and peripheral circulation. Dynamic (real-time) two-dimensional (2-D) B-mode

imaging came into use to present cross-sectional images, and hence measurements, of

the changing myocardium and cardiac cavities throughout the cardiac cycle (Evans *et*

al, 1989; Schmailzl *et al*, 1994). Pulsed Doppler systems then emerged for measuring

and imaging more details of the blood flow at different regions of the heart and great

vessels.

1.2   Clarifying the filling and pumping action (emptying) of the left ventricle

As each new modality in echocardiography came to be applied to diagnostic

problems, new insights were added to the general understanding of the basic

mechanisms and processes in the functioning of the heart in health and disease.

2

Improvements came to be continuously added to the diagnosis, management and treatment of a wide range of cardiac diseases.

In order to establish a conceptual framework or model to develop an understanding of the physiological underpinnings of these new clinical applications, Chapter 3 presents a review of key aspects of cardiac anatomy and microanatomy, as well as relevant theories of cardiac dynamics. Attention is directed in particular at the reciprocal mechanism of emptying and filling of the left atrium and filling and emptying of the left ventricle and the role of the long-axis and circumferential myocardial fibres of the ventricular walls in this mechanism. The main aim of this chapter is to describe the twisting action of the ventricle in systole related to the contraction of the two sets of fibres, then the untwisting in diastole giving rise to a relative vacuum in the ventricle and a resulting early rapid transmitral inflow of blood in advance of the atrial contraction and late inflow due to that. This sets the normal anatomical and functional underpinning for the diagnostic applications of DTI investigated in the main body of the work reported in this thesis.

1.3   Emergence of Doppler tissue imaging (DTI)

A little over ten years ago one of the newest ultrasound modalities, Doppler tissue imaging (DTI), came into clinical use as a means of studying and measuring local myocardial movements in individual regions throughout the heart as well as global cardiac dynamics (Isaaz *et al*, 1989; Isaaz *et al*, 1993; Isaaz, 2000). Chapter 4 presents a brief review of the clinical applications of DTI that have emerged in recent years. The aim of this chapter is to introduce the relatively established clinical

applications of DTI, again as a backdrop to the work reported in this thesis. This
work concerns a number of extensions of the clinical applications of DTI, and its
clinical application in close simultaneous conjunction with other ultrasound
modalities, M-mode, conventional 2-D (B-mode) imaging and pulsed Doppler blood
flow measurement within the heart.

Because DTI is sensitive to cardiac dynamics, it has the potential to be suitable for the
study of cardiac diseases where local or global dynamics are impaired. Two major
cardiac diseases are the focus of the work reported in this thesis, ischaemia, where
collections of myocardial fibres die and are no longer able to contract and relax
autonomously, and hypertrophy, where the volume and mass of the fibres are greatly
increased. In both cases the dynamic behaviour of the tissues concerned is markedly
different from that in the healthy heart. Study of the dynamics is likely to reveal
valuable diagnostic and prognostic information about the heart in each disease.

1.4   Ischaemic cardiac disease

When addressing the Royal College of Physicians of London in 1768, William
Heberden described "a disorder of the breast, marked with strong peculiar symptoms,
considerable for the kind of danger belonging to it, and not extremely rare…" (Dock,
1939). In modern-day parlance, this "disorder" is referred to as ischaemic heart
disease, an umbrella term used to describe the various manifestations of cardiac
ischaemia, essentially oxygen deprivation and death of cells in the myocardium.
Cardiac ischaemia is generally caused by underlying disease of the coronary
circulation whereby atherosclerotic plaque or thromboembolism formation occurs,

such as to narrow or completely block an artery. This reduces perfusion of the

specific area of tissue distal to the site of the occlusion and results in the regional or

segmental infarction and impairment of myocardial contraction, characteristic of the

disease (Heyndrickx *et al*, 1978; Ren *et al*, 1985; Asinger *et al*, 1988).

Ischaemic heart disease described by Heberden in the eighteenth century as "not

extremely rare", has now reached epidemic proportions especially in affluent western

societies where overnutrition, sedentary life styles and an increased life span have

facilitated its development (Braunwald, 1997). According to the World Health

Organisation (WHO Injuries and World Health Report, 1999), ischaemic heart disease

was the leading cause of global mortality in 1998 claiming 7,375,000 lives. This

world-wide incidence is reflected in Irish statistics, which indicate that ischaemic

heart disease was responsible for almost 25% of deaths in 1998. In an ageing Irish

population, this disease is likely to remain prominent despite increasing public

awareness of health issues (New Health Strategy, Department of Health and Children,

2000).

Because ischaemia results in damaged/infarcted myocardial tissue on a regional basis

and this damaged tissue no longer depolarises/ repolarises and contracts/relaxes as

normal, the movement of the affected and neighbouring regions of the myocardium is

changed relative to the normal situation. Therefore, an accurate and quantitative

method of assessing overall as well as regional or segmental heart movement is

required to fully study and diagnose the location and extent of the ischaemic disease.

Echocardiography is a simple and non-invasive diagnostic tool, which can measure many of the functional consequences of cardiac ischaemia. To date however, echocardiographic methods of segmental evaluation have not been ideal in that they are visual, and at best semi-quantitative only. DTI, which give more quantitative measurements of regional myocardial movements, offers greater promise of more objective diagnostic insight into ischaemia.

Chapter 5 presents a pilot study to explore the potential of DTI in conjunction with other ultrasound modalities to offer a quantitative and non-invasive measurement of regional and global (as expressed through ejection fraction) cardiac function in systole. The aims of this chapter are to develop the utility of DTI to the measurement of long axis function in the left ventricle during systole, to provide additional evidence for the reciprocal mechanism of ventricular filling and pumping, and to shed new light on the use of DTI to measure regional and global function of the ventricle. A preliminary aim of this pilot study was to develop the echocardiographic scanning and data analysis/reduction procedures required to study the differences in left ventricular function between these two groups of subjects, and then compare the results obtained with conclusions of similar studies as previously published in peer-reviewed publications.

In Chapter 6 is presented a study of the use of DTI to measure the dynamics of early ventricular filling in normal subjects and in patients with diastolic dysfunction. The main aims of this aspect of the work is to systematically compare and contrast the dynamics of the mitral ring as recorded by DTI and its relationship with transmitral

blood inflow velocity, in normal subjects and in a group of patients with diastolic dysfunction.

1.5   Dynamics of the left ventricle in hypertrophy

Cardiac hypertrophy, principally left ventricular hypertrophy (LVH), consists of increased mass of myofibrils that can lead to myocardial fibrosis, and may be secondary to hypertension or aortic stenosis. Marked LVH may also be caused by fibre disarray secondary to hypertrophic cardiomyopathy which is a primary disorder of the contractile apparatus. However, LVH can be absent in a significant number of mutation-positive individuals until later in life (Nagueh *et al* , 2000).. Cardiac hypertrophy consists of a thickening or swelling of the ventricular walls, due to the individual myocardial cells growing rather than the cells dividing and multiplying. It can be caused by stress on the heart, such as by hypertension, other diseases as well as high athletic activity. If it becomes excessive it can give rise to the death of some of the myocardial cells, thereby increasing the stress on the remainder and producing a positive feedback cycle leading to heart failure.

The first description of the pathology of HCM was by Hallopeau (1869), but it was not recognised as a distinct disease until Teare (1958) did so. He described its main features including hypertrophy of the ventricular walls, especially the septum, reduced cavity sizes, ''disarray'' in the alignment of myocytes, familial, genetic pattern and risk of sudden death. In later years there have been many published papers describing the clinical, electrocardiographic and haemodynamic features of the disease (Braunwald *et al*, 1964). The introduction of echocardiography had a major impact

on the assessment of hypertrophic cardiomyopathy and still remains the cornerstone

of diagnosis (Maron *et al,* 1983).

HCM increases the mass of portions of the myocardium and so affects its

contractility, and its velocity and extent of movement during contraction and

relaxation. The dynamics might be expected to be slower and the overall excursion

possibly reduced in comparison with the normal case. Thus the recoil of the heart

during isovolumic filling in the early part of diastole, which provides energy for rapid

early diastolic filling, is likely to have different dynamics and be slower in cases of

HCM. Such changes, even at an early stage before the development of LVH, might

be expected to be revealed by echocardiography techniques such as DTI that measure

the detailed movement of the cardiac structures (Nagueh *et al*, 2000).

The study reported in Chapter 7 explores and develops the clinical applications of DTI

in making the diagnostic distinction between subjects with normal healthy hearts,

athletes with athlete's heart and patients with HCM. The aim of the study was to

develop and evaluate echocardiographic parameters for the differentiation of

physiological LVH from pathological LVH.

1.6   Summary "Road Map" for this thesis

This thesis falls into four thematic parts, as shown schematically in Figure 1.1.

Part 1, consisting of chapters 1 to 5, reviews the development of the understanding of

in-vivo cardiac dynamics from early theories of left ventricular function. It also

incorporates the theoretical and conceptual underpinnings for the diagnosis of heart

disease. It reviews and discusses the clinical application of echocardiography with

emphasis on Doppler tissue imaging (DTI). Chapter 5 discusses a pilot study of the application of DTI in the assessment of ischaemic heart disease.

Part II of the thesis consists of chapter 6 and presents the theoretical framework and the practical approach to the recognition of an early diastolic mechanism involved in the proper filling of the heart. This describes a study to relate myocardial recoil to the acceleration of blood across the mitral valve using a DTI-derived index as a surrogate for the recoil.

Part III, consisting of chapter 7, presents a review of the athlete's heart and current screening methods for this condition, and their limitations. It explores the potential of DTI in helping to distinguish pathological from physiological left ventricular hypertrophy. It also discusses novel applications of DTI, including measurements of the early diastolic mechanism timing, in making this diagnostic decision.

Part IV, chapter 8, presents a review of the work of the thesis and a number of conclusions.

Thesis

Part I
Introduction and background to theory and experimental clinical approach

Chapter 1: Introduction

Chapter 2: Echocardiography: technical fundamentals of diagnostic ultrasound imaging, including Doppler tissue imaging (DTI)

Chapter 3: Cardiac Anatomy: theories of left ventricular function to provide theoretical and conceptual underpinning of the diagnosis of cardiac diseases

Chapter 4: The developing clinical applications of DTI

Chapter 5: Systolic dysfunction: contribution of DTI, in combination with 2-D imaging and transmitral blood flow measurement by Doppler ultrasound, to assessing infarction arising from ischaemic heart disease

Part II
New concepts relating to early diastolic filling dynamics

Chapter 6: Diastolic dysfunction: contribution of DTI, in combination with 2-D imaging and transmitral blood flow measurement by Doppler ultrasound, to assessing early filling dynamics in normal controls and patients with diastolic dysfunction

Part III
A clinical application of the new concepts: examining the causes of sudden death in athletes

Chapter 7: Causes of sudden death in athletes, current screening methods and their limitations, and the potential of DTI to helping distinguish pathological from physiological LVH

Part IV
Conclusions

Chapter 8: Overall discussion and conclusions

Figure 1.1   The road-map to the structure of the thesis

Chapter 2

Echocardiography: technical fundamentals of diagnostic ultrasound imaging, including Doppler Tissue Imaging (DTI)

Echocardiography is the science and practice of cardiac diagnosis by means of ultrasound. At the present time four broad approaches are used to gather, process and then display the ultrasound diagnostic data. These are

- the M-mode system, the oldest approach

- the 2-D or B-mode imaging system

- the Doppler technique of blood flow measurement

- Doppler colour flow imaging and the related Doppler Tissue Imaging (DTI) approaches.

This chapter introduces the physical principles underlying the technologies of the systems used in these four diagnostic approaches.

The main functional blocks of the ultrasound scanner are the following

- the power supply converts the a.c. voltage supply to controlled d.c. supplies to power the electronic circuits within the scanner

- the electronic circuits drive the transducers to create the diagnostic ultrasound wave, and process the ultrasound signals from the tissues of the body

- the computer controls the timing and logic of operation of the system, stores the ultrasound data about the tissues, processes these data and creates the electronic display, generally on a television monitor

- either the computer memory or a video recorder makes a permanent record of the patient data obtained in the examination, or a camera and hard copy recorder may be used to make an alternative permanent paper record of the display of processed patient data.

Most echocardiography scanners allow the recording of single-lead or multiple-lead electrocardiograms (ECGs) to facilitate correlation between the bioelectrical and mechanical events in the cardiac cycle.

2.1   Ultrasound

Ultrasound is a mechanical wave that travels through the tissues of the body. Initiated by vibratory motion of a surface (the transducer) in contact with the tissue, each successive layer drives the next layer into vibratory motion and so the wave propagates. The tissue particles vibrate and the wave carries mechanical energy from the transducer into the tissues.

At each point in the wave the wave pressure varies sinusoidally above (compression) and below (rarefaction) the normal steady (atmospheric) pressure. This pressure fluctuation is experienced by each part of the tissues through which the wave travels.

The time for one complete cycle of the pressure fluctuation is the *period T*. The number of cycles occurring each second is the *frequency f*, measured in hertz (Hz). Note that $f = 1/T$. Mechanical waves of frequency above 20 kHz are called *ultrasound*.

Ultrasound travels through each tissue at a constant *speed of propagation c*, the distance travelled by the wave in one second (in metres per second, m/s). If the distance travelled is z m in t s, then $c = z/t$. For soft tissues, including blood, $c = 1540$ m/s on average.

At any *instant*, there is a fixed distance between successive compressions along the wave, the distance travelled by the wave in one period T, called the *wavelength (λ)* and measured in metres (m). The wavelength is found from c and f thus $\lambda = c\ T = c/f$. Generally in clinical diagnosis, the use of a shorter wavelength (higher frequency) produces finer spatial resolution and finer detail in the images or displays.

All diagnostic ultrasound techniques rely on the reflection of the wave at boundaries within the tissues. When the ultrasound wave is incident on a boundary between two tissues, a fraction of the wave energy is transmitted into the second tissue and the rest of the energy is reflected backwards as an echo along the original path. Where the wave is obliquely incident on the boundary much less energy is reflected backwards. Therefore most diagnostic applications depend on the original ultrasound wave being very close to perpendicular to the boundaries under investigation, although non-

perpendicular waves scattered from 'rough' surfaces and cells do produce detectible echoes.

As the ultrasound wave travels, some of the energy in the wave is continuously lost and the strength of the wave is attenuated. This *attenuation* is greater at higher frequency and so the depth of field that can be examined tends to be less at higher frequency.

Thus the choice of operating frequency in any instance is broadly a compromise between the depth of tissue required to be investigated and the fineness of spatial detail required in the image.

2.2   Transducers

The transducer is used to create an ultrasound wave with an electrical impulse or signal, and also detect the ultrasound wave and an electronic signal representative of that wave for further processing. The transducer consists of one or more thin discs of piezoelectric crystal, each with thin metal electrodes on the two flat faces, a layer of matching material attached to the front face looking outwards, and a block of damping material against the back face. This ensemble is contained in a holder and electrical leads connect the electrodes to electronic circuits in the main unit of the scanner.

Under the influence of an electric field across the thickness of the disc, the piezoelectric crystal has the property of being deformed, i.e. made thicker or thinner depending on the polarity of the field. Application of an oscillating electric field of

ultrasonic frequency causes the crystal to alternately expand and contract at the same

frequency, thereby producing an ultrasound wave. Conversely, when an ultrasound

pressure wave strikes the crystal, the piezoelectric crystal has the property that the

resulting mechanical distortions of the crystal generates an alternating electrical

voltage between the opposite faces of the disc, proportional to the amplitude and

frequency of the ultrasound wave. If this incident ultrasound wave consists of

reflected echoes returning for instance from intracardiac structures, they may be

converted using the electrodes into signals suitable for electronic processing.

When an electrical signal is supplied to the crystal by the circuit, an ultrasound wave

is transmitted from the front face of the transducer. Conversely, when an ultrasound

wave coming from the tissues strikes this transducer, a replica of this wave in the

form of an electronic signal is generated by the crystal and sent to the electronic

circuits. These transducers can both generate and detect/receive ultrasound waves.

2.2.1   Ultrasound beam

At ultrasound frequencies the transducer creates a directional beam of ultrasound, its

direction being defined by the axis of the beam, the centre-line of the beam, usually

perpendicular to the centre-point of the transducer. Directionality is a key property of

the beam, allowing it to be transmitted along the known direction of the beam axis

into the tissues, and to be reflected from and transmitted by structures along that line

only.

Many echocardiography instruments have multi-crystal array transducers, either linear

or annular. These are arrays of crystal elements mounted in a transducer, but

insulated and isolated from each other. They are activated in distinct groups so that a

composite beam from a group is transmitted. One application of the linear array is the

phased array in which there is electronic sector-steering of the beam while the

composite beam remains within the plane of the array.

The transducer will transmit ultrasound continuously if supplied with an *alternating*

voltage of the appropriate frequency from an oscillator. This is the mode of operation

used in continuous wave (cw) *Doppler* ultrasound instruments. In this case two

separate transducer crystals must be used, one to transmit and the other to receive

continuously.

2.2.2 *Straight line propagation*

Ultrasound propagates or travels in a straight line through homogenous tissue but is

reflected, at interfaces between tissues of different acoustic impedance. The greater

the acoustic mismatch between the two media, the greater the reflection of sound.

Consequently, at boundaries between tissues of high difference in impedance, such as

between soft tissue and bone or between soft tissue and gas, almost all of the

ultrasound is reflected. In such cases the echo reflected is very strong, but the amount

of ultrasound energy remaining in the beam to pass through deeper tissues and

produce echoes from them, tends to be negligible. Such deeper tissues are in the

acoustic shadow of the strongly reflecting boundary. Because the heart lies within the

ribcage, and nestled between the air-filled lungs, it is largely shadowed from an

ultrasound beam approaching from the skin surface. The number of possible acoustic windows to obtain ultrasound access to the heart and cited in Chapter 4, is limited, and hence the number of echocardiographic views of the heart that may be readily obtained is also limited.

2.3   Ultrasound data collection and display

All diagnostic ultrasound systems require the face of the transducer to be placed on the skin of the patient, with a gel or oil coupling-medium between the transducer face and the skin to eliminate air between them.

2.3.1   *Pulse-echo systems*

Most echocardiography instruments are based on *pulse-echo ranging*. In this technique, the transducer transmits a brief pulse of ultrasound, and then remains quiescent while the pulsed wave of ultrasound travels directionally through the tissues at the constant speed of propagation. After some distance, the ultrasound pulse encounters a reflecting boundary, where the incident pulsed wave is partly reflected and partly transmitted. The reflected wave travels back towards the transducer to be detected some time later as an echo by the transducer. By measuring the time (Δt) taken for the echo to return, i.e. to travel the distance $2\,L$ where L is the depth of the boundary producing the echo, L may be calculated thus $L = (c\,\Delta t)/2$, when c is known. Clearly only reflecting structures located in the beam can provide echoes to generate echo signals at the transducer.

Attenuation in the tissues between transducer and reflector reduces the intensity of the echo signal received. The attenuation of the transmitted beam and of the reflected beam(s) depends on the attenuation coefficient of the tissues and the length of the overall path travelled.

2.3.1.1   M-mode

In 1953, Inge Edler and Hellmuth Hertz of Malmo General Hospital in Sweden were the first to use ultrasound for cardiac diagnosis. They placed the transducer of a reflectoscope, used for non-destructive materials testing, over the chests of patients and could detect moving echoes. They thereby recorded the first "ultrasound cardiogram" to examine the mitral valve of the human heart (Edler *et al*, 1954).

In M-mode echocardiography the transducer emits a single pulse of ultrasound along a directional beam in a straight line through a particular region of the chest and heart. Cardiac structures encountered by the beam on its path through the heart reflect some of the ultrasound, which then returns as echoes and are detected by the transducer. The time delays between the original ultrasound transmission and the detection of each subsequent echo allow the depth of each reflecting intracardiac structure to be calculated. The pulse transmission is repeated periodically at a relatively low pulse repetition frequency to sample the positions of the echoing structures in close to real-time.

The M-mode display is essentially a two-dimensional graph. Along one axis is real-time, and along the other axis is pulse-echo delay or depth into the tissues of the

reflecting structures. Points are registered only at those depths from which echoes are returned, at each successive instant during the build-up of the display. If all the reflectors in the tissues are stationary the display is a series of parallel lines at depths corresponding to the reflector depths. When some of the reflectors are moving towards or away from the transducer, the display obtained is a set of graphs of the depths/positions of these reflectors against time. For relative cardiac phase comparisons, an ECG trace is usually displayed along the real-time axis of the M-mode display.

The main advantage of M-mode echocardiography is that it provides a great deal of accurate information every second from a localized straight-line path through the heart, and has adequate temporal resolution of ≥ 1 ms. Another advantage is its ability to allow phases of movement of cardiac structures to be compared in time with the electrocardiogram. It is used to study the thickness of the heart walls and the movement of cardiac structures, as well as to obtain various cardiac dimensions. A limitation of the M-mode modality is that it represents a one dimensional ("ice-pick") view of a line through the heart at each instant. Nevertheless, having located the anterior leaflet of the mitral valve using M-mode provides an ideal landmark for the relative location of other cardiac structures.

2.3.1.2   2-D (B-mode)

The B-mode display or image is a two-dimensional (2-D) representation or map of a cross-section through the tissues. The cross-section in question is that defined by the plane through the tissues scanned by the pulse-echo beams during the acquisition of the

echo data from the tissues. The locations of reflectors in the cross-section are represented in the image by bright (B-mode) spots or pixels on the dark background at all the corresponding or mapped points. Spatial relationships between reflectors in the tissue cross-section are preserved in the spatial relationships of the corresponding bright spots in the image. The brightness or grey level of each spot correlates with the echo signal strengths from the corresponding reflector.

The ultrasound beam is scanned repeatedly, usually in a fan-shaped plane, and the 2-D pattern of reflecting tissues in this fan-shaped cross-section yield the depths and echo strengths from each reflector along each beam line in the scan plane to enable the computer to construct the image. This 2-D image is displayed on a TV monitor, with the image periodically repainted at a frame repetition frequency of 25 Hz, 50 Hz or greater. If features in the image are moving, there is then smooth transition between each frame and the motion is seen as smooth. Such an electronic image is termed a *real-time* or dynamic image.

In a phased transducer array system, as very commonly used in echochardiography, the composite beam from the set of the piezoelectric elements is electronically scanned through the scan plane in sector-fashion to produce a fan- or pie-section-shaped image. Essentially, the transducer produces a fan of scan lines, each of which is created by sending an ultrasound pulse in a specific direction and collecting the corresponding echo train. In this system, a small "footprint" on the skin surface and a large field of view distal to the transducer overcomes the problem of an imaging window limited by the ribs and lungs. The ultrasound fan "slices" the heart to obtain an image similar to a real anatomical section at the level of the examining plane.

Each scan line in the fan-shaped image is created by first sending out a pulsed beam of ultrasound in a specific direction into the issues, and then collecting the corresponding sequence of echoes. A finite time is required to collect the sequence of echoes and hence the data for each scan line, and this time depends on the depth of interest and on the velocity of sound in soft tissue. As a result, the time needed to acquire all the data for one image frame is directly related to the number of scan lines, which, in turn, is indicative of the temporal resolution in the image. It is desirable to have as many scan lines as possible since this improves spatial resolution and the appreciation of small detailed structures. However, imaging fast-moving structures like the heart requires a high frame rate (a number of images per second high enough to exceed the flicker fusion frequency of the eye so that a smoothly changing image is perceived the eye) so that continuous movement can be visualized with no perceived jump from one frame to the next. Therefore, there is trade off between the scan line density and image frame rate. In 2-D imaging, a high frame rate of at least 30 frames per second is desirable for accurate display of cardiac motion. Roughly, this frame rate allows 128 scan lines per 2-D image at a displayed depth of 20 cm.

2.3.2   3-D Echocardiography

Three-dimensional (3-D) imaging systems have recently been introduced which digitally combine a number of 2-D images of the tissues. Progress in computer technology hardware (CPU, memory, networking) and software (computer graphics, network protocols) has allowed this reconstruction of the 3-D image in real-time. In the earliest such systems, the 3-D dynamic image could be viewed from fixed view

points only, but current systems allow the observer to change the view point

instantaneously.

A 3-D dynamic heart imaging system thus allows the observation of a real-time three-

dimensional image of the heart, as seen from various view points. It also allows the

visualisation of a section through the heart. Such a reconstructed 2-D B-mode image

has the same spatial resolution as the basic scanning system and the detail inside the

heart can be presented.

2.3.3   *The Doppler effect*

Doppler echocardiography is based on the Doppler effect, first described in 1842 by

the Austrian physicist, Christian Johann Doppler. If a reflector, with ultrasound of

frequency, f_i, incident on it, is moving away from or towards the stationary

transmitting/receiving transducer, the frequency of the ultrasound reflected and

received at the transducer, f_d, is less or greater than f_i. This change or shift in

frequency is the *Doppler effect* and the change in detected frequency is called the

Doppler shift in frequency, and given by $\Delta f = \pm (2 f_i v \cos\theta)/c$, where v is the speed

of the moving reflector, θ is the angle between the direction of the incident ultrasound

beam and the direction of the reflector motion, and c is the speed of propagation of

ultrasound in the tissues between transducer and reflector. If the reflector is moving

towards the transducer, the shift is positive and if moving away from the transducer,

the shift is negative. Of course if the ultrasound is reflected from a stationary

interface $(v = o)$, the frequency is not shifted at all.

By increasing the operating frequency f_i the Doppler shift increases in direct proportion. In this instance there is the additional advantage of a much longer directional beam. Higher frequency also increases the backscattered echoes from the small moving blood cells, relative to the unwanted strong reflection echoes from the generally larger structures such as blood vessel walls.

By increasing the angle θ, the Doppler shift declines because $\cos\theta$ declines. The Doppler shift is greatest when θ is 0 and this is when the ultrasound beam is travelling in the same direction as the reflector.

2.3.3.1   cw Doppler applications

Conventional Doppler echocardiography measures blood flow velocities in the heart and major vessels. The key reflecting structures are the red blood cell (erythrocyte) membranes within the blood plasma. These are very weak reflectors, some – 100 dB relative to many soft tissue boundaries (Bjaerum et al, 2002). They are also very small in comparison with the wavelength of ultrasound, so that the reflection from them is in many directions and is referred to as scattering. A small portion of that reflected is back towards the transducer. Nevertheless, because of the large number of red blood cells in normal human blood (about 5 million per cubic millimetre), a detectible amount of back-scattered ultrasound is received from moving blood.

Also blood moves at a higher velocity than cardiac tissue. Consequently, the Doppler frequency shift associated with blood flow is greater than that of cardiac tissue in the vicinity, even though the amplitude of the associated signals is lower. In conventional

Doppler echocardiography, the higher amplitude signals from moving tissue are purposely filtered out so that only blood signals are processed.

In a cw Doppler system the ultrasound beam is transmitted continuously and the returning echo signals are also received continuously. This requires two separate side-by-side transducers to be used, one dedicated to transmission and the other dedicated to reception.

Because the beam is propagating continuously and any moving structures in that beam are being reflected continuously, the receiver transducer is constantly receiving all the corresponding Doppler shifted echoes. For instance if both venous flow and arterial flow are located within the same beam, the receiver transducer will simultaneously detect both the spectrum due to the venous flow and the spectrum due to the arterial flow.

Since the transmitter transducer is constantly transmitting ultrasound, all reflecting structures in the beam, both stationary and moving, are constantly returning echoes to the receiver transducer in the probe. This means that the receiver transducer is constantly receiving echoes of frequencies equal to the originally-transmitted frequency (from stationary structures) as well as Doppler-shifted frequency echoes (from moving structures). The spectrum of the received echo signals includes the operating frequency.

There is no provision for time gain compensation (TGC) since there is no way of distinguishing the depth from which echoes are received in this system. However the

echoes from deeper structures are more attenuated than those from more superficial

structures and are therefore generally weaker.

After a receiver amplifier, the cw echo signals are processed through real-time

digitisation and then digital spectrum analysis to yield the amplitude of each

frequency component, especially those Doppler shifted components due to reflections

from moving structures in the tissues. Digital programmes involving fast Fourier

transforms (FFT) in real-time are used for this purpose. The most common form of

display of these processed data is a real-time graph of Doppler-shift frequency against

time with the spectral amplitudes coded into a grey scale or a colour-coded display.

In a grey scale (black on white) display a high amplitude spectral component would

be darker than a low amplitude component. A typical such display is shown in Figure

5.1. In a pseudo-colour or colour-coded display a high amplitude would be displayed

on the frequency/time display as a yellow, a lower amplitude would be red, etc.,

depending upon the colour assignments used.

2.3.3.2   *Doppler blood flow measurement*

To use the Doppler effect to measure blood flow, the beam of ultrasound is made to

pass through the vessel carrying the blood flow of interest. Because there is a range

of speeds in the blood across the vessel, there occurs a range of Doppler shift

frequencies. There is also a Doppler shift due to the motion of the reflecting walls,

but usually much lower than that due to the most rapidly moving blood. Thus the

Doppler shift has a spectrum ranging from 0 to Δf_{max}.

Because the blood flow in an artery or vein is pulsatile, the Doppler spectrum is also pulsatile over time. If the flow is not laminar, there is still a range of speeds present and therefore a Doppler shift spectrum. Because the speeds found in venous flow are less than 10% of those found in arterial flow, the width of the Doppler spectrum from typical venous flow is less than 10% the width of the Doppler spectrum found for the case of arterial flow.

2.3.3.3   *Pulsed Doppler systems*

In a pulsed wave (PW) Doppler system the transmitted ultrasound wave is pulsed, thereby allowing pulse-echo ranging and the measurement of the depth of a moving reflecting structure as in pulse-echo imaging systems.

Because the PW Doppler technique is based on the pulse-echo principle a time gain compensation (TGC) is used to compensate for the greater attenuation suffered by the ultrasound beam while interrogating deeper structures. The received signals are passed through a range gate, which can be opened at any required delay after the original transmitted pulse. By varying the delay used, the pulse-echo signals from different specific depths can be examined in isolation. Also, the duration of the opening of this sampling gate, which can be greater or less than the duration of the transmission pulse, can be varied in order to be able to focus attention on Doppler-shift signals from a particular layer of tissues, of any desired thickness.

Therefore, the final output Doppler signals originate from moving reflectors within a particular layer of tissues within the beam at a particular set depth - the so-called

sample volume. It is an approximation to consider the sample volume as cylindrical. It would be more accurate to note that the cylinder would have some tapering at each end and hence a pear or drop-like shape is more realistic.

This instrumentation allows one to study the Doppler signals from points across the lumen of an artery, or from different points along the cusp of a cardiac valve, etc.

The pulsed system samples the motion of the reflecting structures, red blood cells or other tissues, at the pulse repetition frequency. In the Doppler system it is equivalent to sampling the Doppler-shift frequency signal. The repetitive nature of this signal means that the Doppler pulse repetition frequency, i.e. the sampling frequency, must be at least twice the maximum possible frequency that may be present in the Doppler signal. This is called the Nyquist criterion and means that each cycle of the maximum Doppler shift frequency must be sampled at least twice to detect the positive and negative portions of the Doppler shift oscillations. If the Doppler shift frequency is greater than twice the pulse repetition frequency, an artifact called *aliasing* occurs.

Aliasing is clearly most likely when the highest blood speeds are being measured and the highest Doppler-shifts are therefore occurring. It is manifested on a grey scale or colour spectral display during a part of the pulse of flow, as a full band of (say) positive frequencies up to the maximum of the display and a simultaneous band at the lowest negative frequencies of the display. Aliasing can be eliminated by using a higher pulse repetition frequency or by taking any of the steps which reduce the Doppler-shift frequencies, i.e. decreasing the operating ultrasound frequency f_i or increasing the angle θ between the axis of the ultrasound beam and the axis of the

blood vessel. In some pulsed instruments it is possible to shift the zero frequency axis

of the display, allowing a wider range of Doppler frequencies of either positive or

negative phase. The wider range is often enough to eliminate this wrap-around effect

due to aliasing.

2.3.3.4   *Doppler colour flow imaging*

Doppler (colour flow) imaging is achieved by a duplex system, which combines

conventional real-time 2-D imaging and, in parallel and simultaneously, appropriate

real-time signal processing is carried out to extract the reflector motion data at all

depths for the colour flow display.

The system provides a conventional real-time grey scale image displayed on a colour

TV monitor.

For the colour flow part of the image, the pulse echo delay to a moving reflector for

each transmitted pulse, locates the depth of that structure in real-time and together

with the orientation of the beam projection determines its location in the image. The

Doppler shift detected gives the magnitude and phase (positive or negative) of the

velocity of the reflector at a particular location, is determined by auto-correlation

between two successive echo trains from the same projection, and these date are used

to generate a colour for each pixel corresponding to the voxel from which that moving

echo signal is received. This colour supersedes the grey attributed by the real-time

imaging process to that pixel.

Usually the pixel is coloured blue for flow away from the transducer and red for flow

towards the transducer. The hue of the colour (i.e. its saturation or brightness)

increases with increasing magnitude of the measured velocity.

The result is a real-time grey scale image upon which are superimposed red and/or

blue colours representing movement, located in the lumen of any artery or vein or

other flow or motion within the image.

If streamline or laminar flow occurs throughout the cardiac cycle, the patterns of red

and blue vary during the cycle but are periodic or repetitive from one cycle to the

next, for a fixed position and orientation of the ultrasound transducer. If however

there is some turbulence at some stages of the cardiac cycle the red/blue patterns are

not repetitive from one cycle to the next.

Turbulence in the flow is displayed by the addition of a third colour, green, at

appropriate stages in the image formation. A voxel in which there is laminar flow,

yields a very limited range of blood velocities, since at any instant all of the

streamlines are in the same direction through the voxel. If however, there is turbulent

flow through the voxel, there are streamlines in many random directions through it,

there are many blood cell speeds and many angles of incidence between ultrasound

beam and moving blood cells, and these result in a wide range of measured velocities

for that voxel.

The computer calculates the mean measured velocity and its standard deviation, the latter a measure of the extent of the range of velocities. The mean measured velocity is used in the image formation software to determine the hue or brightness of the red or blue component of the colour of the pixel while the standard deviation is used to determine the hue or brightness of the green component of the colour of the pixel. Thus, in general the colour of the pixel is some mixture of red and green or blue and green.

Forward flow with a high speed and little turbulence is displayed as bright red, while forward flow with high speed and high turbulence is displayed as bright yellow, the result of mixing bright red and bright green. If the flow is in reverse with high speed and high turbulence the display is bright cyan, the result of mixing bright blue and bright green.

2.3.3.5   *Doppler tissue imaging (DTI)*

DTI is a slightly modified colour flow Doppler imaging technique (McDicken *et al*, 1992; Desco *et al*, 1997; Price *et al*, 2000) that concentrates on displaying the mean velocities of the different layers within the myocardium, not just the velocities of the endocardium and epicardium. These tissues usually move with much lower velocity than the blood and so their Doppler shifts are of much lower frequency than those of the blood. Also these tissue are stronger reflectors than blood is and so the echo amplitudes from them is greater than those from blood. These cardiac structures, and particularly the intramyocardial structures, are found to move with a velocity range of

0.06 to 0.24 m/s, some ten times slower than intracardiac blood flow, and produce echo amplitudes some 40 dB above those received from the blood pool.

These two differences allow the DTI system to readily eliminate signals from the blood within the heart from the display. To do so the higher frequency Doppler shift and lower amplitude signals from the more rapidly moving and more weakly reflecting blood, are filtered out using a low-pass filter coupled with a variable threshold set to eliminate the low amplitude signals. The tissue Doppler signals of low frequency and high amplitude are thus preserved for display.

The form of DTI display used in this work is simpler still in that a narrow range-gate is located on a reflecting tissue surface along the axial direction, which is highlighted on the B-mode image. Signals from within the gate only are processed for the final display of average velocity versus real time. An ECG trace is also included in the display to provide phase or time comparisons with different events of the cardiac cycle.

The low frame rates (25 Hz) of early DTI system displays were insufficient to accurately depict each phase of myocardial motion. However digital parallel processing techniques now allow frame rates of up to 80 Hz. This technique has been described in detail by Erbel *et al* (1996).

2.4   Instrumentation used in this work

Appendix A contains the general specifications for the two ultrasound scanning systems, Agilent/Philips 4500 and Agilent/Philips 5500, used to carry out the studies reported in Chapters 5, 6 and 7. It also has a description of the circuit developed to provide a simultaneous timing pulse to both devices to allow accurate relative timing of events simultaneously recorded during individual heartbeats/cardiac cycles in the study described in Chapter 7.

2.5   Bibliography for this chapter

Evans, DH & McDicken, WN, Doppler Ultrasound: Physics, Instrumentation and Signal Processing, 2nd ed., John Wiley & Sons, Chichester, 1999

Hill, CR, Bamber JC & ter Haar, GR (Eds.), Physical Principles of Medical Ultrasonics, 2nd ed., John Wiley & Sons, Chichester, 2004

Chapter 3

Cardiac anatomy: theories of left ventricular function to provide theoretical and conceptual underpinning of the diagnosis of cardiac diseases

Cardiac anatomy and microanatomy are key determinants of the functioning of the heart in health and disease. This chapter presents a review of key aspects of cardiac anatomy and microanatomy, as well as relevant theories of cardiac function and cardiac disease. This is aimed at clarifying the conceptual framework or model underpinning the new diagnostic applications of DTI developed in this work. Attention is directed on the left ventricle, the high-pressure chamber of the heart, where diseases have the most serious consequences. This is the chamber that does most of the physical pumping work, driving the same cardiac output as the right ventricle but to a much higher pressure, and whose functioning principally determines cardiac health and well-being.

3.1   Muscle fibre structure of the heart

The left ventricular wall is composed of three distinct strata, as shown in Figure 3.1. Lining the interior of this wall is the endocardium, a thin layer of epithelial tissue unique to the circulatory system (Rodriguez *et al*, 1996). The epicardium is a thin external membrane that encases the heart. Between these two layers lies the muscular

myocardium, which constitutes the bulk of the heart wall. The myocardium consists

of muscular fibres and fibrous rings. The fibrous rings serve as attachments between

the muscle fibres and the other cardiac structures such as valves. Left ventricular

systolic and diastolic performance is strongly determined, under normal physiological

conditions, by this micro-anatomical arrangement of the myocardial fibres (Streeter *et*

al, 1973).

Mainly long-axis fibres run from the fibrous apex to the fibrous atrio-ventricular

(mitral) ring and are mainly located in the subendocardial and subepicardial layers of

the left ventricular free wall and in the papillary muscles. Such longitudinal fibres are

absent in the septum separating the left ventricle from the right. Systolic shortening

and diastolic lengthening along the longitudinal axis are due, in turn, to contraction

and relaxation of longitudinally aligned sarcomeres within the myocardial cells. The

apex itself remains effectively stationary with relatively little longitudinal motion.

Mainly circumferential myocardial fibres are located in the mid-layer of the left

ventricular free wall and are strongly represented in the intraventricular septum.

They also constitute a sphincter system that is particularly prominent in the basal

portion of the left ventricular cavity, near the mitral ring.

The mitral valve orifice is surrounded by a dense fibrous annulus or ring of

connective tissue, which forms the scaffolding upon which the myocardial mass is

based. This mitral ring frames the mitral orifice and supports the mitral valve that

controls blood flow between the left atrium and the left ventricle. The mitral ring is

continuous with the fibrous mitral valve on the inner side, and with the rest of the so-

called fibrous skeleton of the heart on the outer side (Streeter *et al*, 1973; Turrent, 1973).

The physiological consequence of this anatomical arrangement of myocardial fibers is an unusual heterogeneity of regional contraction and relaxation (Fatenkov *et al*, 1991). In systole the longitudinal and circumferential fibres shorten and the lateral and posterior walls thicken much more than those of the septum. This movement tends to be uniform from the base of the lateral and posterior walls to the apex. On the other hand, the septum shows a reasonably significant increase in circumferential contraction in going from base to apex.

The bands of long-axis fibres constituting the muscular structure of the myocardium are in fact remarkably convoluted and interlaced (Rodriguez *et al*, 1996). The fibres start at the base of the ventricle where they are attached to the fibrous rings around the orifice and pass downwards towards the apex. At the apex the fibres turn inwards into the interior of the ventricular wall forming what is called the vortex (Fatenkov *et al*, 1991). Streeter and coworkers (1973) described this arrangement as continuous bands of fibres forming figures of eight, which sweep from pericardium to endocardium, as they also sweep from base to apex. They also concluded that the fibres present in the pericardium at the base might be in the endocardium where they reach the apex and *vice versa*.

The overall functioning (pumping action) of the left ventricle depends strongly on the normal rhythmic contraction and relaxation of these longitudinal and circumferential fibres in systole and diastole respectively (Fatenkov *et al*, 1991). As the apex of the

heart remains relatively stationary, long axis changes in particular are reflected in alternating movement of the base of the heart.

3.2   Long axis contraction of the fibres of the ventricles

Several studies have shown that left ventricular contraction involves both a reduction of the short axis diameter and a shortening along the longitudinal axis (Alam *et al*, 1990; Alam, 1991; Alam *et al*, 1992).

In fact this description of ventricular motion is not new but goes back to an observation by Leonardo da Vinci who obtained information about the action of the heart by studying the hearts of slaughtered pigs. He observed that the greatest movement in the long axis is approximately the thickness of a finger (Keele, 1983).

In 1932 Hamilton & Rompf stressed the importance of long axis contractions in systole in the left ventricle and concluded that the major pumping action by this ventricle is correlated closely with the caudo-cephalad movement of the atrioventricular septum (Hamilton *et al*, 1932). The mitral ring which forms the base of the ventricle moves towards the apex during systole to reduce the axial length of the ventricle, and away from the apex during diastole to stretch the axial length. This movement in turn ensures the reciprocal action of the two sets of chambers on each side of the heart. Thus the left atrium fills during left ventricular systole, and then during left ventricular diastole the left ventricle fills at the expense of a reduction in the volume of the cavity of the left atrium. This mechanism is represented in Figure 3.2. These dynamic processes occur within an essentially constant outer envelope,

with the overall left ventricular volume (blood cavity plus ventricular walls) and hence the outer contour of each ventricle remaining essentially constant throughout the cardiac cycle.

In contradiction to the mechanism of action advanced by Hamilton & Rompf, Gauer *et al* (1955) concluded from animal studies and from a study of x-ray fluoroscopic ventriculograms in human beings that heart volume does change during the cardiac cycle.

This conflict was not resolved until 1985 when Hoffman & Ritman, using multi-slice computerised tomography, observed that the epicardial apex of the heart remains relatively stationary while the atrioventricular groove moves towards the apex during systole and away from it in diastole (Hoffman *et al*, 1985). They concluded that the atria and ventricles empty and fill reciprocally.

Based on the unchanged mitral orifice area the basal portion of the left ventricle can be regarded as a cylinder with constant diameter, but which changes in length during the heart cycle between systole and diastole. Assuming that the overall volume of the ventricular wall remains constant between diastole and systole, the change in volume of the cylinder between diastole and systole corresponds to the change in blood volume in the ventricle between diastole and systole, i.e. the stroke volume. This model is shown in Figure 3.3. An unchanged outer contour of the ventricle means that the thickening of the wall, caused by long axis shortening, brings an inward movement of the endocardial part of the wall, but not an outward movement of the epicardial part of the wall.

Lundback (1986) carried out comprehensive studies to assess the validity of the simplified Hoffman & Ritman model shown in Figure 3.3, and found an average outer diameter of the left ventricle, 2 to 3 cm below the base of the ventricle, of 68 mm in young healthy subjects. The change in diameter during the heart cycle was on average less then 2 mm, and diminished in the apical direction. In the same study, the excursion or maximum movement of the mitral ring in the left atrioventricular groove was 19 to 22 mm, and he concluded that this finding implied that the ventricular volume shrinks in systole by an almost cylindrical segment 19 to 22 mm in height and 68 mm in diameter. This cylindrical segment corresponds to a volume of 69 to 80 cm^3, which coincides with the range of values for stroke volume found in normal healthy subjects.

It should be noted that this mechanism of ventricular filling and emptying tends to maximise the fraction of the mechanical work of the heart that is directed to pumping the blood and to minimise the fraction used to move the myocardial tissues.

This motion of the mitral ring has been further illustrated in studies that included echocardiography, gated thallium scintigraphy, and coronary cineangiography (Simonson et al, 1989; Pai et al, 1991; Alam et al, 1992). All of these studies confirmed the mode of ventricular pumping presented earlier by Hoffman & Ritman and indicated much earlier by Leonardo Da Vinci. This concept of the mode of ventricular filling and emptying forms the starting point for the work reported in this thesis.

3.3   Mitral ring motion indicative of long axis shortening ?

Studies have shown the apical part of the septum during systole to be almost

stationary compared to the motion of the mitral ring (Hamilton *et al*, 1932; Turrent,

1973). From these studies one may deduce that the mitral ring motion largely reflects

the periodic shortening and lengthening of the long axis of the left ventricle,

measured from the atrioventricular plane to the epicardial part of the apex.

Consequently insights into left ventricular systolic function may be obtained by

studying mitral ring motion, as has been shown in patients with severe left ventricular

dysfunction. One of the challenges is to develop diagnostic measures to detect earlier

stages of dysfunction.

Chapter 5 of this thesis presents a pilot study that examines the potential of a number

of measures derived from DTI for such diagnosis, in systole and diastole.

Diastole begins with the relaxation of the myocardial contraction underpinning

systole. Measurement of the maximal longitudinal relaxation velocity of the mitral

ring during early diastole has been suggested as a means of assessing left ventricular

diastolic function (Greenbaum *et al*, 1981; Galiuto *et al*, 1998; Nagueh *et al*, 2001).

In other studies total ring motion was closely connected to other important indices of

left ventricular function in systole, such as ejection fraction (Simonson *et al*, 1989;

Pai *et al*, 1991; Wandt *et al*, 1999). The linear correlation between mitral ring motion

(displacement or change in position) and ejection fraction (change in volume) was

found to be unexpectedly strong. This conclusion gives support to the model of unchanged outer contour during the cardiac cycle, illustrated in Figure 3.3.

In patients with left ventricular hypertrophy, while ejection fraction is preserved, long axis contraction is found to be impaired and mitral ring motion reduced (Nagueh *et al*, 1999; Wandt *et al*, 1999). In such patients therefore, mitral ring motion may well be a better marker of systolic function than ejection fraction. Besides due to changes associated with ageing, heart size and dimensions, body size, gender, etc, in order to translate mitral ring motion to ejection fraction it is necessary to have established reference values available for patients of different ages, body sizes, genders, etc. (Wandt *et al*, 1997). Such look-up tables have not yet been established.

3.4   The contraction and relaxation of the circumferential fibres

The contraction of the largely circumferential fibres after the QRS wave and during systole does not *per se* produce inward radial movement of the ventricular walls, but rather a torsion or twisting of the ventricle. Viewed from the apex of the heart, this systolic twisting is clockwise at the mitral ring at the base and anti-clockwise at the apex (Streeter *et al*, 1973; Maier *et al*, 1992; Nagel *et al*, 2000). This winding or screwing action of the ventricle as if it were a coiled spring works in tandem with the longitudinal fibres to contribute to the long-axis shortening movement of the ventricle and the consequential emptying of the ventricle. Thus the ventricle has essentially a 'belt and braces' mechanism of contraction. The combination of the two contractions and the accompanying torsion gives rise to a thickening inwards of the ventricular wall and a reduction of the cross-sectional area of the ventricular cavity.

Ventricular pumping therefore results from the long-axis shortening of the ventricular wall and hence of the ventricular cavity, as well as the wall thickening which reduces the cross-sectional area of the blood-filled cavity.

After systole, these both sets of fibres relax, leading to the relaxation of the twist and the recoil of the spiral spring of the ventricular myocardium. This unwinding action contributes to the early diastolic movement of the mitral ring and the lengthening widening of the ventricular cavity. The early diastolic movement of the mitral ring is indicative of the unwinding recoil action of the ventricular wall. In unwinding in this way it creates a pressure gradient across the closed mitral valve, tending to open the valve and draw the blood into the ventricle from the atrium. It produces a rapid augmented filling of the ventricle after mitral valve opening in the normal heart under the influence of preload (Radamakers *et al*, 1992) in advance of atrial systole. This array of phenomena, early diastolic unwinding, mitral valve opening and initial rapid transmitral blood flow, is referred to as the early diastolic mechanism. The work reported in Chapters 5, 6 and 7 of this thesis provides important new evidence that the relative timing of these dynamic activities in the heart using echocardiographic techniques including DTI, can readily reveal valuable diagnostic information about the heart. Furthermore, understanding this early diastolic mechanism helps with the interpretation of the echocardiographic findings.

3.4.1   Early diastolic mechanism

Rademakers *et al* (1992) showed that elastic recoil has a role in left ventricular filling and untwisting occurs principally during the isovolumic period before filling. The relaxation recoil of the systolic deformation was shown to be independent of filling in the canine heart. The potential energy that causes rapid ventricular suction is proportional to the amount of the initial untwisting or unwinding, the majority of which takes place during the isovolumic period before the valve opens. The findings of Rodriguez *et al* (1996) support the concept of this early diastolic mechanism, which exists when the peak mitral ring velocity precedes the peak transmitral blood flow. This mechanism, with its critically timed phases, is disrupted or lost in patients with significant left ventricular hypertrophy and in such cases the patient is deprived of efficient early diastolic filling which is essential for efficient cardiac function. This proposition is examined in the work described in Chapter 6 of this thesis.

3.4.2   Relevance of fibre orientation to early diastolic filling

The twisting motion of the heart is believed to be consequent to the arrangement of the muscle fibers. Conceptually, the heart has been treated mainly as a pressure chamber. The rotary or twisting motion of the heart has been poorly understood by the scientists and has lacked clinical relevance. The counter-clockwise torsion (when viewed from the base of the ventricle) that occurs during ventricular contraction is in the direction of the epicardial fibres (Streeter *et al*, 1973). Buchhalter *et al* (1994) used magnetic resonance imaging to show that the mean angle of torsion in the apical

slice relative to the mean angle in the basilar slice in the endocardium was 19.1° ± 2.0° counterclockwise when viewed from the apex.

It has also been proposed that epicardial contraction dominates the direction of torsion because these epicardial fibres are at larger radii and produce greater torque than those fibres in the mid-layer of the myocardium (Streeter *et al*, 1973; Turrent, 1973). The epicardial fibres relax and begin to lengthen along their circumferential fibre direction during the isovolumic period. This therefore dominates the direction of untwisting as the epicardium begins to move outwards as it unwinds. The early diastolic filling and its extent therefore are related to relaxation or torsion reversal. The most of the torsion reversal normally has occurred by the time of mitral valve opening and this movement releases potential energy in the form of a negative transmural pressure creating the atrioventricular pressure gradient for early diastolic filling as part of the early diastolic mechanism (Hammerstrom *et al*, 1991).

3.5   Ischaemic heart disease and ventricular function

Ischaemia damages regions of the myocardium. The location and extent of the damage determine the degree of infarction and consequent dysfunction and impairment to the ventricular function.

3.5.1   Assessment of regional left ventricular function with ultrasound

2-D echocardiography employs a planar fan of ultrasound beams and this fan 'slices' the heart to obtain an image of the anatomical cross-section or plane to be examined.

Regional left ventricular (LV) function is most commonly assessed by real-time

visual examination of the heart in several two-dimensional planes. In this way,

echocardiographers can identify and subjectively assess the extent of myocardial

dysfunction. However, such a qualitative method lacks objectivity and the observer,

however experienced, may overlook subtle abnormalities when confronted with more

obvious findings. Recognising these failings, the American Society of

Echocardiography has devised a more systematic approach where the left ventricular

wall is divided into sixteen segments corresponding to coronary artery anatomy

(Henry *et al*, 1980). Each segment is individually examined using 2-D

echocardiography and is subjectively assigned a score on the scale of 0 to 5,

indicating the extent of segmental wall thickening. Although this semi-quantitative

method forces the echocardiographer to examine the ventricle in its entirety, it

remains subjective. Because it is involved, it is generally used for experimental

purposes only. It has however been shown that patients with poor acoustic windows,

chest wall deformities or who are obese may not be ideal subjects for 16-segment

analysis due to suboptimal endocardial visualisation. Recent studies indicate that

tissue harmonic imaging provides the potential for evaluating previously suboptimal

endocardial definition. (DeCara & Lang, 2003)

3.5.2   Diagnostic information from the mitral ring movement

During the late nineteen eighties and the nineteen nineties many echocardiographic

studies were performed on mitral ring movement and a marked interest in the method

developed after it was shown that it could be used for the assessment of left

ventricular function (McDonald, 1970; Höglund *et al*, 1988; Alam *et al*, 1990; Alam, 1991; Alam *et al*, 1992).

In this approach, M-mode recordings were taken from four sites on the mitral ring, situated about 90° apart as shown in Figure 3.4, according to the method introduced by Höglund *et al* (1988). Ring motion as recorded by M-mode echocardiography had good reproducibility in studies by Höglund *et al* (1988), Hammarstrom *et al* (1991) and Alam *et al* (1992).

Previous research indicated that mitral ring descent reflects the pumping ability of the left ventricle as a whole. Höglund *et al* (1988) measured the magnitude of atrioventricular plane displacement during ventricular systole in healthy subjects of different ages. Using M-mode echocardiography, they measured the displacement at four specific sites on the ring as described above in Figure 3.4. The mean displacement was comparable to that found by Zaky *et al* (1967), amounting to 16 mm ± 2 mm, but was found to decrease significantly with increasing age. Since myocardial contractility decreases with age, this result supports the conclusion that mitral ring displacement reflects left ventricular function.

3.5.3   *Comparison of echocardiographic measurements of ejection fraction and its measurement by radionuclide imaging*

Pai *et al* (1991) measured the left ventricular ejection fraction using radionuclide ventriculography and compared these measurements with those from a variety of echocardiographic techniques. This method correlated well with all other ultrasound

methods used and showed a strong linear correlation with the excursion of the mitral ring during systole. Further supporting evidence was provided by Alam *et al* (1990), who examined the ring descent at the same four sites in patients with severe congestive heart failure following dilated cardiomyopathy or myocardial infarction. They reported a good correlation between mean ring descent and left ventricular ejection fraction measured using radionuclide angiography. In addition, an ejection fraction less than 30 %, generally regarded as severely depressed, corresponded to a mean ring displacement of less than 7 mm.

Jensen-Urstad *et al* (1998) also measured left ventricular ejection fraction using radionuclide imaging and atrioventricular plane displacement in ninety-six patients, 70 men and 26 women, with acute myocardial infarction. A positive correlation between these two variables was demonstrated with r = .64, for atrioventricular plane displacement, and r = 0.72, for radionuclide angiography. The velocity of the mitral ring in its periodic displacement has also been investigated with respect to global cardiac function, indicated by ejection fraction.

Gulati and colleagues (1996) measured the velocity of descent at six sites on the mitral ring using colour Doppler tissue imaging, and compared the mean descent velocity with the left ventricular ejection fraction as measured by radionuclide techniques. A strongly positive linear correlation (r = 0.70) was found, extending over a large range of values of ejection fraction. In addition, a peak mitral ring descent velocity average greater than 5.4 cm/s was indicative of an ejection fraction greater than 50%.

As previously mentioned, Fukuda *et al* (1998) studied peak mitral ring descent velocity (Sw) at six sites on the ring, and the time taken to reach peak velocity (Q-Sw) in patients with previous myocardial infarction. These parameters were then compared with global function expressed as ejection fraction. A significant positive correlation ($r = 0.86$) was found to exist between ejection fraction and the mean Sw of all six ring sites. A poor negative correlation ($r = - 0.01$) between ejection fraction and the mean Q-Sw of all sites was also found. However, stronger correlation was found between the left ventricular ejection fraction and the mean parameters of sites corresponding to infarcted regions. For instance, when the mean Sw and mean Q-Sw at the mitral sites corresponding to the infarct regions, were higher than 7.6 cm/s and shorter than 200 ms respectively, ejection fraction could be accurately predicted to be greater than 50% in the patient. This result differs from that of Gulati *et al* (1996). However, Gulati's study included a range of disease conditions other than ischaemic heart disease. Furthermore, the mean peak systolic descent velocity of all six ring sites was used whereas Fukuda and colleagues used the mean velocity of sites corresponding to infarcted regions only, and this correlated more closely with ejection fraction in their study. It has been shown that mitral ring motion is related to age, height and heart rate (Wandt *et al*, 1997). Consequently reference values for mitral ring motion should be calculated.

3.5.4   Ejection fraction as a function of mitral ring movement

A number of these early studies (Simonson, 1989; Alam *et al*, 1990; Alam, 1991; Pai *et al*, 1991; Alam *et al*, 1992) did yield approximate empirical relationships between the ejection fraction (EF) independently measured by a reference or standard

technique, and the mitral ring movement (MRM) measured echocardiographically, of the following form,

EF = a (MRM) + c

where **a** and **c** are constants. Table 3.1 summarises the outcomes of these studies and the different values of the two constants found for normal individuals and patients with various cardiac dysfunctions. The values of the two constants in the various disease conditions investigated would appear to differ to varying degrees from the normal.

In addition patients with hypertension or hypertrophic cardiomyopathy have thickened walls with decreased mitral ring motion despite a sustained ejection fraction (Gulati *et al*, 1996: Zaky *et al*, 1967). These limitations have led to studies relating overall systolic and diastolic left ventricular function to mitral ring velocities obtained by DTI (Hammarstrom *et al*, 1991; Rademakers *et al*, 1992).
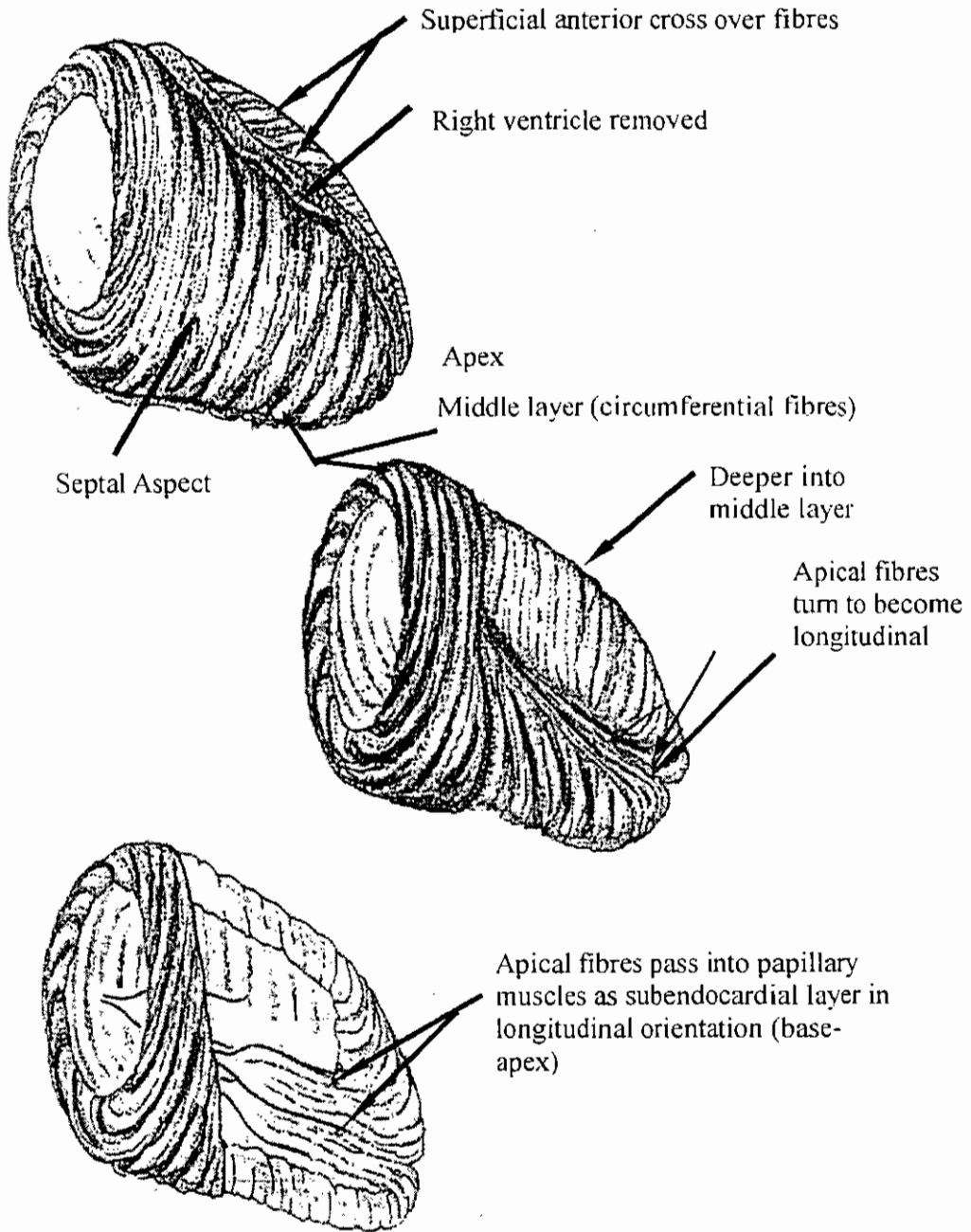
Figure 3.1   **Anatomical arrangement of myocardial fibres**
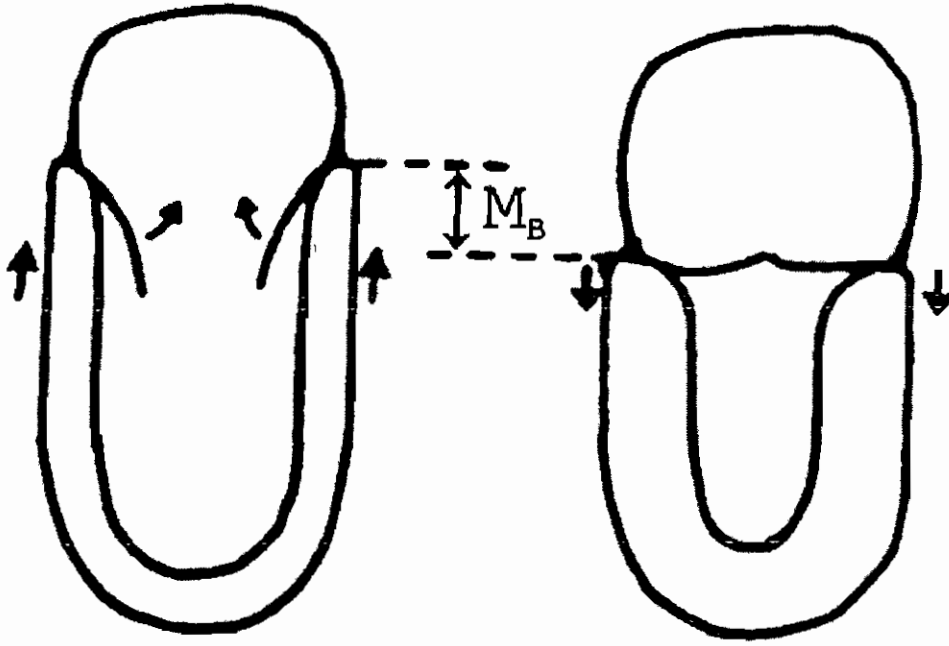
Figure 3.2   Schematic figure of the description by Hamilton & Rompf of the

heart pumping, which illustrates constant volume, movement of

the base toward and away from the apex by an amount Mb, and

reciprocal filling of each ventricle and atrium

Total volume of the left ventricle (including walls and blood)

Diastole

Systole

$Vol_c = \pi \times r^2 \times \ell$

Invariable outer diameter:

$\pi \cdot r^2$ is constant

$\Delta Vol_c = \text{constant} \times \Delta \ell$

↕ **Mitral ring motion**

ℓ

Volume change during the heart cycle = stroke volume
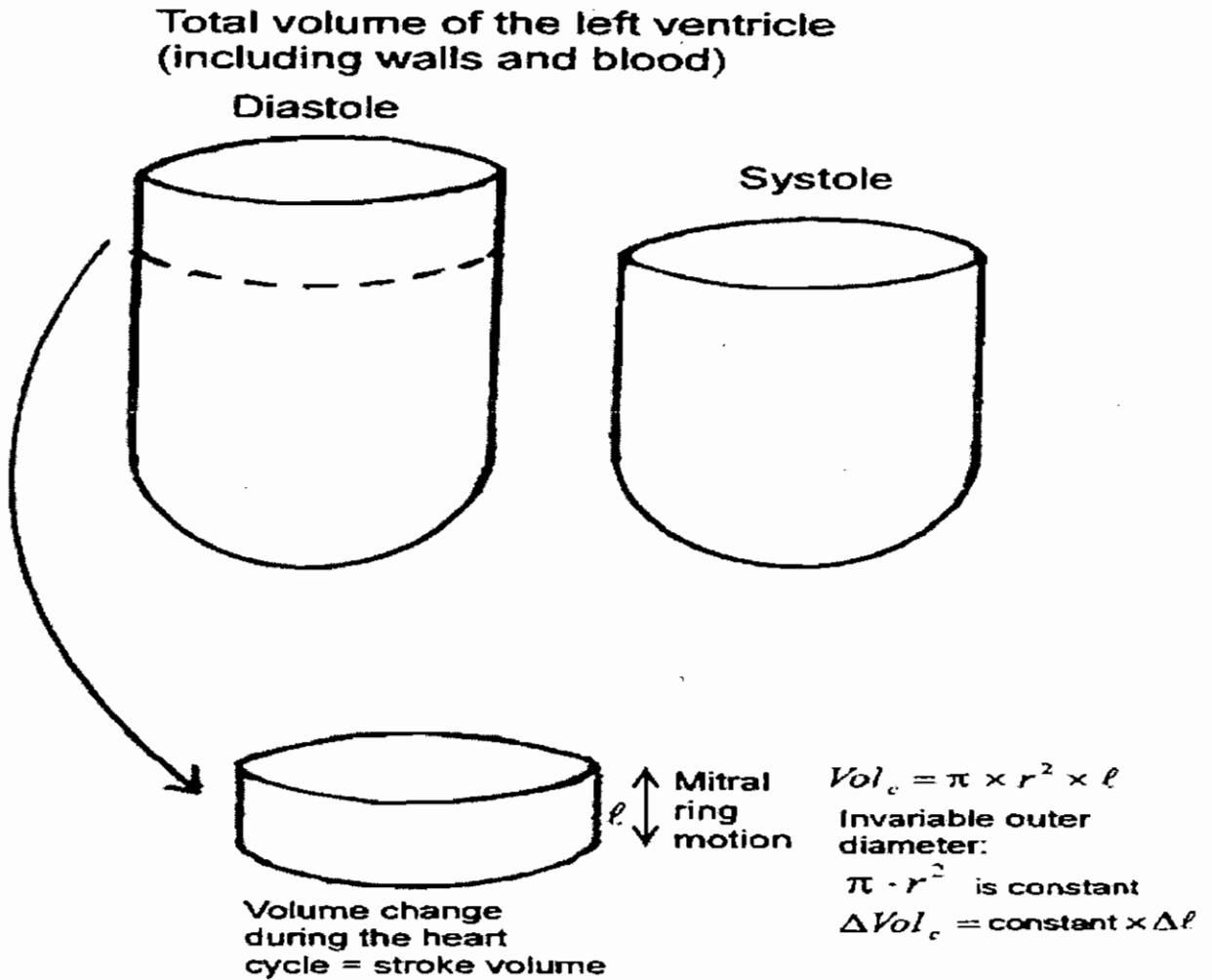
Figure 3.3   **A schematic drawing of the linear relation between ventricular length and volume, according to the model of unchanged outer diameter of the ventricle during the heart cycle described by Hamilton & Rompf, Hoffman & Ritman, Lundback and others.**
[Here Vol_c is the volume of the cylinder, l its length and r its radius]

septal | lateral   posterior | anterior

4-chamber view   2-chamber view
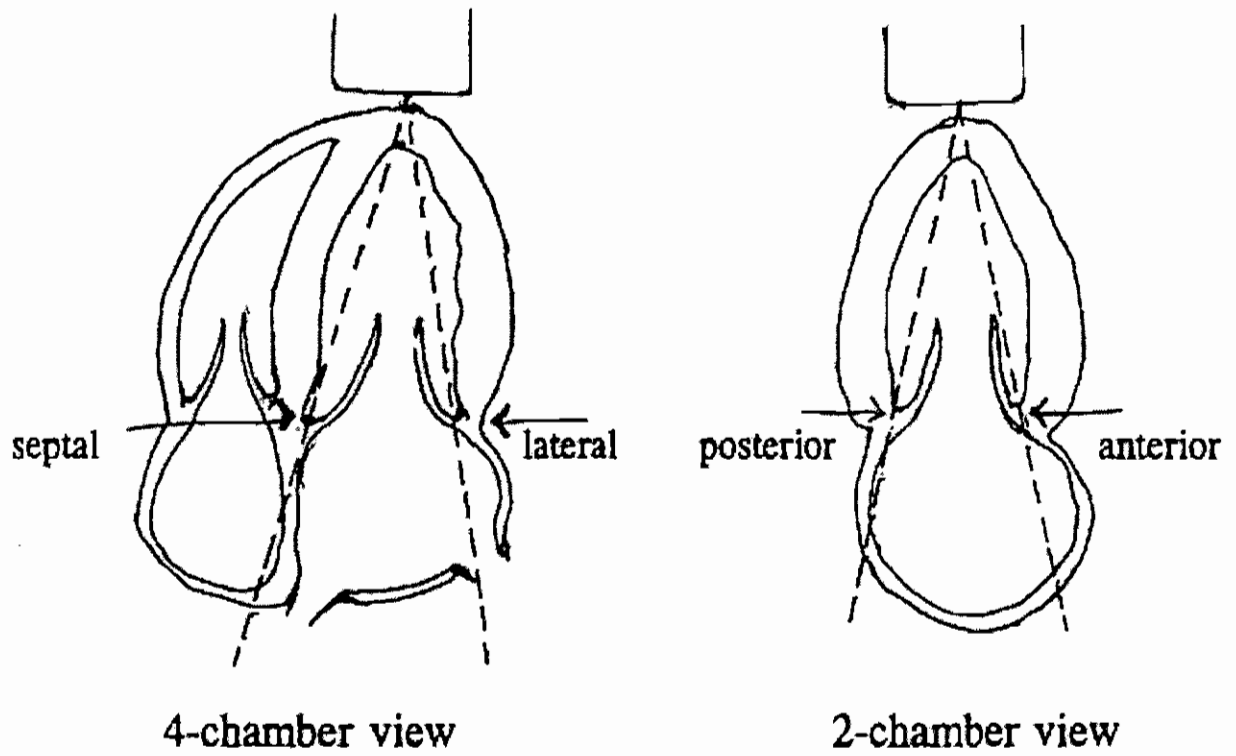
Figure 3.4   Schematic illustration of the four sites on the mitral ring, where measurements are obtained for calculation of mitral ring motion

Table 3.1   Correlations between different echocardiographically measured mitral ring movement (MRM) and ejection fraction (EF)

Study	Echocardiographic Method	Method for investigation of ejection fraction	Study population	Equation of regression line EF vs MRM (%) (mm)	Correlation Coefficient	SEE (EF)
Simonson *et al* (1989)	2-D measurements from 2- and 4-chamber views	2-D echocardiographic volume measurements	Healthy volunteers (n=26), patients with different heart diseases (n=74)	2-chamber view EF=3.8 x MRM + 21 4-chamber view EF=4.1x MRM + 17	r = 0.78 r = 0.84	0.14 0.12
Alam *et al* (1990)	Apical M-mode from 2- and 4-chamber views (4 sites)	Radionuclide angiography	Patients with chronic congestive heart failure (n=30)	EF=5.0 x MRM - 5.6	r = 0.82	--
Pai *et al* (1991)	2-D measurements from lateral and septal sites from 4-chamber apical view	Radionuclide angiography	Consecutive patients referred for both echocardiography and radionuclide angiography (n=57)	EF = 4.4 x MRM + 1.5	r = 0.95	0.059
Alam *et al* (1991)	Apical M-mode from 2-and 4-chamber views (4 sites)	Radionuclide angiography	Patients 2-10 days after first-time acute myocardial infarction (n=37)	EF = 5.5 x MRM – 5	r = 0.87	0.062
Alam *et al* (1992)	Apical M-mode from 2- and 4-chamber views (4 sites)	Biplane left ventricular	Patients with coronary artery disease (n = 106)	EF = 4.4 x MRM + 11.5	r = 0.89	0.064

Chapter 4

The developing clinical applications of DTI

The technical principles underpinning DTI were outlined in chapter 2. This relatively new mode of diagnostic ultrasound was developed as an extension of colour flow Doppler and has been applied mainly in cardiology, to study and measure the movements of cardiac structures, including the relative movements of intra-myocardial structures. A number of these clinical applications are introduced in this chapter to provide an additional backdrop to the main work reported in this thesis.

4.1 DTI applied to study myocardial movements

It is understood that the motions of the myocardium and its substructures, their magnitudes, directions and velocities, are strongly indicative of the function and viability of the myocardium (Galiuto *et al*, 1998). Consequently, attempts to quantitatively measure global and regional left ventricular function using DTI have focused directly on ventricular wall motion.

4.1.1 Performance of DTI compared to that of M-mode echocardiography

The pulsed ultrasound DTI system was originally developed by Karl Isaaz and his colleagues (Isaaz *et al*, 1989; Isaaz *et al*, 1994; Isaaz, 2000) to measure the velocity of the left ventricular posterior wall. In order to assess the validity of the technique,

DTI-measured posterior wall velocities were compared with analogous M-mode measurements. A good correlation between the two sets of data was observed by Isaaz and colleagues.

The value of DTI measurement of tissue velocity was further endorsed by Garcia *et al* (1996), who compared DTI-measured velocities with velocities obtained from highly accurate, off-line, digitised M-mode echocardiography. This work showed that DTI has several advantages over M-mode echocardiography in the assessment of myocardial velocity. One is the capacity to measure velocity at multiple levels within the myocardium without being limited to the endocardial surface. A second advantage is the time resolution possible with DTI ($\pm$ 5 ms) which provides the capacity to measure instantaneous spectral velocity at any stage in the cardiac cycle. A third is the capacity to assess the ring motion on-line rapidly, whereas digitised M-mode analysis must be performed off-line and is time-consuming. To validate the use of pulsed DTI that measures wall velocities and to define the characteristics of these velocities in normal subjects Garcia *et al* (1996) compared the anteroseptal and posterior wall velocities in 24 volunteers using pulsed DTI and digitised M-mode echocardiography. There was a good correlation between DTI and M-mode derived velocities ($r = 0.95$, $p < 0.001$), with higher reproducibility for DTI ($r = 0.99$). Garcia *et al* concluded that wall velocities obtained by pulsed DTI are accurate and reproducible.

4.1.2   Characteristic DTI record for posterior wall of the left ventricle

In 1989, Isaaz *et al* described a normal pattern of DTI velocities in the left ventricular posterior wall. Three dominant waves, a negative, early diastolic wave (E-wave), a late diastolic wave (A-wave), and a positive systolic wave (S-wave), were described, as shown in Figure 5.1. This pattern was confirmed by Severino *et al* (1998) and described in detail by García-Fernández *et al* (1999).

Accordingly, the early diastolic E-wave is observed shortly after the T wave of the electrocardiogram (ECG) and is associated with the rapid filling phase after the opening of the mitral valve. There ensues a phase with no appreciable wall motion which corresponds to diastasis. The late diastolic A-wave follows the P wave of the ECG and is due to late myocardial relaxation after mechanical contraction of the left atrium. Finally, the systolic S-wave corresponds to ventricular ejection and follows the QRS complex of the ECG, which initiates and signals ventricular depolarisation and then contraction.

4.1.3   Alteration of DTI record for case of damaged myocardium

In areas of damaged myocardium, this normal profile is disturbed. Using DTI, Isaaz *et al* (1989) measured the longitudinal velocity of the left ventricular posterior wall in control subjects and in patients with coronary artery disease, in an attempt to identify and characterise any regional dysfunction. The peak systolic velocity was greater than or equal to 7.5 cm/s in all control subjects and in patients with normal left ventricular posterior wall motion. However, in ten out of twelve patients with

56

posterior dysfunction, the peak systolic velocity was less than 7.5 cm/s, an indicator

of abnormal left ventricular wall motion with a sensitivity of 83%, a specificity of

100% and an accuracy of 95%. Wall motion abnormalities during diastole were also

notable within this patient group. All patients had lower peak E-wave velocity than

the healthy controls and a higher peak A-wave velocity. Those patients with

abnormal left ventricular posterior wall motion exhibited the most severe decreases in

peak E-wave velocity but only slight increases in peak A-wave velocity.

A similar, but more extensive, study by García-Fernández *et al* (1999) showed that

regional diastolic wall motion is impaired at baseline in infarcted myocardial

segments, even when systolic contraction is preserved. In this study, the myocardium

was divided into sixteen segments according to the anatomy of the coronary

circulation. DTl was then performed in each of these segments in both healthy

controls and in 43 patients with infarctions consequent on ischaemic heart disease. In

diseased wall regions within the patient group, the mean peak early diastolic velocity

and the E/A diastolic velocity ratio were reduced, indicating abnormal myocardial

relaxation in those areas. In addition, the regional isovolumic time, defined as the

time interval from the high-pitched second heart sound (produced by the closing of

the aortic and pulmonic valves at the end of ventricular systole) to the onset of the E

wave, was prolonged. No differences were observed in any of these parameters

between the normally perfused segments of ischaemic patients and the corresponding

segments of the control group. These results suggest that by measuring myocardial

velocities, DTl can be used to assess regional left ventricular function.

4.2   DTI used to measure longitudinal intra-myocardial movements at different sites across the posterior wall as an another indicator of myocardial viability

Fleming and coworkers (1994) used a scanner whose colour Doppler mode was adapted to display tissue motion (instead of blood flow), and they presented the concept of velocity gradients, detected across the myocardial thickness. This velocity gradient is a gradual spatial change in the value of velocity estimates and has the potential for indicating regional myocardial contractility. Fleming and coworkers showed that velocity gradients are consistant with wall thickness changes, strongly suggesting that these gradients have potential for the assessment of myocardial contractility.. In this study colour DTI was used as described by McDicken *et al* (1992). This mode of display superimposes a colour-coded representation of velocity onto an M-mode (time-motion) trace or a 2-D real-time image. The relationship between these wall thickness changes as measured by M-mode echocardiography and the velocity gradients of the left ventricular posterior wall was explored in this study. A good qualitative agreement was reported, indicating again that DTI velocity gradients can be used to express left ventricular regional function.

The existence of transmyocardial longitudinal velocity gradients was confirmed by Donovan *et al* (1995), who characterised the normal velocities of the endocardium, mid-myocardium and epicardium, in the anteroseptal and inferoposterior walls. This study also validated colour DTI in measuring myocardial velocity, by comparing maximal systolic velocities determined using this method with those found by M-mode echocardiography. An 'excellent correlation' was found to exist between the

two sets of results, implying that colour DTI is a reliable method with which to

quantify regional myocardial velocities.

4.3   Use of DTI in mapping and quantifying regional left ventricular dysfunction

Garot *et al* (1999) carried out a study aimed at determining whether velocity gradients

assessed quantitatively by M-mode or colour DTI could reliably indicate regional left

ventricular dysfunction after acute myocardial infarction. Peak endocardial and

epicardial excursion velocities in the left ventricular posterior and anteroseptal walls

were recorded in patient and control groups. It was found that both systolic and

diastolic transmyocardial velocity gradients were consistently lower in the recently

infracted myocardial walls compared with corresponding segments in the normal,

control group. In addition, compensatory hyperkinesis of wall regions some distance

from the infarcted area was indicated by increased systolic and diastolic velocity

gradients. These results suggest that DTI, by measuring systolic and diastolic velocity

gradients, has the potential to quantitatively assess segmental left ventricular function,

identifying both infarct areas and regions of compensatory kinetics.

4.4   Limitations of DTI in cardiology due to limited acoustic windows

Direct DTI of the myocardium has revealed several parameters of systolic and

diastolic ventricular motion that reportedly reflect regional myocardial contractility

and viability. Despite this seeming success however, this approach has some

disadvantages. According to the Doppler equation, the Doppler shift is directly

proportional to the cosine of the intercept angle, θ, between the direction of the ultrasound beam and the direction of the interface motion. When $\theta = 0°$ and the direction of the ultrasound beam and that of the motion of the interface are identical, the cosine of $0°$ is 1 and the Doppler shift recorded is the maximum possible. The cosine of $90°$ is 0 and so there is no Doppler shift recorded if the ultrasound beam is perpendicular to the direction of interface motion. Because of this angle-dependence, optimum positioning of the ultrasound beam, as close to parallel to the movement of the structure being examined as possible, is essential. For example, a beam position at $0 \pm 25°$ to the motion of the structure can give an error of $\pm 10\%$.

In addition, the ribs and lungs shelter the heart and obstruct the ultrasound beam, severely limiting the number of echocardiographic windows available. The combination of these factors reduces the number of ventricular walls to which the beam has diagnostically useful access, and therefore, the number of walls that can be imaged. This is a considerable drawback when attempting to assess regional function across the heart. The accuracy of direct imaging of the myocardium has also been questioned. To obtain an optimal Doppler signal and consequently, an accurate velocity measurement, the ultrasound beam must be parallel to the direction of myocardial motion. However, due to the anatomical arrangement of the myocardial fibres, left ventricular wall motion is complex and multidirectional.

Furthermore, the heart is rotated, contorted, and displaced as a whole during the cardiac cycle and this may cause the region of interest to move out of the sample volume. Since the transducer is positioned on the chest rather than the heart wall, these movements can introduce an amount of error.

4.5 Extraction of full diagnostic information from the motion of the mitral ring

Because of these limitations, a more indirect approach has been proposed based on the excursion of the mitral ring during the cardiac cycle. The mitral ring is one of four inter-linked rings of dense connective tissue that form the scaffolding upon which the myocardial mass is based. In 1967 using M-mode ultrasound, Zaky *et al* (1967) investigated the movement of the mitral ring during the cardiac cycle and found it to be 'remarkably constant' in 25 normal subjects. Specifically during ventricular systole, the ring was found to descend towards the apex of the heart. In this study, the total displacement amounted to 16 mm ± 4. Since the cardiac apex does not move significantly, this 'pulling down' of the ring towards the apex has been attributed to the contraction of longitudinally orientated fibres in the myocardium between the subendocardial and subepicardial layers of the ventricular wall, together with contraction of the papillary muscles (Höglund *et al*, 1988; Jones *et al*, 1990; Pai *et al*, 1991; Rodriguez *et al*, 1996).

4.5.1 Mitral ring displacement and performance of longitudinal fibres in the left ventricular myocardium

Suggestions that the descent of the mitral ring is due to haemodynamic factors rather than contraction and shortening of the left ventricle have been disproved (Keren *et al*, 1988). It has therefore been proposed that mitral ring displacement is an expression and index of the systolic performance of the left ventricular longitudinal fibres. Such

an index might be particularly pertinent in cases of ischaemic heart disease.

According to Jones and his colleagues (1990), non-uniformity of fibre orientation

results in non-uniform susceptibility of the various layers to injury. They cite

previous necropsy studies in patients with coronary disease, which showed that the

longitudinal fibres of the subendocardium are most vulnerable to ischaemic damage.

Subendocardial dysfunction is likely to manifest itself as abnormal long axis

shortening, reflected in the movements of the mitral ring.

Höglund *et al* (1988) described the magnitude of the atrioventricular plane

(containing the mitral ring) displacement during ventricular systole in healthy subjects

of different ages. Using M-mode echocardiography, they measured the displacement

at four specific sites on the ring, corresponding to the anterior, septal, posterior, and

lateral parts of the left ventricular wall. Previous reports of a significant ring descent

towards the apex during ventricular systole were confirmed in this study. The mean

displacement was comparable to that found by Zaky *et al* (1967), amounting to 16

mm ± 2, but was found to decrease significantly with increasing age. Since

myocardial contractility decreases with age, this result supports the assertion that

mitral ring displacement reflects left ventricular function. Further supporting

evidence was provided by Alam *et al* (1990), who examined ring descent at the same

four sites in patients with severe congestive heart failure following dilated

cardiomyopathy or myocardial infarction. They found a significant generalized

reduction in atrioventricular plane displacement in these patients compared with the

age-matched control group (5.6 mm vs. 14.5 mm), which they maintained reflects the

overall reduction in left ventricular contractility associated with this dilated

cardiomyopathy.

4.5.2   Mitral ring displacement and localised cardiac ischaemia in the left ventricular myocardium

As mentioned previously, ischaemic damage to the myocardium impairs the mechanical contraction of myocardial fibres, especially those longitudinally orientated, and this in turn decreases mitral ring displacement. It is possible that regional left ventricular dysfunction, as occurs in ischaemic heart disease, affects the descent of a specific area of the mitral ring. This would then represent a potential method of indicating and even identifying dysfunctional regions in segmental diseases. With this in mind, Höglund et al (1989) studied the effects of acute myocardial infarction on the extent of atrioventricular plane displacement. They determined the ring descent at four ring sites using M-mode echocardiography. In patients with anterior or posterior myocardial infarction, all four sites showed significantly decreased AV plane displacement compared to age-matched, healthy controls. Furthermore, at sites corresponding to the infarct area, the excursion of the ring was decreased compared to other sites. The authors believed the decreased displacement to be an expression of regional systolic dysfunction and felt that this method could be used to identify regional damage following myocardial infarction.

Alam et al (1991) studied the effects of exercise on the displacement of the atrioventricular plane in patients with coronary artery disease, and stable angina pectoris without prior myocardial infarction. In healthy subjects, exercise was found to significantly increase mitral ring excursion from 14.5 mm to 19.2 mm. On cessation of the test, displacement returned to the pre-exercise level. According to the

authors, this was due to the higher heart rates that accompany exercise. In order to achieve normal systolic emptying within the reduced ejection period increased rate of tension development and appropriate shortening of myocardial fibres is necessary. There is consequently an obvious need for a quantitative method of regional left ventricular assessment. Measuring the descent of the mitral ring is an attractive candidate because it can be quantified by DTI and it is less reliant on endocardial definition. In addition, because its direction of motion is virtually parallel to the Doppler beam, the accuracy of the technique is not compromised by variation of the intercept angle.

Any movement of the region of interest in and out of the sample volume could give rise to error in these measurements. Experiments have not been reported quantifying such errors. However further studies, such as multiple repetitions of these measurement on groups of subjects or patients, would be required to provide estimates of errors due to this phenomenon.

Finally, unlike previous approaches, this method can assess all areas of the left ventricle. In this study, we attempted to quantify regional left ventricular systolic dysfunction arising from coronary artery disease. The word 'regional' in this context denotes sites around the mitral ring corresponding to the positions of the posterior, posteroseptal, lateral, anterior and inferior wall of the ventricle as described by Fukuda *et* al (1998). The peak velocity of ring descent and the time taken to reach this peak velocity will be measured at six distinct sites around the circumference of the mitral ring. At sites corresponding to hypokinetic regions, it is expected that the

velocity of ring descent will be decreased and the time taken to reach this peak
velocity increased.

Post-systolic shortening is a wall motion abnormality defined as shortening of cardiac
muscle after the end of ejection and usually regarded as a manifestation of infarction
resulting from ischaemia. The amount of post-systolic shortening depends on the
volume status, which therefore has to be taken into account in interpreting regional
wall motion abnormalities, such as those detected by echocardiography and DTI.

Chapter 5

Systolic Dysfunction: DTI, 2-D Imaging and Transmitral Blood Flow Measurement by Doppler Ultrasound for Assessing Infarction Arising from Ischaemic Heart Disease

As indicated in chapters 3 and 4, cardiac ischaemia generally results from reduced

perfusion of a specific area of myocardial tissue distal to the site of coronary

obstruction and resulting in regional or segmental impairment of myocardial

contraction characteristic of the disease (Heyndrickx *et al*, 1978; Ren *et al*, 1985;

Asinger *et al*, 1988).

5.1   Assessment of left ventricular function in systole

5.1.1   Development of systolic descent of the mitral ring as an index of regional left ventricular function

Pulsed Doppler tissue imaging (DTI), detailed in chapter 2, is an echocardiographic

technique with which cardiac tissue velocities can be determined. When originally

devised, it was hoped that this technique could provide some means of quantifying

regional ventricular function. Initially, a pragmatic approach was adopted where DTI

was used to attempt to directly measure the velocity of the ventricular wall, which is

lower in diseased regions (Isaaz *et al*, 1989; Severino *et al*, 1998; Garcia-Fernandez *et

al*, 1999; Garot *et al*, 1999). Some success was reported, but ultimately, this strategy

had several fundamental failings, which disqualified it as a method of segmental

evaluation (Donovan *et al*, 1995; Garcia *et al*, 1996; Severino *et al*, 1998; Zamorano,

1998; Garcia-Fernandez *et al*, 1999; Garot *et al*, 1999). Because of these limitations,

and including the facts that in many subjects much of the myocardium falls in the

acoustic shadow of ribs and lung tissues, and there is oblique incidence of the

ultrasound beam from the available acoustic windows on many myocardial surfaces

and therefore the failure to obtain useful echoes from them, an indirect approach has

been proposed based on the excursion of the mitral ring during the cardiac cycle.

Although M-mode echocardiography has been used successfully to measure the

magnitude of mitral ring excursion, it does not reflect the motion of all ring sites and

its assessment of regional function is thus limited. Ischaemic damage to the

myocardium impairs not only the extent of its contraction but also the velocity at

which it contracts (Isaaz *et al*, 1989; Garot *et al*, 1999). This reduced velocity of

myocardial contraction should be accompanied by a reduction in the velocity of

descent of the mitral ring. DTI can be used to measure this velocity and unlike M-

mode echocardiography, can access the entire circumference of the ring (Garcia *et al*

1996).

The Doppler pattern characteristic of mitral ring motion, shown in Figure 5.1, consists

of three distinct waves (Garcia *et al*, 1996). An early diastolic wave (E-wave) is

observed shortly after the T wave of the electrocardiogram and is associated with the

rapid filling phase that follows mitral valve opening. The wall is then temporarily

static during the slow filling phase, diastasis, after which, a late diastolic wave (A-

wave) is observed. This is due to late myocardial relaxation and follows the ECG P

wave, which is associated with atrial contraction. Finally, the systolic wave (S-wave)

corresponds to ventricular ejection and follows the QRS complex, which represents

ventricular depolarisation.

Fukuda *et al* (1998) studied the relationship between the velocity of ring descent

during systole and regional left ventricular function in patients with previous

myocardial infarction. Infarct regions were identified by two-dimensional

echocardiography and coronary angiography and DTI was then performed at six sites

on the mitral ring, corresponding to the anteroseptal, posterior, posteroseptal, lateral,

anterior and inferior walls of the left ventricle as shown in Figure 5.2. An ECG trace

was recorded simultaneously. The peak systolic descent velocity (Sw) and the time

from the ECG Q wave, signalling ventricular depolarisation, to the peak of the

systolic wave (Q-Sw) were measured at each site in each subject. The mean Sw of

the sites corresponding to the infarct areas was significantly lower in the patient group

than in the controls, and the mean Q-Sw was significantly longer. Conversely, there

were no differences in either of these variables at the mitral ring sites corresponding

to the non-infarct regions between the patient and control groups. Thus regional left

ventricular dysfunction was reflected in the DTI-determined velocity of mitral ring

descent.

5.1.2   Assessment of global left ventricular function

In patients with regional wall motion abnormalties arising from ischaemia ejection

fraction (EF), as a measure of global left ventricular pumping function, is a crucial

variable in clinical decision-making and stratifies the risk of mortality after

myocardial infarction (Volpi *et al*, 1993; St. John Sutton *et al*, 1994; Naik *et al*,

1995). Ejection fraction is the percentage of the end-diastolic volume that is ejected from the left ventricle during systole and is calculated using the following equation:

EF   =   LV (end-diastolic volume) – LV (end-systolic volume) x 100%

LV (end-diastolic volume)

To solve this equation, ventricular volume at both end-diastole and at end-systole must be determined. At present, the most accurate echocardiographic method for calculating ventricular volume is based on Simpson's rule where an object is divided into parallel slices of predetermined thickness, as shown in Figure 5.3. The volume of the object is then simply the sum of the slice volumes.

Because of the limited number of echocardiographic windows, it is virtually impossible to obtain the multiple short axis images required to "slice" the ventricle as described. Consequently, the American Society of Echocardiography has recommended that a modified form of Simpson's rule be employed where the length of the ventricle is divided into a fixed number of discs from base to apex with the diameter of each disc determined in one or more apical views (Schiller *et al*, 1989; Senior *et al*, 1994; Naik *et al*, 1995; Otterstad *et al*, 1997). The end-diastolic volume is calculated from end-diastolic images and similarly, the end-systolic volume is derived from end-systolic images. For each volume, the endocardial border must be manually defined. This technique is therefore limited by a dependence on high quality images and clear ventricular endocardial definition (Schiller *et al*, 1996; Jensen-Urstad *et al*, 1998). In addition, this method assumes symmetrical ventricular shape throughout the cardiac cycle and calculations may therefore be confounded by

regional asynergy, often characteristic of ischaemic heart disease. Consequently, there is a need for a quantitative echocardiographic method of assessing global function, independent of endocardial function and of ventricular dimensions.

5.2   Aims of this pilot study

The aims of this pilot study were

1. to develop the echocardiographic scanning and data analysis/reduction procedures required to study the differences in left ventricular function in systole between a population of normal control subjects and a number of patients with infarctions arising from ischaemia.

2. to benchmark the results obtained with data and conclusions previously published in peer-reviewed publications and hence confirm the validity of the techniques and procedures used

3. to investigate measurements of mitral ring descent velocity by DTI as a means of quantitatively assessing regional left ventricular dysfunction in systole arising from ischaemic heart disease.

Global left ventricular function is generally expressed in terms of left ventricular ejection fraction, a clinical variable of diagnostic, prognostic, and therapeutic importance. Currently, the most accurate echocardiographic method of measuring ejection fraction is based upon a modified form of Simpson's rule. This method is not ideal however, for reasons previously outlined. It has been demonstrated previously that both the excursion of the mitral ring (Höglund *et al.* 1988; Alam *et al*, 1990; Pai *et al*, 1991; Jensen-Urstad *et al*, 1998) and the velocity of its descent (Gulati *et al*,

1996; Fukuda *et al*, 1998) reflect the pumping ability of the left ventricle as a whole in a variety of pathologies. The major secondary aim of this study was to investigate the relationship between ejection fraction determined by the Simpson's rule approach using 2-D images of the 4-chamber view of the heart, as an expression of global function, and the velocity of ring descent in ischaemic heart disease.

5.2.1   *Population sample*

Patients with regional wall motion abnormalties due to infarctive coronary artery disease visiting the Cardiology Department of St James's Hospital were reviewed for inclusion in the study. Any patient with one of the following conditions was not considered for the study - inadequate imaging windows, global left ventricular hypokinesis, mitral valvular disease, hypertrophic, dilated or restrictive cardiomyopathy or congestive heart failure. Over an eight-week period, twenty-two patients with heart disease and consequent regional left ventricular asynergy in systole were considered, but three patients were subsequently excluded due to poor quality echocardiographic images. One of these patients was a heavy smoker with poor acoustic windows and two were excessively obese.

The remaining nineteen fell into two groups, the first group of eight patients (7 male, 1 female, mean age 67.3 ± 7.2 years) with hypokinetic anterior LV walls (the anterior infarction group) and the second group of eleven patients (8 male, 3 female, mean age 61.7 ± 12.6 years) with hypokinesis of the inferior LV wall (the inferior infarction group). A third overall infarction group was formed by combining the above two groups. Diagnosis of ischaemic heart disease was based on a combination of typical

anginal pain, dyspnoea, electrocardiographic features, changes in cardiac enzyme profiles, angiography and regional left ventricular asynergy, as identified by 2-D echocardiography.

A normal control group of eight slightly younger volunteers (5 male, 3 female, mean age 54.3 ± 10.1 years) was selected, all with clear acoustic windows and no clinical or echocardiographic evidence of cardiovascular disease. All participants were normotensive and in normal sinus rhythm. This study was not controlled for drug administration. All treatment decisions were based solely on clinical grounds. However, the use of drugs in both patients and controls that might directly or indirectly affect cardiac function was noted. Informed consent was obtained from all participants prior to inclusion.

5.2.2   Subject assessment

Patient medical charts were reviewed retrospectively and information concerning blood pressure, age, medication administered and, in the infarction groups, the initial diagnostic criteria were retrieved and recorded. Those control subjects who were not patients at St James's Hospital were asked to complete a medical questionnaire, a copy of which is given in Appendix B. Systemic blood pressure was determined by auscultation so that hypertensive individuals could be excluded. Prior to inclusion in this study, all participants underwent a conventional echocardiographic examination to confirm diagnosis in the patient groups and rule out any cardiac abnormalities in the controls.

5.2.3   *Instrumentation*

In this study echocardiographic data were obtained using a commercially available ultrasound scanner (SONOS 2500, now Philips 2500) with two variable frequency, phased array transducers (2.5/2.0 MHz, model no. 21215 A; 3.5/2.7 MHz, model no. 21243 A). The specifications of this scanner are provided in Appendix A. The system was equipped with all major modalities, including 2-D sector scanning and steerable colour, and pulsed-wave DTI. It housed an in-built, standard Super-VHS PAL videocassette recorder (Panasonic AG-MD830) and a video graphic printer (Sony UP-890MD). Analysis functions allowed measurements to be made from VCR playback and frozen images and an 'extended physiological measurement' option facilitated ECG monitoring. Echocardiographic imaging controls were initially set at 'standard' values, as given in Table 5.1, but due to variation in size between subjects, it was necessary to adjust these during each examination in order to optimise image quality.

5.2.4   *Subject preparation*

Each subject was required to attend the echocardiographic laboratory in St James's Hospital only once in order to undergo a cardiac ultrasound scan. On arrival, subjects were asked to strip to the waist and lie supine on the examination bench. Three self-adhesive electrodes were positioned on the chest and abdomen and a lead 1 electrocardiogram (ECG) trace was established. This aided identification of cardiac events and allowed heart rate to be measured. The subject was then asked to assume a left semi-lateral decubitus position as recommended by Schiller *et al* (1996). This

position gives access to the left lateral ribs and allows ample room for transducer manoeuvring by rotating the heart out from under the sternum and expanding the left intercostal spaces. A left-handed (Mayo Clinic) examining technique was adopted (Asmi *et al*, 1995), where the examiner sits to the left of the subject and uses their left hand to hold and manipulate the transducer while operating the imaging controls with their right hand.

5.2.5   Subject positioning and apical imaging window

Because the heart lies within the ribcage, and nestled between the air-filled lungs, it is effectively shielded from the ultrasound beam. Therefore, it may only be viewed through one of a small number of echocardiographic windows through which ultrasound may travel unimpeded.

Ultrasound gel (Henley's Medical) was applied to the chest for acoustic matching with the transducer, which was positioned so as to view the heart through the apical imaging window as shown in Figure 5.4. This window is located on the anterior chest wall, over the palpable apex beat of the heart. The transducer was therefore placed between the 6th and 7th ribs, slightly lateral and inferior to the left nipple. However, because the position of the heart within the thorax varies to a small degree between individuals it was often necessary to move the transducer in a trial-and-error fashion in this vicinity in search of the apical window.

5.2.6   Apical imaging planes

Once the apical window had been located, it was possible to visualise the heart in

three standard apical two-dimensional views by altering the orientation of the

transducer. A four-chamber view was produced by directing the transducer superiorly

and medially towards the right scapula, parallel to the major axis of the heart as

shown in Figure 5.5. The ultrasound beam thus sectioned the heart from apex to base

along the septum. This allowed simultaneous visualisation of all four cardiac

chambers demarcated by the mitral and tricuspid valves, and the interatrial and

interventricular septa. In this view, the left ventricle is bounded by the lateral and

posteroseptal walls. By convention, the image was displayed with the left ventricle at

the top left hand area of the screen.

By rotating the transducer clockwise and angling it slightly anteriorly towards the

sternum, the so-called 5-Chamber view was obtained. In addition to the four

chambers, this image included the left ventricular outflow tract and the aortic root,

which represented the 'fifth' chamber displayed. In this view, the anteroseptal and

posterior/inferolateral walls of the left ventricle were visualised as shown in Figure

5.6.

Further clockwise rotation (60 ° to 90 ° from the 4-Chamber view) gave rise to the 2-

chamber view, which displayed the left atrium and left ventricle with the interposed

mitral valve, as shown in Figure 5.7. In this view, the left ventricle was bounded by

the anterior wall to the right of the image and posterior/inferior wall to the left.

These three 2-D views were used to confirm the original diagnosis of cardiac infarction and to identify any dysfunctional area, to obtain an ejection fraction for each subject by the Simpson's rule method, and to guide the Doppler cursor to specific measurement sites around the mitral ring.

5.2.7   Ejection fraction

A modified form of Simpson's rule carried out in the apical views and averaged was used to measure ejection fraction in each subject. Similar techniques have been detailed elsewhere (Senior *et al*, 1994; Naik *et al*, 1995; Schiller *et al*, 1996; Otterstad *et al*, 1997). Real-time 2-D imaging of the heart over ten cardiac cycles was recorded on S-VHS videotape for this off-line analysis.

The tape was reviewed and frozen at ventricular end-diastole. This was defined as the point at which the mitral valve leaflets were at maximal opening and the ventricular cavity was maximally dilated, and occurred near the end of the T wave of the ECG trace. Having located this end-diastolic image, the cursor was placed on the mitral ring at the base of the left ventricle and the inner contours of the left ventricle were outlined manually using the trace function of the scanner. The cursor was then positioned at the apical end of the ventricular cavity and a line perpendicular to the mitral plane was drawn to obtain the long-axis length. This allowed the internal software to section the cavity into discs of equal height and to estimate the volume of the ventricular cavity by summing the disc volumes. These data were entered into the ejection fraction analysis programme.

The imaging frame displaying the left ventricle at end-systole of the same heartbeat was then selected. This coincided with the QRS complex of the ECG and corresponded to the minimum size of the ventricular cavity prior to mitral valve opening. Again, the endocardial surface was traced, the cavity divided into discs and the volume computed as before. Using the end-diastolic and end-systolic ventricular volumes, ejection fraction was calculated according to the equation given in section 5.1.2. Values obtained were confirmed approximately by real time visual examination of left ventricular function using 2-D imaging, performed by an experienced echocardiographer. The values of ejection fraction are tabulated in Appendix C.

5.2.8   Heart rate

Heart rate was derived from the ECG trace by measuring the time interval (ms) between consecutive R waves, and dividing this value into 60,000 ms to obtain the number of cardiac cycles per minute. The results are tabulated in Appendix C.

5.2.9   Mitral ring interrogation

In each of the three apical 2-D views (4-chamber, 2-chamber, 5-chamber), pulsed Doppler sample volumes were placed on the mitral ring on either side of the valve. In this way, 2-D views were used to guide the Doppler cursor to a total of six sites around the mitral ring, corresponding to the anteroseptal, posterior, posteroseptal, lateral, anterior and inferior walls of the left ventricle as shown in Figure 5.2. Correct positioning of the cursor on the ring was aided by colour DTI of the mitral area. This

modality assigns one of a range of colours to cardiac tissue according to the velocity of tissue motion and was used to help distinguish the mitral ring from the valve leaflets and from the ventricular wall but not on the same heartbeats as the 2-D images were taken. The pulsed wave DTI mode was then engaged and the Doppler velocity pattern characteristic of mitral ring motion was visualised in real time, as shown in figure 5.1. Imaging controls were adjusted to optimise signal clarity. The image was then frozen and the peak velocity of ring descent (Sw) and the time interval from the Q wave of the ECG to the peak descent velocity (Q-Sw) were recorded at least three times for each sampling location on the mitral ring. This was repeated at each of the six ring sites in each subject. This procedure has been previously described in the literature (Gulati *et al*, 1996; Fukuda *et al*, 1998).

5.3   Data processing

Peak systolic descent velocity (Sw) and the time taken to reach this peak velocity (Q-Sw) were determined at each mitral ring site, in each subject. The data are tabulated in Appendix C. Four subject groups were established thus, the control group, the two different infarction groups, and a fourth combined overall infarction group comprising all subjects with infarctive heart disease. The mean values of the two parameters, Sw and Q-Sw, measured at each of the six ring sites, were calculated. In relation to the three infarction groups, mean values were obtained for sites corresponding both to hypokinetic ventricular regions and to non-hypokinetic regions. This was repeated for analogous sites in the control group. The effect of regional left ventricular hypokinesis due to ischaemic heart disease on mitral ring motion was then statistically assessed.

5.3.1   Statistical analysis

Values relating to subject characteristics are expressed as the mean ± the standard deviation (SD). All other values refer to the mean ± the standard error of the mean (SEM). All statistical analyses were performed using the BMDP statistical package. Groups were statistically compared using student's t test, analysis of variance (ANOVA) and Bonferroni's multiple comparisons test. Correlations between paired values were examined using Pearson's linear correlation analysis. A p value < 0.05 was considered statistically significant.

Ejection fraction was determined in each subject, as described earlier, from the 2-D apical view. The data are also tabulated in Appendix C. The relationship between ejection fraction and each of the two measured parameters of mitral ring motion, was assessed by linear correlation analysis in all four subject groups.

5.4   Subject characteristics

The physical characteristics of the four subject groups, control, anterior and inferior infarction groups and the fourth group comprising all subjects with cardiac infarction are summarised in Table 5.2. These variables were compared statistically using analysis of variance (ANOVA) and, when appropriate, Bonferroni's multiple comparisons test, using BMDP software. The groups did not differ significantly with only a small increase in the mean age of the control group and no difference in the mean heart rate. The mean left ventricular ejection fraction, however, was

significantly lower in all three infarction groups than in the control group ($p < 0.001$), an indication of compromised pumping performance in these patients. This is illustrated in Figure 5.8.

5.4.1 Mitral ring descent velocity (Sw)

Figure 5.9 shows the mean of the descent velocities (Sw) measured at sites corresponding to hypokinetic myocardial regions. In the anterior infarction group, velocities measured at site 5 in each subject were averaged while velocities obtained from site 6 were averaged in the inferior infarction group. In the overall infarction group, mean Sw was derived from measurements obtained at both site 5 and site 6. In the normal control group, Sw values obtained from analogous sites to sites 5 and 6 were averaged. Mean Sw was found to be significantly lower than control group values in both the anterior and the overall infarction groups ($p < 0.05$). A lower mean Sw relative to that of the controls was also noted in the inferior infarction group, although the difference was not statistically significant.

5.4.2 Q-Sw interval

The time interval (Q-Sw) between the Q wave of the ECG trace and the peak velocity of descent (Sw) was determined at each of the six ring sites, in each subject. The mean Q-Sw derived from sites corresponding to hypokinetic myocardial regions was calculated for each of the three infarction groups. In the control group, analogous sites were selected. The infarction groups were compared with their respective controls using the student's t test. Mean Q-Sw was fractionally greater in all three

infarction groups but differences were not statistically significant and so this parameter would appear to have only some slight promise as an indicator of infarction.

5.5   Relationship between ring motion and ejection fraction

In each subject, the means of the two parameters of ring motion, derived from all sites, sites corresponding to non-hypokinetic ventricular regions and sites corresponding to hypokinetic regions, were paired with the ejection fraction for that subject. The relationship between the two variables in each group was then assessed using Pearson's linear correlation analysis. No significant correlations between ejection fraction and mean Sw or mean Q-Sw were found in any of the subject groups. The correlation coefficients and p values are given in Appendix C   Therefore, only those graphs pertaining to regional wall motion in all the infarction subjects are included here. The remaining graphs are given in appendix C.

These graphs show that there was no statistically significant correlation found to exist between ejection fraction and mean Sw at sites corresponding to hypokinetic myocardium. Graphically, however, mean Sw appeared to be positively related to ejection fraction but no significant correlation was found. Mean Sw measured at sites corresponding to non-hypokinetic ventricular regions did not correlate significantly with ejection fraction (Appendix C).

The Q-Sw interval measured at sites corresponding to hypokinetic ventricular regions was paired in each subject with ejection fraction. The relationship between the two

was then investigated and no significant correlation emerged. This analysis was repeated for the mean Q-Sw intervals derived from all six sites and from sites corresponding to non-hypokinetic myocardium (Appendix C). Again, no significant correlations were found.

5.6   Main findings and discussion

Ischaemic heart disease is generally characterised by regional rather than global left ventricular dysfunction. At present however, no adequate means of quantifying regional function exists and in practice, regional assessment is achieved primarily by visual estimation of mobility or kinesis in dynamic 2-D images of the heart. Current echocardiographic methods of global assessment are similarly operator-dependent and, because they assume symmetrical ventricular geometry throughout the cardiac cycle, tend to be unsuitable for use in patients with regional diseases. The purpose of this study was to investigate the relationship between the velocity of mitral ring descent and both regional and global left ventricular function in patients with ischaemic heart disease. It is hoped that this approach will provide a much-needed noninvasive means of quantifying left ventricular function.

At ring sites corresponding to hypokinetic ventricular regions, mean Sw was reduced in all groups, but only significantly so in the anterior group. Conversely, mean Q-Sw was non-significantly greater in any of the infarction groups.

5.6.1   Assessment of regional function

As previously discussed, a considerable body of research over recent years has

explored ring descent with a view to quantifying regional left ventricular systolic

function. Importantly, Fukuda et al, (1998) demonstrated that the velocity of ring

descent (Sw) is markedly lower at sites corresponding to infarcted ventricular regions.

This finding was confirmed to an extent in the present study. In the anterior group,

the mean Sw was significantly lower at the ring site (site 5) corresponding to

myocardial hypokinesis.

Only nineteen acute (within 24 hours) ischaemic subjects were included in this pilot

study whereas the study by Fukuda and his colleagues involved forty-five patients

with acute myocardial infarction, essentially the damage to the ventricular

myocardium resulting from ventricular ischaemia. In addition, the methodology of

the present study differed somewhat from that of Fukuda et al (1998). Infarctive

areas were identified in this study by visual 2-D examination of the heart, which

allowed only a crude estimation of the location of dysfunctional regions. In contrast,

Fukuda and co-workers used invasive coronary angiography to identify occluded

coronary arteries as well as assessing the entire left ventricle systematically by

segment. Their approach probably resulted in a more accurate location of

dysfunctional regions than was possible in this study.

In order to assess the motion of the ring as a whole in infarction patients, parameters

derived from all six mitral ring sites were averaged and compared with control values.

The mean Q-Sw was greater than in normals, albeit non-significantly, in all three

infarction groups. Conversely, the mean descent velocity was found to be lower than normal in the infarction groups, but only significantly so in anterior subjects.

These results are expected from earlier work. Previous research focusing on the excursion of the mitral ring in patients with acute myocardial infarction found an overall reduction in the extent of ring displacement as well as a marked decrease at sites closely related or corresponding to diseased areas (Höglund *et al*, 1989). This may be attributed, at least in part, to the complicated but well-defined anatomical arrangement of myocardial fibres. Fibres spiral gradually across the myocardium, varying in obliquity from circumferential, in the middle, to longitudinal in the subendocardial and subepicardial layers (Gray, 1918; Jones *et al*, 1990; Galiuto *et al*, 1998). Damage to a specific area of the myocardium may be expected to directly affect the motion of more remote mitral ring sites by impairing the function of longitudinally and circumferentially orientated fibres. The effect of regional dysfunction on the velocity of descent of the ring as a whole has not been described previously.

Regional ventricular infarction often induces compensatory motion of functional myocardium, which helps to maintain an adequate ejection fraction (Fukuda *et al*, 1998). To determine whether or not this occurred in the infarction subjects, the motion of the ring at sites corresponding to functional myocardium was examined. Mean Sw was found to be lower in the anterior group, although the difference was not found to be significant. The inferior group, in contrast, displayed a modest increase in this variable, but neither was this difference significant. Mean Q-Sw at non-hypokinetic sites was non-significantly greater in any of the three infarction groups.

It seems contradictory that both mean Q-Sw and mean Sw were greater in the inferior

infarction group. A greater mean Sw suggests compensatory hyperkinesis of non-

ischaemic ventricular regions (Isaaz *et al*, 1989; Fukuda *et al*, 1998; Garot *et al*,

1999) whereas a greater mean Q-Sw is indicative of myocardial dysfunction (Jones *et*

al, 1990; Fukuda *et al*, 1998). Clearly, these two conditions are not expected to

coexist where the time to peak Sw and the peak Sw were both prolonged.

Nevertheless, changes in both parameters were not statistically significant in this pilot

study. These results were found to be consistent with those of Fukuda *et al* (1998),

who saw no significant differences between either mean Sw or mean Q-Sw and

control values at sites correponding to non-hypokinetic regions.

5.6.2   Differences between the anterior and inferior infarction groups

The mean Q-Sw, measured at all ring sites, those corresponding to hypokinetic

ventricular regions only and those corresponding to non-hypokinetic regions, was not

found to be statistically significant different between the anterior and inferior

ischaemic groups. However, the increase in the anterior group was consistently more

pronounced. Several factors may have contributed to these differences.

The anterior wall and indeed most of the left ventricle is supplied by the left coronary

artery while the right coronary artery feeds the inferior left ventricular wall as well as

the right ventricle. The former is usually, but not always, larger in calibre, and

perfuses a greater volume of myocardium than the latter (Gray, 1918). Occlusion of

this artery therefore results in a larger region of myocardial infarction and consequent

hypokinesis. As the ischaemic zone increases in size, the amount of functional myocardial tissue remaining decreases and ventricular ejection suffers (Aversano *et al*, 1990). In the present study, the suggestion of a larger anterior ischaemic zone is supported by the lower ejection fraction found in the anterior infarction group than in the inferior infarction group and shown in Figure 5.9. A greater area of anterior hypokinesis is likely to directly impair a greater proportion of the circumference of the mitral ring because of damage to both longitudinal and spiral fibres. In this context therefore, the lower mean Sw of non-hypokinetic sites recorded in the anterior infarction group might have been expected.

Furthermore ischaemic damage to the inferior wall is likely to induce compensatory motion of the opposing anteroseptal wall. The non-significant increase in mean Sw recorded at mitral ring sites corresponding to non-hypokinetic regions in the inferior ischaemic group may be attributable to compensatory hyperkinesis of functional myocardium. Larger ischemic zone size can impair function in nonischaemic myocardium by reducing the erectile component of end-systolic performance (Aversano *et al*, 1990).

Although, the general infarctive area was identified by real-time 2-D echocardiography, its exact location and extent were not determined in this study. If such localization were required, angiography would be the gold standard and the technique of choice. As a result, it is possible that the location of the dysfunctional region did not correspond precisely and exclusively to the ring site attributed to it. The descent velocity at this ring site might still be reduced to some degree, due to tethering or to impairment of spirally positioned myocardial fibres. With the data

available, it is not possible to predict how pronounced such tethering might be. Certainly a potentially larger ischaemic, and so infarctive, zone in the anterior infarction group would be expected to minimise the possibility of this occurring. This may account for the greater deviation from control values observed in the anterior group. As mentioned previously this problem was overcome by Fukuda *et al* (1998) by identifying occluded coronary vessels using coronary angiography.

On the other hand, the inferior ventricular wall is in closer proximity to the pericardium, the dense fibroserous sac that surrounds the heart. Due to pericardial constraint, it tends to be less dynamic than the anterior wall, which is relatively free-moving. Therefore, differences in the two parameters of mitral ring motion studied, Sw and Q-Sw, between the inferior wall abnormalities and control groups would not be expected to be as marked as those with anterior regional wall abnormalities.

Q-Sw intervals are indeed greater in the inferior infarction group but to a less pronounced degree than in the anterior infarction group. This can be attributed to the possible difference in the extent of the ischaemic zone or to the constraint by the pericardium. In addition, there is a small, non-significant difference in mean heart rate between the two groups (table 5.2). An increased heart rate shortens the time available for completion of the functions of contraction and relaxation of the cardiac cycle. For instance, in order to achieve normal systolic emptying within the reduced ejection period, a greater rate of tension development and shortening of the myocardial fibres is necessary (Alam *et al*, 1991). Thus, increased heart rate might reduce the Q-Sw interval in the inferior infarction group, and attenuate increases at sites corresponding to hypokinetic ventricular regions.

5.6.3   Assessment of global function

The results of previously published studies on the relationship between mitral ring descent and global left ventricular function, expressed in terms of ejection fraction, are summarised in table 5.3.

Of particular relevance was the research carried out by Fukuda *et al* (1998) to measure the mean Sw and mean Q-Sw at six ring sites in patients with myocardial infarction. Both parameters were then compared with ejection fraction measured using the Simpson's rule echocardiographic area-length method. No contrast agent was used because the system had second harmonics imaging if needed. As indicated in table 5.3, a significant positive correlation was found to exist between ejection fraction and the mean Sw of all six ring sites. Conversely, a significant negative correlation between ejection fraction and the mean Q-Sw of all sites was evident ($r = -0.71$, $p < 0.0001$, $n = 45$). Stronger correlations existed however, between the ejection fraction and the mean parameters of sites corresponding to infarct regions only ($r = 0.8$ for Sw and $r = -0.75$ for Q-Sw).

In the present study, ejection fraction was compared with the mean Sw and the mean Q-Sw derived from all six ring sites, from sites corresponding to non-hypokinetic ventricular regions only, and from sites corresponding to hypoknetic regions, and no significant correlations were found. As regards the relationship between ejection fraction and mean Sw measured at sites corresponding to hypokinetic regions in all infarction subjects, no statistically significant correlation was found ($r = 0.3$, $p = 0.21$, $n = 19$) although graphically these two parameters appear to be related in a positive linear manner.

88

As regards the relationship between ejection fraction and mean Q-Sw derived from ring sites corresponding to hypokinetic ventricular regions, again no significant correlation emerged (r = - 0.01, p = 0.69, n = 19).

5.7   Conclusions

The number of subjects in this pilot study is smaller than the numbers studied in previous work reported in the literature. The visual identification of ischaemic regions in this study may have been somewhat too crude. In addition, ejection fraction was measured in this study using a modified form of Simpson's rule, a method undermined by its dependence on endocardial definition and operator skill. Although noninvasive quantification of left ventricular function was a core aim of this study, research leading to the development of such techniques may require more sensitive and possibly more invasive techniques.

Anterior hypokinesis associated with ischaemic heart disease reduces the velocity of descent of the corresponding portion of the mitral ring. Inferior hypokinesis did not significantly affect the velocity of mitral ring descent. The current method of quantifying ring descent velocities may not be sensitive enough to identify smaller areas of dysfunction. An increase in the number of ring sites investigated might improve sensitivity. However, because of the limited number of two-dimensional views, this does not seem viable at present.

Previous reports of a greater time interval between ventricular depolarisation and the peak velocity of mitral ring descent were not confirmed in this study.

Since no significant correlations were found to exist between ejection fraction and either of the parameters of mitral ring motion measured, this study does not support earlier suggestions that mitral ring descent velocity or delay reflects global left ventricular function.
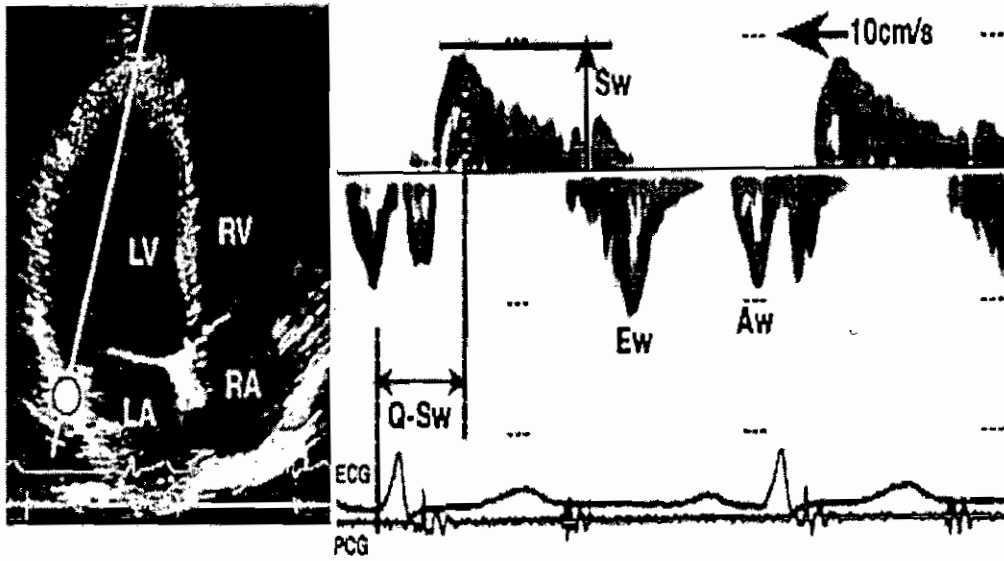
A
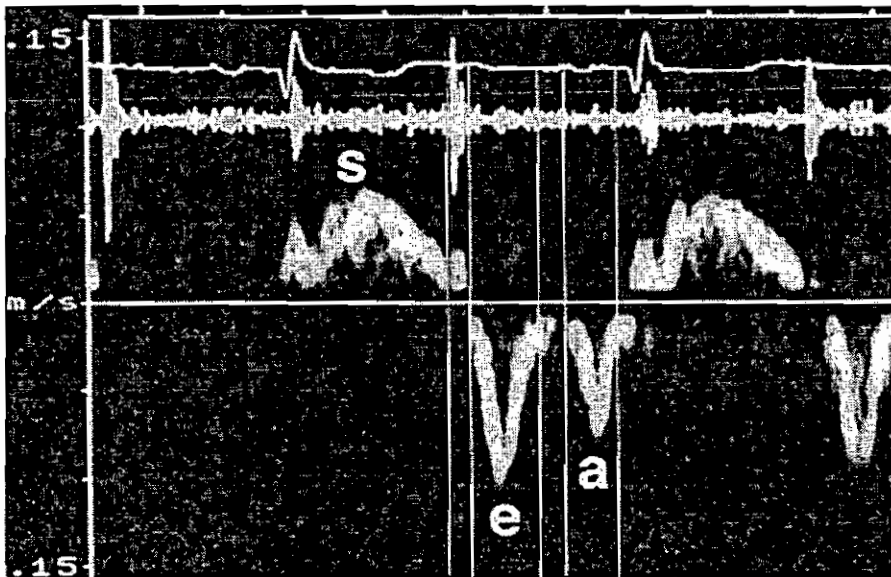
B

Figure 5.1   Characteristic TDI pattern for mitral ring motion
In A the patterns are those recorded by Fukuda *et al* (1998) and in B
are the patterns recorded in this study. S represents the peak mitral
ring descent velocity and Q-Sw the time interval between the Q-wave
of the ECG and S.
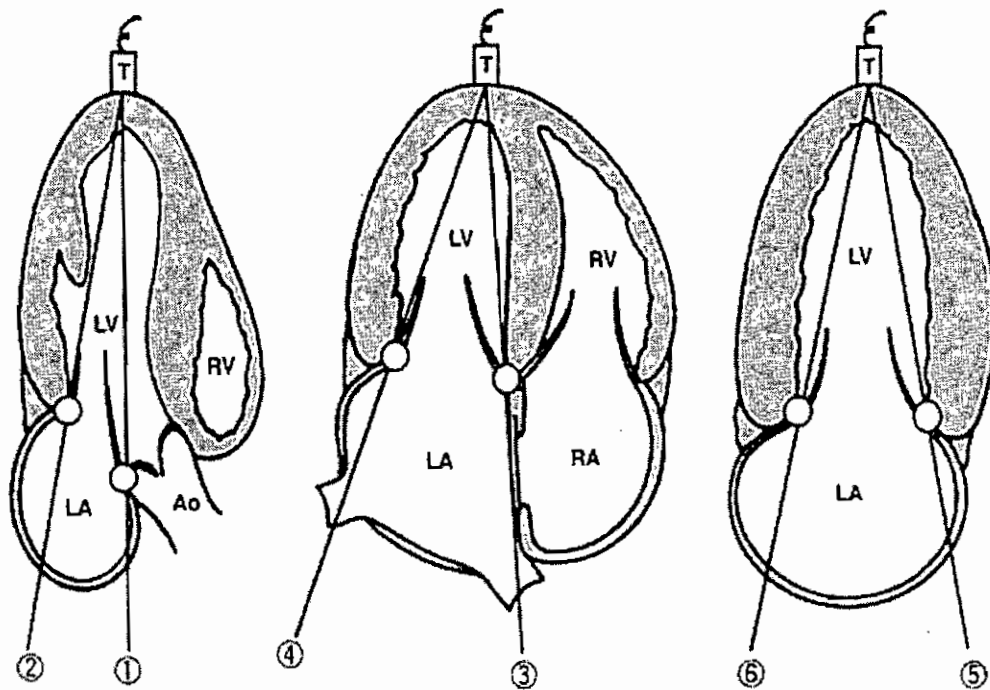
Figure 5.2   Sites at which the parameters of mitral ring motion were recorded
The Doppler cursor was positioned at six ring sites, (1) anteroseptal,
(2) posterior, (3) posteroseptal, (4) lateral, (5) anterior and (6) inferior
walls of the left ventricle. (Fukuda *et al*, 1998)
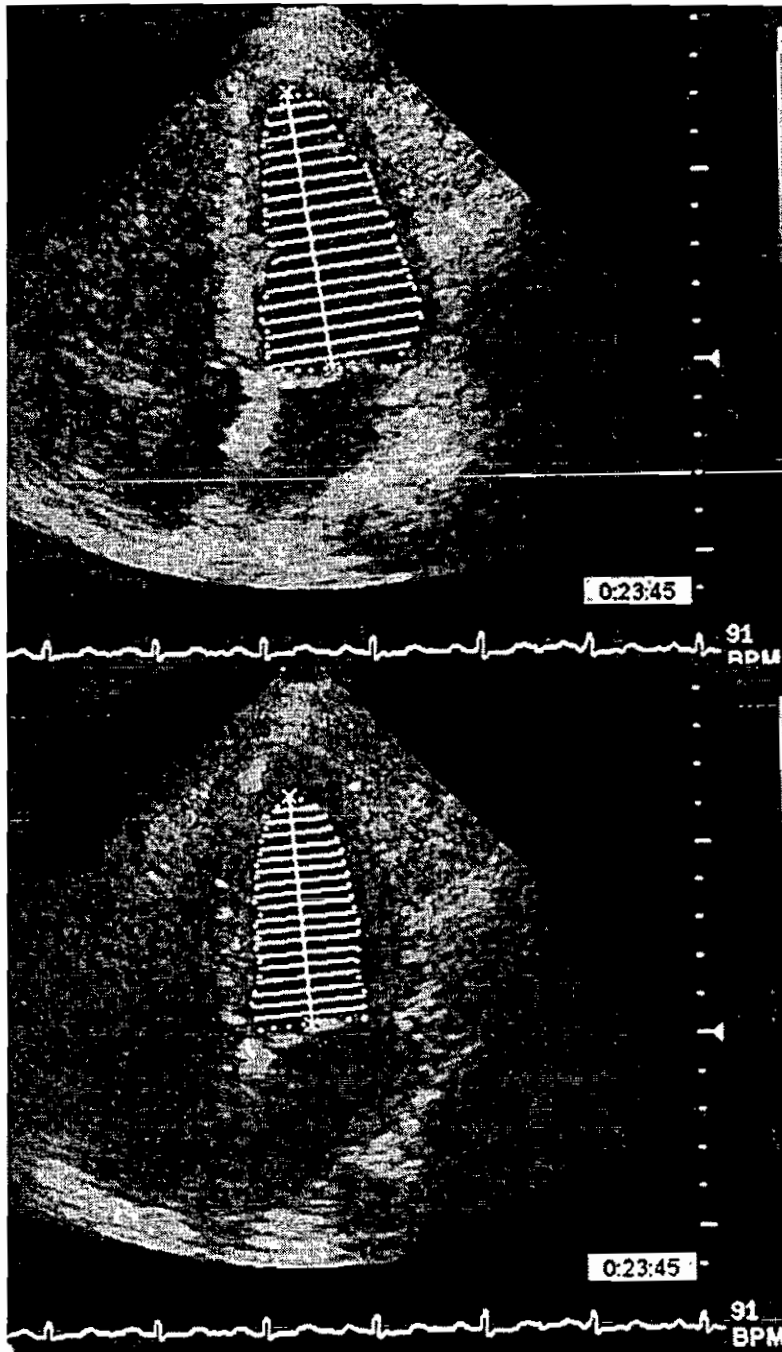
Figure 5.3   Application of Simpson's rule
The left ventricular cavity is divided into a number of 'slices' of fixed known height and diameter. The volume of the left ventricle as a whole is the sum of the volumes of the individual discs. [Asmi *et al*, 1995]
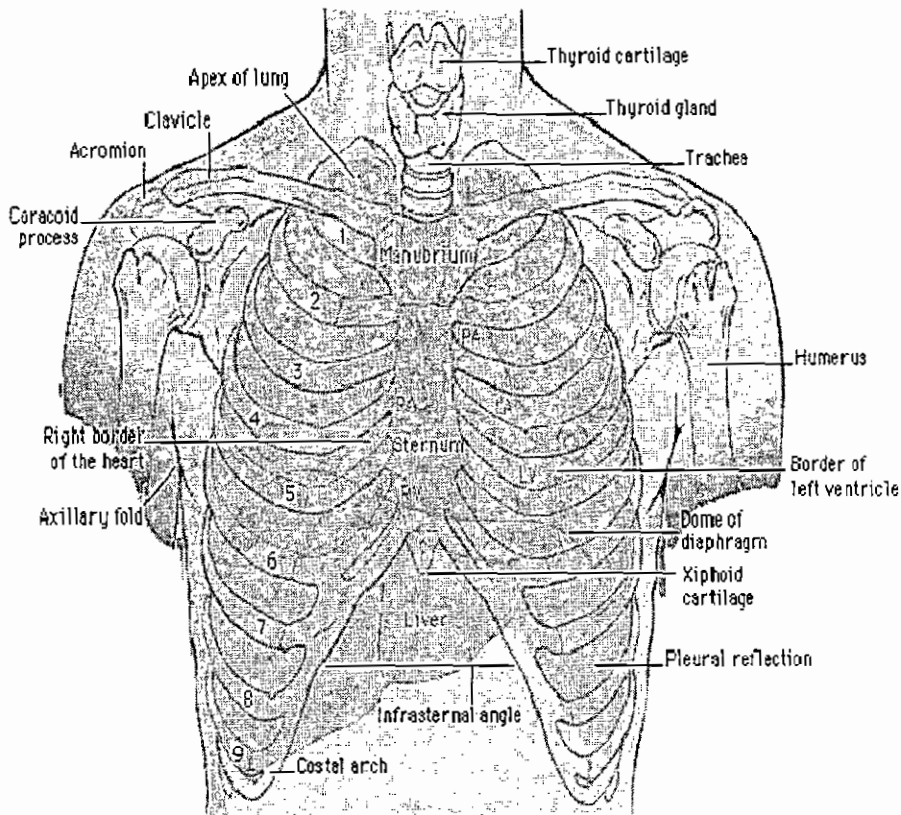
Figure 5.4   Echocardiographic apical imaging window
The apical window is located on the anterior chest wall, slightly lateral
and inferior to the left nipple (Atlas of Echocardiography 1999 Yale
University Press, © 1999 Yale University)

95
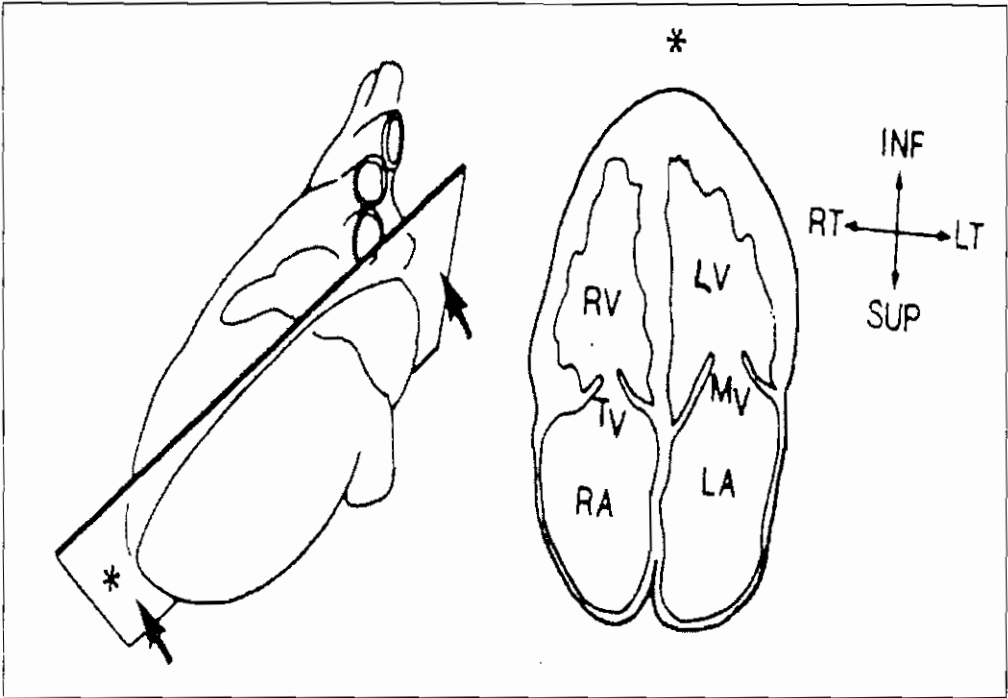
Figure 5.5   Apical four-chamber view
The heart is divided into four chambers by the interatrial and
interventricular septa and by the atrioventricular valves (Walsh &
Wilde, 1999)
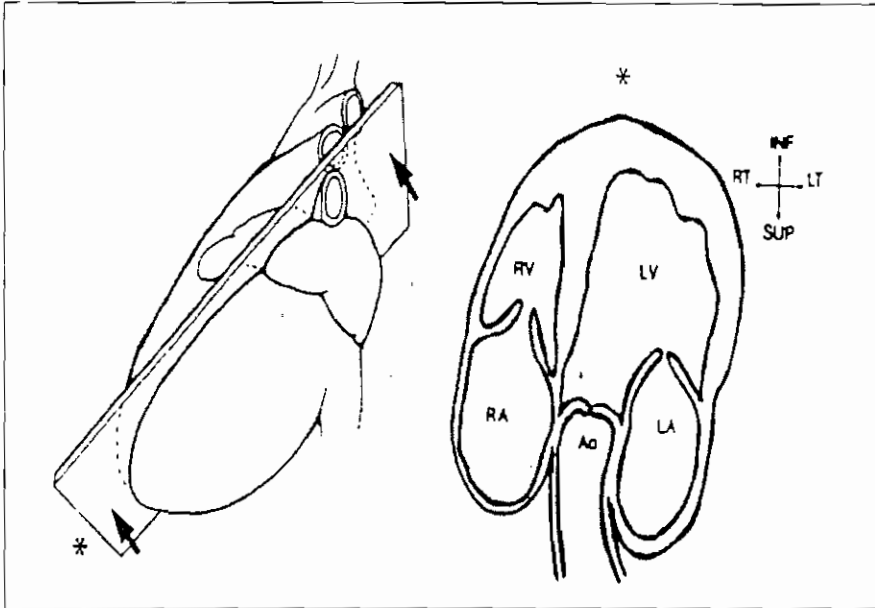
Figure 5.6   Apical five-chamber view
This view is produced by slight anterior angulation of the transducer
from the position used to obtain the four chamber view (Walsh &
Wilde, 1999)
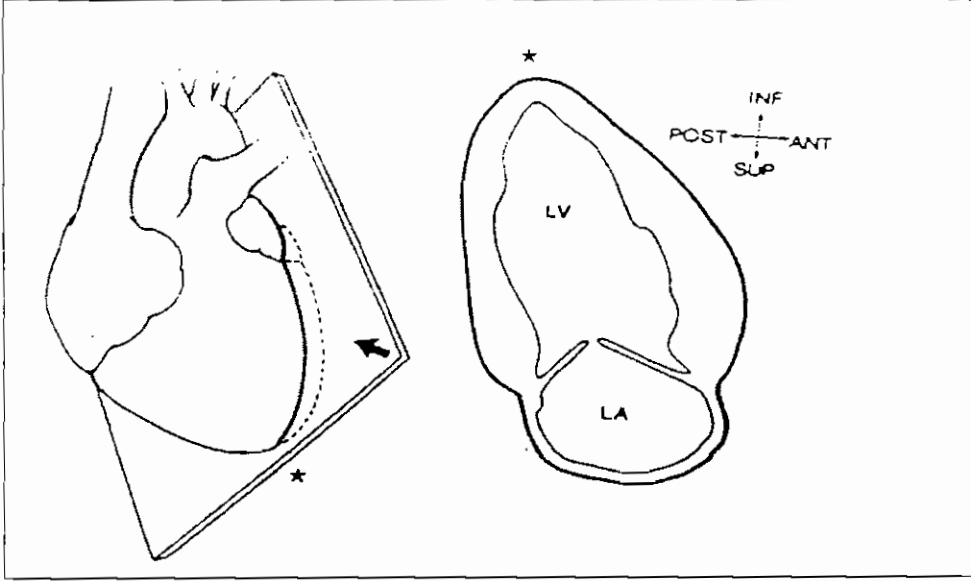
Figure 5.7   Apical two-chamber view
This view is obtained by rotating the transducer 60° to 90° from the
four-chamber view (Walsh & Wilde, 1999)
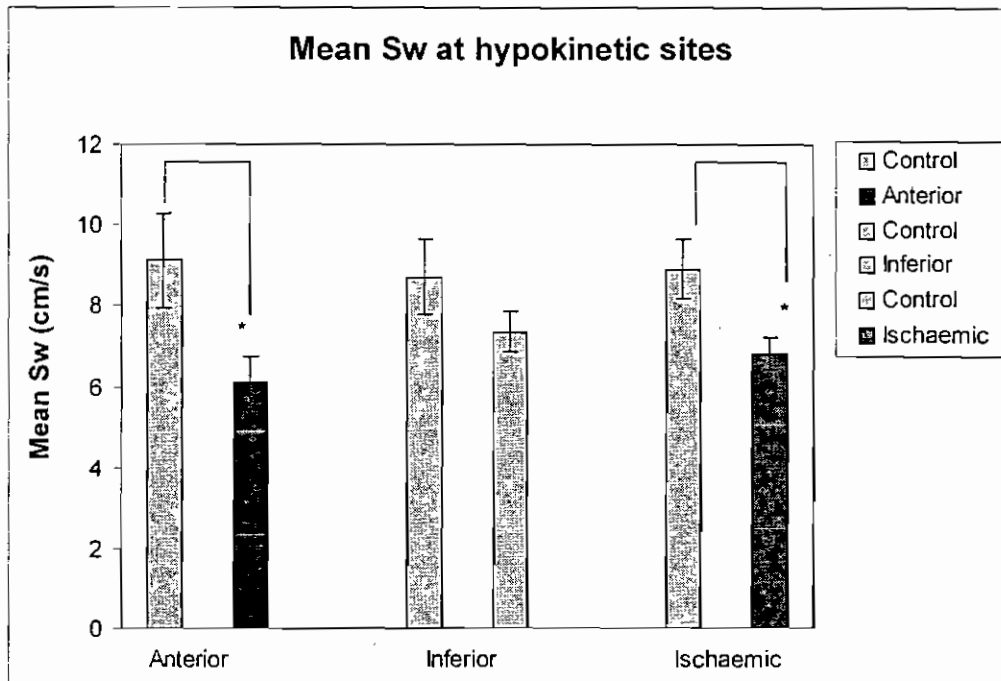
Figure 5.8   **Mean Sw measured at ring sites corresponding to hypokinetic**
ventricular regions only
Values are expressed as mean ± SEM. Significant differences between
infarction groups and their respective controls are denoted by * p <
0.05

Fig 5.12 Mean Q-Sw at hypokinetic sites
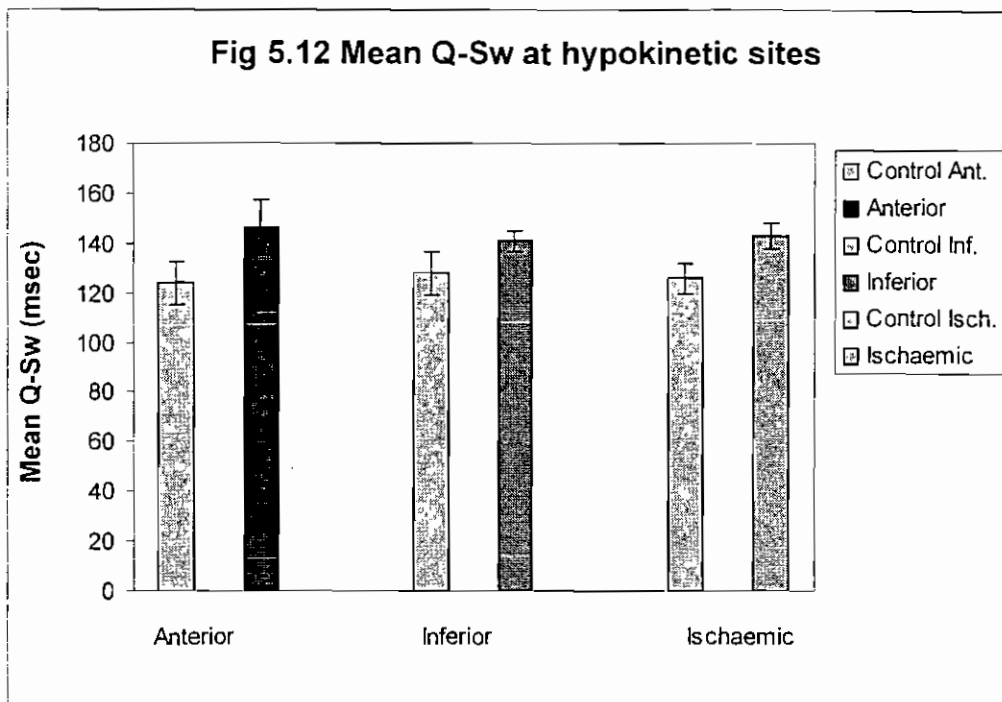
Figure 5.9   Mean Q-Sw measured at ring sites corresponding to hypokinetic ventricular regions
Values are expressed as mean ± SEM. No significant differences between the groups were recorded although small increases from control values were observed in all three infarction groups.

Table 5.1   Standard imaging control settings for the Hewlett Packard
SONOS 2500 system

Imaging control	Standard settings
Sweep speed	50 cm/s
Depth	10 to 20 cm
Gain	50%
Power	17 dB
Filter	Low

Table 5.2   Subject Characteristics

Subject Group	Control	Anterior infarction	Inferior infarction	Overall infarction
Number of Subjects	8	8	11	19
Number of Males	5	7	8	15
Mean Age (Years ± SD)	54.3 ± 10.1	67.3 ± 7.2	61.4 ± 12.6	63.8 ± 10.8
Mean Heart Rate (Beats/min ± SD)	72.4 ± 13.0	68.6 ± 15.0	72.7 ± 9.0	71.0 ± 11.7
Mean Ejection Fraction (% ± SD)	63.6 ± 5.8	41.0 ± 10.0	46.1 ± 7.5	44.0 ± 8.8

Table 5.3   **A summary of the results of several previous studies examining the relationship between mitral ring motion and ejection fraction (EF)**

Study	No of sites	EF Vs mean mitral ring movement (MRM)	EF vs mean Sw
Alam *et al*, 1990	4	r = 0.82; p < 0.001; n = 30	
Pai *et al*, 1991	4	r = 0.95; p < 0.001; n = 54	
Jensen-Urstad *et al*, 1998	4	r = 0.64; p < 0.001; n = 94	
Gulati *et al*, 1996	6		r = 0.86; n = 54
Fukuda *et al*, 1998	6		r = 0.71; p < 0.0001; n = 45

Chapter 6

Diastolic Dysfunction: DTI, 2-D Imaging and Transmitral Blood Flow Measurement by Doppler Ultrasound for Assessing Early Filling Dynamics in Normal Controls and Patients with Diastolic Dysfunction [1]

It is been proposed that post-systolic recoil of the left ventricle provides the potential energy for rapid early diastolic filling, occurring as it does during the isovolumic relaxation time before left ventricular filling, and that the rate of early diastolic inflow blood velocity is influenced by preload conditions. These preload conditions are those forces acting to stretch the ventricular fibres at end-systole. In diastolic dysfunction, recoil is delayed and can occur during or after left ventricular filling, and the early diastolic inflow velocity is not then influenced by preload in the stiff (dysfunctional) heart (Oki *et al*, 1997). The study reported in this chapter seeks to evaluate this proposition indirectly by exploring the relationship between peak early diastolic mitral ring velocity (Ea) (as a surrogate for recoil) measured using DTI, and the acceleration of early diastolic transmitral flow measured by pulsed Doppler in patients with and without diastolic dysfunction.

---

[1] The substance of this chapter was published in King, GJ, Foley, JB, Almane, F, Crean, PA & Walsh, MJ, Early diastolic filling dynamics in diastolic dysfunction, Cardiovasc Ultrasound, 2003; 1: 9. A copy of this paper is provided in Appendix D.
On 14 May 2004, this paper was reported to be the most accessed article ever in Cardiovasc Ultrasound. This report is also provided in Appendix D.

6.1   Dissociation between left ventricular untwisting and filling

Cardiac torsion was described for the first time in the 1960s and 1970s in transplant

recipients (Carlsson *et al*, 1967; Ingels *et al*, 1975). These investigators used

intramyocardial markers implanted in the myocardium during open-heart surgery.

Later, studies by Maier *et al* (1992) using echocardiography and echo-dense crystals

implanted in the subendocardium on special catheters measured the wall thickness

dynamics of the inner and outer walls of the heart. These authors described a twisting

motion of the left ventricle with angular displacement (torsion) of the apex relative to

the base.

There were various limitations in these studies. The echo-dense markers had to be

precisely located by means of catheter techniques or surgery. The idea of implanting

cardiac markers was not without its critics. This type of implantation may cause local

scarring or arrhythmias, and may induce regional wall motion abnormalities due to

the implantation. Other problems were associated with the weight of these markers

affecting local myocardial mobility.

With new technologies such as magnetic resonance imaging and myocardial tagging

the non-invasive analysis of regional cardiac motion has become possible.

Myocardial regions were labelled non-invasively with a star-like pattern, parallel lines

or rectangular grid. This allowed left ventricular rotation to be assessed.

Nagel *et al* (2000) studied cardiac rotation and relaxation in patients with aortic valve

disease using myocardial tagging and concluded that patients with left ventricular

hypertrophy had a reduction in the torsion at the base and an increase in the torsion at

the apex of the ventricle. These authors concluded that diastolic untwisting is delayed

and prolonged in hypertrophy. In this condition the ventricle is not able to stretch

effectively and can not accept preload changes due to physical activity. In

consequence there is a rise in left atrial pressure and this would help to explain the

occurrence of diastolic dysfunction in patients with pressure overload hypertrophy.

Rademakers *et al* (1994) used magnetic resonance tagging to show that the untwisting

occurs principally during the isovolumic relaxation before filling. They also showed

that left ventricular torsion is observed to be counter-clockwise rotation, as observed

from the apex, of the left ventricle during systole. It is dependent on relaxation of the

myocardial fibres in diastole, but also on other preload conditions such as left atrial

pressure, atrial contraction and passive left ventricular compliance. When one of

these parameters is impaired or defective, or when, for instance, the left ventricular

filling period is shortened and stroke volume increased during physiological stress,

maintaining cardiac output is more and more dependent on rapid early filling. The

subsequent untwisting during diastole has been postulated to generate recoil forces

that account for diastolic suction. Ventricular suction in diastole is a means of

achieving efficient early filling. However the mechanism for diastolic suction has not

been clearly identified. Untwisting however occurs before mitral valve opening and

this has been postulated to generate recoil forces that account for diastolic suction in

the normal. That potential energy which causes rapid ventricular suction is broadly

proportional to the amount of the initial untwisting and is stored during the

isovolumic period pending the opening of the mitral valve.

6.2   Importance of the early diastolic mechanism revealed by DTI

The study of left ventricular filling dynamics in diastole has only recently begun to receive detailed attention. DTI is fundamental in this assessment as it allows for the determination of systolic and diastolic velocities in the myocardium (McDicken *et al*, 1992; Erbel *et al*, 1996). Simultaneous pulsed Doppler blood flow measurement gives the accompanying transmitral flow to complement the tissue movement data.

In normal left ventricular relaxation after systole, the peak mitral ring velocity (Ea) recorded by DTI precedes the peak early passive diastolic transmitral flow (E) recorded by conventional pulsed wave (PW) Doppler ultrasound. In situations where this relaxation is impaired, Ea follows E (Rodriguez *et al*, 1996; Nagueh *et al*, 2001). This supports the proposition that elastic recoil is related to mitral ring motion and this early diastolic mechanism of augmenting the onset of mitral flow velocity is lost in patients with diastolic dysfunction (Rodriguez *et al*, 1996). Ea appears to be more reflective of events at the very early diastolic stage in the cardiac cycle, including untwisting or recoiling of the ventricle (Nagueh *et al*, 1999; Nagueh *et al*, 2001).

There are animal and human data that show a good correlation between the lowest early left ventricular diastolic pressure (minimal pressure) and Ea, where subjects with low left ventricular minimal pressure have a normal Ea and those with a high minimal left ventricular pressure have a low Ea (Ohte *et al*, 1998; Nagueh *et al*, 1999; Nagueh *et al*, 2001). This minimal left ventricular pressure is likely to reflect the early diastolic recoil, in that subjects with normal or enhanced recoil tend to have low

pressures. Recoil may also be dependent on myocardial interstitial composition, which is altered in patients with diastolic dysfunction (Villari *et al*, 1993).

6.3   Acceleration of early diastolic filling and its relationship to peak mitral ring velocity (Ea) as recorded by DTI

The effect of left ventricular twist has been postulated to be the storing of potential energy, which ultimately provides energy to aid in diastolic recoil leading to ventricular suction. According to Rothfeld *et al* (1998), the magnitude of ventricular twist is strongly positively correlated with the acceleration of the mitral E wave. These investigators measured ventricular twist in 40 patients with normal hearts, the end-systolic twist being determined by measuring rotation of the antero-lateral papillary muscle about the centre of the ventricle.

However previous work by Choong *et al* (1988) had shown that E is strongly dependent on both preload and relaxation. In the latter investigators' study on dogs, they showed through changes in left atrial pressures and ventricular relaxation that the acceleration of early diastolic filling E was directly related to left atrial V-wave on the left atrial pressure trace and inversely related to the index of myocardial relaxation, tau, defined by Choong *et al*. If the acceleration of early diastolic filling is strongly dependent on preload variables it is unlikely that it will correlate with ventricular twist in normal subjects. Previous work has shown that myocardial velocities such as Ea measured in the regions of the mitral ring are inversely related to tau and thereby ideally suited to offset the effects of relaxation on the acceleration of early diastolic

filling E in estimating pulmonary capillary wedge pressure (or indirectly left atrial

pressure).

Work by Firstenburg *et al* (2000) has shown no relationship between either E/Ea

septal or E/Ea lateral and pulmonary capillary wedge pressure, thereby limiting the

global application of this index. In this circumstance it is reasonable to suggest that

E/Ea can be applied to estimating pulmonary capillary wedge pressure in patients with

impaired relaxation because the influence of preload is diminished with impaired

relaxation.

6.4   Aim of this study

A number of studies have shown that early diastolic tissue velocity (Ea) is reflective

of events in early diastole, including ventricular recoil (Nagueh *et al*, 2001). The aim

of this study was to determine the relationship between Ea (peak early mitral ring

velocity in diastole) recorded with DTI and assumed to be representative of recoil,

and early transmitral inflow velocity E (recorded using pulsed Doppler ultrasound) in

patients with diastolic dysfunction and to compare this with the corresponding

relationship in a normal control population.

6.5   Experimental methods

6.5.1   Patient selection

The study proposal was assessed and approved by the Hospital and Institute Ethics

Committees. Individuals attending the Cardiology Department for echocardiography

assessment were screened. Those with echocardiography features suitable for

enrolment in the study were asked to participate, as described by King *et al* (2003).

Diastolic dysfunction, defined by the European Study Group on Diastolic Heart

Failure, 1998, as preserved systolic function but with evidence of LVH, reversed E/A

ratio and a prolonged isovolumic relaxation period, was determined using 2-D

echocardiography and Doppler techniques. Patients were not asked to participate if

they had abnormal rhythm, known coronary artery disease, or valvular incompetence

beyond a modest degree, or if echocardiographic images were technically inadequate

for complete analysis.

Over a seven month period, a group of 22 controls with normal echocardiograms and

25 patients with clinical echocardiography and Doppler ultrasound evidence of

diastolic dysfunction gave informed consent and were enrolled in the study.

6.5.2   The study population

The 25 patients in the diastolic dysfunction group had a mean age of 61.5 (SD 13.3)

years. The 22 normal controls had a mean age of 33.4 (SD 18) years. Comparisons

between these two groups were adjusted for the mean age differences, by regression

analysis using JMP software (SAS version 3), as outlined in section 6.5.4 below.

Fifteen patients from the diastolic dysfunction group (10 males, 5 females) had been

referred to the Hypertension Clinic. These patients had been evaluated for essential

hypertension and sent for an echocardiography examination as part of their

evaluation. Patients selected for the study had echocardiographic evidence of

diastolic dysfunction without pseudonormalisation, which would have been unmasked

on the tissue Doppler profile. They were subsequently diagnosed as having essential

hypertension and treated appropriately. At the time of the echocardiographic

evaluation they were not on any anti-hypertensive therapy. Eight of the patients had

electrocardiographic evidence of LVH of various degrees. Ten other patients (2 male,

8 female) with diastolic dysfunction consisted of an elderly group with age-related

diastolic dysfunction, who were also free of cardiac drugs. These patients had been

referred for echocardiography to investigate the possible presence of a systolic

murmur. Three of these patients had mild calcific aortic stenosis gradient (< 25

mmHg) only, 4 patients had basal septal hypertrophy only and 3 patients had both

mild aortic stenosis gradient (< 25 mmHg) and basal septal hypertrophy.

The group of 22 normal controls (12 males, 10 females) had clear acoustic windows

and no clinical or echocardiographic evidence of cardiovascular disease.

6.5.3   Echocardiography

Echocardiograms were obtained with an Agilent/Philips 5500 cardiac ultrasound

system with colour flow imaging and DTI capabilities. The system specifications are

given in Appendix A. The system was equipped with 2.5 MHz and 3.5 MHz

transducers. 2-D imaging echocardiography was performed followed by a pulsed

Doppler blood flow study. The images obtained included the apical four-chamber and

two-chamber views so that blood flow measurements could be made across the mitral

valve as outlined in chapter 4. Also these views made it possible to locate the sample

volume, for recording the DTI, at the lateral mitral ring. Pulsed wave DTI was

performed by activating this function on the Agilent/Philips 5500 system. The

characteristic velocity profile of diastole was obtained in all subjects.

Peak early (E) and late (A) diastolic mitral ring velocities were recorded, as well as

the E/A ratio, acceleration time, along with acceleration and time/velocity integrals of

early and late filling in each case. Acceleration time of the early diastolic velocity

was defined as twice the interval between the point at peak velocity and that at half of

the peak velocity in the acceleration phases. Acceleration (in units of cm/s^2) was

represented by the slope of the line between an anchored point and a movable

crosshair on the display, and calculated by the software package in the scanner. E

wave acceleration was defined as the slope of the up-stroke of the E wave. This linear

measurement was made on the velocity recording. These recordings were made on a

paper strip chart with a sweep speed of 100 mm/s. Measurements were performed

off-line by an independent observer who had no knowledge of the pulsed Doppler or

DTI findings. At least three measurements were taken of each parameter and these

were averaged. The raw data are tabulated in Appendix G.

Using 2-D echocardiography, the end-systolic (ESV) and end-diastolic (EDV)

volumes were recorded by the method of disc summation based on Simpson's rule, as

outlined in chapter 4. This method treats the ventricle as a stack of discs and is

recommended because it is independent of preconceived ventricular shape (Otterstad

et al, 1997). The endocardial border was traced in each phase of the cardiac cycle and

the system computer partitioned the ventricle into 20 discs of equal thickness. The

computer then summed the individual disc volumes to give the total volume of the

cavity. The data obtained are tabulated in Appendix G.

All echocardiography examinations were performed by an experienced sonographer

and/or by an experienced physician. To test for inter-observer variability, DTI

measurement of Ea and pulsed Doppler ultrasound profiles (determined by

conventional pulsed wave Doppler) were analysed by one experienced observer who

was blind to the first examination. A value of $p \leq 0.05$ was considered to indicate

statistical significance. Inter-observer agreement was measured using the method

described by Bland *et al* (1986). Mean differences and correlations close to zero

would indicate negligible bias in one observer compared with the other.

6.5.4   *Statistical Analysis*

All statistical analyses were performed using the JMP version 5 statistical package

[SAS Institute Inc.]. Paired and unpaired student's t-tests were used, as appropriate, to

evaluate the difference between the means of the two selected groups and the

difference between repeated measures. Because of the wide age range in both groups

the means were adjusted for age using regression analysis for each variable. This is a

standard method, (Bland, 2000), for relating a continuous response variable to several

predictor variables. It simultaneously examines each predictor variable while

adjusting for other variables in the regression model. For each group the relationship

between DTI diastolic early velocity and mitral acceleration (Ea) was expressed using

the Pearson correlation coefficient. A linear regression model was constructed to

examine the relationship between these variables and to test whether the slopes of the

regression lines differed between the control and diastolic dysfunction groups, using a

test for interaction. The F-ratio was used to test for significance, and significance at

$p < 0.05$ was assumed throughout.

6.6   Results

The main results are tabulated in Tables 6.1 (a) and 6.1 (b).

6.6.1   *Inter-observer variability for Ea and Doppler profiles*

Mean differences and correlations for inter-observer variability for Ea ($r = 0.07$) and

other Doppler profiles indicated negligible inter-observer variability or bias.

6.6.2   *Standard Doppler echocardiographic analysis*

The early diastolic tissue velocity detected by DTI was lower in the diastolic

dysfunction group than in the normal group (6.1 cm/s $\pm$ 0.7 and 11.8 cm/s $\pm$ 0.7

respectively, $p = 0.001$). The acceleration was lower in the diastolic group (549.2

cm/s^2 $\pm$ 151.9 versus 871.1 cm/s^2 $\pm$ 128.1, $p = 0.001$) as was the time-velocity integral

of early diastolic flow (7.8 cm $\pm$ 2.5 versus 10.6 cm $\pm$ 2.9, $p = 0.003$). There were no

appreciable differences between the two groups in relation to the end-diastolic volume

or the end-systolic volume. There was no difference with age in the ejection fraction.

The E/A ratio was lower in the diastolic dysfunction group compared with the normal

group (0.7 $\pm$ 0.2 versus 1.9 $\pm$ 0.5, $p = 0.001$), while the time-velocity integral of the

atrial component was greater in the diastolic dysfunction group compared with the

normal group (11.7 cm ± 3.7 versus 5.5 cm ± 2.1, p = 0.0001). In view of the age

difference between the control and diastolic dysfunction groups the data were

adjusted for age. The same differences were seen in the various parameters after

adjusting for age. The results of the unadjusted univariate analyses are presented in

Table 6.1 (a) and the results for the multivariate analysis, adjusted for age, are given

in Table 6.1 (b).

6.6.3   *DTI assessment of the mitral ring descent velocities recorded at the lateral mitral ring*

All of the patients with diastolic dysfunction had a lower Ea than all of the subjects in

the normal control group. Patients with diastolic dysfunction and an E/A ratio less

than one had consistently lower mitral ring velocities, as determined by DTI. A

positive correlation was found between the mitral ring tissue velocity (Ea) with the

acceleration of mitral inflow in the diastolic dysfunction group (r = 0.66). Such a

correlation was not found in the control group. Figure 6.1 shows these relationships

for the two groups of subjects. The F ratio test, comparing the two regression lines

for the two groups, indicated a significant difference (F = 4.44, p = 0.0176) between

them.

6.7   Discussion

In the control group, Ea had no relationship to the acceleration of early diastolic filling. In the group with diastolic dysfunction, Ea had a positive correlation to the acceleration of early diastolic filling.

It is known from previous studies that recoil occurs during the isovolumic relaxation period before filling and that mitral ring tissue velocities and transmitral inflow velocities are influence by preload conditions in a normal study population (Rodriguez *et al*, 1996; Nagueh *et al*, 2001). Therefore because of the dissociation between filling and recoil described already by Buchalter *et al* (1994) and the influence of preload conditions on the rate of filling, the two variables are unlikely to correlate. However in the stiff heart, recoil is delayed and filling takes place at the same time. In addition preload dependency of these variables is also reduced in the stiff diseased ventricle. Therefore a strong relationship between the rate of filling and recoil occurs. In the stiff heart a slow release of restoring forces during recoil reduces the early diastolic filling across the mitral valve. In the normal heart the rate of flow is a result of the potential energy of the maximum restoring forces held when recoil has terminated, and this results in the typical normal ventricular filling pattern in early diastole.

This study provides evidence that ventricular filling is associated with early diastolic motion of the mitral ring, which is a marker for left ventricular recoil in the control group. This positive correlation is the result of the absence or reduction of the early diastolic mechanism essential for proper filling. It may be argued that in the normal

state most people have normal filling pressures and it is primarily the left ventricular

relaxation and recoil that influences the transmitral pressure gradient. Preload

however is the force that extends the ventricle in diastole or the force acting to stretch

the ventricular fibres at end diastole (European Study Group on Diastolic Heart

Failure, 1998). Therefore even though the filling pressures are normal, preload will

affect the rate of blood flow across the mitral valve depending on the degree of stretch

of the left ventricular cavity in diastole. Taking into account the physiological

changes that affect preload there should be a varying degree of acceleration of blood

flow across the mitral valve, which is dissociated from left ventricular recoil in the

normal.

6.7.1 *Early diastolic velocity of the mitral ring - an index of left atrial*
filling pressures

Evidence that Ea declines progressively with age and is reduced in LVH led

investigators to suggest that Ea could be an index of left ventricular relaxation (Garcia

et al, 1996; Rodriguez *et al*, 1996; Nagueh *et al*, 1997). From these observations it

was suggested that Ea, as measured from the diastolic velocity profiles produced by

DTI may provide an index of left ventricular relaxation not strongly influenced by

preload variables such as heart rate and left atrial pressure. Therefore mitral E-wave

velocity or the velocity of passive early diastolic filling determined by conventional

pulsed Doppler ultrasound might be corrected for the influence of relaxation by

applying the dimensionless index, E/Ea. Ea has been shown to be related inversely to

the time constant of relaxation (Nagueh *et al*, 1997). In previous studies, the ratio

E/Ea related well to left atrial pressure and was used to estimate left ventricular filling

pressures in stiff hearts (Kim *et al*, 2000). Firstenberg *et al* (2000) showed that E/Ea

did not correlate with pulmonary capillary wedge pressure in normal volunteers and

that Ea was strongly preload independent with preserved relaxation. This observation

agrees with the results of this study. In a canine study, left ventricular relaxation,

minimal pressure and transmitral pressure gradients determined Ea in normal

conditions. In cases of impaired relaxation the influence of filling pressures was very

small (Firstenberg *et al*, 2000; Nagueh *et al*, 2001).

In a study looking at the differentiation between constrictive and restrictive

cardiomyopathy using DTI, Ea was found to be low even when the mitral inflow

pattern was pseudonormal or restrictive (Garcia *et al*, 1996). This indicates that low

Ea values are symptomatic of abnormal left ventricular relaxation and are not

influenced by preload variables such as high left ventricular filling pressures. The

findings of the current study also agree with these observations. We have observed a

better correlation between the rate of early diastolic filling and Ea in the diastolic

dysfunction group without pseudonormalisation than in the control group.

Patients with diastolic dysfunction have increased endocardial and perivascular

fibrosis as a feature of altered interstitial structure (Waldman *et al*, 1998; Brilla *et al*,

1992). The relationship of tissue velocities determined by DTI to the regional amount

of interstitial fibrosis has also been established (Isaaz, 2000; Shan *et al*, 2000).

Therefore altered interstitial composition should manifest itself in the behaviour of

Ea. This study provides further evidence to support the use of the E/Ea ratio to

estimate pulmonary capillary wedge pressure in patients who have impaired cardiac

relaxation. Since diastolic dysfunction develops with age and is prevalent in all myocardial pathologies, the potential use of the E/Ea ratio in estimating left ventricular filling pressure is important. Therefore this additional evidence to support its use in assessing accurately this significant clinical parameter is a further indication of its potential diagnostic value.

6.7.2 Limitations of this study

The main limitation of this study may be the age bands of the two groups compared. The study set out to assess the mechanics of early diastolic filling in stiff and normal hearts regardless of the aetiology of the stiffness. However mean values adjusted for age were calculated. The strength of the associations was found to be low, possibly because the numbers in the normal control group were relatively small (n = 22), and random variations tend to diminish associations with small study populations. Nevertheless, with this number there would have been sufficient power (80%) to detect a correlation of 0.55 or above as being statistically significant in this group.

Transmitral flow presents a parabolic distribution during progression from normal to advanced diastolic dysfunctions characterised by a restrictive pattern. Therefore patients with a restrictive physiology and pseudo-normalisation were excluded from the study. However a further study to show the association between the deficits of elastic recoil estimated by Ea velocity with early left ventricular inflow acceleration in patients with pseudo-normalisation unmasked by the valsalva manoeuvre could yield interesting results.

6.8   Conclusions

In patients with diastolic dysfunction a strong relationship was found between mitral ring relaxation recorded by DTI and the acceleration of early diastolic flow recorded by conventional pulsed Doppler ultrasound. This relationship was not found in the normal control group. This provides a new insight into diastolic filling events in patients with diastolic dysfunction and further supports not only the premise that recoil is an important mechanism for rapid early diastolic filling, but also the existence of an early diastolic mechanism in the normal subject.

The existence of the early diastolic mechanism is fundamental to normal cardiac function. The novel experiment described above in this chapter clarifies this mechanism. It is known that the elongation of the ventricles taking place while the atrioventricular valves are still closed is due to the active distension which is not affected by flow volume but depends on the energy stored by myocardial elastic components during ventricular systole. The results of the work reported here are novel as they help to explain the mechanics of diastole and also indicate that mitral ring diastolic peak tissue velocity occurs earlier than the peak of early mitral inflow velocity in normal human hearts. This work also supports the suggestion that this relationship may be altered in the presence of diastolic dysfunction and elevated atrial pressure. It may be postulated that the flow across the mitral valve exhibits decelerating qualities once the stretch of the multitude of molecular springs begins. It would then seem logical to postulate that the myocardium becomes slack, with the expectation of preload depending on physical activity within a period between the peak myocardial tissue velocity measured at the mitral ring and the peak of the E wave of ventricular inflow via the mitral valve. The conclusion drawn from the

experimental observations shows that the preload influence on the myocardial E wave gradually decreases as diastolic dysfunction worsens. This then would validate the use of the ratio, E/Ea, to estimate filling pressures in cardiac patients. Such an estimate would be extremely valuable especially in the light of recent work by Skaluba *et al* (2004), who suggest that left ventricular filling pressures rather than slow relaxation reduces exercise capacity.

As a consequence of these results the method described in chapter 7 was developed to allow the measurement of the relative timings in the early diastolic mechanism. With this timing method a study was carried out into the clinical diagnostic utility of the time difference between the peak Ea diastolic velocity of the mitral ring by DTI and the peak mitral inflow demonstrated by the maximum opening of the mitral valve determined by M-mode echocardiography.

The next stage of this thesis focuses on the evaluation and potential role of the "slack" period of the cardiac cycle that appears to be mediated by the unique properties of the myocardium and the dynamics of filling. Multiple echocardiographic parameters including Doppler most often derived from 2-D assessments were developed for the assessment of left ventricular systolic and diastolic functions. No "slack" myocardial status or diastolic mechanism has yet been correlated echocardiographically. Myocardial hypertrophy is a common pathology with many causes and diastolic dilemmas. The study reported in the following chapter was designed to test the diagnostic utility of the new timing mechanism to differentiate between pathological and physiological hypertrophy.
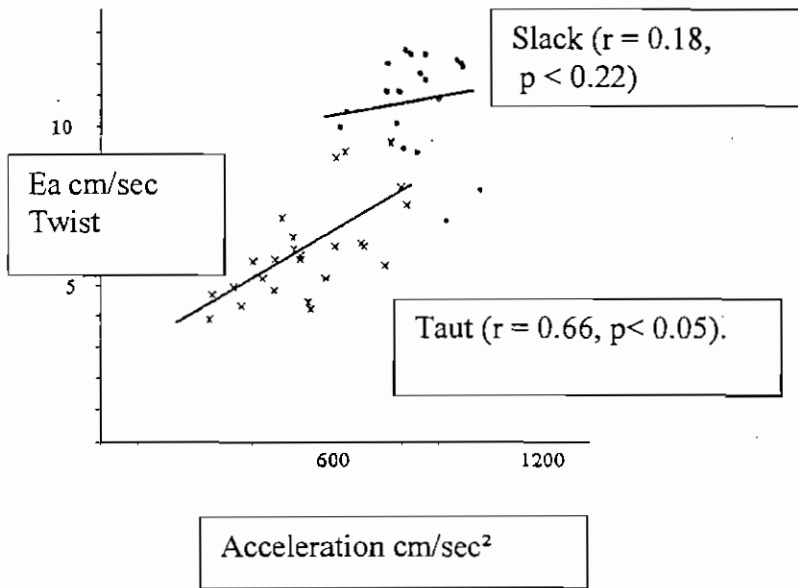
Figure 6.1   Correlation between mitral ring tissue velocity Ea and the acceleration of mitral inflow for normal subjects (•) and patients with diastolic dysfunction (x)
There is a good positive correlation for the diastolic dysfunction group but very weak correlation for the normal group.

Table 6.1 (a) Echocardiographic characteristics of the study population

	Normal controls (n = 22)	Diastolic dysfunction (n = 25)	p value
Age (years)	33.0 ± 18	61.9 ± 13.3	< 0.001
EDV (ml)	90.0 ± 23.5	98.7 ± 40.3	0.418
ESV (ml)	35.0 ± 11.2	43.2 ± 24.4	0.175
EF (%)	62.7 ± 5.3	61.1 ± 6.5	0.37
Ea (cm/s)	10.1 ± 1.6	6.1 ± 1.6	0.001
E Acc (cm/s^2)	871.5 ± 128.1	549.2 ± 151.9	0.001
E/A	1.9 ± 0.5	0.7 ± 0.2	< 0.001
Et VI (cm)	10.6 ± 2.9	7.8 ± 2.5	0.003
At VI (cm)	5.5 ± 2.1	11.7 ± 3.7	0.0001
Time to acc (ms)	86.7 ± 15	93.2 ± 2.5	0.114
Heart period (ms)	920.1 ± 168.7	895.7 ± 208.5	0.675

Values expressed as mean ± standard deviation

EDV (ml)   End diastolic volume in millilitres
ESV (ml)   End systolic volume in millilitres
EF (%)   Ejection fraction as a percentage of blood ejected per cardiac cycle
Ea (cm/s)   Peak early mitral ring tissue velocity recorded by DTI
E Acc (cm/s^2)   Acceleration of blood across the mitral valve in early diastole
E/A   Ratio of peak early diastolic flow over peak late diastolic flow
Et VI (cm)   Time velocity integral of early diastole in centimetres
At VI (cm)   Time velocity integral of late diastole in centimetres
Time to Acc (ms)   Time to peak acceleration of early diastole in milliseconds
Heart period (ms)   R to R interval in milliseconds

Table 6.1 (b) Means adjusted for age

	Normal controls (n = 22)	Diastolic dysfunction (n = 25)	p value
EDV (ml)	90.2 ± 8.53	99.2 ± 8.79	0.473
ESV (ml)	36.0 ± 4.91	43.4 ± 5.06	0.165
EF (%)	62.2 ± 1.47	61.1 ± 1.38	0.144
Ea (cm/s)	11.8 ± 0.73	6.08 ± 0.67	< 0.001
E Acc (cm/s^2)	870.1 ± 39.0	548.3 ± 35.8	< 0.0001
E/A	1.81 ± 0.11	0.69 ± 0.10	< 0.001
Et VI (cm)	10.4 ± 0.70	8.00 ± 0.7	0.042
At Vl (cm)	5.2 ± 2.20	12.20 ± 3.8	0.09
Time to Acc (ms)	83.18 ± 13.0	87.60 ± 12.0	0.466
Heart period (ms)	825.4 ± 45.9	848 .9 ± 42.1	0.998

Values expressed as mean ± standard deviation

Chapter 7

The potential of DTI in distinguishing pathological from physiological LVH [1]

Because cardiac hypertrophy gives rise to ventricular dysfunction in systole and diastole, it was decided to investigate the ability of DTI to reveal fine details of the early diastolic mechanism, and its potential therefore to provide diagnostic differentiation between pathological and physiological left ventricular hypertrophy (LVH), as well as between LVH and the normal heart. Furthermore a novel index of myocardial stiffness was investigated to help make this crucial differentiation.

In elite young athletes, the differentiation of hypertrophic cardiomyopathy (HCM) from physiological left ventricular hypertrophy associated with training (commonly referred to as 'athlete's heart') with the risk of sudden death, is an important clinical problem (Rost, 1982; Hutson *et al*, 1985; Maron, 1986; Maron *et al*, 1994). It is important to differentiate between those who have a thickened heart that is normal, from those who have a thickened heart due to a disease process like HCM. This vital diagnostic distinction most frequently involves HCM (Maron *et al*, 1994). Most exercise-related sudden cardiac deaths from HCM occur in adolescence (14 to 18 years old) (Maron *et al*, 1980; Maron *et al*, 1986; Maron *et al*, 1993). Awareness of

---

[1] A paper based on the study reported in this chapter, King G, JB Foley, J Cosgrave, G Boyle, M Hussey, K Bennett, P Crean, M Walsh, "Differentiation in the 'grey zone': novel applications of Doppler Tissue Imaging to distinguish physiological left ventricular hypertrophy in athletes from hypertrophic cardiomyopathy", has been submitted to Journal of the American College of Cardiology and a copy of the paper is provided in Appendix F.

this issue, as well as the corresponding consideration of athletic screening before

training, has been heightened by a number of recent high-profile cases of elite

basketball and football players who died suddenly and unexpectedly from suspected

cardiovascular disease.

Differentiation between athlete's heart and left ventricular hypertrophy associated

with cardiac disease has important implications, because identification of

cardiovascular disease in an athlete may be the basis for disqualification from

competition in an effort to minimize risk (Maron *et al*, 1994). Conversely, an

improper diagnosis of cardiac disease in an athlete may lead to unnecessary

elimination, thereby depriving that individual of a career in sports.

The application of non-invasive techniques to aid in making this diagnostic distinction

and planning subsequent clinical tactics has increased in recent times. This issue has

not been examined in a comprehensive fashion, and the work reported in this chapter

is a contribution to this examination. In preparation for this, it is of value to review

the available data to develop a practical approach to the decision-making process in

the identification of cardiovascular disease and risk of sudden death in athletes.

Because athlete's heart results in an increase in the size and mass of the myocardium,

most frequently that of the left ventricle, it is to be expected that this will result in

changes to the dynamics of that myocardium, and be readily studied by

echocardiographic techniques such as DTI. This technique measures the mobility of

the cardiac tissues and blood, including the relative phasing in time of the elements of

the early diastolic mechanism.

7.1   Causes of sudden death in athletes

Many cardiovascular diseases have been identified as potential causes of sudden death in young athletes.

The most common cause among athletes under 35 years of age appears to be HCM (Maron *et al*, 1980; Maron *et al*, 1986; Maron *et al*, 1993; Burke *et al*, 1991). There are many more less common causes and they incorporate a variety of congenital coronary artery anomalies, myocarditis, dilated cardiomyopathy, Marfan's syndrome, and right ventricular dysplasia (Thiene *et al*, 1988; Corrado *et al*, 1990). The more uncommon causes of these athletic field catastrophes include sarcoid, mitral valve prolapse, aortic valve stenosis, atherosclerotic coronary artery disease, and QT-interval prolongation syndromes.

Among athletes over 35 years of age, mainly those interested in individual activities such as long-distance running, sudden death tends to be caused mainly by coronary artery disease (McKeag, 1989).

7.1.1   Dilated cardiomyopathy

Increases in left ventricular diastolic cavity dimensions that occur with training is similar to and overlaps with the characteristic findings of dilated cardiomyopathy. For example, while left ventricular end-diastolic cavity diameter in athletes is usually in the range of 53 to 58 mm, in some individuals it may extend into what may be

regarded as the pathological range of > 58 mm and thereby resemble dilated cardiomyopathy (Pelliccia *et al*, 1991). However, the absence of left ventricular systolic and diastolic dysfunction and the presence of an acceptable ejection fraction are usually sufficient to distinguish this physiological ventricular enlargement induced by training from that due to the pathological condition of dilated cardiomyopathy.

7.1.2   *Myocarditis*

Myocarditis, a rare disorder usually caused by viruses, has recently been implicated as the possible cause of some highly publicized deaths in athletes (Maron, 1993; Maron *et al*, 1994). While myocarditis usually has an infectious origin, it can also be a consequence of drug abuse such as the intake of cocaine. Sudden death with myocarditis is usually associated with a ventricular arrhythmia (Isner *et al*, 1986; Tazelaar *et al*, 1987; Kloner *et al*, 1992). In an athlete with myocarditis, left ventricular cavity enlargement may be due to the disease, to athletic training, or to a combination of these, but the differential diagnosis with athlete's heart is usually resolved by the presence of tachycardia in the absence of fever and, more importantly, arrythmias, syncope, presyncope, or heart failure with systolic dysfunction. The diagnosis may also be clarified by histological examination of myocardium obtained by endomyocardial biopsy during cardiac catheterisation. Routine assessment by this technique is not normally practicable.

7.1.3   *Arrythmogenic right ventricular dysplasia (ARVD)*

Arrythmogenic right ventricular dysplasia (ARVD) (or cardiomyopathy) is a heart muscle disorder of unknown cause that is characterized pathologically by fibrofatty replacement of the right ventricular myocardium (Thiene *et al*, 1988; Corrado *et al*, 1990; McKenna *et al*, 1994). This disease may be hereditary and includes structural and functional abnormalities of the right ventricle, ventricular and supraventricular arrhythmias. It carries the risk of sudden cardiac death (Thiene *et al*, 1988; McKenna *et al*, 1994). Autopsy studies identified right ventricular dysplasia as a cause of death in six of twenty seven young athlete deaths studied in northern Italy (Thiene *et al*, 1988; Corrado *et al* 1990).

The problem of differentiating from healthy physiological responses also arises in this group of patients.

Because highly trained athletes may demonstrate right ventricular enlargement and a variety of conduction abnormalities on the ECG, the differential diagnosis between athlete's heart and right ventricular dysplasia may arise (Rost, 1982; Hauser *et al*, 1985; Hutson *et al*, 1985; Zehender *et al*, 1990). Identification of right ventricular dysplasia may be difficult because of technical limitations inherent in 2-D echocardiography imaging of right ventricular structure and assessing function in these patients and because the spectrum of the disease is broad and includes mild morphological forms with subtle manifestations (Robertson *et al*, 1985; McKenna *et al*, 1994). Suspicion of ARVD on the echocardiogram is revealed by abnormal shape and wall motion of the right ventricle. The best current solution seems to be magnetic

resonance imaging because this technique provides enhanced non-invasive diagnosis of this condition (Ricci *et al*, 1992). A standardised diagnostic criterion for diagnosis of ARVD was proposed by McKenna *et al* (1994). ARVD should be strongly suspected in a patient with ventricular tachycardia of left bundle branch block morphology or in a young adult who has died suddenly. Echocardiography and angiographic studies showing dilated right ventricle with outpouching in the free wall are useful in making the diagnosis. Also, the demonstration of right ventricular segmental or global dysfunction or substantial right ventricular cavity enlargement would support the diagnosis of right ventricular dysplasia; alternatively, thickening or enlargement of the left ventricle would be most consistent with athlete's heart (Rost, 1982; Hutson *et al*, 1985; Maron, 1986).

7.1.4   *Hypertrophic cardiomyopathy*

Hypertrophic cardiomyopathy is an autosomal-dominant congenital disorder usually characterised by left ventricular outflow tract obstruction with asymmetrical septal hypertrophy and marked disarray of ventricular muscle fibres. The left ventricular cavity is usually not dilated. A pathological description by Hallopeau (1869) is often cited as the first description of the disease. However the first real recognition of this condition as a distinct entity was made by a British pathologist, Teare (1958). He described the major features, namely hypertrophy of the ventricles, predominantly involving the septum, with a reduced cavity size, "disarray" in the alignment of myocytes, a familial pattern and a risk of sudden death. Brock is credited with a case report about the same time (Brock, 1957). Electrocardiography may show left ventricular hypertrophy or other changes, but interestingly the ECG may be normal.

Several studies were published describing the clinical, electrocardiographic and

haemodynamic features of the disease (Braunwald *et al*, 1964). The introduction of

echocardiography had a major impact on the assessment of hypertrophic

cardiomyopathy and still remains the cornerstone of diagnosis.

The mechanisms of sudden death and syncope in hypertrophic cardiomyopathy

remain controversial, probably because a number of mechanisms may be responsible

and the predominant mechanism may vary with age. It is likely however that in

adults, ventricular arrhythmia is the cause of sudden death. The diagnosis of HCM is

based on the WHO definition of the disease, the finding of a non-dilated left ventricle

on 2-D echocardiography in the absence of hypertension, valvular disease or any

other systemic cause of hypertrophy (Maron, 2002). It must be remembered that an

athlete's heart undergoes adaptive changes in response to regular physical exercise

that can mask some abnormal characteristics such as pathological left ventricular

hypertrophy. Therefore, it is often difficult to distinguish physiological (normal)

LVH adaptations from pathological (disease) processes.

The problem with the definition of hypertrophic cardiomyopathy lies in the concept

that the criterion for clinical diagnosis is a maximum wall thickness greater or equal

to 15 mm. It has been shown that depending on the mutant gene, virtually any wall

thickness (including those in the normal range) could be compatible with HCM.

The clinical study reported in this chapter aims to provide clinical criteria to

distinguish pathological from physiological LVH.

7.2   Current screening methods and their limitations

7.2.1   Epidemiological Studies

Several echocardiographic studies have estimated the prevalence of HCM in the

general population to be 0.2% (Maron *et al*, 1980; Maron *et al*, 1986). The

investigators in the Coronary Artery Risk Development in Adults (CARDIA) study

reported an almost identical prevalence of HCM (Maron *et al*, 1993). The CARDIA

study was initially designed to investigate the longitudinal influence of lifestyle and

other factors on the risk of coronary heart disease in a biracial cohort of adults 18 to

30 years old (Lewis *et al*, 1989). Recruitment to the study was from four urban areas.

In a subset of this population, the CARDIA investigators identified 7 patients with

HCM out of 4111 study subjects. HCM was estimated to be 2.9 times more common

in men than women and 2.4 times more common in blacks than whites. HCM was

mild in almost every case. Only 1 patient had significant LV outflow tract

obstruction. Two of the 7 patients had normal 12-lead ECGs. An additional 5 subjects

with LV wall thickness of 15 to 21 mm were not thought to have HCM because of

coexisting hypertension.

It is possible to either underestimate or overestimate the prevalence of HCM through

the choice of the locality from which subjects are recruited. For example, it has been

observed in family/genetic studies that it is not uncommon for many members of an

extended HCM family to reside in rural areas around a small town (Rost, 1982;

Hutson *et al*, 1985). It is therefore possible that the disease is under-represented in the

four urban areas that were part of the CARDIA study. Conversely, if by chance an

epidemiological study includes one of these large local families, a false impression

would be created that HCM is very prevalent among young and otherwise healthy

adults.

7.2.2   Echocardiography definitions

The echocardiogram is considered to be a sensitive and specific means of detecting

HCM. Several studies have reported on the application of echocardiography to

assessing athlete's heart. In the majority of elite athletes, left ventricular wall

thickness is normal or only mildly increased (≤12 mm) (Morganroth et al, 1975;

Gilbert et al, 1977; Ehsani et al, 1978; Ikaheimo et al, 1979; Longhurst et al, 1980;

Nishimura et al, 1980; Bekaert et al, 1981; Keul et al, 1981; Longhurst et al, 1981;

Rost, 1982; Fagard et al, 1983; Shapiro et al, 1983; Shapiro, 1984; Hauser et al, 1985;

Hutson et al, 1985; Douglas et al, 1986; Maron, 1986; Milliken et al, 1988; Fisher et

al, 1989; Pelliccia et al, 1991; Pelliccia et al, 1993; Spirito et al, 1994). In some

athletes, however, the increase in left ventricular wall thickness may be more

substantial, up to 16 mm, therefore unavoidably raising the possibility of HCM

(Pelliccia et al, 1991). In the majority of patients with HCM an increase in left

ventricular wall thickness exists and is usually substantial. Wall thickness reported in

this disease is about 20 mm and ranging to >50 mm (Maron et al, 1981; Maron et al,

1984; Louie et al, 1986; Spirito et al, 1989). However, an important minority of

patients with HCM show relatively mild left ventricular hypertrophy with wall

thickness values in the range of about 13 to 15 mm, and many of these patients are

asymptomatic (Spirito et al, 1986; Maron et al, 1987; Spirito et al, 1989; Klues et al,

1993). The important question to be resolved once an athlete is diagnosed as having

LVH is whether it is a normal physiological response of a pathological phenomenon, with hypertrophic cardiomyopathy being the most serious possibility. A diagnostic dilemma arises in those athletes who fall into this "grey zone" between physiological hypertrophy and HCM (Maron, 1986). This is indicated schematically in Figure 7.1. While this distinction cannot be resolved with certainty in some of these athletes, careful analysis of several echocardiographic and clinical features permits this diagnostic differentiation in most cases.

In highly trained athletes, thickening always involves the anterior septum, while the thicknesses of other walls are similar (with differences in the range of 1 to 2 mm). In patients with HCM, wall thickening, and the pattern of hypertrophy, is usually asymmetrical. Other areas such as the anterior septum may show the most marked thickening (Maron *et al*, 1981; Ciró *et al*, 1983; Maron *et al*, 1987; Klues *et al*, 1993). The diagnosis of HCM in asymptomatic athletes is frequently based solely on the echocardiographic assessment of the size and extent of the hypertrophy. Exact measurements are essential and care should be taken not to include any right ventricular structures when measuring the septum. In these circumstances the mis-diagnosis of HCM may occur. This, in turn, creates considerable stress and anxiety to the athlete by creating an unnecessary perception of heart disease.

Since a marked increase in left ventricular wall thickness often occurs during adolescence in patients with HCM, young athletes with HCM (<18 years old) may not demonstrate their maximum magnitude of hypertrophy until full physical maturation and development is achieved (Maron *et al*, 1986). Therefore, an athlete with HCM may initially be evaluated with echocardiography when the hypertrophy is still only

mild and within the borderline range. The differential diagnosis with athlete's heart

may be difficult at that point in time. However, this uncertainty can be resolved by

serial echocardiographic examinations, which, within months or years, may show

more definite left ventricular wall thickening and confirm the diagnosis of HCM.

It is possible to distinguish the athlete's heart from HCM on the basis of left

ventricular internal cavity dimensions. An enlarged left ventricular end-diastolic

internal cavity dimension (> 55 mm) appears to be present in more than one third of

highly trained elite male athletes, especially rowers (Pelliccia *et al*, 1991; Spirito *et al*,

1994). Conversely, the diastolic cavity dimension is small, usually <45 mm, in most

patients with HCM, and it is >55 mm only in those patients who evolve to the end-

stage phase of the disease with progressive heart failure and systolic dysfunction

(Spirito *et al*, 1987). For example, a cavity >55 mm in an athlete with borderline wall

thickness would constitute strong evidence against the presence of HCM; conversely,

a cavity dimension < 45 mm would be inconsistent with the athlete's heart. However,

cardiac alterations associated with training differ somewhat depending on the

particular sport in which the individual participates. Cavity dimension alone would

not resolve this differential diagnosis.

Because of the wide variety of ECG alterations present in both athletes without

cardiovascular disease and patients with HCM, the 12-lead ECG is not particularly

useful in distinguishing between these two entities (Klemola, 1951; Zehender *et al*,

1990). However, it has been shown that peculiar ECG patterns with markedly

increased voltages, prominent Q waves, or deep, negative T waves are a feature of

HCM and suggest strongly a positive diagnosis (Maron *et al*, 1983; Alfonso *et al*, 1990; Lemery *et al*, 1990).

When assessing whether an athlete with increased wall thickness has HCM or not, detailed knowledge of the training regimen is relevant. Different types of athletic training have important effects on the way the left ventricle adapts and on the magnitude of the changes in the dimensions of the left ventricle major (Morganroth *et al*, 1975; Gilbert *et al*, 1977; Ikaheimo *et al*, 1979; Longhurst *et al*, 1980; Nishimura *et al*, 1980; Bekaert *et al*, 1981; Keul *et al*, 1981; Longhurst *et al*, 1981; Shappiro *et al*, 1983; Hauser *et al*, 1985; Fisher *et al*, 1989; Pelliccia *et al*, 1991; Pelliccia *et al*, 1993; Spirito *et al*, 1994). For example, in a study of almost 1000 elite Italian athletes, only about 2% had a left ventricular wall thickness ≥ 13 mm (in the 'gray zone' between physiological hypertrophy and HCM), and this subgroup was confined to rowing sports and cycling (Pelliccia *et al*, 1991). Another important conclusion related to other forms of training, including isometric (or power) sports such as weight-lifting and wrestling, which showed mild increases in wall thickness beyond 12 mm (Pelliccia *et al*, 1993). Left ventricular wall thickness is different in trained athletes of various ethnic and racial origins, although this issue has not yet been resolved.

This definition, however, has significant limitations.

1.   It fails, even in adults, to identify many patients with HCM who have inherited a disease gene but who have not developed LVH.

135

2.   It excludes patients who do have HCM but who have another coexisting

        disease that may contribute to the LVH, such as hypertension or valvular heart

        disease.

3.   The clinical outcome of HCM patients may correlate poorly with the severity

        of the LVH.

7.2.3   Genetic testing

The absence of HCM in family members, however, does not exclude HCM, since the

disease may be sporadic (i.e. absent in relatives other than the index case), possibly as

a result of de novo mutations (Watkins *et al*, 1992). In 1989 a group in Boston

reported the first positive genetic linkage study in hypertrophic cardiomyopathy

(Jarcho, 1989). They found strong linkage to an area of chromosome 14 near the

locus for the cardiac myosin heavy chain gene. The most definitive evidence for the

presence of HCM in an athlete with a significant increase in wall thickness would

probably come from the demonstration of the disease in a relative of that particular

athlete (Ricci *et al*, 1992; Geisterfer-Lowrance *et al*, 1990; Thierfelder *et al*, 1994).

Echocardiographic screening of family members, in those athletes in whom the

distinction between HCM and athlete's heart cannot be achieved might be one way of

resolving this diagnostic uncertainty.

Recent advances in the understanding of the genetic alterations responsible for HCM

raise the possibility of DNA diagnosis in athletes suspected of having this disease

(Geisterfer-Lowrance *et al*, 1990; Watkins *et al*, 1992; Thierfelder *et al*, 1994). The

genetic abnormalities that cause HCM, however, are greatly heterogeneous. At

present, mutations responsible for HCM have been identified in three genes located on

chromosomes 14, 1, and 15; these genes encode the contractile proteins ß-myosin

heavy chain, cardiac troponin T, and α-tropomyosin, respectively. A fourth gene locus

on chromosome 11 has been shown to be involved (Carrier *et al*, 1993). Thus,

mutations of at least four different genes can cause HCM. This substantial genetic

heterogeneity of the disease makes it extremely difficult and time consuming at

present to use the techniques of molecular biology for the purpose of resolving

clinically the differential diagnosis between athlete's heart and HCM.

7.2.4   *Doppler transmitral flow waveforms*

Abnormalities of left ventricular diastolic filling have been identified noninvasively

with pulsed Doppler echocardiography in many patients with a variety of cardiac

diseases associated with left ventricular hypertrophy, such as systemic hypertension

and HCM (Maron *et al*, 1987; Phillips *et al*, 1987; Appleton *et al*, 1988; Stoddard *et

al*, 1989; Lewis *et al*, 1992). Most patients with HCM, including those with relatively

mild hypertrophy that could be confused with athlete's heart, show abnormal Doppler

diastolic indexes of left ventricular filling. These abnormalities can be subtle and

independent of whether symptoms or outflow obstructions are present or not (Maron

et al, 1987; Lewis *et al*, 1992). Typically, the early peak of transmitral flow-velocity

("E," due to rapid filling) is decreased and deceleration time of the early peak is

prolonged; the late peak ("A," due to atrial contraction) is increased, inverting the

normal E/A ratio in stage 1 diastolic dysfunction. Other stages of diastolic

dysfunction such as pseudo-normalisation may present in HCM. Trained athletes

have demonstrated normal left ventricular filling patterns (Colan *et al*, 1985; Granger

et al, 1985; Finkelhor *et al*, 1986; Pearson *et al*, 1986; Fagard *et al*, 1987; Nixon *et al*,

1991; Pelliccia *et al*, 1991; Lewis *et al*, 1992). Consequently, athletes suspected of

having HCM should show a distinctly abnormal Doppler pattern of transmitral flow-

velocity along with an increase in the isovolumic relaxation time and this should

strongly support the diagnosis, while a normal Doppler pattern can be compatible with

either HCM or athlete's heart. A comprehensive Doppler echocardiographic study

should be performed on all athletes to rule out pseudo-normalisation. This should

include pulmonary vein velocities and DTI.

7.2.5   *Ultrasound myocardial reflectivity measured by integrated backscattered signal*

The acoustic properties of the myocardium have been used for the purpose of

resolving the differential diagnosis between athlete's heart and HCM (Lattanzi *et al*,

1991; Lattanzi *et al*, 1992). Initial observations suggest that most asymptomatic (or

mildly symptomatic) patients with HCM show increased intensity of the ultrasound

signal from the septum and posterior free wall (including patients with mild and

localized hypertrophy), while highly trained athletes with physiological hypertrophy

show normal myocardial tissue reflectivity. However this technology is limited and is

mostly available in research laboratories only. In addition, it is not known whether

differences in the backscatter signal identified by group comparisons can be used, or

not, to distinguish athlete's heart from cardiac disease in the individual subject.

7.2.6   *Transoesophageal echocardiography*

Transoesophageal echocardiography provides little additional information other then a better visualisation of the proximal coronary artery (Pelliccia *et al,* 1993).

7.2.7   *Magnetic resonance imaging*

Changes in the athlete's heart are due to the need to sustain continuous muscular work by increasing oxygen transportation. Magnetic resonance imaging is a useful tool in evaluating myocardial hypertrophy and function of the athletic heart. It is also useful in visualizing the increase in cross-sectional area of the left coronary artery system. Different studies using magnetic resonance imaging have previously demonstrated a direct relationship between coronary artery size and myocardial mass. Hypertrophic hearts however show an increase in fibrous tissue but coronary vascular dilation would not be proportional to the increased total muscle mass in this disease entity. This might be seen as a method to differentiate HCM from athletic heart, i.e. coronary artery size in the absence of cardiovascular disease would be greater in the athletes with physiological left ventricular hypertrophy compared to the HCM patient. However the enlargement of the coronary arteries did not appear to keep pace with that of myocardial mass up to a certain size. In a study by MacAlpin (1996) in patients with hypertrophic cardiomyopathy the left main coronary artery measured 4.4 mm ± 0.7 compared with left main diameters of 5.4 mm ± 0.9 in athletes, suggesting the increase in capacity of the left coronary system in the athletes.

Magnetic resonance imaging is a useful tool in evaluating myocardial physiological hypertrophy and functional changes of athlete's heart. Myocardial mass and coronary diameter can all be accurately assessed by magnetic resonance imaging.

7.2.8 Detraining

Various studies have shown that increases in left ventricular cavity size or wall thickness are physiological consequences of athletic training. For example, elite athletes with left ventricular hypertrophy have shown a reduction in wall thickness of about 2 to 5 mm within 3 months of deconditioning (Maron et al, 1993). Serial echocardiographic examinations showing a clear decrease in cardiac dimensions and mass after athletic deconditioning have been carried out (Ehsani et al, 1978; Fagard et al, 1983; Shapiro et al, 1983; Maron et al, 1993). Identification of such changes in wall thickness with deconditioning, however, requires serial echocardiographic studies of optimal technical quality. It is important to remember that changes in left ventricular wall thickness with deconditioning are inconsistent with the presence of pathological hypertrophy and HCM. However obtaining compliance from highly motivated and competitive athletes to interrupt training to prove the diagnosis may prove difficult.

7.2.9 DTI

The potential contribution of DTI, in combination with other echocardiography modalities, to distinguish pathological from physiological LVH is developed experimentally in the remainder of this chapter.

7.2.10 Conclusions

In highly trained athletes with substantial left ventricular hypertrophy, it is of critical

importance to clarify whether the increased left ventricular wall thickness represents

the expression of the physiological adaptation of the heart to athletic training or a

pathological condition such as HCM. While at present there is no single approach that

will definitively resolve this question in all such athletes, several strategies are

described here that, alone or in combination, offer a large measure of clarification in

most instances for this often compelling diagnostic dilemma. However problems with

routine widespread screening of athletes include the limitations inherent in the

analytical value of available diagnostic procedures and the cost of testing large

populations.

7.3   Using DTI to measure the early diastolic mechanism and peak early tissue velocity (Ea) in order to distinguish pathological from physiological LVH

Recoil in the normal heart provides the potential energy for rapid early diastolic

filling and occurs during the isovolumic relaxation time before left ventricular filling.

However, in patients with left ventricular hypertrophy (LVH) recoil can occur during

or after filling. In LVH, if peak early tissue velocity (Ea) is taken as a marker of

recoil then Ea would be expected to reach its peak before mitral inflow. In normal

subjects the reverse would be expected to be true. The aim of the study reported in

this chapter is to investigate the clinical utility of both the timing of the early diastolic

mechanism and peak early tissue velocity (Ea), obtained with Doppler tissue imaging

(DTI) to differentiate between pathological and physiological LVH.

The elite athlete invariably suggests someone of excellent health and well-being.

Therefore sudden death in athletes is one of the great catastrophes in sport because of

its unexpectedness (Maron *et al*, 1996). As outlined above, screening athletes to

identify and counsel those at risk of sudden death remains a great challenge because

the athlete's heart undergoes adaptive changes in response to regular physical exercise

that can mask some pathological abnormalities (Spirito *et al*, 1994). It is often

difficult to distinguish physiological adaptations from pathological processes. The

many methods currently employed to help guide athletes through the medical

conundrum of left ventricular hypertrophy (physiological) or left ventricular

hypertrophy (pathological) are not comprehensive and are frequently bypassed

(Fananapazir *et al*, 1995).

DTI is a relatively new ultrasound modality that can be used to record systolic and

diastolic velocities within the myocardium (Mc Dicken *et al*, 1992; Erbel *et al*, 1996).

A number of studies have recorded mitral ring displacement and velocity both in

systole and diastole as indicators of overall cardiac performance (Fukuda *et al*, 1998;

Galiuto *et al*, 1998; Nagueh *et al*, 2001). Long axis dynamics, apical displacement of

the mitral ring, are associated with fibres in the subendocardium, which are aligned

longitudinally from apex to base. The velocities of the mitral ring can be quantified

using DTI (Greenbaum *et al*, 1981; Keele, 1983).

In the normal subject, during ventricular diastole, the peak mitral ring velocity (Ea) recorded by DTI precedes the peak early passive diastolic transmitral flow (E) recorded by conventional pulsed wave (PW) Doppler systems. In situations where diastole is impaired, Ea follows E (Rodriguez *et al*, 1996). This observation supports the concept that elastic recoil is related to mitral ring motion and that this early diastolic mechanism of augmenting the onset of mitral flow velocity is lost in patients with diastolic dysfunction and pathological LVH (Buchalter *et al*, 1994; Rodriguez *et al*, 1996).

This study was designed to evaluate the relative timing of the peak early diastolic tissue velocity (Ea) by DTI and the peak opening of the mitral valve by M-mode, both recorded simultaneously. A novel index of myocardial stiffness was developed and used to diagnostically distinguish hypertrophic cardiomyopathy (HCM) from athletic physiological left ventricular hypertrophy in the Maron 'grey zone'.

7.3.1   Experimental approach used

7.3.1.1 Study group selection

This study was approved by the local hospital research ethics committee, and each subject gave informed consent to their participation. Copies of the ethics approval and the subject consent form are given in Appendix B. The study population was composed of three age- and sex-matched adult groups.

Between 2002 and 2004 ongoing research of 27 patients diagnosed with hypertrophic cardiomyopathy (HCM) led to the identification of 11 (30%) adults with characteristics of mild HCM without left ventricular outflow tract obstruction. They were identified as having HCM based on a combination of clinical presentation, family history of HCM, absence of hypertension or of training that would induce LVH, and exclusion of other conditions that could cause cardiac infiltration. Resting Doppler and DTI indices of diastolic dysfunction were also recorded and each patient had a left ventricular wall thickness of > 13 mm.

The physiological LVH group were identified among 34 highly trained international rowers who had trained intensively 15 to 20 hours/week for more then 5 years and who underwent 2-D echocardiography and DTI evaluation. None had a family history of HCM or premature sudden cardiac death and all were normotensive. Of the 34 rowers 17 (50%) had a left ventricular wall thickness (LVWT) ≥ 12 mm. A control group of 30 sedentary normal subjects was recruited from hospital personnel who included young hospital doctors and medical students.

Following informed consent the participants were enrolled in their groups. Patients were excluded if they had abnormal rhythm, including atrial fibrillation, known coronary artery disease, valvular incompetence beyond a modest degree, or if echocardiographic images were technically inadequate for complete analysis. The general characteristics of the study groups are presented in Table 7.1.

7.3.1.2 Echocardiographic examination

Images were obtained with the Agilent/Philips 5500 and Agilent/Philips 4500 cardiac
ultrasound systems. The specifications for these scanners are given in Appendix A.
Standard apical views made it possible to record the DTI at four sites - medial, lateral,
inferior and anterior - around the mitral ring. The characteristic velocity profile of
diastole was obtained in all patients. In each case, peak early (E) and late (A)
diastolic mitral ring velocities were recorded, as well as the E/A ratio, acceleration
time, acceleration and time/velocity integrals of early and late filling. Recordings at a
sweep speed of 100 mm/s allowed for correct temporal observations. Measurements
were performed from these recordings off-line by an independent observer with no
knowledge of the M-mode timings, Doppler or DTI findings. At least three
measurements of each parameter were taken and the average of these calculated.

7.3.1.3 Triggering the time bases on the two separate scanners at the same time

The time delay between peak tissue ring velocity Ea and peak mitral opening was
measured by taking simultaneous DTI and M-mode measurements with the two
scanners. A rectangular time reference pulse was introduced into unused ECG
channels on both machines by pressing a footswitch activated circuit, as described in
Appendix A. The time intervals from this pulse edge to Ea on one machine and to
peak mitral opening on the other were measured using the machines' electronic
callipers. The difference between these values yielded the time delay. Calliper time

resolution at the sweep speed used was 10 ms (i.e. ± 5 ms) and so that the time

difference measurement resolution was then ± 10 ms.

7.3.1.4 Echocardiographic data analysis

Echocardiographic data analysis was performed off-line for calculation of left

ventricular volume, ejection fraction and left ventricular mass. Left ventricular mass

was estimated by the method of Devereux (1987) by applying the Penn convention.

7.3.1.5 Long axis function by DTI

The four-site mean velocity was calculated thus, (M+L+I+A)/4, where M, L, I and A

are the peak velocities of the medial, lateral, inferior, and anterior points on the

selected in the 2-D image of the mitral ring respectively. With the sample volume

(gate 6 mm) placed over each of these points in turn on the mitral ring, the cursor was

aligned to ensure an angle of incidence as close as possible to $0°$.

7.3.1.6 New non-invasive index of passive diastolic stiffness

Diastolic stiffness was assessed with the use of three indices transmitral E blood

velocity, TDI Ea velocity, and the left ventricular end diastolic diameter in diastole

(LVIDd). The ratio E/Ea represents an index of left ventricular filling pressure and

has been shown to be related inversely with the time constant of relaxation (Nagueh *et

al*, 1999), and LVIDd was used as an index of ventricular volume. The ratio of these

two parameters, (E/Ea)/(LVIDd) provides a novel index of diastolic performance and

is a rough estimate of end diastolic stiffness. This index was calculated for each subject in the study.

7.3.2   *Statistical analysis*

Results are presented as mean values and standard deviations (SD) where the data are normally distributed and median values with inter-quartile ranges (IQR) where the data are non-normally distributed. For comparisons between athletes and HCM patients, a student's t-test or non-parametric Wilcoxon rank sum test was used where appropriate. Box and whisker plots are used for displaying the data. Sensitivity, specificity and accuracy were assessed using standard methods. Inter-observer variability was examined for Ea (average) and time difference using a non-parametric correlation of association between the measurements (Dickhuth *et al, 1994*). A $p < 0.05$ for a 2-tailed test was considered statistically significant. All statistical analyses were performed using the JMP statistical analysis package (SAS Inst. Inc). One-way analysis of the differences in the new index of diastolic stiffness between the groups was assessed by the Kruskal-Wallis test.

Using the method of Bland & Altman (1986), where the difference between measurements is plotted against the average, and the correlation calculated. If the correlation is close to zero there is little or no bias associated with the measurements. The correlation r was found to be 0.0097 ($p = 0.622$) for reproducibility for each four-site average, and r was found to be 0.061 ($p = 0.758$) for the time difference. This suggests that there was negligible inter-observer bias in the measurements.

7.3.3 Results

The general characteristics of the study group are presented in Table 7.1. The raw data for all measurements taken are tabulated in Appendix G and the summary echocardiographic data obtained are listed in Table 7.2.

The mean age between the HCM patients, athletes and normals was not statistically significant. Body surface area in m^2 (BSA) in the athlete group was slightly higher than in the normal/control and HCM groups, 2.0 (2.0, 2.0) vs. 1.84 (1.6, 2.0) m^2 and 1.93 (1.9,1.9) respectively. As might be expected heart rate (per minute) was lower in the athletes compared with the normal and HCM groups (65 ± 11 vs. 70.0 ± 5.0 and 67.0 ± 5.0 respectively) (Table 7.1).

Patients with HCM without pseudo-normalisation had a longer isovolumic relaxation time (in ms) than the athlete and normal groups, median 90 (IQR 80, 10) vs 80 (71, 80) and 80 (70, 80) respectively, as shown in Table 7.2, and greater LV mass index than the normals. The athletes had a greater LV mass index than the HCM patients. Patients with HCM had lower long axis systolic and early diastolic velocities compared with the athlete and normal groups at all four sites of the mitral ring (Table 7.2 and Figure 7.2). They had a higher calculated left ventricular filling pressure E/Ea index (mean = 10.1 ± 2.8) than the normal (mean 7.1 ± 1.1) and athletic group (mean = 6.4 ± 1.63), p = 0.0001.

7.3.3.1 Timing of the early diastolic mechanism

In the athlete group the **peak early diastolic ring tissue velocity preceded the peak mitral E** of the M-mode on average by a median of 20 ms (1QR 20, 10), and in the normals by a median of 15 ms (IQR 0, 30), compared with the HCM group where the situation is reversed and the **peak mitral E observed by the M-mode display preceded the peak early diastolic tissue velocity** by a median of 10 ms (1QR 0, 20), with $p < 0.0001$, as shown in Figure 7.3.

7.3.3.2 A novel index of left ventricular performance (E/Ea)/(LVIDd)

The pressure index E/Ea was found to be higher and LVIDd lower in the HCM group compared with the controls and the athletes,, as shown in Table 7.2. Furthermore, E/Ea was lower and LVIDd higher in athletes compared with normals and HCM patients. This suggests that the ratio, (E/Ea)/(LVIDd), could prove an index of left ventricular performance that might readily provide distinctions between HCM patients, athletes and normals, as shown also in Table 7.2. The athletes have a lower value of this index of left ventricular performance than the normals and HCM patients, 1.2 (0.9, 1.4) compared with the normal average 1.5 (1.3, 1.6) and the HCM average 2.2 (2.0, 2.3), $p < 0.0001$, and this is shown in Figure 7.4.

7.3.3.3 Differentiating between pathological and physiological hypertrophy

As shown in Figure 7.2, a mean diastolic velocity < 10 cm/s differentiated pathological from physiological hypertrophy. Also the time delay from early diastolic tissue velocity peak Ea to the early M-mode peak E provided a strong differentiation between the HCM and the athlete's heart in the 'grey zone'. All patients with HCM had values ≥ 0 for the four-site average time difference, and all athletes had values < 0 and therefore there was complete discrimination between these two groups. Testing all seven criteria listed in Table 7.3 (a), the best differentiation was provided by (1) a novel index of myocardial performance of < 1.7 and (2) the association of the time delay between the early mitral M-mode E and the early diastolic tissue velocity of 0.0 ms (i.e. both occurring at the same time or are possibly reversed), based on standard statistical methods to calculate sensitivity and specificity (Bland *et al*, 1994). Tables 7.3 (a) show a range of echocardiographic criteria for differentiating between patients with pathological LVH and athletes with LVH.

Testing all six criteria listed in Table 7.3 (b), the best differentiation was provided by the association of a mean early diastolic mitral ring velocity < 10 cm/s, a ratio of (septum+ posterior wall thickness) to (end diastolic diameter) > 0.6 and the time delay between the early mitral M-mode E and the early diastolic tissue velocity of 0.0 ms (i.e. both occurred at the same time or are possibly reversed).

Based on standard statistical methods to calculate sensitivity and specificity, Tables 7.3 (a) and 7.3 (b) show a range of echocardiographic criteria for differentiating between patients with pathological LVH and athletes with LVH (Bland *et al*, 1994).

7.3.3.4 Pseudo-normalisation

Of particular interest, five patients in the pathological LVH group who demonstrated pseudo-normalisation and stage II diastolic dysfunction showed the appropriate timing reversal directly, even though the isovolumic relaxation time was pseudo-normal (median = 20 (10, 30)) in the pseudo-normal group compared with median = 10 (0, 13) in the remainder, with p = 0.059.

7.3.3.5 Reproducibility

Using the method of Bland *et al* (1986), the correlation found was r = - 0.0047 (p = 0.653) for reproducibility for each 4-site average, and r = - 0.077 (p = 0.466) for the time delay. This suggests that there was negligible inter-observer bias in the measurements.

7.3.4   Discussion

We report on two non-invasive measurements using DTI which can help to differentiate pathological LVH from athletic physiological hypertrophy in the Maron 'grey zone'. One is a novel method of measuring left ventricular performance by using the ratio, (E/Ea)/(LVIDd), and the other is a novel application of a timing

measurement which, along with measurement of early tissue velocity E, is effective in detecting changes of diastolic dysfunction in individuals with HCM. From this study several echo features that permitted demarcation from pathological LVH are identified and set out in Table 7.2. For example, left ventricular cavity dimension exceeded the upper limits of 5.5 cm ± 0.5. In contrast the HCM patient group showed small or normal-sized left ventricular cavities of 4.7 cm ± 0.6. However cardiac alterations associated with training differ somewhat depending on the particular sport in which the individual participates (Fisher *et al*, 1989). Cavity dimension alone would not resolve this differential diagnosis.

7.3.4.1 Early diastolic tissue velocity (E)

Studies by Ho *et al* (2002) and Nagueh *et al* (2001) suggest that DTI can be used to identify a group of individuals without hypertrophy as well as individuals with pathological hypertrophy. Our study groups included patients with left ventricular hypertrophy due to disease and exercise and we have shown an Ea < 10 cm/s had a sensitivity of 73% and specificity 100% for differentiating between athlete (physiological) hypertrophy and pathological hypertrophy in the 'grey zone' (Table 7.3 (a)). We found a similar result between the normal and pathological groups with the same sensitivity and specificity but with slightly increased accuracy (Table 7.3 (b)). Accuracy is an average of sensitivity and specificity and is calculated by summing those with a negative test result not having the disease and those with a positive test having the disease and dividing the sum by the total sample. We did not consider positive predictive value in this setting.

7.3.4.2 Novel index of myocardial performance

Our novel index of myocardial performance, (E/Ea)/(LVIDd), was shown to be increased in the HCM group compared with the normal and athlete groups (Figure 7.4). We have also shown that (E/Ea)/(LVIDd) has a sensitivity of 86% and specificity 94% for differentiating between athletic (physiological) hypertrophy and pathological hypertrophy in the 'grey zone' similar to the early diastolic tissue (Ea) but slightly better in sensitivity and accuracy.

7.3.4.3 Timing of the early diastolic interval

We have previously demonstrated that mitral diastolic peak ring tissue velocity occurs earlier than the peak of the early mitral inflow velocity in normal human hearts (King *et al*, 2003). Our findings of altered timing between peak tissue velocity (Ea) and peak mitral (E) valve opening on M-mode are similar to those reported by Rodriguez *et al*, 1996 (Table 7.2). Rodriguez also compared DTI with M-mode of the ring and mitral inflow Doppler velocities in patients with LVH (Table 7.2). Patients with LVH showed a delay in peak early diastolic mitral ring velocity (21 ms $\pm$ 5.5 ms, p = 0.002, after the E wave). In Rodriguez's study M-Mode and DTI measurements were measured on different heart beats, with times of the peak velocities measured with reference to the ECG R-wave. In the current study M-Mode and DTI measurements were taken simultaneously and actual time differences measured between events in a single heartbeat, with the scheme shown in Figure 7.5.

The canine experiments of Rivas-Gotz *et al* (2003) showed a strong relationship

between the time interval between the onset of mitral inflow (Tea) and the time onset

of early diastolic velocity of the mitral ring by DTI (E). However it has been

demonstrated that a variation in passive myocardial tension exists in different

mammalian species (Greaser *et al*, 2002). This discovery raises reasonable doubt as

to the validity of simple extrapolation of related experimental data from animal

studies to humans. Rodriguez *et al* (1996) also found that in a group with no heart

disease the onsets of mitral flow and diastolic ring motion were simultaneous, but the

peak ring velocity preceded the peak mitral M-mode E by an average of 20 ms. This

was in contrast to patients with LVH where the timing was reversed. These findings

and ours support the notion of elastic recoil, but differ in principle from those reported

by Rivas-Gotz where a definite time delay between the onsets was reported (Table

7.2). In patients with LVH and HCM we found that peak mitral opening preceded

early diastolic ring tissue velocity by approximately 20 ms (Figure 7.3).

Our patients with mild HCM showed abnormal diastolic indices of left ventricular

filling. However we have shown that measuring the diastolic mechanism has a

sensitivity of 100% and specificity 100% for differentiating between athletic

(physiological) hypertrophy and pathological hypertrophy in the 'grey zone', far

exceeding the sensitivity and accuracy of other techniques to detect diastolic

dysfunction in our HCM group (Table 7.3 (a)). Another potential future advantage

other than its sensitivity and accuracy, is the ability of this technique to

simultaneously measure on a beat to beat basis, and so follow the effects of

medication and intervention directly irrespective of preload variables. Our ability to

visualise this timing interval in milliseconds can also enhance our understanding of

the coordinated sequence of diastolic dysfunction in HCM.

Cardiac time intervals such as the early diastolic mechanism will become more

precise and practical for clinical use when DTI technology improves so as to allow

automatic simultaneous overlay of DTI and M-mode displays. This will allow the

direct assessment of the early diastolic mechanism, automatic calculation of the index

of myocardial stiffness and left ventricular filling pressures even in patients with atrial

fibrillation (Sohn *et al*, 1999) which cannot be assessed by conventional Doppler.

Conventional transmitral flow and pulmonary venous flow velocity patterns are

affected by multiple factors that alter preload. Tissue Ea alone, although diagnostic,

may be inconclusive as a lone index where its peak compared to blood inflow might

yield finer diagnostic information. This new timing measurement and the novel index

of ventricular stiffness have several other potential advantages over conventional

Doppler parameters. It was possible to obtain them readily in all subjects included in

this study. In previous reports by Masuyama *et al*, 1991 and Nagueh *et al*, 1995,

adequate pulmonary venous flow signals, for example could not be obtained in up to

18% of normals and up to 84% of patients in intensive care units. It is essential that

all important diagnostic parameters or equally useful alternatives be obtained in all

patients, especially for the critical diagnosis of what is physiological and what is

pathological left ventricular hypertrophy.

It is not clinically practical to perform the technique as reported in this work, as it

requires two echo machines. But future technological innovation to allow the

simultaneous overlay of M-mode or conventional Doppler with DTI spectra using a single ultrasound system will improve the ease and reliability of the timing technique.

7.3.5   Limitations

The number of elite athletes with LVH in this study was small due to the low prevalence of LVH in this group. The number of individuals studied with clinically proven mild HCM was also small due to the low prevalence of patients with LVH in the range associated with physiological hypertrophy. The HCM patients in the study were somewhat older that the other subjects, although not significantly so. Patients and subjects aged > 55 years were excluded to avoid any confusing effects of aging. However, in most cases, the differences between these two groups were large enough to have sufficient (> 80%) statistical power to detect such a difference with confidence. For example, the comparison in the Ea four-site average between HCM patients and athletes with n = 11 and n = 17 respectively in the groups, would indicate over 90% confidence. The Canadian consensus guidelines (Rakowski *et al*, 1996) were not followed exactly because the pulmonary venous flow velocity patterns were omitted but conventional blood flow Doppler indices and LV ring DTI were obtained on each patient.

The technical limitations with regard to time resolution of the ultrasound systems did not allow us to measure time differences below 5 ms. With further technical advances we would expect to see an improvement in this time resolution in ultrasound systems and hence finer diagnostic differentiation.

7.3.6   Conclusions

The timing measurement between peak tissue velocity Ea and peak mitral opening (by M-Mode) and the novel index of left ventricular performance in diastole, introduced in this work can be used together or separately to differentiate hypertrophic cardiomyopathy from athletic physiologic left ventricular hypertrophy in the Maron 'grey zone'.
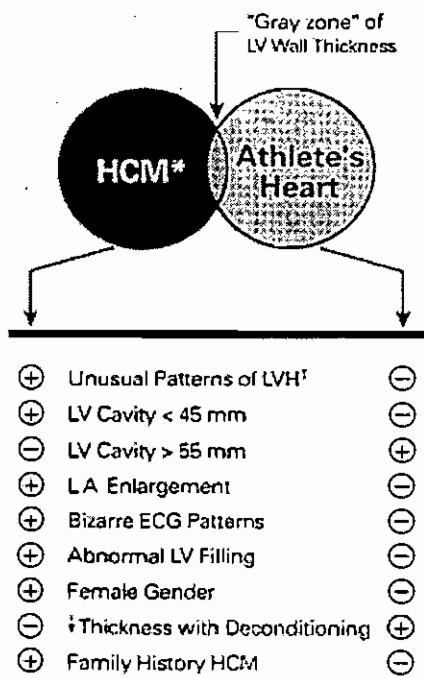
Figure 7.1   **Schematic representation of the quantitative and qualitative points**

of difference between the athlete's heart and the patient with

HCM, and indicating the 'gray zone' of overlap in LV wall

thickness for the two conditions (Maron *et al, 1995*)
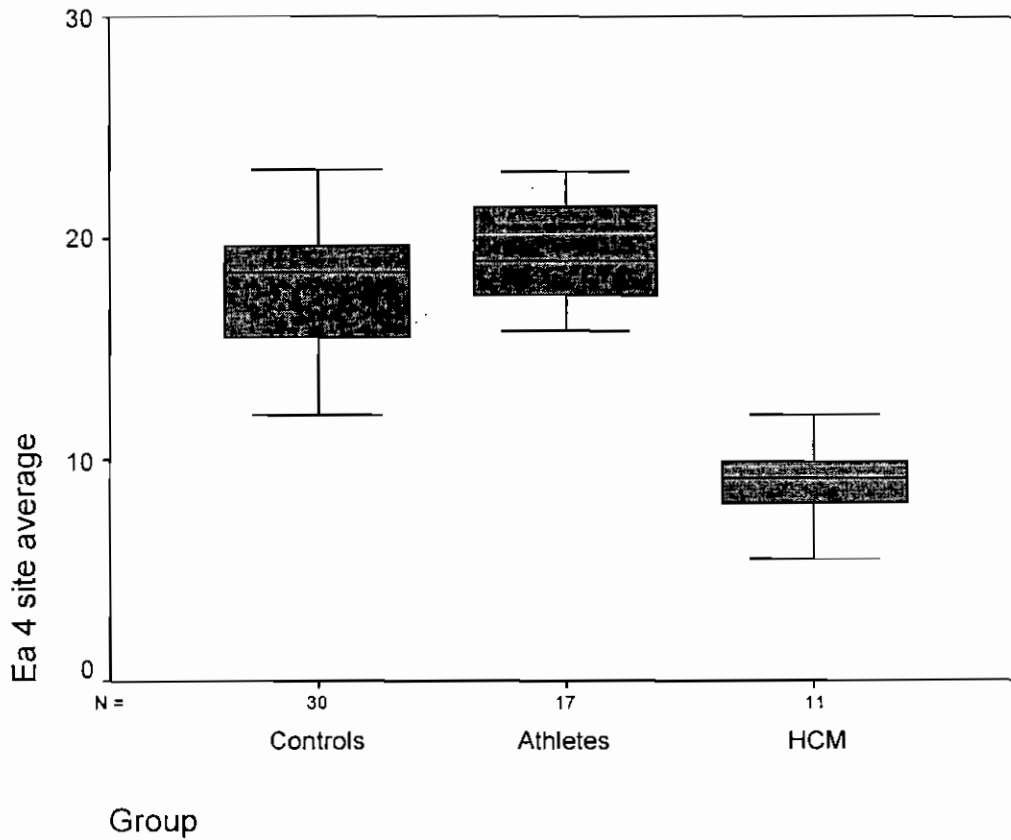
Figure 7.2   Box and whisker plots of 4-site average early diastolic tissue

(mitral ring) velocity, Ea (cm/s), in patients with HCM (H),

athletes (A) and normal subjects (N)
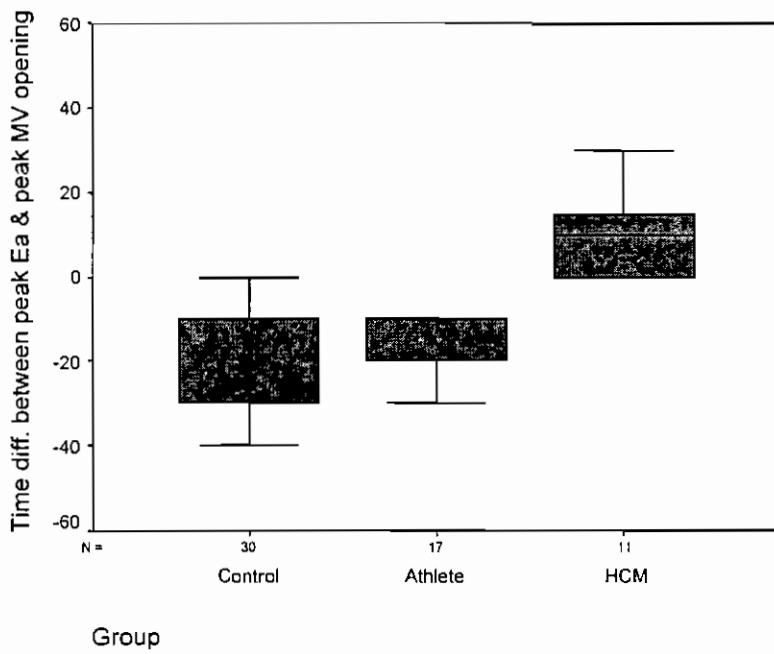
Figure 7.3   **Box and whisker plots for the early diastolic mechanism (ms) in**

patients with HCM (H), athletes (A) and normal subjects (N)
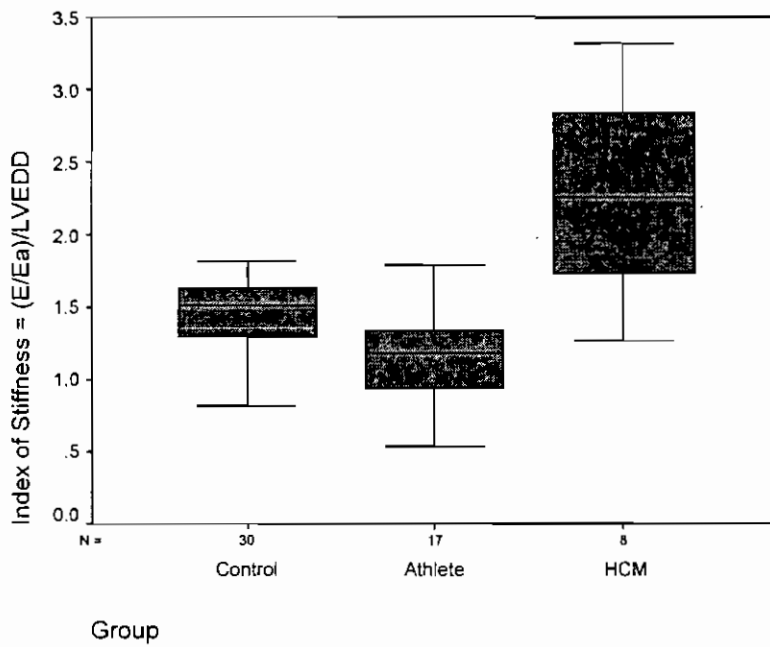
Figure 7.4   Box and whisker plots for the novel index of myocardial

performance in diastole, (E/Ea)/(LVIDd) in patients with HCM

(H), athletes (A) and normal subjects (N)
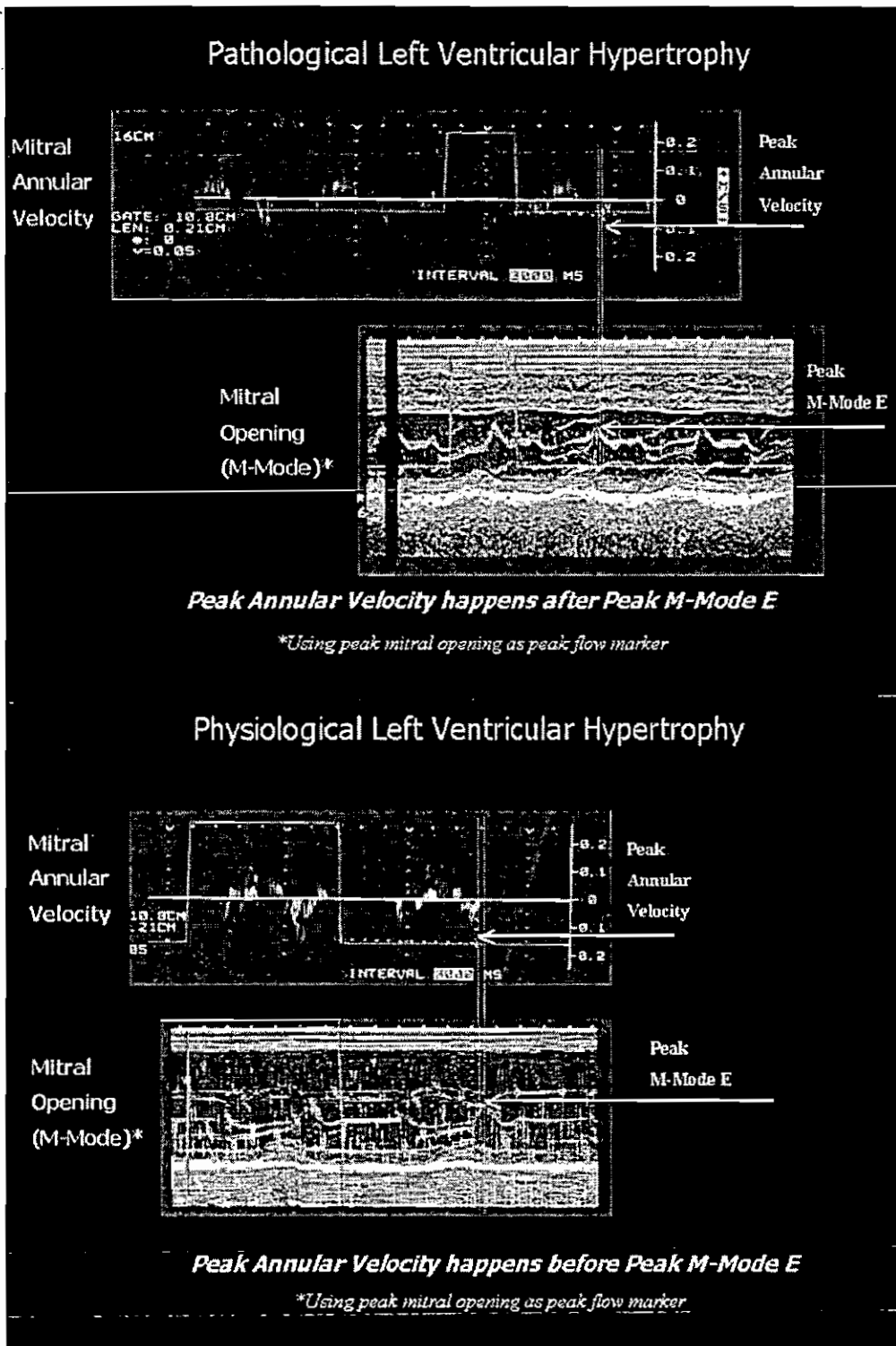
Figure 7.5   A time reference pulse was introduced into the displays of both

machines simultaneously. The time from pulse edge to Ea (DTI)

on one machine and to peak mitral (M-mode) opening were

measured simultaneously.

Table 7.1   General characteristics of the study groups

	HCM (n = 11)	Athletes (n = 17)	Normals (n = 30)	p-value [#]
Age (years) [†]	31 (13, 40)	28 (24, 31)	26 (24, 28)	ns
Men/Women	9/2	14/3	25/5	ns
Heart rate (/min)*	67 ± 5	65 ± 11	70 ± 5	ns
Body surface area (m²) [†]	1.9 (1.9, 2.0)	2.0 (2.0, 2.0)	1.8 (1.6, 1.9)	ns

[#] adjusted for age

[†] median and IQR presented for non-normal data

* mean ± SD

Table 7.2   Summary echocardiographic data for the study groups

	HCM	Athletes	Normals	p-value
Aortic root diameter (cm) *	3.5 ± 0.4	3.8 ± 0.4	3.2 ± 0.4	0.003
Left atrial diameter (cm) [†]	4.0 ± 0.4	3.8 ± 0.4	3.5 ± 0.4	<0.002
Septal thickness (cm) [&]	1.3 (1.3, 1.5)	1.3 (1.3, 1.3)	0.9 (0.8, 1.0)	<0.0001
Posterior wall thickness (cm) *	1.3 ± 0.1	1.3 ± 0.1	1.0 ± 0.2	<0.0001
LVIDd (cm) *	4.6 ± 0.2	5.6 ± 0.1	4.8 ± 0.4	<0.0001
LVIDs (cm) *	3.0 ± 0.5	3.6 ± 0.6	3.1 ± 0.5	0.015
Ejection fraction % *	67 ± 5	64 ± 5	64 ± 5	0.164
Left ventricular mass index (g/m²) [†]	167 ± 22.	188 ± 24.	102 ± 27.	<0.0001
E wave (cm/s)*	60 ± 18	71 ± 15	74 ± 14	0.09
A wave (cm/s) [†]	41 (22, 70)	37 (33, 48)	40 (35, 49)	0.94
E/A ratio *	1.1 ± 0.5	1.8 ± 0.4	1.8 ± 0.4	0.0012
IVRT (ms) [†]	93 ± 16	82 ± 12	75 ± 10	0.014
Dec	223 ± 69	185 ± 40	169 ± 39	< 0.01
Ea averaged four-site velocity (cm/s) [†]	9 (7, 10)	19 (17, 22)	18 (15, 20)	<0.0001
E/Ea *	10.1 ± 2.8	6.4 ± 1.6	7.1 ± 1.1	0.0014
Systolic wave velocity (cm/s) *	8.7 ± 2.5	12.2 ± 1.6	10.3 ± 1.4	<0.0001
Novel index of myocardial performance (E/Ea)/(LVIDd) [†]	2.2 (1.9, 2.30)	1.2 (0.9, 1.4)	1.5 (1.3, 1.6)	<0.0001

[†] median and IQR presented for non-normal data   * mean ± SD
There was no consideration here of inter-observer variations. One observer only took all measurements.

Table 7.3 (a) Performance of possible echocardiographic criteria for

discriminating between patients with HCM and athletes

	Sensitivity	Specificity	Accuracy
4-site average Ea < 9 cm/s	27%	100%	71%
4-site average Ea < 10 cm/s	73%	100%	89%
Systolic shortening P velocity < 9 cm/s	64%	100%	86%
(IVS+LVPW)/(LVIDd) > 0.6	36%	100%	75%
E/A ratio < 1.0	36%	100%	75%
Flow propagation velocity < 50 cm/s	27%	100%	71%
* 4-site average time difference between Ea and E (M-mode) ≥ 0 ms	100%	100%	100%
(E/Ea)/(LVIDd) < 1.7	86%	94%	92%

* All patients with HCM had values ≥ 0 for the four-site average time difference and all athletes had values < 0 and therefore there was complete differentiation between the groups.
See page 152 for further explanation.

Table 7.3 (b) Performance of possible echocardiographic criteria for

discriminating between patients with HCM and normals

	Sensitivity	Specificity	Accuracy
4-site average Ea < 9 cm/s	27%	100%	81%
4-site average Ea < 10 cm/s	73%	100%	93%
Systolic P velocity < 9 cm/s	36%	93%	78%
(IVS+LVPW)/(LVIDd) > 0.6	37%	100%	83%
E/A ratio < 1.0	27%	100%	83%
Flow propagation velocity < 50 cm/s	27%	97%	78%
4-site time difference between Ea and E (M-mode) ≥ 0 ms	100%	77%	83%
(E/Ea)/(LVIDd) < 1.7	86%	87%	86%

[See page 153 for further explanation]
Accuracy is not a positive predictive value.

Chapter 8

Overall Discussion and Conclusions

This thesis presents the development of clinical applications of the relatively new

ultrasound modality, Doppler Tissue Imaging (DTI), in conjunction with the earlier

more established modalities of echocardiography. The contents of this thesis outline

the investigations leading up to the recognition of the early diastolic mechanism.

From there we examine the usefulness of a new timing parameter of diastole which

allows us to measure the early diastolic mechanism. The confirmation of a delay in

Ea tissue velocity compared with mitral inflow velocity when myocardial relaxation is

impaired, can contribute greatly to the understanding of the mechanics of diastolic

filling. Our ability to measure these millisecond intervals has the potential to enhance

our understanding of the well-orchestrated timing of cardiac events and will improve

the diagnostic assessment of cardiac function.

The clinical applications reported in this thesis relate especially to the early diastolic

mechanism and to new diagnostic insights possible through measurement of the fine

detail of cardiac mechanics even to milliseconds intervals of this relatively less

understood functional aspect of the heart that can be readily examined with DTI.

Cardiac time intervals in which the motions of the myocardium occur can be recorded

non-invasively by this new measurement. We investigated also the clinical utility of a

new index based on the ratio, (E/Ea)/(LVIDd), which is an indicator of myocardial

performance in diastole.

These two new measurements of the duration of the early diastolic mechanism and myocardial performance, permit quantitative evaluation of a range of cardiac diseases. It also introduces improved diagnostic differentiation between pathological and athletic physiological LVH.

Chapter 3 introduces a conceptual framework/mechanism of left ventricular filling and emptying that relates the microanatomy of the myocardial fibres in the left ventricle to the function of the ventricle. In early ventricular diastole, when the early diastolic mechanism takes place, the longitudinal and circumferential fibres relax, the torsion of the left ventricle unwinds, pulling the mitral ring towards the apex thus creating a relative vacuum below the closed mitral valve. As this valve opens there is a rapid burst of transmitral blood flow that tends to rapidly fill the ventricle just before the left atrium contracts to complete the filling of the ventricle.

Then in systole the two types of myocardial fibres contract to produce the torsion of the left ventricle, thereby pulling the mitral ring towards the base of the ventricle and pumping the blood into the aorta.

In Chapter 3 the long axis motion of the atrioventricular/mitral ring and how this reflects longitudinal ventricular shortening and lengthening, are discussed. The extent and timing of cardiac systole and diastole can be conveniently assessed with M-mode echocardiography. The velocity of shortening and lengthening can also be measured using DTI. DTI examination of the mitral ring is eminently suited for providing useful information about myocardial function and a valuable technique for the

assessment of left ventricular regional and global systolic function. These parameters, together with pulsed Doppler measurement of transmitral inflow and aortic outflow profiles, are useful to describe the normal systolic state and to quantify and classify the degree of cardiovascular pathology.

8.1   Earlier development of DTI applications

Myocardial stiffening from whatever cause disrupts the action of some of the ventricular fibres of both types, thereby disrupting to one extent or another the early diastolic mechanism as well as the emptying/pumping action of the left ventricle. DTI allows the assessment of myocardial tissue velocities, which are substantially lower than the blood flow velocities recorded by conventional pulsed wave (PW) and continuous wave (CW) Doppler (Mc Dicken *et al*, 1992; Isaaz *et al*, 1993; Erbel *et al*, 1996). This technique has enabled the characterization of regional myocardial systolic and diastolic function, both by recording myocardial velocities and different time indices in the cardiac cycle.

Regional myocardial function, assessed by DTI, is abnormal in patients with HCM. Both systolic and diastolic functional parameters are altered in both the left ventricle and right ventricle and evidence of significant diastolic abnormalities has been found (Lewis *et al*, 1992).

One of the clinical applications of DTI has been to identify indices of diastolic function that are less dependent on the loading conditions, compared to the conventional Doppler indices used. Recent studies have shown that the early-diastolic

myocardial wave velocity (Ea), measured by tissue Doppler echocardiography, is useful in the study of left ventricular relaxation in patients with diastolic dysfunction caused by different cardiac diseases. Indeed, it has been found that early diastolic LV lateral annular velocity (Em) can be used as a preload-independent index of LV filling pressure and can be used to correct for the influence of relaxation on transmitral velocity (E) in the evaluation of filling pressures in patients with stiff hearts, including patients with HCM. We have shown further evidence in chapter 5 to support the usefulness of the E/Ea ratio in patients with diastolic dysfunction.

Lateral walls have higher systolic tissues velocities without a gradient between basal to mid-wall segments. Also posterior wall tissue Doppler signals are higher in the lateral walls indicating that relaxation activity in the long axis is prominent in the lateral aspects of the left ventricular wall. Early diastolic velocities corresponding to the phase of rapid ventricular filling were high in the basal lateral segments.

HCM can increase the mass of each or different segments of the myocardium and so affects its contractility, and its velocity and extent of movement during relaxation and contraction. The dynamics in both phases of cardiac function might be expected to be slower and possibly of reduced excursion in comparison with the normal case. Thus the recoil of the heart during isovolumic filling in the early part of diastole, which provides energy for rapid early diastolic filling, is likely to have different dynamics and be slower in cases of HCM. The ratio of conventional Doppler transmitral velocity E to Em was shown to correlate well with left ventricular filling pressures (Nagueh *et al*, 1999). Important clinical parameters in HCM, like NYHA functional class and exercise capacity have also been found to correlate to this E/Em ratio.

Another clinical application of the technique has been to identify markers that are

present early in the disease, even preceding the development of cardiac hypertrophy.

Again, Em (at the lateral, septal, anterior and inferior LV base) was shown to be a

sensitive index, showing reduced velocities in patients carrying a mutation for HCM,

before any sign of hypertrophy or abnormality in any of the conventional Doppler

measurements was evident (Nagueh *et al*, 2000). Thus, DTI seems to be more

sensitive than conventional echocardiographic techniques and can provide a novel

means for early diagnosis in HCM. The use of DTI to measure the detailed

movement of the cardiac structures forms the basis for the study outlined in Chapter 7

to improve the diagnosis of HCM within the range of physiological LVH and its

distinction from pathological LVH.

8.2   General discussion on and conclusions of the work reported in this thesis

8.2.1   Study of systolic dysfunction due to infarction arising from ischaemia

In the pilot study of left ventricular dysfunction in systole due to ischaemia, reported

in Chapter 5, three groups with different regional ischaemias and a normal control

group were investigated. The average values of the peak mitral ring systolic descent

velocity (Sw) for hypokinetic sites (proximate to ischaemic areas of ventricle) tended

to be lower than in corresponding sections of the ring in normal subjects. These

average values also correlated slightly with ejection fraction. Values of Sw for non-

hypokinetic sites (associated with normal, non-ischaemic ventricular areas) were not

significantly different among all the subjects, but a small decrease from the corresponding control value was recorded in the anterior ischaemia group while a modest increase was observed in the inferior ischaemia group.

Furthermore the time interval (Q-Sw) between the Q wave of the ECG trace and the mean value of Sw from hypokinetic sites on the ring were fractionally greater in all three ischaemia groups relative to the normals. The Q-Sw intervals for all non-hypokinetic sites showed slight increases above the normal controls.

No significant correlations were found to exist between ejection fraction and either mean Sw or mean Q-Sw, derived from sites corresponding either to non-hypokinetic ventricular areas or to hypokinetic myocardium.

The ways in which the microanatomy of the ventricle, as outlined in Chapter 3, together with the way in which the heart is located and tethered in the chest, might explain these effects is discussed in some detail in Chapter 5.

In this study dysfunctional ischaemic areas were relatively crudely identified by visual inspection of 2-D images of the heart. A more definitive means of identification, well correlated with the coronary arteries and applied to a more extensive population of subjects in the different categories of regional and global ischaemia, would be expected to yield more robust conclusions. An increase in the number of ring sites investigated, to the extent that this would be feasible might also improve sensitivity.

8.2.2 *Further evidence to validate E/Ea in estimating LV filling pressures*

In chapter 5 the partial return of the left ventricle to its pre-ejection configuration before mitral valve opening is considered as an important mechanism for the release of potential energy stored in elastic elements during the systolic deformation. These myocardial restoring forces have to be enhanced by physiological changes such as exercise producing catecholamines, offsetting shortening of the filling period. This idea is fundamental to the whole idea of the thesis. In diastolic dysfunction the physiological changes do not enhance systolic deformation and they are dependent on the elastic elements of recoil that dictates filling only. In other words the absence of the early diastolic mechanism would be related to the absence of compensation for shortening of the filling period. This provides the reason for the direct correlation between the acceleration of blood across the mitral valve in early diastole with the early diastolic tissue velocity E, which acts as a surrogate measurement for twist.

In chapter 5 we showed that mitral annular diastolic peak tissue velocity occurs earlier than the peak of early mitral inflow velocity in normal human hearts. This study also demonstrated that such a relationship may be altered in the presence of diastolic dysfunction and elevated atrial pressure. The understanding that in normal hearts rapid 'relaxation' results in creation of a negative sucking pressure inside the ventricle has already been described (Yastrebov *et al*, 2004). This effect may be largely determined by Ig-like segments of titin exhibiting a recoil 'spring' effect in addition to the pressure exhibited by the left atrium. Once the multitude of 'molecular springs' returns to a neutral state, the flow of blood between the chambers becomes a function only of the pressure gradient between the atrium and the ventricle created by the

contraction of the atrium. It is likely that the flow exhibits decelerating qualities once the stretch of the multitude of molecular springs begins. It therefore would seem logical to postulate that the 'slack myocardium' status occurs within a period between the peak myocardial tissue velocity measured at the mitral valve annulus and the peak of the E.

We have already shown a relationship between Ea and the acceleration across the mitral valve in patients with diastolic dysfunction. The stiffer ventricles are less likely then, as previously shown in other studies, to be influenced by preload conditions. This study provides further evidence for the usefulness of E/Ea to estimate pulmonary capillary wedge pressure in patients who have impaired cardiac relaxation. Since diastolic dysfunction exists in all myocardial pathologies its potential use in estimating left ventricular filling pressure is important. Therefore the availability of further evidence to support its use in assessing accurately this clinical useful parameter is important.

8.2.3   *Diastolic recoil and identification of the early diastolic mechanism*

It is been proposed that recoil of the left ventricle, the relaxation of its systolic torsion, during the isovolumic relaxation time before left ventricular filling, provides potential energy in the form of a relative vacuum in the ventricular cavity to produce rapid early diastolic inflow, and that the blood velocity of this early diastolic inflow is influenced by preload conditions. In diastolic dysfunction, recoil can occur during or after left ventricular filling, and the acceleration of early diastolic inflow is not influenced by preload in the stiff heart. The study reported in Chapter 6 seeks to

evaluate this proposition indirectly by exploring the relationship between peak early

diastolic mitral ring velocity (Ea) (as a surrogate for recoil), measured using DTI, and

the acceleration of early diastolic transmitral blood flow in patients with and without

diastolic dysfunction, measured with a pulsed Doppler system.

Indeed all of the patients with diastolic dysfunction in the study reported in Chapter 6

had a lower Ea than all of the subjects in the normal control group. Patients with

diastolic dysfunction and an E/A ratio less than one had consistently low mitral ring

velocities, as determined by DTI. The mitral ring tissue velocity (Ea) was found to

correlate positively with the acceleration of mitral inflow in the diastolic dysfunction

group and this correlation was not present in the normal control group.

This showed that ventricular filling is associated with early diastolic motion of the

mitral ring, which is a marker for left ventricular recoil in the control group. This is

the result of the absence or reduction of the early diastolic mechanism that is essential

for proper filling. It may be argued that in the normal state most people have normal

filling pressures and it is primarily the left ventricular relaxation and recoil that

influences the transmitral pressure gradient. Preload however is the force that extends

the ventricle in diastole or the force acting to stretch the ventricular fibres at end

diastole (European Study Group on Diastolic Heart Failure, 1998). Therefore even

though the filling pressures are normal, preload will affect the rate of blood flow

across the mitral valve depending on the degree of stretch of the left ventricular cavity

in diastole. Taking into account the physiological changes that effect preload there

should be a varying degree of acceleration of blood flow across the mitral valve,

which is dissociated from left ventricular recoil in the normal.

In patients with diastolic dysfunction a strong relationship was found between mitral

ring relaxation recorded by DTI and the acceleration of early diastolic flow recorded

by conventional pulsed Doppler ultrasound, and this relationship was not found in the

normal control group. This provides a new insight into diastolic filling events in

patients with diastolic dysfunction and further supports the premise that recoil is an

important mechanism for rapid early diastolic filling.

8.2.4   Study to distinguish pathological from physiological LVH

The upper normal limit of LV hypertrophy attributable to physical training in men

seems to be 16 mm (Pelliccia *et al*, 1991), sometimes creating a diagnostic dilemma

between physiological hypertrophy and HCM with mild hypertrophy. Female elite

athletes do not show the same hypertrophic response to intensive training. In a study

of 600 elite female athletes, LV wall thickness was within normal values, ranging

from 6-12 mm, but LV end diastolic cavity dimension was increased in 8% of the

subjects (Pelliccia *et al*, 1996).

It is generally accepted that strenuous physical activity is associated with an increased

risk of sudden death in patients with HCM (Maron *et al*, 1996). This includes

endurance sports, sports with burst exercise (e.g. sprinting) and heavy isometric

exercise (e.g. weightlifting). The magnitude of the increase in risk associated with

exercise is difficult to quantify. Not all athletes with HCM will die suddenly during

competition and, overall, only some of the sudden deaths in HCM occur during

exercise. Nevertheless, patients with HCM are recommended to discontinue

competitive athletic activity to reduce the risk of sudden death and this modification

of lifestyle can be regarded as a treatment *per se* (Maron *et al*, 1994).

In the athlete group the peak early diastolic ring tissue velocity **preceded** the peak

mitral E of the M-mode on average by a median of 20 ms, and in the normal by a

median of 15 ms, compared with the HCM group where the situation is reversed and

the peak mitral E observed by the M-mode display **preceded** the peak early diastolic

ring tissue velocity by a median of 20 ms.

A novel timing measurement is reported here which, along with the novel index of

myocardial performance in diastole, (E/Ea)/(LVlDd), is effective in detecting subtle

changes of diastolic dysfunction in individuals with HCM. This combination of

measurements can improve the differentiation of pathological LVH from

physiological hypertrophy seen in athletes.

In a recent study by the authors we noted that mitral diastolic peak ring tissue velocity

occurs earlier then the peak of the early mitral inflow velocity in normal human hearts

(King *et al*, 2003). Also our findings of altered timing between peak tissue velocity

(Ea) and peak mitral (E) valve opening on M-mode are similar to those reported by

Rodriguez *et al* (1996).

In this work the timing intervals were measured on the same heartbeat and so the

cardiac cycle durations for both measurements were identical. These measurements

were then independent of intracardiac processes giving rise to beat-to-beat variations.

Our result concurred numerically with that of Rodriguez *et al* (1996) and conceptually

with those reported by an earlier study by Maier *et al* (1992) who, using magnetic

resonance imaging and myocardial tagging, showed a prolongation of diastolic

untwisting in patients with HCM. This timing interval between peaks represents an

index of relaxation in early diastole. But more importantly the positive value seen in

the normal control can be considered positive for the presence of the early diastolic

mechanism essential for normal cardiac filling. The presence or absence of the early

diastolic mechanism can also be used alone or in conjunction with other established

echocardiographic indices to differentiate pathological from physiological LVH.

The technical limitations with regard to time resolution of the ultrasound systems did

not allow us to measure time differences below 5 ms. With further technical advances

we would expect to see an improvement in this time resolution in ultrasound systems

and hence finer diagnostic differentiation.

The clinical application of this novel idea of overlay (simultaneous recording) of the

DTl spectral velocities and the M-Mode or conventional Doppler blood flow

velocities depends on its practicality and incremental value in comparison with other

more easily available measures such a deceleration time, Ea and E/Ea ratio.

Measuring time intervals can be more difficult than measuring peak velocities.

However, the simultaneous recording of the peak of both mitral Ea and E by the

overlay of the spectral displays is possible. This time delay measurement will

therefore be more practical in routine noninvasive assessment of diastolic function

and in patients with cardiac arrhythmias.

Our novel index of myocardial performance in diastole, (E/Ea)/(LVIDd), was shown

to increase in the HCM group compared with the normals and athletes as shown in

Figure 7. 4. With increased myocardial stiffness, left ventricular relaxation is slowed

and delayed, and accordingly transmitral inflow becomes dependent on increased left

atrial pressure generated by left atrial contraction. Under these situations, annular

recoil in early diastole is delayed and follows the transmitral inflow. This gives rise

to the timing delay or timing reversal in the early diastolic mechanism. The slow rate

of ventricular relaxation in our patients with stiff ventricles due to HCM would

preclude full relaxation of the myocardium in early diastole. The incomplete

relaxation at the point of left ventricular minimal diastolic pressure would cause E/Ea

to be higher causing the inevitable absence or reversal of the early diastolic

mechanism. The work reported in this thesis suggests that the novel idea of using

simultaneous overlay of the Doppler tissue imaging over M-mode recordings in

conjunction with the new novel index of myocardial performance may increase the

sensitivity for the detection of pathological hypertrophy and stiffness.

8.2.5   *Advantages over other methods of assessing diastolic dysfunction*

Our novel index of passive myocardial stiffness is simply calculated using one

ultrasound system. The timing measurement uses two echocardiographic machines

operated simultaneously, and this is not normally clinically practical. But when

newer technology emerges, with better resolution and simultaneous overlay of tissue

Doppler spectral traces with conventional blood velocity spectral traces or M-mode

spectral traces, the timing measurements will become possible using one ultrasound

system. Then measuring cardiac time intervals such as the early diastolic mechanism

will become more precise as well as being readily done. This will allow the direct

assessment of the early diastolic mechanism, automatic calculation of left ventricular

filling pressures and automatic calculation of the index of myocardial performance,

(E/Ea)/(LVIDd), even in patients with atrial fibrillation who cannot be assessed by

conventional Doppler. Tissue Ea alone is diagnostic, but may be inconclusive as a

lone index, whereas its peak compared to blood inflow would yield more useful

diagnostic information. This technology will reduce the need for provocative

manoeuvres such as valsalva because both the early diastolic mechanism and peak

tissue velocities are preload independent to some extent. Automatic overlay will also

be more useful in terms of monitoring the dynamic continuum of pharmacological

intervention. Eventually this technology, including estimation of passive diastolic

stiffness, could alter the Canadian consensus report for the assessment of diastolic

dysfunction.

8.3   Conclusions

Along with the four-site average early diastolic tissue relaxation velocity (Ea) and the

novel index of myocardial stiffening, this simple new measurement of the time

interval between peak early diastolic tissue E and mitral valve opening is useful in

differentiating pathological from physiological left ventricular hypertrophy. Reversal

of the early diastolic mechanism is a strong indicator of pathological hypertrophy.

Sudden cardiac deaths of young athletes, which are usually associated with physical

exertion, continue to stimulate intense and persistent public interest. To much of the

public and, indeed, the medical community, the young competitive athlete is among

the healthiest members of society. Hypertrophic cardiomyopathy is one of the main

causes of sudden death and is more common than previously believed. HCM is

identified by echocardiography. However young athletes who have died suddenly

sometimes have only modest increases in left ventricular mass so there is an

unresolved issue as to whether or not such athletes have a mild expression of HCM or

degrees of physiological hypertrophy.

The new indices and experimental results described in this thesis differentiate between

these different morphological expressions but future experiments on larger

populations are needed so that they might provide a preclinical diagnosis. It is evident

that whatever future therapies evolve the hope would be that they would help to treat

the disease at the stage at which such new indices are positive but no other

manifestations are evident.

The simultaneous use of DTI to measure tissue dynamics, and pulsed Doppler to

measure hemodynamics, allows the relationships of these vital cardiac functions to be

described in time and space. This opens an exciting vista of diagnostic measurements,

hitherto available in highly invasive situations, using mild and non-invasive

procedures. However an improvement of the resolution in the time interval

measurement below ± 5 ms would be highly desirable. We need also to develop

studies of the relative phase of other DTI, M-mode and pulsed Doppler blood flow

measurements, in health and disease, together with the correlation of these studies

with features of the ECG.

The general applicability of our findings will have to be confirmed and deepened in future studies, with larger number of subjects with different mutations of hypertrophic cardiomyopathy. However this work has contributed to the strong potential of DTI and other echocardiographic techniques to contribute to the understanding and prevention of sudden death in our young population and, in particular, in young athletes.

References

Alam M, Höglund C, Thorstrand C & Hellekant C, Haemodynamic significance of the atrioventricular plane displacement in patients with coronary artery disease, Eur Heart J, 1992; 13: 194-200

Alam M, Höglund C, Thorstrand C & Philip A, Atrioventricular plane displacement in severe congestive heart failure following dilated cardiomyopathy or myocardial infarction, J Intern Med, 1990; 228: 569-575

Alam M, The atrioventricular plane displacement as a means of evaluating left ventricular systolic function in acute myocardial infarction, Clin Cardiol, 1991; 14: 588-594

Alfonso F, Nihoyannopoulos P, Stewart J, Dickie S, Lemery R & McKenna WJ, Clinical significance of giant negative T waves in hypertrophic cardiomyopathy, J Am Coll Cardiol, 1990; 15: 965-971

Appleton CP, Hatle LK & Popp RL, Relation of transmitral flow velocity patterns to left ventricular diastolic function: new insights from a combined hemodynamic and Doppler echocardiographic study, J Am Coll Cardiol, 1988; 12: 426-440

Asmi, M, & Walsh M, A practical guide to echocardiography, London: Chapman and Hall Medical, 1995
HYPERLINK
"mailto:Chapman@Hall"

Aversano T & Marino PN, Effect of ischemic zone size on nonischemic zone function, Am J Physiol, 1990 June; 258(6 Pt 2): H1786-1795

Bekaert I, Pannier JL, Van de Weghe C, Van Durme JP, Clement DL & Pannier R, Non-invasive evaluation of cardiac function in professional cyclists, Br Heart J, 1981; 45: 213-218
HYPERLINK
"http://circ.ahajournals.org/cgi/ijlink?linkType=ABST&journalCode=heartjnl&resid=45/2/213" [Abstract]

Bjaerum S, Torp H & Kristoffersen, Clutter filter design for ultrasound color flow imaging, IEEE Trans Ultrasonics, Ferroelectrics and Frequency Control, 2002; 49 (2): 204-216

Bland JM, An Introduction to Medical Statistics, Oxford, Oxford University Press, 3rd ed, 2000

Bland JM & Altman DG, Statistical methods for assessing agreement between two methods of clinical measurement, Lancet, 1986; 1: 307-310

Bland JM & Altman DG, Statistics notes: diagnostic tests 1: sensitivity and specificity, BMJ, 1994; 308: 1552

Braunwald E, Lambrew IT, Rockoff SD, Ross J Jr & Morrow G, Idiopathic hypertrophic subaortic stenosis. I. Description of the disease based upon an analysis of 64 patients, Circulation, 1964; 30 (Suppl IV): 3-119

Braunwald E, Shattuck Lecture: Cardiovascular medicine at the turn of the millennium: triumphs, concerns and opportunities, New England J Med, 1997; 337: 1360-1369

Brilla CG, Maisch B & Weber KT, Myocardial collagen matrix remodelling in arterial hypertension, Eur Heart J, 1992; 13(suppl. D): 24-32

Brock R, Functional obstruction of the left ventricle (acquired subvalvular aortic stenosis), Guy's Hosp Rep, 1957; 106: 221-238

Buchalter MB, Rademakers FE, Weiss JL, RogersWJ, Weisfeldt ML & Shapiro EP, Rotational deformation of the canine left ventricle measured by magnetic resonance tagging: effects of catecholamines, ischaemia and pacing, Card Res, 1994; 28: 629-635

Burke AP, Farb A, Virmani R, Goodin J & Smialek JE, Sports-related and non-sports-related sudden cardiac death in young athletes, Am Heart J, 1991; 121: 568-575

Carlsson E & Milne ENC, Permanent implantation of endocardial tantalum screws: a new technique for functional studies of the heart in the experimental animal, J Can Assoc Radiol, 1967; 19: 304 – 309.

Carrier L, Hengstenberg C, Beckmann JS, Guicheney P, Dufour C, Bercovici J, Dausse E, Berebbi-Bertrand I, Wisnewsky C, Pulvenis D, Fetler L, Vignal A, Weissenbach J, Hillaire D, Feingold J, Bouhour J-B, Hagege A, Desnos M, Isnard R, Dubourg O, Komajda M & Schwartz K, Mapping of a novel gene for familial hypertrophic cardiomyopathy to chromosome 11, Nature Genet, 1993; 4: 311-317

Choong CY, Abascal VM, Thomas JD, Guerrero JL, McGlew S & Weyman AE, Combined influence of ventricular loading and relaxation on the transmitral flow velocity profile in dogs measured by Doppler echocardiography, Circulation, 1988; 78: 672-683

Ciró E, Nichols PF & Maron BJ, Heterogeneous morphologic expression of genetically transmitted hypertrophic cardiomyopathy: two-dimensional echocardiographic analysis, Circulation, 1983; 67: 1227-1233

Colan SD, Sanders SP, MacPherson D & Borow KM, Left ventricular diastolic function in elite athletes with physiologic cardiac hypertrophy, J Am Coll Cardiol, 1985; 6: 545-549

Corrado D, Thiene G, Nava A, Rossi L & Pennelli N, Sudden death in young competitive athletes: clinicopathologic correlations in 22 cases, Am J Med, 1990; 89: 588-596

DeCara JM & Lang RM, Interpretation of left ventricular wall motion during stress testing, J CV Ultrasound and Allied Tech, 2003, 20: 643-658

Desco M & Antoranz JC, Technical principles of Doppler tissue imaging, in Garcia-Fernández MA (ed), Doppler Tissue Imaging, New York, McGraw-Hill, 1997

Devereux RB, Detection of left ventricular hypertrophy by M-mode echocardiography: anatomic validation, standardisation and comparison with other methods, Hypertension, 1987; 9: 119-126

Dickhuth HH, Rocker K, Hipp A, Heitkamp HC & Keul J, Echocardiographic findings in endurance athletes with hypertrophic non-obstructive cardiomyopathy (HNCM) compared to non-athletes with HNCM and to physiological hypertrophy (athlete's heart), Int J Sports Med, 1994; 15: 273-277

Dock G, Historical notes on coronary occlusion: from Heberden to Osler, JAMA, 1939, No 7; 133

Donovan CL, Armstrong WF & Bach DB, Quantitative Doppler tissue imaging in the left ventricular myocardium: validation in normal subjects, Am Heart J, 1995; 130: 100-104

Douglas PS, O'Toole ML, Hiller DB & Reichek N, Left ventricular structure and function by echocardiography in ultraendurance athletes, Am J Cardiol, 1986; 58: 805-809

Edler I & Hertz CH, The use of ultrasonic reflectoscope for the continuous recording of the movement of the heart walls, Kungl. Fysiografiska Sallskapets i Lund Forhandlingar 1954; 24: 40-58

Edler I, Early echocardiography, Ultrasound Med & Biol 1991; 17: 425-431

Edler I, The diagnostic use of ultrasound in heart disease, Acta Med Scandinav 1955; 152 (suppl. 308): 32-63 [Abstract]

Ehsani AA, Hagberg JM & Hickson RC, Rapid changes in left ventricular dimensions and mass in response

to physical conditioning and deconditioning, Am J Cardiol, 1978; 42: 52-56

Erbel R, Wallbridge DR, Zamorano J, Drozdz J & Nesser HJ, Tissue Doppler echocardiography (editorial), Heart, 1996; 76 (3): 193-196

European Study Group on Diastolic Heart Failure, How to diagnose diastolic heart failure, Eur Heart J. 1998; 19: 990-1003

Evans D, McDicken WN, Skidmore R & Woodcock J, Doppler Ultrasound: Physics, Instrumentation and Clinical Applications, Chichester: John Wiley & Sons, 1989

Fagard R, Aubert A, Lysens R, Staessen J, Vanhees L & Amery A, Noninvasive assessment of seasonal variations in cardiac structure and function in cyclists, Circulation, 1983; 67: 896-901

Fagard R, Van den Broeke C, Bielen E, Vanhees L & Amery A, Assessment of stiffness of the hypertrophied left ventricle of bicyclists using left ventricular inflow Doppler velocimetry, J Am Coll Cardiol, 1987; 9: 1250-1254

Fananapazir L & Epstein ND, Prevalence of hypertrophic cardiomyopathy and limitations of screening methods, Circulation, 1995; 92: 700-704

Fatenkov VN, Bukhvalova S, Fatenkov SV & Silke B, Computerised analysis of the apexcardiogram: New insights into cardiac biomechanics, Automedia, 1991; 13: 227-237

Finkelhor RS, Hanak LJ & Bahler RC, Left ventricular filling in endurance-trained subjects, J Am Coll Cardiol, 1986; 8: 289-293

Firstenberg MS, Levine BD, Garcia MJ, Greenberg NL, Cardon L, Morehead AJ, Zuckerman J & Thomas JD, Relationship of echocardiographic indices to pulmonary capillary wedge pressures in healthy volunteers, J Am Coll Cardiol, 2000; 36: 1664-1669

Fisher AG, Adams TD, Yanowitz FG, Ridges JD, Orsmond G & Nelson AG, Noninvasive evaluation of world class athletes engaged in different modes of training, Am J Cardiol, 1989; 63: 337-341

Fleming AD, Xia X, McDicken WN, Sutherland GR & Fenn L, Myocardial velocity gradient detected by Doppler imaging, Brit J Radiol, 1994; 67: 679-688

Fukuda K, Oki T, Tabata T, Luchi A & Ito S, Regional left ventricular wall motion abnormalities in myocardial infarction and mitral annular descent velocities studied with pulsed tissue Doppler imaging, J Am Soc Echocardiogr, 1998; 11(9): 841-848

Galiuto L, Ignone G & DeMaria AN, Contraction and relaxation velocities of the normal left ventricle using pulsed-wave tissue Doppler echocardiography, Am J Cardiol, 1998; 81: 609-614

Garcia MG, Rodriguez L, Ares M, Griffin BP, Thomas JD & Klein AL, Differentiation of constrictive pericarditis from restrictive cardiomyopathy: assessment of left ventricular diastolic velocities in longitudinal axis by Doppler Tissue Imaging, J Am Coll Cardiol, 1996; 27: 108-114

Garcia MJ, Ares MA, Asher C, Rodriguez L, VanderVoort P & Thomas JD, Color M-Mode flow velocity propagation: an index of early left ventricular filling that combined with pulsed Doppler E-velocity may predict capillary wedge pressure. J Am Coll Cardiol, 1997; 29: 448-454

Garcia MJ, Rodriguez L, Ares M, Griffin BP, Klein AL, Stewart WJ & Thomas JD, Myocardial wall velocity assessment by pulsed Doppler tissue imaging: characteristic findings in normal subjects, Amer Heart J, 1996; 132(3): 684-656

Garcia-Fernandez MA, Azevedo J, Moreno M, Bermejo J, Perez-Castellano N, Puerta P, Desco M, Antoranz C, Serrano JA, Garcia E & Delcan JL, Regional diastolic function in ischaemic heart disease using pulsed wave Doppler tissue imaging, Eur Heart J, 1999; 20: 496-505

Garot J, Derumeaux GA, Monin JL, Duval-Moulin AM, Simon M, Pascal D, Castaigne A, Dubois-Rande JL, Diebold B & Gueret P, Quantitative systolic and diastolic transmyocardial velocity gradients assessed by M-mode colour Doppler tissue imaging as reliable indicators of regional left ventricular function after acute myocardial infarction, Eur Heart J, 1999; 20: 593-603

Gauer OH, Volume changes of the left ventricle during blood pooling and exercise in the intact animal: three effects on left ventricular performance. Physiol Rev, 1955: 35: 143-155

Geisterfer-Lowrance AAT, Kass S, Tanigawa G, Vosberg H-P, McKenna WJ, Seidman CE & Seidman JG, A molecular basis for familial hypertrophic cardiomyopathy: a ß-cardiac myosin heavy chain gene missense mutation, Cell, 1990; 62: 999-1006
HYPERLINK
"http://circ.ahajournals.org/cgi/external_ref?access_num=1975517&link_type=MED"

Gilbert CA, Nutter DO, Felner JM, Perkins JV, Heymsfield SB & Schlant RC, Echocardiographic study of cardiac dimensions and functions in the endurance-trained athlete, Am J Cardiol, 1977; 40: 528-533
HYPERLINK
"http://circ.ahajournals.org/cgi/external_ref?access_num=910717&link_type=MED"

Granger CB, Karuimeddini MK, Smith VE, Shapiro HB, Katz AM & Riba AL, Rapid ventricular filling in left ventricular hypertrophy, I: physiologic hypertrophy, J Am Coll Cardiol, 1985; 5: 862-868
Gray, Henry, Anatomy of the Human Body, Philadelphia: Lea & Febiger, 1918 (www.bartleby.com/107/)

Greaser H, Berri M, Warren CM & Mozdziak PE, Species variations in cDNA sequence and exon splicing patterns in the extensible I-band region of cardiac titin: relation to passive tension, J Muscle Res Cell Motil, 2002; 23(5/6): 473-482

Greenbaum RA, Ho SY, Gibson DG, Becker AE & Anderson RH, Left ventricular fibre architecture in man, Br Heart J, 1981; 45: 248-263

Gulati VK, Katz WE, Follanbee WE & Gorcsan WP, (1996) Mitral annular descent velocity by tissue Doppler echocardiography as an index of global left ventricular function, Am J Cardiol, 1996; 77: 979-984

Hallopeau M, Retrecissement ventriculo-aortique, Gaz Med Paris, 1869; 24: 683-687 (cited in Seidman C (2002))

Hamilton WF & Rompf JH, Movements of the base of the ventricle and relative constancy of the cardiac volume, Am J Physiol, 1932; 102: 559-565

Hammarstrom E, Wranne B, Pinto FJ, Puryear J & Popp RL, Tricuspid annular motion. J Am Soc Echocardiogr, 1991; 4: 131-139.

Hauscr AM, Dressendorfer RH, Vos M, Hashimoto T, Gordon S & Timmis GC, Symmetric cardiac enlargement in highly trained endurance athletes: a two-dimensional echocardiographic study, Am Heart J, 1985; 109: 1038-1044
HYPERLINK
"http://circ.ahajournals.org/cgi/external_ref?access_num=3158184&link_type=MED"

Helmes M, Lim CC, Liao R, Bharti A, Cui L & Sawyer DB, Titin determines the Frank-Starling relation in early diastole, J Gen Physiol, 2003; 121(2): 97-110

Henry WL, De Maria A, Gramiak R, King DL, Kisslo JA, Popp RL, Sahn DJ, Schiller NB, Tajik A,

Teichholz LE & Weyman AE, Report of the American Society of Echocardiography Committee on Nomenclature and Standards in 2D Echocardiography, Circulation, 1980; 62: 212-217

Heyndrickx GR, Depression of regional blood flow and wall thickening after brief coronary occlusions, Am J Physiol, 1978; 234(6): 653-659

Hildick-Smith DJR & Shapiro LM, Echocardiographic differentiation of pathological and physiological LVH, Heart 2001; 85: 615-619

Ho CY, Sweitzer NK, McDonough B, Maron BJ, Casey SA, Seidman JG, Seidman CE & Solomons D, Assessment of diastolic function with Doppler tissue imaging to predict genotype in preclinical hypertrophic cardiomyopathy, Circulation 2002; 105: 2992 - 2997

Hoffman EA & Ritman EL, Invariant total heart volume in the intact thorax, Am J Physiol, 1985; 249: 883-890

Höglund C, Alam M & Thorsrand C, Atrioventricular valve plane displacement in healthy persons: an echocardiographic study, Acta Med Scand, 1988; 224: 557-562

Höglund C, Alam M & Thorsrand C, Effects of acute myocardial infarction on the displacement of the atrioventricular plane: an echocardiographic study, J Intem Med, 1989; 77: 979-984

Horowitz P & Winfield H, The Art of Electronics, New York, Cambridge University Press, 2nd ed, 1989

Hutson TP, Puffer JC & MacMillan W, The athlete heart syndrome, New England J Med, 1985; 313: 24-32
HYPERLINK
"http://circ.ahajournals.org/cgi/external_ref?access_num=3158817&link_type=MED"

Ikaheimo MJ, Palatsi IJ & Takkunen JT, Noninvasive evaluation of the athletic heart: sprinters versus endurance runners, Am J Cardiol, 1979; 44: 24-30
HYPERLINK
"http://circ.ahajournals.org/cgi/external_ref?access_num=156493&link_type=MED"

Ingels NB, Daughters GT, Stinson EB & Alderman EL, Measurement of midwall myocardial dynamics in intact man by radiography of surgically implanted markers, Circulation, 1975; 52: 859-867

Isaaz K, del Romeral LM, Lee E & Schiller NB, Quantitation of the motion of the cardiac base in normal subjects by Doppler echocardiography, J Am Soc Echocardiogr, 1993; 6: 166-176

Isaaz K, Thompson A, Ethevenot G, Cloez JL, Brembilla B & Pernot C, Doppler echocardiographic measurement of low velocity motion of the left ventricular posterior wall, Amer J Cardiol, 1989; 64, 66-75

Isaaz K, What are we actually measuring by Doppler tissue imaging? J Am Coll Cardiol, 2000; 36: 897-899

Isner JM, Estes NAM, Thompson PD, Costanza-Nordin MR, Subramanian R, Miller G, Katsas G, Sweeney K & Sturner WQ, Acute cardiac events temporally related to cocaine abuse, New England J Med 1986; 315: 1438-1443

Jensen-Urstad K, Bouvier F, Hojer J, Ruiz H, Hulting J, Samad B, Thorstrand C & Jensen-Urstad M, Comparison of different echocardiographic methods with radionuclide imaging for measuring left ventricular ejection fraction during acute myocardial infarction treated by thrombolytic therapy, Am J Cardiol, 1998 Mar 1; 81(5): 538-544

Jones CJH, Raposo L & Gibson DG, Functional importance of the long axis dynamics of the human left ventricle, Brit Heart J, 1990; 63: 215-220

Kassirer JP, Diagnosis in the public domain, New England J Med, 1993; 329: 50-51

Keele KD, Leonardo da Vinci's Elements of the Science of Man, London, Academic Press, 1983; p320

Keren G, Sonnenblick EH & Lejemtel TH, Mitral annulus motion: relation to pulmonary venous and transmitral flows in normal subjects and in patients with dilated cardiomyopathy, Circulation, 188; 78: 621-629

Keul J, Dickhuth H-H, Simon G & Lehmann M, Effect of static and dynamic exercise on heart volume, contractility, and left ventricular dimensions, Circ Res, 1981; 48(suppl I): I-162-I-170

Kim YJ & Sohn DW, Mitral annulus velocity in the estimation of left ventricular filling pressure: prospective study in 200 patients. J Am Soc Echocard 2000; 13: 980-985

King GJ, Foley JB, Almane F, Crean PA & Walsh MJ, Early diastolic filling dynamics in diastolic dysfunction, Cardiovasc Ultrasound, 2003; 1:9

Klemola E, Electrocardiographic observations of 650 Finnish athletes, Ann Med Intern Fenn, 1951; 40: 121-132

Kloner RA, Hale S, Alker K & Rezkalla S, The effects of acute and chronic cocaine use on the heart, Circulation, 1992; 85: 407-419
HYPERLINK
"http://circ.ahajournals.org/cgi/ijlink?linkType=ABST&journalCode=circulationaha&resid=85/2/407"
[Abstract]

Klues HG, Schiffers A & Maron BJ, Patterns of hypertrophy and morphologic spectrum in 600 patients with hypertrophic cardiomyopathy, Circulation, 1993; 88(suppl I): I-211 [Abstract]

Lattanzi F, Di Bello V, Picano E, Caputo MT, Talarico L, Di Muro C, Landini L, Santoro G, Giusti C & Distante A, Normal ultrasonic myocardial reflectivity in athletes with increased left ventricular mass: a tissue characterization study, Circulation, 1992; 85: 1828-1834
HYPERLINK
"http://circ.ahajournals.org/cgi/ijlink?linkType=ABST&journalCode=circulationaha&resid=85/5/1828"
[Abstract]

Lattanzi F, Spirito P, Picano E, Mazzarisi A, Landini L, Distante A, Vecchio C & L'Abbate A, Quantitative assessment of ultrasonic myocardial reflectivity in hypertrophic cardiomyopathy, J Am Coll Cardiol, 1991; 17: 1085-1090
HYPERLINK
"http://circ.ahajournals.org/cgi/external_ref?access_num=1826118&link_type=MED"

Lemery R, Kleinebenne A, Nihoyannopoulos P, Aber V, Alfonso F & McKenna WJ, Q waves in hypertrophic cardiomyopathy in relation to the distribution and severity of right and left ventricular hypertrophy, J Am Coll Cardiol, 1990; 16: 368-374
HYPERLINK
"http://circ.ahajournals.org/cgi/external_ref?access_num=2373813&link_type=MED"

Lewis JF, Maron BJ, Diggs JA, Spencer JE, Mehrotra PP & Curry CL, Pre-participation echocardiographic screening for cardiovascular disease in a large predominantly black population of collegiate athletes, Am J Cardiol, 1989; 64: 1029-1033
HYPERLINK
"http://circ.ahajournals.org/cgi/external_ref?access_num=2816733&link_type=MED"

Lewis JF, Spirito P, Pelliccia A & Maron BJ, Usefulness of Doppler echocardiographic assessment of

diastolic filling in distinguishing 'athlete's heart' from hypertrophic cardiomyopathy, Br Heart J, 1992; 68: 296-300
HYPERLINK
"http://circ.ahajournals.org/cgi/ijlink?linkType=ABST&journalCode=heartjnl&resid=68/3/296"
[Abstract]

Longhurst JC, Kelly AR, Gonyea WJ & Mitchell JH, Chronic training with static and dynamic exercise: cardiovascular adaptation and response to exercise, Circ Res, 1981; 48(suppl I): I-171-I-178

Longhurst JC, Kelly AR, Gonyea WJ & Mitchell JH, Echocardiographic left ventricular masses in distance runners and weight lifters, J Appl Physiol, 1980; 48: 154-162
HYPERLINK
"http://circ.ahajournals.org/cgi/ijlink?linkType=ABST&journalCode=jap&resid=48/1/154"
[Abstract]

Louie EK & Maron BJ, Hypertrophic cardiomyopathy with extreme increase in left ventricular wall thickness: clinical significance, functional and morphologic features, J Am Coll Cardiol, 1986; 8: 57-65
HYPERLINK
"http://circ.ahajournals.org/cgi/external_ref?access_num=2940288&link_type=MED"

Lundback S, Cardiovascular pumping and function of the ventricular septum, Acta Physiol Scand (Suppl), 1986; 550: 1-101

MacAlpin R, Assessment of coronary vasoreactivity, Circulation, 1996; 94: 589-590

Maier SE, Fischer SE, McKinnon GC, Hess OM, Krayenbuehl HP & Boesiger P, Evaluation of left ventricular segmental wall motion in hypertrophic cardiomyopathy with myocardial tagging, Circulation, 1992; 86: 1919-1928

Maron BJ & Epstein SE, Hypertrophic cardiomyopathy: a discussion of nomenclature, Am J Cardiol, 1979; 43: 1242-1244
HYPERLINK
"http://circ.ahajournals.org/cgi/external_ref?access_num=571671&link_type=MED"

Maron BJ & Garson A, Arrhythmias and sudden cardiac death in elite athletes, Cardiol Rev, 1994; 2: 26-32

Maron BJ & Mitchell JH, 26th Bethesda Conference: recommendations for determining eligibility for competition in athletes with cardiovascular abnormalities. J Am Coll Cardiol, 1994; 24: 845-899
HYPERLINK
"http://circ.ahajournals.org/cgi/external_ref?access_num=7798484&link_type=MED"

Maron BJ & Mitchell JH, Revised eligibility recommendations for competitive athletes with cardiovascular abnormalities: the introduction to Bethesda Conference #26. J Am Coll Cardiol, 1994; 24:846-848

Maron BJ, Bodison S, Wesley Y, Tucker E & Green KJ, Results of screening a large population of intercollegiate athletes for cardiovascular disease, J Am Coll Cardiol, 1987; 10: 1214-1222
HYPERLINK
"http://circ.ahajournals.org/cgi/external_ref?access_num=2960727&link_type=MED"

Maron BJ, Bonow RO, Cannon RO, Leon MB & Epstein SE, Hypertrophic cardiomyopathy: interrelation of clinical manifestations, pathophysiology, and therapy, New England J Med, 1987; 316: 780-789, 844-852
HYPERLINK
"http://circ.ahajournals.org/cgi/external_ref?access_num=3547130&link_type=MED"

Maron BJ, Epstein SE & Roberts WC, Causes of sudden death in the competitive athlete, J Am Coll

Cardiol, 1986; 7: 204-214
HYPERLINK
"http://circ.ahajournals.org/cgi/external_ref?access_num=3510233&link_type=MED"

Maron BJ, Gottdiener JS & Epstein SE, Patterns and significance of the distribution of left ventricular hypertrophy in hypertrophic cardiomyopathy: a wide-angle, two-dimensional echocardiographic study of 125 patients, Am J Cardiol, 1981; 48: 418-428

Maron BJ, Gottdiener JS, Bonow RO & Epstein SE, Hypertrophic cardiomyopathy with unusual locations of left ventricular hypertrophy undetectable by M-mode echocardiography: identification by wide-angle, two-dimensional echocardiography, Circulation, 1981; 63: 409-418
HYPERLINK
"http://circ.ahajournals.org/cgi/ijlink?linkType=ABST&journalCode=circulationaha&resid=63/2/409"
[Abstract]

Maron BJ, Hypertrophic cardiomyopathy: a systematic review, JAMA, 2002; 287: 1308-1320

Maron BJ, Isner JM & McKenna WJ, 26th Bethesda Conference: recommendations for determining eligibility for competition in athletes with cardiovascular abnormalities. Task Force 3: hypertrophic cardiomyopathy, myocarditis and other myopericardial diseases and mitral valve prolapse, J Am Coll Cardiol, 1994; 24: 880-885

Maron BJ, Nichols PF, Pickle LW, Wesley YE & Mulvihill JJ, Patterns of inheritance in hypertrophic cardiomyopathy: assessment by M-mode and two-dimensional echocardiography, Am J Cardiol, 1984; 53: 1087-1094
HYPERLINK
"http://circ.ahajournals.org/cgi/external_ref?access_num=6538384&link_type=MED"

Maron BJ, Pelliccia A & Spirito P, Cardiac disease in young trained athletes: insights into methods for distinguishing athlete's heart from structural heart disease with particular emphasis on hypertrophic cardiomyopathy, Circulation, 1995; 91: 1596-1601

Maron BJ, Pelliccia A, Spataro A & Granata M, Reduction in left ventricular wall thickness after deconditioning in highly trained Olympic athletes, Br Heart J, 1993; 69: 125-128
HYPERLINK
"http://circ.ahajournals.org/cgi/ijlink?linkType=ABST&journalCode=heartjnl&resid=69/2/125"
[Abstract]

Maron BJ, Roberts WC, McAllister HA, Rosing DR & Epstein SE, Sudden death in young athletes, Circulation, 1980; 62: 218-229
HYPERLINK
"http://circ.ahajournals.org/cgi/ijlink?linkType=ABST&journalCode=circulationaha&resid=62/2/218"
[Abstract]

Maron BJ, Shirani J, Mueller FO, Cantu RC & Roberts WC, Cardiovascular causes of "athletic field" deaths: analysis of sudden death in 84 competitive athletes, Circulation, 1993; 88(suppl I): I-50, Abstract

Maron BJ, Shirani J, Poliac LC, Mathenge R, Roberts WC & Mueller FO, Sudden death in young competitive athletes: Clinical, demographic, and pathological profiles, JAMA, 1996; 276: 199-204

Maron BJ, Spirito P, Green KJ, Wesley YE, Bonow RO & Arce J, Noninvasive assessment of left ventricular diastolic function by pulsed Doppler echocardiography in patients with hypertrophic cardiomyopathy, J Am Coll Cardiol, 1987; 10: 733-742
HYPERLINK
"http://circ.ahajournals.org/cgi/external_ref?access_num=3655141&link_type=MED"

Maron BJ, Spirito P, Wesley Y & Arce J, Development and progression of left ventricular hypertrophy in children with hypertrophic cardiomyopathy, New England J Med, 1986; 315: 610-614
HYPERLINK
"http://circ.ahajournals.org/cgi/ijlink?linkType=ABST&journalCode=nejm&resid=315/10/610"
[Abstract]

Maron BJ, Structural features of the athlete heart as defined by echocardiography. J Am Coll Cardiol, 1986; 7:190-203.
HYPERLINK
"http://circ.ahajournals.org/cgi/external_ref?access_num=2934463&link_type=MED"

Maron BJ, Sudden death in young athletes: lessons from the Hank Gathers affair, New England J Med, 1993; 329: 55-57

Maron BJ, Wolfson JK, Ciró E & Spirito P, Relation of electrocardiographic abnormalities and patterns of left ventricular hypertrophy identified by two-dimensional echocardiography in patients with hypertrophic cardiomyopathy, Am J Cardiol, 1983; 51: 189-194
HYPERLINK
"http://circ.ahajournals.org/cgi/external_ref?access_num=6217739&link_type=MED"

McDicken WN, Sutherland GR, Moran CM & Gordon LN, Colour Doppler velocity imaging of the myocardium, Ultrasound in Med & Biol, 1992; 18: 651-654

McDonald IG, The shape and movements of the human left ventricle during systole: a study by cineangiography and by cineradiography of epicardial markers, Am J Cardiol, 1970; 26: 221-230

McKeag DB, Preparticipation screening of the potential athlete, Clin Sports Med, 1989; 8: 373-397

McKenna WJ, Thiene G, Nava A, Fontaliran F, Blomstrom-Lundqvist C, Fontaine G & Camerini F (on behalf of the Task Force of the Working Group Myocardial and Pericardial Disease of the European Society of Cardiology and of the Scientific Council on Cardiomyopathies of the International Society and Federation of Cardiology), Diagnosis of arrhythmogenic right ventricular dysplasia/ cardiomyopathy, Br Heart J, 1994; 71: 215-218
HYPERLINK
"http://circ.ahajournals.org/cgi/external_ref?access_num=8142187&link_type=MED"

Milliken MC, Stray-Gundersen J, Peshock RM, Katz J & Mitchell JH, Left ventricular mass as determined by magnetic resonance imaging in male endurance athletes, Am J Cardiol, 1988; 62: 301-305
HYPERLINK
"http://circ.ahajournals.org/cgi/external_ref?access_num=2969673&link_type=MED"

Miyatake K, Yamagishi M, Tanaka N, Uematsu M, Yamazaki N, Mine Y, Sano A & Hirama M, New method for evaluating left ventricular wall motion by color-coded tissue Doppler imaging: in vitro and in vivo studies, J Am Coll Cardiol, 1995; 25: 717-724

Morganroth J, Maron BJ, Henry WL & Epstein SE, Comparative left ventricular dimensions in trained athletes, Ann Intern Med, 1975; 82: 521-524
HYPERLINK
"http://circ.ahajournals.org/cgi/external_ref?access_num=1119766&link_type=MED"

Nagel E, Stuber M, Lakatos M, Scheidegger MB, Boesiger P & Hess OM, Cardiac rotation and relaxation after anterolateral myocardial infarction, Coron Artery Dis, 2000; 11: 261-267

Nagueh SF, Bachinski LL, Meyer D, Hill R, Zoghbi WA, Tam JW, Quinones MA, Roberts R & Marian AJ. Tissue Doppler imaging consistently detects myocardial abnormalities in patients with hypertrophic cardiomyopathy and provides a novel means for an early diagnosis before and independently of

hypertrophy, Circulation, 2001; 104: 128-130

Nagueh SF, Kopelen HA, Lim DS, Zoghbi WA, Quinones MA, Roberts R & Marian AJ, Tissue Doppler imaging consistently detects myocardial contraction and relaxation abnormalities, irrespective of cardiac hypertrophy, in a transgenic rabbit model of human hypertrophic cardiomyopathy, Circulation, 2000; 102: 1346-1350

Nagueh SF, Lakkis NM, Middleton KJ, Spencer III WH, Zoghbi WA & Quinones MA, Doppler estimation of left ventricular filling pressures in patients with hypertrophic cardiomyopathy, Circulation 1999; 99: 254-261

Nagueh SF, Middleton KJ, Kopelen HA, Zoghbi WA & Quinones MA, Doppler Tissue Imaging: a non-invasive technique for evaluation of left ventricular relaxation and estimation of filling pressures, J Am Coll Cardiol, 1997; 30: 1527-1533

Nagueh SF, Sun H, Kopelen HA, Middleton KJ & Khoury DS, Haemodynamic determinants of the mitral annulus diastolic velocities by tissue Doppler, J Am Coll Cardiol, 2001; 37: 278-285

New Health Strategy, Department of Health and Children, Dublin, 2000
Nishimura T, Yamada Y & Kawai C, Echocardiographic evaluation of long-term effects of exercise on left ventricular hypertrophy and function in professional bicyclists, Circulation, 1980; 61: 832-840
HYPERLINK
"http://circ.ahajournals.org/cgi/ijlink?linkType=ABST&journalCode=circulationaha&resid=61/4/832"
[Abstract]

Nixon JV, Wright AR, Porter TR, Roy V & Arrowood JA, Effects of exercise on left ventricular diastolic performance in trained athletes, Am J Cardiol, 1991; 68: 945-949
HYPERLINK
"http://circ.ahajournals.org/cgi/external_ref?access_num=1927955&link_type=MED"

Odqvist H, A roentgen cinematographic study of the movements of the mitral ring during heart action, Acta Radiol, 1945; 26: 392-396

Ohte N, Narita H, Hashimoto T, Akita S, Kurokawa K & Fujinami T, Evaluation of left ventricular early diastolic performance by Tissue Doppler Imaging of the mitral annulus, Am J Cardiol, 1998; 82: 1414-1417

Oki T, Tabata T, Yamada H, Wakatsyki T, Shinohara H, Nishikado A, Iuchi A, Fukuda N & Ito S, Clinical application of pulsed Doppler tissue imaging for assessing abnormal left ventrieular relaxation, Am J Cardiol, 1997; 79: 921-928

Ormiston JA, Shah PM, Tei C & Wong M, Size and motion of the mitral valve annulus in man: 1. A two-dimensional echocardiographic method and findings in normal subjects, Circulation, 1981; 64: 113-120

Otterstad JE, Froeland G, St. John Sutton M & Holme I, Accuracy and reproducibility of bi plane two-dimensional echocardiographic measurements of left ventricular dimensions and function, Eur Heart J, 1997; 18 (3): 507-513

Paelinck BP, van Eck WM, De Hert SG & Gillebert TC, Effects of postural changes on cardiac function in healthy subjects, Eur J Echocardiogr, 2003; 4: 196-201

Pai RG, Bodenheimer MM, Pai SM, Koss JH & Adamick RD, Usefulness of systolic excursion of the mitral annulus as an index of left ventricular systolic function, Am J Cardiol, 1991; 67: 222-224

Palka P, Lange A & Fleming AD, Doppler tissue imaging: myocardial wall motion velocities in normal subjects, J Am Soc Echocardiogr, 1995; 8: 659-668

Pearson AC, Schiff M, Mrosek D, Labovitz AJ & Williams GA, Left ventricular diastolic function in weight lifters, Am J Cardiol, 1986; 58: 1254-1259
HYPERLINK
"http://circ.ahajournals.org/cgi/external_ref?access_num=2947454&link_type=MED"

Pelliccia A, Maron BJ, Culasso F, Spataro A & Caselli G, Athlete's heart in women: echocardiographic characterization of highly trained elite female athletes, JAMA, 1996; 276: 211-215

Pelliccia A, Maron BJ, Spataro A & Caselli G, Absence of left ventricular hypertrophy in athletes engaged in intense power training, Am J Cardiol, 1993; 72: 1048-1054
HYPERLINK
"http://circ.ahajournals.org/cgi/external_ref?access_num=8213586&link_type=MED"

Pelliccia A, Maron BJ, Spataro A, Biffi A, Caselli G & Culasso F, Physiological limits of 'athlete's heart' in women, Circulation, 1993; 88(suppl I): I-57 Abstract

Pelliccia A, Maron BJ, Spataro A, Proschan MA & Spirito P, The upper limit of physiologic cardiac hypertrophy in highly trained elite athletes, New Engl J Med, 1991; 324: 295-301
HYPERLINK
"http://circ.ahajournals.org/cgi/ijlink?linkType=ABST&journalCode=nejm&resid=324/5/295"
[Abstract]

Pérez JE & Lang RM (eds), Echocardiography and Cardiovascular Function: Tools for the Next Decade, Dordrecht: Kluwer Academic, 1997

Phillips RA, Coplan NL, Krakoff LR, Yeager K, Ross RS, Gorlin R & Goldman ME, Doppler echocardiographie analysis of left ventricular filling in treated hypertensive patients, J Am Coll Cardiol, 1987; 9: 317-322
HYPERLINK
"http://circ.ahajournals.org/cgi/external_ref?access_num=3805521&link_type=MED"

Price DJ, Wallbridge DR & Stewart MJ, Tissue Doppler imaging: current and potential clinical applications, Heart, 2000; 84 Suppl 2:II: 11-18

Rademakers FE, Buchalter MB, Rodgers JW, Zerhouni EA, Weisfeldt ML, Weiss JL & Shapiro EP, Dissociation between left ventricular untwisting and filling: rotational deformation of the canine left ventricle measured by magnetic resonance tagging: effects of catecholamines, ischaemia and pacing, Circulation, 1992; 85: 1572-1581

Rademakers FE, Rogers JW, Guier WH, Hutchins GM, Siu CO, Weisfeldt ML, Weiss JL & Shapiro EP, Relationship of cross-fiber shortening to wall thickening in the intact heart: 3-D strain analysis using NMR tagging, Circulation, 1994; 89: 1174-1181

Ricci C, Longo R, Pagnan L, Dalla Palma L, Pinamonti B, Camerini F, Bussani R & Silvestri F, Magnetic resonance imaging in right ventricular dysplasia, Am J Cardiol, 1992; 70: 1589-1595
HYPERLINK
"http://circ.ahajournals.org/cgi/external_ref?access_num=1466328&link_type=MED"

Riley-Hagen M, Peshock RM, Stray-Gundersen J, Katz J, Ryschon TW & Mitchell JH, Left ventricular dimensions and mass using magnetic resonance imaging in female endurance athletes, Am J Cardiol, 1992; 69: 1067-1074
HYPERLINK
"http://circ.ahajournals.org/cgi/external_ref?access_num=1561980&link_type=MED"

Rivas-Goetz KD, Manolios M, Rao L, Kopelen H, Nagueh SF, Time interval between onset of mitral

Appendix A

Specifications for the ultrasound scanning systems used in this work and a description of the set-up for making simultaneous DTI and M-mode examinations using both scanners together

SONOS 4500

Ultrasound Imaging System
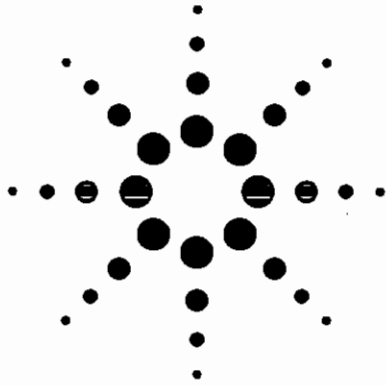
Data Sheet

- 512-channel digital system

- Fusion Imaging with Adaptive Power

- Harmonic Fusion Imaging with Power Modulation

- Ultraband transducers (sector, linear array and curved linear array)

- New s3 Ultraband transducer
  − 1.3/2.6; 1.6/3.2 MHz Harmonics

- New c3540 Ultraband CLA transducer
  − 2.1/4.2; 2.5/5.0 MHz Harmonics

- LVD imaging with Power Modulation

- Soft Echo Enhancement

- 300 Hz frame rate (maximum)

- Optional stress echo package

- High-Definition Acoustic Zoom with flexible pan capability

- Color compare mode

- Full-screen and split-screen M-mode and Doppler spectral display

- DICOM print capability

- Remote support capability
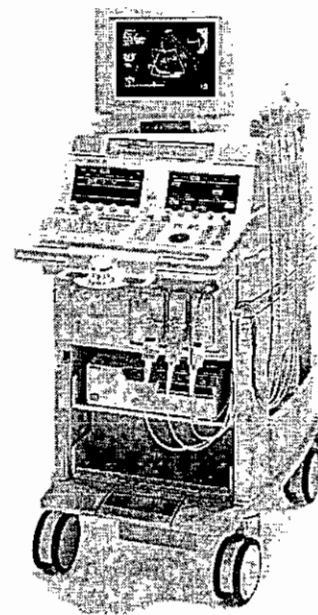
Agilent Technologies

SONOS 4500
Digital Echocardiography System
Product No. M2424A, option A06

Upgrade to SONOS 4500 Revision B.2
Product No. M2425A

STANDARD FEATURES & OPTIONS

Anatomy

- Fusion Imaging

- Harmonic Fusion Imaging with
  Power Modulation

- Ultraband 1–12 MHz 2-D sector imaging

- Ultraband 3–15 MHz B-mode linear array
  imaging

- M-mode

- High-frame-rate scanning up to 300 Hz

- Acoustic Cine

- Colorization

- Lateral Gain Control (LGC)

- High-Definition Acoustic Zoom with
  flexible pan capability

Function

- Adaptive Color Flow

- Adaptive Doppler

- Steerable pulsed- and continuous-
  wave Doppler

- Color compare mode

- Full-screen and split-screen M-mode and
  Doppler spectral display

- Acoustically-optimized stereo Doppler
  speakers (2 front-mounted mid-range;
  2 rear-mounted low-range)

- 1.9 MHz CW Doppler non-imaging
  pencil transducer

- Angio

- Tissue Doppler

- Contrast imaging capability for
  Left Ventricular Opacification (LVO)*

Viability

- Optional stress echo package

Information Management

- Study Manager option

- Digital Storage and Retrieval (DSR) —
  optional 8x drive can read media from 1x,
  2x, 4x and 8x drives; can write to
  4x and 8x media (2.3 and 4.8 Gbyte
  optical disks)

- Integrated Digital Interface (IDI) —
  option provides network connectivity
  to EnConcert echo information
  management system; configured for
  EnConcert or third-party DICOM server

* Use contrast agents approved for commercial
distribution for the intended use under applicable
U.S. and international regulations.

S O N O S
5 5 0 0

Ultrasound Imaging System
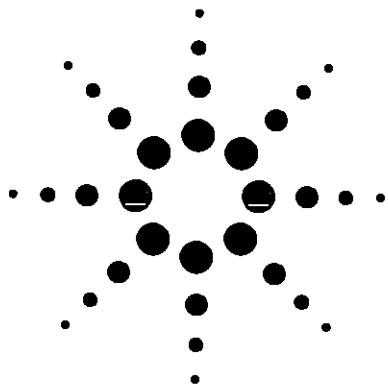
Data Sheet

- 512-channel digital system

- Fusion Imaging with Adaptive Power

- Harmonic Fusion Imaging with
  Power Modulation

- Ultraband transducers (sector, linear
  array and curved linear array)

- s3 Ultraband transducer
  − 1.3/2.6; 1.6/3.2 MHz Harmonics
  − 1.3/3.6 MHz Ultraharmonics

- Comprehensive contrast capabilities
  for research and LVO:

  − Real-time MCE imaging with
    Power Modulation (optional)

  − Ultraharmonics and enhanced
    Harmonic Angio for triggered
    MCE imaging

  − LVO imaging with Power Modulation

  − Acoustic Densitometry

- Soft Echo Enhancement

- High-Definition Acoustic Zoom with
  flexible pan capability

- Color compare mode

- Full-screen and split-screen M-mode and
  Doppler spectral display

- Optional Acoustic Quantification,
  Color Kinesis, Dynamic Stress Echo,
  Integrated 3-D Acquisition

- DICOM print capability
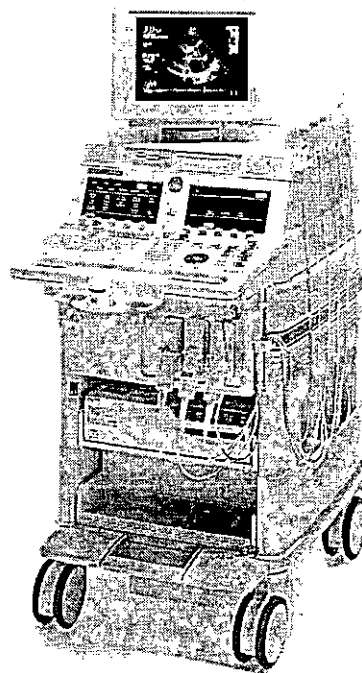
Agilent Technologies

S O N O S   5 5 0 0
Digital Echocardiography System
Product No. M2424A, option A05

Upgrade to SONOS 5500 Revision B.2
Product No. M2425A, option K25

STANDARD FEATURES AND OPTIONS

Anatomy

- Fusion Imaging with Adaptive Power

- Harmonic Fusion Imaging with
Power Modulation

- Frequency Fusion control

- Ultraband 1–12 MHz 2-D sector imaging

- Ultraband 3–15 MHz B-mode
linear array imaging

- M-mode

- High-frame-rate scanning up to 300 Hz

- Acoustic Cine

- Colorization

- Lateral Gain Control (LGC)

- High-Definition Acoustic Zoom with
flexible pan capability

Function

- Adaptive Color Flow

- Adaptive Doppler

- Steerable pulsed- and continuous- wave
Doppler

- Color compare mode

- Full-screen and split-screen M-mode and
Doppler spectral display

- Acoustically-optimized stereo Doppler
speakers (2 front-mounted mid-range;
2 rear-mounted low-range)

- 1.9 MHz CW Doppler non-imaging
pencil transducer

- Angio

- Tissue Doppler

- Contrast imaging capability for Left
Ventricular Opacification (LVO)*

Viability

- Contrast imaging capabilities for
research and LVO:

  – Real-time MCE: low-MI non-
destructive technique using
Power Modulation for real-time
MCE (optional)

  – Ultraharmonics: higher-MI 2-D
technique to burst bubbles for
triggered MCE imaging

  – Harmonic Angio: higher-MI angio
technique to burst bubbles for
triggered MCE imaging

- Harmonic Imaging in all modes, including
2-D, Doppler, Color Flow, Angio, Tissue
Doppler, Dynamic Stress Echo, Acoustic
Quantification, Color Kinesis, Multiple
Frame Trigger with dual display

- Acoustic Densitometry

Information Management

- Study Manager

- Digital Storage and Retrieval (DSR) — 8x
drive can read media from 1x, 2x,
4x and 8x drives; can write to 4x and 8x
media (2.3 and 4.8 Gbyte optical disks)

- Integrated Digital Interface (IDI) —
option provides network connectivity to
EnConcert echo information manage-
ment system; configured for EnConcert
or third-party DICOM server

* Use contrast agents approved for commercial
distribution for the intended use under applicable
U.S. and international regulations.

Measurement of time difference between peak tissue velocity and peak mitral valve opening

Technical Set-up

The parameter of interest in this experiment is the time difference between peak tissue velocity as measured by DTI and peak mitral valve opening as detected by M-Mode. Currently available technology does not support simultaneous DTI and M-Mode measurements using a single ultrasound machine. In order to measure the time difference of interest two simultaneous measurements, one DTI and one M-Mode, were made using two different machines, Agilent 4500 and Agilent 5500.

Each machine provides an on-screen calliper to measure temporal differences between events displayed on that machine. In order to measure time differences between events seen on one machine versus events seen on the other, it is necessary to introduce a common temporal reference to both machines.

The machines used allow a number of physiological signals to be input and displayed as overlays on the M-Mode or DTI velocity traces. Initially the R-wave of the subject's ECG was considered for use as a temporal reference signal. The ECG was fed into the ECG input jacks of both machines and displayed as an overlay on the M-Mode and DTI images. The time from peak ring velocity to an R-wave on one machine and from peak mitral opening to the corresponding R-wave on the other were measured. The difference between these two values gave the time difference between peak mitral opening and peak ring velocity in the same heartbeat. In practice it was found to be difficult to identify the same R-wave consistently on both machines and so this approach was considered to be unsatisfactory.

As shown in Figure A1, simple footswitch-operated circuit was built to introduce a clear temporal reference. The circuit is connected to a free ECG channel on each machine. When a satisfactory image quality is obtained on both ultrasound machines, one operator depresses the footswitch. The circuit generates a voltage pulse 'high' while the switch is depressed and a voltage 'low' otherwise. The circuit incorporates a standard switch debouncing circuit to eliminate the possibility of multiple signal

transitions on depressing or releasing the footswitch. The voltage pulse appears as an overlay on the M-Mode and DTI traces as shown in Figure A2. The rising edge is then used as the temporal reference, rather than the R-wave as described above.

Temporal resolution

The temporal resolution of the on-screen callipers varies with the scan sweep setting. With a scan sweep setting of 100 ms/s, the callipers gives an on-screen resolution of 5ms. A time difference between any two events on the screen of one machine can therefore be measured to within ± 2.5 ms. When measuring temporal differences between events on the two machines, the calliper resolution results in a theoretical accuracy of ± 5ms.

Timing errors due to differences in sound propagation time to each of the two probes will be negligible.

Validation of Method

In this test a signal generator was use to introduce a triangular waveform into one of the physiological signal inputs on each ultrasound machine. The footswitch was connected in the usual way to an ECG input jack. Depressing the footswitch introduces the pulse waveform as seen in the figure. The display of each machine, shown in Figure A3, displays both the footswitch pulse and the triangular waveform. The time from the rising edge of the footswitch pulse to the peak of the nearest triangular wave was measured on each machine using the on-screen callipers. The measurement was made a large number of times and in all cases the measurements differed by no more than ± 5 ms, as expected.

This test demonstrates that the physiological input channels are temporally 'stable' and do not introduce any additional timing measurement error.

In an ideal test of the accuracy of the timing difference measurement method, a DTI velocity 'event' and an M-Mode 'event' would be generated in a phantom at a known temporal separation. The error between the actual and measured time difference

between these events could then be found, and the accuracy of the timing measurement method assessed. In practice it is difficult to envisage a practical phantom implementation for this purpose, and the simpler test described was adopted.
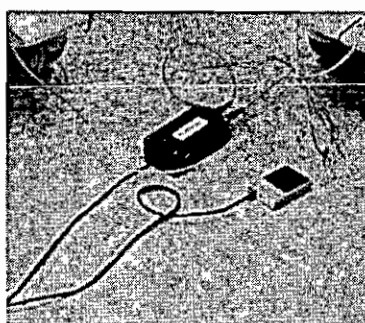
Figure A1   **Footswitch used to introduce reference timing pulse in traces of both ultrasound machines**
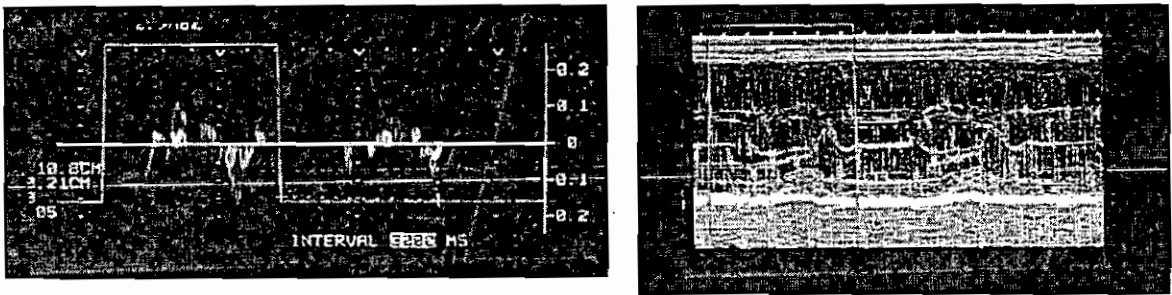
Figure A2   Timing pulses on DTI and M-Mode traces
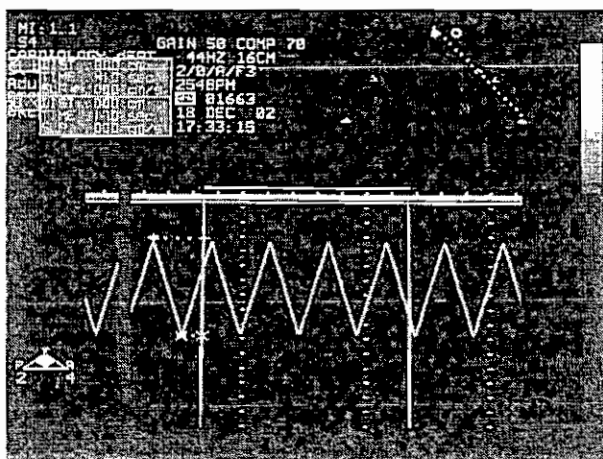
Figure A3   Test waveform used in validation of the method of measuring the
time delay between peak tissue velocity as measured by DTI and
peak mitral valve opening as detected by M-Mode

Appendix B

Ethical approvals for the work reported in this thesis, a copy of the information leaflet for subjects and a copy of the approval form signed-off by each subject

Dan Lynch, Joint Research Ethics Committee Secretariat.
Telephone: 4142860. Fax: 4142371. Email: dan.lynch@amnch.ie

Professor Michael Walsh,
Consultant Cardiologist,
St. James's Hospital,
James's Street,
Dublin 8

25th October 2001

Re: **Early diastolic filling and its relationship to mitral annular velocity, as
recorded by Doppler tissue Imaging.**

Please quote this reference in all communications regarding this study : 011006 / 16801

Dear Professor Walsh,

The Joint Research Ethics Committee at its meeting on 9th October 2001 agreed to
give ethical approval to the above study.

Yours sincerely,

Daniel R. Lynch,
Senior Executive Officer.

cc   Mr. Gerard King

Dan Lynch, Joint Research Ethics Committee Secretariat.
Telephone: 4142860. Fax: 414237. Email: dan.lynch@amnch.ie

Mr. Gerard King,
Cardiology Department,
St. James's Hospital,
James's Street,
Dublin 8

19th March 2002

Re: **Mitral Annular dynamics and the hypertrophied heart: Differentiation between pathological and physiological hypertrophy, a new method.**

Please quote this reference in all communications regarding this study : 020207 / 2302

Dear Mr King,

The Joint Research Ethics Committee at its meeting on 19th February 2002 agreed to give ethical approval to the above study subject to the following condition:

❑   The Investigator is asked to confirm that this proposed study will comply with the Ethics Committee's recommendations in relation to genetic testing in a clinical trial.

I should emphasise that these recommendations are in preparation and may be finalised at the next meeting of the Joint Research Ethics Committee which will take place on 26th March. I will send the recommendations to you as soon as they are available.

Yours sincerely,

Daniel R. Lynch,
Senior Executive Officer.

This letter also sent to Dr. J. B. Foley, Consultant Cardiologist, St. James's Hospital

PATIENT INFORMATION LEAFLET FOR FOR AN ECHOCARDIOGRAPHIC STUDY TO DIFFERENTIATE BETWEEN THE INCREASE IN HEART MUSCLE SIZE CAUSED BY HYPERTROPHIC CARDIOMYOPATHY FROM THAT CAUSED BY EXTENSIVE PHYSICAL TRAINING

Hypertrophic cardiomyopathy is an inherited condition, which causes abnormal thickening of heart muscle. It can cause symptoms of chest pain, breathlessness, palpitations or collapse. It is rarely associated with sudden death, which may be precipitated by heavy physical exercise.

Athletes who train heavily also develop a thickened heart muscle, which is a normal response to training. It is important to differentiate between those who have a thickened heart, which is normal to those who have a thickened heart due to a disease process.

Standard Echocardiography which is a routine ultrasound scan of the heart is unable to reliably differentiate between these groups. Doppler tissue imaging is a new addition to the Echo machine, which allows us to make measurements of how the heart muscle contracts and relaxes.

If you become involved in the study an Echocardiogram will be performed by two operators on the same day. A routine physical examination will be carried out and an electrocardiogram or tracing of your heart will be performed. The scan is non invasive, painless and does not expose you to any risk. If you are on any cardiac medications these will be stopped for forty eight hours prior to the procedure.

All information will be confidential and your identity will be protected throughout.

If you require any further information you can contact Dr Brendan Foley Consultant Cardiologist or Gerard King through the Cardiology Department of St James's Hospital.

**ST JAMES'S HOSPITAL AND FEDERATED DUBLIN VOLUNTARY HOSPITALS
JOINT RESEARCH ETHICS COMMITTEE
CONSENT FORM** (template)

Title of research study: Mitral Annular dynamics and the hypertrophied heart.
Differenciation between pathological and physiological hypertrophy .A new Method .

This study and this consent form have been explained to me. My doctor has answered all my questions to my satisfaction. I believe I understand what will happen if I agree to be part of this study.
I have read, or had read to me, this consent form. I have had the opportunity to ask questions and all my questions have been answered to my satisfaction. I freely and voluntarily agree to be part of this research study, though without prejudice to my legal and ethical rights. I have received a copy of this agreement and I understand that, if there is a sponsoring company, a signed copy will be sent to that sponsor.
Name of sponsor:

PARTICIPANT'S NAME:

PARTICIPANT'S SIGNATURE:

Date::
Date on which the participant was first furnished with this form:`

Where the participant is incapable of comprehending the nature, significance and scope of the consent required, the form must be signed by a person competent to give consent to his or her participation in the research study (other than a person who applied to undertake or conduct the study). If the subject is a minor (under 18 years old) the signature of parent or guardian must be obtained:-

NAME OF CONSENTOR, PARENT or GUARDIAN:
SIGNATURE:
RELATION TO PARTICIPANT:

Where the participant is capable of comprehending the nature, significance and scope of the consent required, but is physically unable to sign written consent, signatures of two witnesses present when consent was given by the participant to a registered medical practitioner treating him or her for the illness.

NAME OF FIRST WITNESS: SIGNATURE:
NAME OF SECOND WITNESS: SIGNATURE:

Statement of investigator's responsibility: I have explained the nature, purpose, procedures, benefits, risks of, or alternatives to, this research study. I have offered to answer any questions and fully answered such questions. I believe that the participant understands my explanation and has freely given informed consent.

Physician's signature:
Date:
(Keep the original of this form in the participant's medical record, give one copy to the participant, keep one copy in the investigator's records, and send one copy to the sponsor (if there is a sponsor).

Appendix C

Tables of raw measured data for the study described in chapter 5 and four figures showing low correlations between ejection fraction and mean Sw and mean Q-Sw corresponding to hypokinetic regions in the infarcted group at all ring sites.
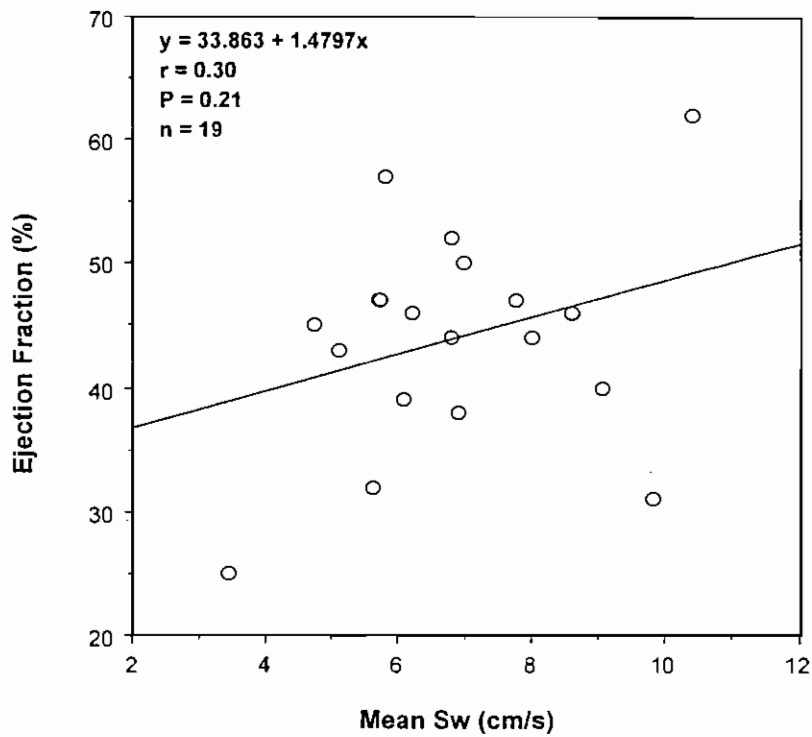
Figure C1 **Relationship between ejection fraction and mean Sw derived from ring sites corresponding to hypokinetic myocardial regions in the infarcted group.**
Although ejection fraction appears to correlate positively with mean Sw, there was no statistically significant relationship.
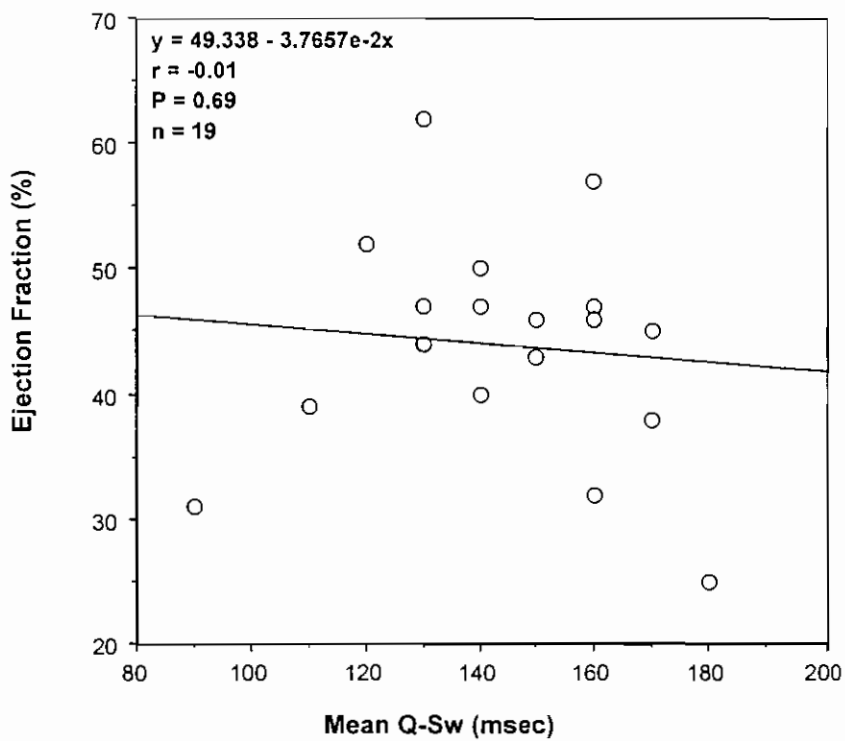
Figure C2   **Relationship between ejection fraction and mean Q-Sw obtained at ring sites corresponding to hypokinetic ventricular regions in the infarcted group.**
No statistically significant correlation between ejection fraction and mean Q-Sw was found.
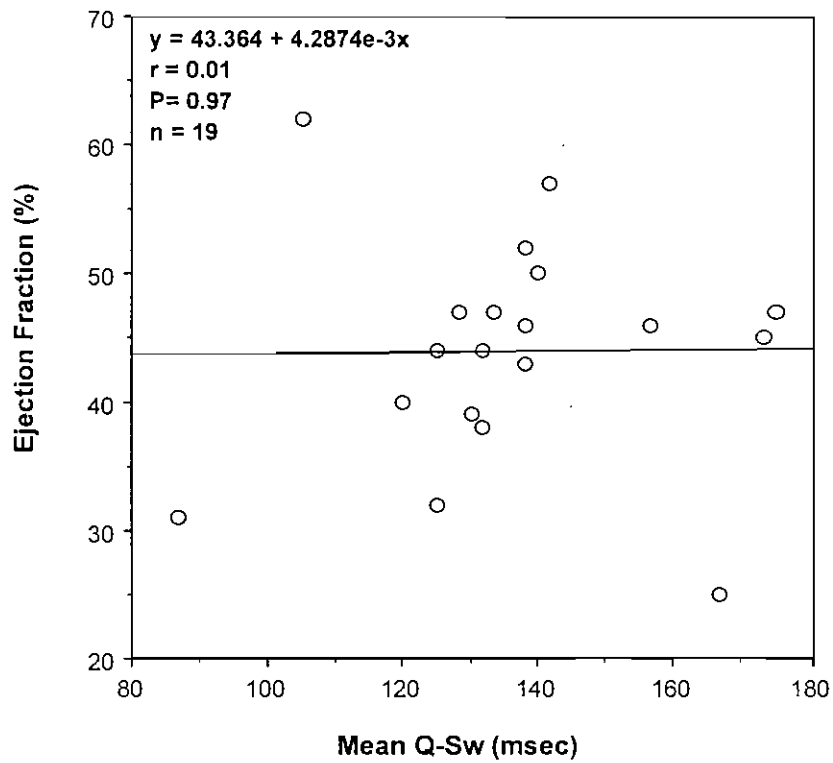
Figure C3 **Relationship between ejection fraction and mean Q-Sw derived from all six ring sites.**
No significant correlation between this variable and ejection fraction was revealed.
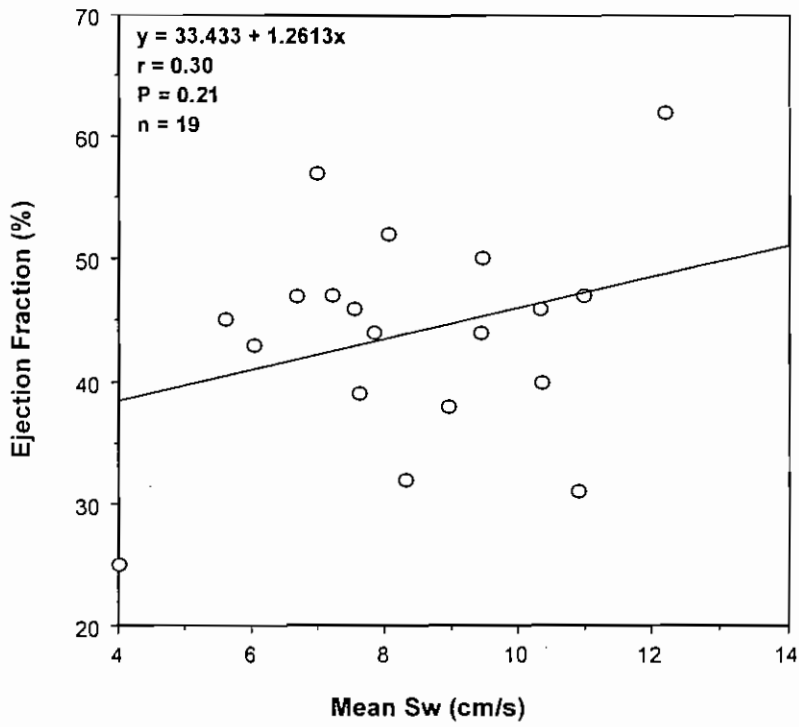
Figure C4   Relationship between ejection fraction and mean Sw derived from all ring sites
No significant correlation between this variable and ejection fraction was found.

Mean data for each ring site in the anterior *(The lower mean Sw and the slightly higher mean Q-Sw at site 6, correspond to inferior infarction.)*, **inferior** *(The slightly lower mean Sw at site 5 corresponds to anterior infarction.)* **and control groups**

Ring site	Measurement	Anterior	Inferior	Controls
1	mean Sw (cm/s)	7.0 ± 0.6	10.0 ± 0.9	8.9 ± 1.0
1	mean Q-Sw (ms)	128.8 ± 8.8	131.8 ± 8.1	129.1 ± 9.7
2	mean Sw (cm/s)	8.0 ± 0.9	9.3 ± 0.6	8.1 ± 0.8
2	mean Q-Sw (ms)	160.0 ± 10.9	137.3 ± 8.2	149.1 ± 6.0
3	mean Sw (cm/s)	6.6 ± 0.7	9.4 ± 0.7	8.7 ± 1.1
3	mean Q-Sw (ms)	127.5 ± 13.3	132.7 ± 5.4	124.0 ± 9.0
4	mean Sw (cm/s)	8.8 ± 1.0	9.1 ± 0.6	8.7 ± 1.2
4	mean Q-Sw (ms)	141.3 ± 11.6	134.6 ± 9.7	135.4 ± 10.7
5	mean Sw (cm/s)	6.1 ± 0.7	9.2 ± 0.6	9.2 ± 1.2
5	mean Q-Sw (ms)	146.3 ± 11.2	124.6 ± 4.7	124.1 ± 8.9
6	mean Sw (cm/s)	7.6 ± 0.9	7.4 ± 0.5	8.7 ± 0.9
6	mean Q-Sw (ms)	132.5 ± 12.8	140.9 ± 4.4	127.9 ± 8.9

Ejection fraction (EF) data *(Values are percentages of the end-diastolic volume ejected from the heart during systole)*, **age data and heart rate (HR) data for the three groups** The overall infarcted group is not included in this table.

Subject number	Measurement	Anterior	Inferior	Controls
1	EF (%)	47	40	56
	Age (years)	79	55	48
	HR (beat/min)	45	77	78
2	EF (%)	57	43	56
	Age (years)	62	50	60
	HR (beat/min)	65	75	72
3	EF (%)	45	52	66
	Age (years)	71	63	47
	HR (beat/min)	63	65	78
4	EF (%)	46	32	69
	Age (years)	67	78	57
	HR (beat/min)	64	66	57
5	EF (%)	39	44	60
	Age (years)	57	32	62
	HR (beat/min)	76	88	70
6	EF (%)	25	47	68
	Age (years)	68	68	48
	HR (beat/min)	65	66	97
7	EF (%)	40	62	68
	Age (years)	73	72	49
	HR (beat/min)	73	71	71
8	EF (%)	31	44	71
	Age (years)	73	61	74
	HR (beat/min)	98	90	56
9	EF (%)		46	
	Age (years)		72	
	HR (beat/min)		68	
10	EF (%)		47	
	Age (years)		63	
	HR (beat/min)		64	
11	EF (%)		50	
	Age (years)		61	
			70	

Appendix D

Copy of the published paper on the work described in Chapter 6, and a recent evaluation of the extent of peer interest in the paper

Cardiovascular Ultrasound

Research

Early diastolic filling dynamics in diastolic dysfunction

Gerard J King*, Jerome B Foley, Faisal Almane, Peter A Crean and Michael J Walsh

Address: Trinity College, Dublin and St. James's Hospital, Dublin 8, Ireland

Email: Gerard J King* -gking@stjames.ie; Jerome B Foley -bfoley@stjames.ie; Faisal Almane · Cardiology@stjames.ie; Peter A Crean -Creansec@stjames.ie; Michael J Walsh · walshsec@stjames.ie

* Corresponding author

Abstract Background: The aim of the study was to determine the relationship between the rate of peak early mitral inflow velocity and the peak early diastolic mitral annular tissue velocities in normal controls and to compare them with subjects with diastolic dysfunction.

Methods: The relationship between early passive diastolic transmitral flow and peak early mitral annular velocity in the normal and in diastolic dysfunction was studied. Two groups comprising 22 normal controls and 25 patients with diastolic dysfunction were studied.

Results: Compared with the normal group, those with diastolic dysfunction had a lower E/A ratio (0.7 ± 0.2 vs. 1.9 ± 0.5, $p < 0.001$), a higher time-velocity integral of the atrial component (11.7 ± 3.2 cm vs. 5.5 ± 2.1cm, $p < 0.0001$), a longer isovolumic relaxation time 73 ± 12 ms vs. 94 ± 6 ms, $p < 0.01$ and a lower rate of acceleration of blood across the mitral valve (549.2 ± 151.9 cm/sec^2 vs. 871 ± 128.1 cm/sec^2, $p < 0.001$). They also had a lower mitral annular relaxation velocity (Ea) (6.08 ± 1.6 cm/sec vs 12.8 ± 0.67 cm/sec, $p < 0.001$), which was positively correlated to the acceleration of early diastolic filling ($R = 0.66$), $p < 0.05$.

Conclusions: This investigation provides information on the acceleration of early diastolic filling and its relationship to mitral annular peak tissue velocity (Ea) recorded by Doppler tissue imaging. It supports not only the premise that recoil is an important mechanism for rapid early diastolic filling but also the existence of an early diastolic mechanism in normal.

Background

The study of left ventricular filling dynamics has only recently received the same attention historically associated with systolic dynamics. Doppler Tissue Imaging (DTI) is fundamental in this assessment as it allows for the determination of systolic and diastolic velocities in the myocardium [1,2]. A number of studies have proposed that recorded mitral annular displacement and velocity in both systole and diastole may be used as indicators of overall cardiac performance [3,4].

In normal left ventricular relaxation after systole, the peak mitral annular velocity (Ea) recorded by DTI precedes the peak early passive diastolic transmitral flow (E) recorded by conventional pulsed wave (PW) Doppler ultrasound. In situations where this relaxation is impaired, Ea follows E [5,6]. This supports the suggestion that elastic recoil is related to mitral annular motion and this early diastolic mechanism of augmenting the onset of mitral flow velocity is lost in patients with diastolic dysfunction [6]. Ea appears to be more reflective of events at the very early

Table 1: Echocardiographic characteristics of the study population

	Normal Controls (n =	22). Diastolic Dysfunction	(n = 25) P value
Age (years)	33.0 ± 18	61.9 ± 13.3	< 0.001
EDV (ml)	90.04 ± 23.5	98.7 ± 40.3	0.418
ESV (ml)	35.0 ± 11.2	43.2 ± 24.4	0.1747
EF%	62.7 ± 5.3	61.1 ± 6.5	0.37
Ea (cm/s)	11.08 ± 1.6	6.1 ± 1.6	0.001
E Acc (cm/s2)	871.5 ± 128.1	549.2 ± 151.9	0.001
E/A	1.9 ± 0.5	0.7 ± 0.2	< 0.001
Et VI (cm)	10.6 ± 2.9	7.8 ± 2.5	0.0027
At VI (cm)	5.5 ± 2.1	11.7 ± 3.7	0.0001
Time to Acc(ms)	86.7 ± 15	93.2 ± 2.5	0.114
Heart Rate(ms)	920.1 ± 168.7	895.7 ± 208.5	0.6748
IVRT	73 ± 12	94 ± 6	0.01

Results expressed as mean ± standard deviation. EDV (ml) = End diastolic volume in millilitres. ESV (ml) = End systolic volume in millilitres. EF % = Ejection fraction as a percentage of blood ejected per cardiac cycle. Ea (cm/sec) = Peak early mitral annular tissue velocity recorded by Doppler tissue imaging. E Acc (cm/sec2) = Rate of acceleration of blood across the mitral valve in early diastole. E/A = Ratio of peak early diastolic flow over peak late diastolic flow. Et VI cm = Time velocity integral of early diastole in centimetres At VI cm = Time velocity integral of late diastole in centimetres. Time to Acc (ms) = Time to peak acceleration of early diastole in milliseconds. Heart Rate (ms) = R to R interval in milliseconds IVRT (ms) = Isovolumic relaxation time.

diastolic stage in the cardiac cycle, including untwisting or recoiling of the ventricle. [5,7]. There are animal and human data showing a good but not perfect correlation between the lowest very early left ventricular diastolic pressure (minimal pressure) and Ea, where subjects with low left ventricular minimal pressure have a normal Ea and those with a high minimal left ventricular pressure have a low Ea [5,7,8]. This minimal left ventricular pressure reflects the early diastolic recoil where subjects with normal or enhanced recoil tend to have low pressures [5,7]. Recoilmay also be dependent on myocardial interstitial composition, which is altered in patients with diastolic dysfunction [9]. The aim of the study was to determine the relationship between Ea and early transmitral flow in patients with diastolic dysfunction and to compare this with a normal population.

Methods

Patient selection

The study proposal was assessed and passed the Institutional Ethics Committee. Individuals coming for echocardiographic assessment were screened. Those with echocardiographic features suitable for enrolment in the study were asked to participate. Following informed consent the participants were enrolled. Between March 2002 and

September 2002, a group of 22 controls with completely normal echocardiograms and 25 patients with clinical echocardiographic and Doppler evidence of diastolic dysfunction were entered into the study. These patients were asymptomatic and had no previous cardiac failure. Diastolic dysfunction was defined using two-dimensional echocardiography and Doppler techniques as preserved systolic function but with evidence of LV hypertrophy, reversed E/A ratio and a prolonged isovolumic relaxation period [10]. Patients were excluded if they had abnormal rhythm, known coronary artery disease, or valvular incompetence beyond a modest degree, or if echocardiographic images were technically inadequate for complete analysis.

The study population

We studied twenty-five patients of mean age 61.5 (SD 13.3) years in the diastolic dysfunction group and twenty-two normal controls of mean age 33.4 (SD 18) years. Fifteen patients from the diastolic dysfunction group (10 male, 5 female) had been referred to the Hypertension clinic. These patients were evaluated for essential hypertension and were sent for echocardiography as part of their evaluation. Patients selected for the study had echo evidence of diastolic dysfunction without pseudonormalisation, which would have been unmasked on the tissue Doppler profile. They were subsequently diagnosed as having essential hypertension and treated appropriately. At the time of echocardiographic evaluation they were not on any anti-hypertensive therapy. Eight had electrocardiographic evidence of left ventricular hypertrophy of various degrees. Ten other patients (2 male, 8 female) with diastolic dysfunction consisted of an elderly group who had age-related diastolic dysfunction and were also free of cardiac drugs. These patients were referred for echocardiography for investigating of a systolic murmur. Three of these patients had mild calcific aortic stenosis gradient < (25 mmHg), four patients had basal septal hypertrophy only and three patients had both mild aortic stenosis gradient (< 25 mmHg) and basal septal hypertrophy.

These were compared to a group of 22 controls (12 males, 10 females) with clear acoustic windows and no clinical or echocardiographic evidence of cardiovascular disease.

Echocardiography

Echocardiograms were obtained with an Agilent 5500 cardiac ultrasound system with colour flow imaging and DTI capabilities. The system was equipped with 2.5 and 3.5 MHz transducers. Two-dimensional (2-D) echocardiography was performed followed by a PW Doppler study. The images obtained included the apical four-chamber and two-chamber views so that blood flow measurements could be made across the mitral valve. Also these views made it possible to record the DTI at the lateral mitral annulus. Pulsed wave DTI was performed by activating this function on the Agilent 5500 system. A sample volume was located at the lateral side of the mitral annulus. The characteristic velocity profile of diastole was obtained in all patients. Peak early (E) and late (A) diastolic mitral annular velocities were recorded, as well as the E/A ratio, acceleration time, along with acceleration and time/veloc-ity integrals of early and late filling in each case. Patients who were relatively tachycardic were repeated at another time when the rate had reduced enough to allow us to measure the time velocity integral accurately. Acceleration time of the early diastolic velocity was defined as twice the interval between the point at peak velocity and that at half of the peak velocity in the acceleration phases. Acceleration rate (cm/sec^2) was represented by the slope of the line between an anchored point and a crosshair. This linear measurement was made on the velocity spectrum. These recordings were shown on a strip chart with a sweep speed of 100 mm/s to determine correct temporal observations. Measurements were performed off line by an independent observer who had no knowledge of the Doppler or Tissue Doppler findings. At least three measurements were taken of each parameter and these were averaged.

Using 2-D echocardiography the end-systolic (ESV) and end-diastolic (EDV) volumes were recorded by the method of disc summation based on Simpson's rule. This method treats the ventricle as a stack of discs and is recommended because it is independent of preconceived ventricular shape [11]. The endocardial border was traced in each phase of the cardiac cycle and the system computer partitioned the ventricle into 20 discs of equal thickness. The computer then summed the individual disc volumes to give the total volume of the cavity.

All echocardiographic examinations were performed by an experienced sonographer and / or an experienced physician. To test for inter-observer variability, pulsed wave

Doppler tissue imaging measurement of Ea and Doppler profiles (determined by conventional pulsed wave Doppler) were analysed by one experienced observer who was blind to the first examination. A $p = 0.05$ was considered to indicate statistical significance.

Statistical Analysis

All statistical analyses were performed using the BMDP statistical package. Paired and unpaired Student's t-tests were used, as appropriate; to evaluate the difference between the means of the two selected groups and the difference between repeated measures. Because of the wide age range in both groups the means adjusted for age for each variable were calculated using multiple regression. For each group the relationship between DTI diastolic early velocity (Ea) and parameters of left ventricular mitral inflow including the rate of mitral acceleration was expressed using the Pearson correlation coefficient and separate linear regression models that were compared using an R test.

Results

Inter-observer variability For Ea and Doppler profiles

Inter-observer agreement is measured using the method described by Bland and Altman (1986)[12]. Mean differences and correlations close to zero indicate no bias in one observer compared with the other. Mean differences and correlations for inter-observer variability for Ea ($r = 0.07$) and other Doppler profiles were insignificant.

Standard Doppler echocardiographic analysis

The early diastolic tissue velocity detected by Doppler tissue imaging was lower in the diastolic dysfunction group than in the normal group (6.08 ± 0.67 cm/sec and $12.8 \pm$

1. 0.73 cm/sec respectively, $p = 0.001$). The rate of acceleration was lower in the diastolic group (549.2 ± 151.9 cm/s^2 versus 871.1 ± 128.1 cm/s^2, $p = 0.001$) as was the time-velocity integral of early diastolic flow (7.8 ± 2.5 cm versus 10.6 ± 2.9 cm, $p = 0.0027$). There was a longer isovolumic relaxation time in the diastolic group then the normal (94 ± 6 ms versus 73 ± 12 ms $p < 0.01$). There were no differences between the two groups in relation to the end-diastolic volume or in the end-systolic volume. There was no change with age for ejection fraction. The E/A ratio was lower in the diastolic dysfunction group compared with the normal group (0.7 ± 0.2 versus 1.9 ± 0.5, $p = 0.001$), while the time-velocity integral of the atrial component was greater in the diastolic dysfunction group compared with the normal group (11.7 ± 3.7 cm versus

2. 5.5 ± 2.1 cm, $p = 0.0001$). In view of the age difference between the control and diastolic dysfunction group the data was adjusted for age. The same differences were seen in the various parameters after adjusting for age. The results are given in table 1 and the means adjusted for age are given in table 2.

Table 2: Means adjusted for age. The values presented are adjusted means ± standard deviation.

	Normal Controls (n = 22)	Diastolic Dysfunction (n = 25)	P value
EDV (ml)	90.2 ± 8.53	99.2 ± 8.79	0.473
ESV (ml)	36.0 ± 4.91	43.4 ± 5.06	0.165
EF%	62.2 ± 1.47	61.1 ± 1.38	0.144
Ea (cm/sec)	12.8 ± 0.73	6.08 ± 0.67	< 0.001
E Acc (cm/sec2)	870.1 ± 39.0	548.3 ± 35.8	< 0.0001
E/A	1.81 ± 0.11	0.690 ± 0.10	< 0.001
Et VI (cm)	10.4 ± 0.70	8.000 ± 0.7	0.042
At VI (cm)	5.2 ± 2.20	12.20 ± 3.8	0.09
Time to Acc (ms)	83.18 ± 13.0	87.60 ± 12.0	0.466
Heart Rate (ms)	825.4 ± 45.9	848.9 ± 42.1	0.998
IVRT (ms)	71 ± 11	90 ± 6	0.01

Doppler tissue imaging assessment of the mitral annular descent velocities recorded at the lateral mitral annulus

By individual patient analysis patients with diastolic dysfunction had a reduced Ea compared to the normal group. Patients with diastolic dysfunction and an E/A ratio less than one had consistently low mitral annular velocities determined by DTI. There was a positive correlation between the mitral annular tissue velocity with the acceleration of mitral inflow in the diastolic dysfunction group($r = 0.66$), which was not present in the control group (Figure 1). The F ratio test, comparing the two regression lines for the two groups, indicated a significant difference ($F = 4.44$, $p = 0.0176$). There were positive correlations between the mitral annular tissue velocity with the E/A ratio ($r = 0.64$, $p < 0.001$), the time velocity integral of early diastolic filling ($r = 0.50$, $p < 0.02$), and the time velocity integral of late filling ($r = 0.44$, $p < 0.05$) which was also not present in the control group.

Discussion

We have found that in the group with diastolic dysfunction, Ea had a positive correlation to the acceleration of early diastolic filling and in the control group there was no relationship. We know from previous studies that recoil occurs during the isovolumic relaxation period before filling and Doppler mitral annular tissue velocities and Doppler mitral inflow velocities are influence by preload conditions in a normal study population [5,6]. Therefore because of the dissociation between filling and recoil described already by Buchalter et al [13] and the influence of preload conditions on the rate of filling the two variables are unlikely to correlate. In the stiff heart however recoil is delayed and filling takes place at the same time under the influence of high filling pressures. In addition preload dependency of these variables is also reduced in the stiff diseased ventricle. Therefore a relationship between the rate of filling and recoil occurs. In the stiff heart a slow release of restoring forces during recoil reduces the early diastolic filling across the mitral valve. In the normal heart however the rate of flow is a result of the potential energy of the maximum restoring forces held when recoil had terminated which results in normal early diastolic filling [14].

This study provides evidence that ventricular filling is associated with early diastolic motion of the mitral annulus, which is a marker for left ventricular recoil in the control group. However this positive correlation is the result of the absence or reduction of the early diastolic mechanism essential for proper filling. It may be argued that in the normal state most people have normal filling pressures and it is primarily the left ventricular relaxation and recoil that influences the trans mitral gradient. Preload however is the force that extends the ventricle in diastole or the force acting to stretch the ventricular fibres at end diastole [10]. Therefore even though the filling pressures are normal preload will affect the rate of blood velocity across the mitral valve depending on the degree of stretch of the left ventricular cavity in diastole. Taking into account the physiological changes that effect preload there should be a varying degree of acceleration of blood flow across the mitral valve, which is dissociated from left ventricular recoil in the normal.

Early diastolic velocity of the mitral annulus – an index of left atrial filling pressures

Evidence that Ea declines progressively with age and is reduced in left ventricular hypertrophy led investigators to suggest that Ea could be an index of LV relaxation [6,15,16]. From these findings it was suggested that Ea measured from the diastolic velocity profiles produced by DTI may provide an index of left ventricular relaxation not strongly influenced by preload variables such as heart rate and left atrial pressure [16]. Therefore mitral E-wave velocity or the velocity of passive early diastolic filling determined by conventional Doppler was corrected for
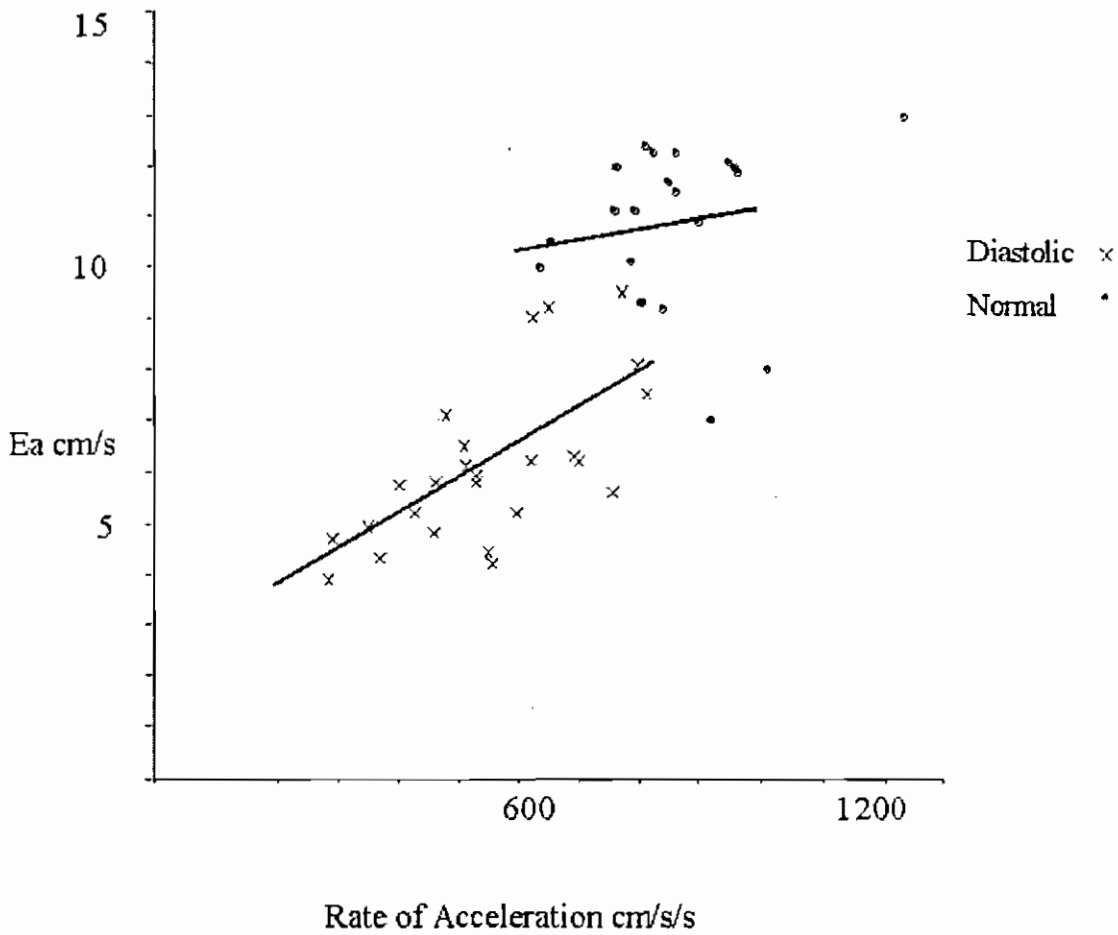
Figure 1
Scatter plot showing the correlation between DTI early diastolic mitral annular velocity (Ea) and acceleration of diastolic flow in patients with diastolic dysfunction and in normal subjects.

the influence of relaxation by applying the dimensionless index of E/Ea. Ea has been shown to be related inversely to the time constant of relaxation [16]. In previous studies, the ratio E/Ea related well to left atrial pressure and was used to estimate left ventricular filling pressures in stiff hearts [17]. In a canine study, left ventricular relaxation, minimal pressure and transmitral pressure gradients determined Ea in normal conditions. In cases of impaired relaxation the influence of filling pressures was very small [5,18]. In a study looking at the differentiation between constrictive and restrictive cardiomyopathy using Doppler tissue imaging Ea was found to be reduced even when the mitral inflow pattern was pseudonormal or restrictive [19]. We have observed a better correlation between the rate of early diastolic filling, and Ea in the diastolic dysfunction group without pseudonormalisation than in the normal group. We have also observed a better correlation with three other parameters of left ventricular mitral inflow in the diastolic dysfunction group, the early and late time velocity integrals and the E/A ratio supporting the results of this study.

Patients with diastolic dysfunction have increased endocardial and perivascular fibrosis as a feature of altered interstitial structure [20,21]. The relationship of tissue velocities determined by DTI to the regional amount of interstitial fibrosis has also been established [22,23]. Therefore altered interstitial composition should manifest itself in the behaviour of Ea. Since diastolic dysfunction exists in all myocardial pathologies and aging its potential use in estimating left ventricular filling pressure is important. Therefore the availability of further evidence to support its use in assessing accurately this clinical parameter is reassuring. The association between elastic recoil estimated by E annular velocity and early inflow acceleration in stiff hearts may be partly due to the relationship in time if the peak E annulus was delayed in the patients with diastolic dysfunction. Therefore if E annulus peaked earlier in normal than in patients with left ventricular dysfunction the timing of this interval or early diastolic mechanism could be of enormous clinical benefit in different clinical settings.

Study limitations

The major limitation of this study may be the comparison from different age groups. The purpose of the study was to assess the mechanics of early diastolic filling in stiff and normal hearts regardless of the aetiology of that stiffness. However the mean values adjusted for age are presented. The power of the associations may have been low, as the numbers in the normal group were relatively small (n = 22), however with this number we would have sufficient power (80%) to detect a correlation of 0.55 or above as being statistically significant in this group.

Transmitral flow presents a parabolic distribution during progression from normal to advanced diastolic dysfunction characterised by a restrictive pattern. Therefore patients with restrictive physiology and pseudonoarmalisation were excluded from the study. However a further study to show the association between the deficits of elastic recoil estimated by E annular velocity with early left ventricular inflow acceleration in patients with pseudonormalisation unmasked by the valsalva manoeuvre could yield interesting results.

Conclusion

This investigation provides information on the acceleration of early diastolic filling and its relationship to mitral annular peak tissue velocity (Ea) recorded by Doppler tissue imaging. It supports not only the premise that recoil is an important mechanism for rapid early diastolic filling but also the existence of an early diastolic mechanism in   normal.

Competing interests

None   declared.

Authors' Contributions

GK: lead Author.

JBF: Editing, advice, quality control, and coordination of the manuscript.

FAM. Performed and read the echocardiograms.
  http://www.cardiovascularultrasound.com/content/1/1/9

PC. Performed quality control.

MW.   Performed   quality   control.

References

1. McDicken WN, Sutherland GR, Moran M and Gorden LN: Colour Doppler velocity imaging of the myocardium *Ultrasound in Med Biol* 1992, **18(6/7)**:651-654.
2. Erbel R, Wallbridge DR, Zamorano J, Drozdz J and Nesser HJ: Tissue Doppler echocardiography (editorial) *Heart* 1996, **76(3)**:193-196.
3. Galiuto L, Ignone G and DeMaria AN: Contraction and relaxation velocities of the normal left ventricle using pulsed-wave tissue Doppler echocardiography *Am J Cardiol* 1998, **81**:609-614.
4. Fukuda K, Oki T, Tabata T, Luchi A and Ito S: Regional left ventricular wall motion abnormalities in myocardial infarction and mitral annular descent velocities studied with pulsed tissue Doppler imaging *J Am Soc Echocardiography* 1998, **11(9)**:841-848.
5. Nagueh SF, Sun H, Kopelen HA, Middleton KJ and Khoury DS: Haemodynamic determinants of the mitral annulus diastolic velocities by tissue Doppler *J Am Coll Cardiology* 2001, **37**:278-285.
6. Rodriguez L, Garcia M, Ares MA, Gritlin BP, Nakatani S and Thomas JD: Assessment of mitral annular dynamics during diastole by Doppler tissue imaging: comparison with mitral Doppler inflow in subjects without heart disease and in patients with left ventricular hypertrophy *Am Heart J* 1996, **131**:982-987.
7. Nagueh SF, Lakkis NM, Middleton KJ, Spencer WH III, Zoghbi WA and Quinones MA: Doppler estimation of left ventricular filling pressures in patients with hypertrophic cardiomyopathy *Circulation* 1999, **99**:254-261.
8. Ohte N, Narita H, Hashimoto T. Akita S, Kurokawa K and Fujinami T: Evaluation of left ventricular early diastolic performance by Tissue Doppler Imaging of the mitral annulus *Am J Cardiology* 1998, **82**:1414-1417.
9. Villari B, Campbell SE and Hess OM: Influence of collagen network on left ventricular systolic and diastolic function in aortic valve disease *J Am Coll Cardiology* 1993, **22**:1477-1484.
10. European Study Group on Diastolic Heart Failure: How to diagnose diastolic heart failure *Eur Heart J* 1998, **19**:990-1003.
11. Otterstad JE, Froeland G, St John Sutton M and Holme I: Accuracy and reproducibility of bi plane two-dimensional echocardiographic measurements of left ventricular dimensions and function *Eur Heart J* 1997, **18**:507-513.
12. Bland JM and Altman DG: Statistical methods for assessing agreement between two Methods of clinical measurement *Lancet* 1986, **1**:307-310.
13. Buchalter MB, Rademakers FE, Weiss JL, Rogers WJ, Weisfeldt ML and Shapiro EP: Rotational deformation of the canine left ventricle measured by magnetic resonance tagging: effects of catecholamones, ischaemia, and pacing *Card Res* 1994, **28**:629-635.
14. Garcia MJ, Rodriguez L, Ares M, Griffin BP, Klein AL and Stewart WJ: Myocardial wall velocity assessment by pulsed Doppler tissue imaging: characteristic findings in normal subjects *Am Heart J* 1996, **132(2)**:648-656.
15. Garcia MJ, Ares MA, Asher C, Rodriguez L and VanderVoort P: Thomas JD. Color M-Mode flow velocity propagation: an index of early left ventricular filling that combined with pulsed Doppler e velocity may predict capillary wedge pressure *J Am Coll Cardiology* 1997, **29**:448-454.
16. Nagueh SF, Middleton KJ, Kopelen HA, Zoghbi WA and Quinones MA: Doppler Tissue Imaging: a non-invasive technique for evaluation of left ventricular relaxation and estimation of filling pressures *J Am Coll Cardiology* 1997, **30**:1527-1533.
17. Kim YJ and Sohn DW: Mitral annulus velocity in the estimation of left ventricular filling pressure: prospective study in 200 patients *J Am Soc Echocardiography* 2000, **13**:980-985.
18. Firstenberg MS, Levine BD, Garcia MJ, Greenberg NL, Cardon L, Morehead AJ, Zuckerman RN and Thomas JD: Relationship of echocardiographic indices to pulmonary capillary wedge pressures in healthy volunteers *J Am Coll Cardiology* 2000, **36**:1664-1669.
19. Garcia MG, Rodriguez L, Ares M, Griffin BP, Thomas JD and Klein AL: Differentiation of constrictive pericarditis from restrictive cardiomyopathy: assessment of left ventricular diastolic velocities in longitudinal axis by Doppler Tissue Imaging *J Am Coll Cardiol* 1996, **27**:108-14.
20. Waldman LK, Nosan D, Villarreal F and Covell JW: Relationship between transmural deformation and local myofiber direction in canine left ventricle *Circ Res* 1988, **63**:550-562.
21. Brilla CG, Maisch B and Weber KT: Myocardial collagen matrix remodelling in arterial hypertension *Eur Heart J* 1992, **13(suppl D)**:24-32.
22. Shan K, Bick RJ, Poindexter BJ, Shimoni S, Letsou GV, Reardon MJ, Howell JF. Zoghbi WA and Nagueh SF: Relation of tissue Doppler derived myocardial velocities to myocardial structure and beta-adrenergic receptor density in humans *J Am Coll Cardiology* 2000, **36**:891-896.
23. Isaaz K: What are we actually measuring by Doppler tissue imaging? *J Am Coll Cardiology* 2000, **36**:897-899.

Cardiovascular Ultrasound | Top 10 most accessed articles of all time
12-May-2005

Browse Cardiovascular Ultrasound for Top 10 most accessed articles of all
timeresearch | case report | editorial | hypothesis | review |
technical notes | top 10 most
accessed articles

Top 10 most accessed articles of all time / last 30 days
1.
Accesses
7849Research
Tissue Doppler imaging of carotid plaque wall motion: a pilot
study
Kumar V Ramnarine, Tim Hartshorne, Yvonne Sensier, May Naylor,
Joanne Walker, A Ross Naylor, Ronney B Panerai, David H Evans
Cardiovascular Ultrasound 2003, 1:17 (19 December 2003)
[Abstract] [Full Text] [PDF] [PubMed] [Related articles]

2.
Accesses
5808Research
Early diastolic filling dynamics in diastolic dysfunction
Gerard J King, Jerome B Foley, Faisal Almane, Peter A Crean,
Michael J Walsh
Cardiovascular Ultrasound 2003, 1:9 (25 July 2003)
[Abstract] [Full Text] [PDF] [PubMed] [Related articles]

3.
Accesses
5215Technical notes
Imaging of all three coronary arteries by transthoracic
echocardiography. an illustrated guide
Marek Krzanowski, Wojciech Bodzoń, Paweł Petkow Dimitrow
Cardiovascular Ultrasound 2003, 1:16 (17 November 2003)
[Abstract] [Full Text] [PDF] [PubMed] [Related articles]

4.
Accesses
4646Research
Low-dose adenosine stress echocardiography: Detection of
myocardial viability
Ana Djordjevic-Dikic, Miodrag Ostojic, Branko Beleslin, Ivana
Nedeljkovic, Jelena Stepanovic, Sinisa Stojkovic, Zorica
Petrasinovic, Milan Nedeljkovic, Jovica Saponjski, Vojislav
Giga
Cardiovascular Ultrasound 2003, 1:7 (3 June 2003)
[Abstract] [Full Text] [PDF] [PubMed] [Related articles]

5.

Accesses
4223Review
Tissue Doppler echocardiography and biventricular pacing in heart failure: Patient selection, procedural guidance, follow-up, quantification of success
Fabian Knebel, Rona Katharina Reibis, Hans-Jürgen Bondke, Joachim Witte, Torsten Walde, Stephan Eddicks, Gert Baumann, Adrian Constantin Borges
Cardiovascular Ultrasound 2004, 2:17 (15 September 2004)
[Abstract] [Full Text] [PDF] [PubMed] [Related articles]

6.
Accesses
4004Review
Transthoracic Doppler echocardiography – noninvasive diagnostic window for coronary flow reserve assessment
Paweł Petkow Dimitrow
Cardiovascular Ultrasound 2003, 1:4 (11 April 2003)
[Abstract] [Full Text] [PDF] [PubMed] [Related articles]

7.
Accesses
3831Research
Strain and strain rate parametric imaging. A new method for post processing to 3-/4-dimensional images from three standard apical planes. Preliminary data on feasibility, artefact and regional dyssynergy visualisation
Asbjørn Støylen, Charlotte B Ingul, Hans Torp
Cardiovascular Ultrasound 2003, 1:11 (25 August 2003)
[Abstract] [Full Text] [PDF] [PubMed] [Related articles]

8.
Accesses
3574Review
Assessment of left ventricular function by three-dimensional echocardiography
Boudewijn J Krenning, Marco M Voormolen, Jos RTC Roelandt
Cardiovascular Ultrasound 2003, 1:12 (8 September 2003)
[Abstract] [Full Text] [PDF] [PubMed] [Related articles]

9.
Accesses
3483Research
Flow propagation velocity is not a simple index of diastolic function in early filling. A comparative study of early diastolic strain rate and strain rate propagation, flow and flow propagation in normal and reduced diastolic function
Asbjørn Støylen, Gunnar Skjelvan, Terje Skjaerpe
Cardiovascular Ultrasound 2003, 1:3 (1 April 2003)
[Abstract] [Full Text] [PDF] [PubMed] [Related articles]

10.
Accesses
3284Research
Comparison of m-mode echocardiographic left ventricular mass
measured using digital and strip chart readings: The
Atherosclerosis Risk in Communities (ARIC) study
Donna K Arnett, Thomas N Skelton, Philip R Liebson, Emelia
Benjamin, Richard G Hutchinson
Cardiovascular Ultrasound 2003, 1:8 (27 June 2003)
[Abstract] [Full Text] [PDF] [PubMed] [Related articles]

Cardiovascular Ultrasound
BioMed Central
Current Controlled
Trials
PubMed
PubMed Central

Appendix E

Two tables of raw measured data for the study described in Chapter 6 and a third table of data to show the inter-observer variability for two observers (1, 2) for a range of measured variables

name	age yrs	sex	EDV ml	ESV ml	SV ml	EF %	TWDEG °	EACM cm/s	EACC cm/s²
kd	34	2	64	23	67	67	12	9	840
mmcc	17	1	101	55	.	65	14	11	900
jl	24	1	80	38	65	65	9	12	956
jjg	35	1	83	44	10	65	11	9	798
amc	28	1	72	31	65	65	15	12	860
ld	40	2	85	40	.	65	·9	9	802
sa	24	1	93	35	65	65	9	23	851
dod	25	1	131	62	55	55	12	12	860
jm	17	2	60	28	60	60	17	11	790
mh	61	1	120	70	.	55	10	6	690
gh	45	1	99	49	55	55	17	22	1134
uk	32	1	95	29	70	70	9	9	624
cog	25	1	152	52	70	70	15	13	1230
rc	49	1	107	48	.	60	17	10	771
rg	65	1	125	68	50	55	.	5	351
rs	70	1	172	82	55	55	.	8	811
bl	70	2	162	78	.	55	.	6	700
lp	71	1	70	26	62	60	.	8	795
ss	32	1	95	33	60	60	7	12	823
jb	57	1	175	101	50	50	.	9	650
er	72	2	61	28	55	55	15	8	1010
aam	35	2	80	40	60	60	13	10	634
rf	71	2	.	.	50	50	.	5	292
dd	55	1	90	33	55	55	.	6	404
gr	63	1	45	28	67	67	.	6	462
pg	32	2	110	27	.	66	.	11	654
ss	70	2	100	18	55	55	.	12	850
ot	24	1	66	38	65	65	18	7	481
mh	88	2	.	.	68	68	10	6	756
fs	29	1	74	32	56	56	12	11	757
mm	58	2	.	.	65	65	14	6	621
doc	19	2	85	42	70	70	8	·12	949
tm	78	2	65	24	60	60	14	5	459
nf	19	2	90	32	68	68	8	12	964
sm	69	1	42	11	70	70	18	5	427
ec	74	1	113	55	51	51	.	4	555
mcn	72	2	64	22	.	65	18	6	529
ck	58	1	77	21	70	70	18	5	596
dr	34	1	64	25	60	60	12	10	785
wk	60	1	55	19	64	64	22	7	508
mg	65	2	74	22	.	65	22	6	513
ed	65	1	129	42	67	67	.	4	285
nod	55	1	137	50	63	63	.	6	529
th	55	1	.	.	.	.	.	4	549
rob	63	1	91	39	62	62	.	4	371
ma	50	2	90	25	55	55	.	7	919
ps	34	1	112	30	65	65	.	12	807

name	age yrs	E/A	ETVI Cm	ATVI Cm	IVRT ms	NAB 1 N 2 AB	LVH 1 no 2 yes	R-R ms
kd	34	1.5	0.09	0.06	80	1	1	850
mmcc	17	1.7	0.07	0.06	70	1	1	720
jl	24	1.2	0.06	0.03	70	1	1	980
jjg	35	1.5	0.09	0.05	80	1	1	650
amc	28	2.2	0.08	0.06	85	1	1	854
ld	40	1.2	0.15	0.13	80	1	1	789
sa	24	1.6	0.09	0.04	70	1	1	1000
dod	25	2.0	0.16	0.06	75	1	1	960
jm	17	2.8	0.16	0.04	80	1	1	980
mh	61	0.8	0.08	0.07	70	2	2	855
gh	45	1.1	0.09	0.06	80	1	1	680
uk	32	1.1	0.07	0.06	80	2	2	920
cog	25	2.2	0.10	0.05	80	1	1	980
rc	49	0.9	0.15	0.09	100	2	2	870
rg	65	0.6	0.08	0.08	120	2	2	1100
rs	70	1.3	.	.	90	2	2	952
bl	70	0.4	0.06	0.05	60	2	2	690
lp	71	0.7	0.10	0.08	70	2	2	750
ss	32	2.0	0.13	0.06	100	1	2	780
jb	57	0.7	0.08	0.07	100	2	2	780
er	72	2.9	0.09	0.04	80	1	1	980
aam	35	1.2	0.06	0.03	90	1	1	1000
rf	71	0.5	0.08	0.05	120	2	2	980
dd	55	0.7	0.04	0.04	80	2	2	1000
gr	63	0.9	0.10	0.08	100	2	2	698
pg	32	2.1	0.12	0.04	80	1	1	780
ss	70	2.0	0.12	0.05	100	1	1	790
ot	24	1.0	0.06	0.14	90	2	2	720
mh	88	0.7	0.09	0.06	90	2	2	890
fs	29	1.5	0.10	0.05	90	1	1	930
mm	58	0.6	.	.	80	2	2	980
doc	19	2.7	0.11	0.04	90	1	1	85
tm	78	0.7	.	.	80	2	2	930
nf	19	2.2	0.11	0.04	90	1	1	780
sm	69	0.4	0.06	0.11	60	2	2	930
ec	74	0.5	0.04	0.14	70	2	2	850
mcn	72	0.7	0.10	0.06	100	2	2	670
ck	58	0.8	0.09	0.04	90	2	2	722
dr	34	1.5	0.11	0.05	100	1	1	722
wk	60	0.8	0.09	0.07	80	2	2	850
mg	65	0.6	0.10	0.07	90	2	2	700
ed	65	0.3	0.04	0.10	70	2	2	550
nod	55	0.5	0.06	0.10	80	2	2	1080
th	55	0.7	.	.	100	2	2	952
rob	63	0.5	0.08	0.10	120	2	2	800
ma	50	1.2	0.09	0.08	80	1	1	850
ps	34	1.8	.	.	80	1	1	1021

Inter-observer variability for two observers (1 and 2) for a number of measured variables

e/arate1	e/arate2	atvi1	atvi2	etvi1	etvi2	timeacc1 ms	timeacc2 ms
1.6	1.6	11.4	11.2	10.4	10.4	85	85
1.2	1.1	5.6	5.7	7.9	7.8	69	69
0.7	0.8	10.2	10.2	8.7	8.7	71	72
0.6	0.6	3.9	4.0	6.8	6.7	68	68
1.7	1.7	9.2	9.2	11.8	11.7	105	108
0.9	1.0	5.8	5.8	7.4	7.5	90	90
1.1	1.0	12.0	11.8	8.0	8.0	95	95
1.6	1.6	10.6	10.4	8.2	8.2	85	85
0.8	0.8	4.2	4.1	7.0	7.0	66	66
8.2	8.2	11.0	11.0	12.0	11.8	70	72

erate1	erate2	arate1	arate2	brate1	brate2
67	65	9.2	9.0	840	830
65	62	10.9	11.1	900	890
65	60	12.0	11.8	960	940
65	62	9.3	9.0	800	800
65	62	11.5	11.2	860	850
70	68	9.0	8.9	620	620
70	66	13.0	13.0	1230	1200
60	65	9.5	9.2	770	790
55	52	4.9	4.8	350	360
55	55	7.5	7.3	810	810

Appendix F

Copy of the draft paper on the work described in Chapter 7, recently submitted to Heart

Novel applications of Doppler tissue imaging to distinguish physiological hypertrophy in athletes from hypertrophic cardiomyopathy: Differentiation in the "grey zone"

G King MSc, JB Foley MD, J Cosgrave MRCP, G Boyle PhD, M Hussey PhD, K Bennett PhD, P Crean FRCPI, M Walsh MD

Gerard King MSc*
Jerome Brendan Foley MD*
John Cosgrave MRCP*
Gerard Boyle PhD°
Matthew Hussey PhD†
Kathleen Bennett PhD*
Peter Crean FRCPI*
Michael Walsh MD*

Cardiology Department, St James's Hospital, Dublin*
Medical Physics Department, St James's Hospital, Dublin°
Dublin Institute of Technology, Kevin Street, Dublin†

Gerard King
Cardiology Department, St James's Hospital
James's Street
Dublin 8
Ireland

Tel   (00353-1) 416 2792
Fax (00353-1) 4103467
Email gking@stjames.ie

Novel applications of Doppler tissue imaging to distinguish physiological hypertrophy in athletes from hypertrophic cardiomyopathy: Differentiation in the "grey zone"

G King MSc, JB Foley MD, J Cosgrave MRCP, G Boyle PhD, M Hussey PhD, K Bennett PhD, P Crean FRCPI, M Walsh MD

Objectives
To evaluate two novel applications of Doppler tissue imaging in distinguishing athletic physiological hypertrophy in the "grey zone" from hypertrophic cardiomyopathy.

Methods and Results
We compared eleven patients with characteristics of mild HCM without left ventricular outflow tract obstruction and seventeen international rowers with LVWT (13mm) with a control group of thirty age matched sedentary normal subjects. Each subject under went echocardiography where the time interval between Ea (by Doppler tissue imaging) and peak mitral opening (by M-mode) were measured simultaneously on the same heartbeat. A novel index of left ventricular stiffness was also measured using (E/Ea)/LVEDd (pressure/volume) in the three groups. In the athlete group the peak early diastolic annular tissue velocity preceded the peak mitral E of the M-mode by median 20 ms (IQR 10, 20) and in the control group by median 15 ms (0, 30), compared with the HCM group where the peak early diastolic annular tissue velocity was delayed relative to the peak mitral inflow by a median 10 ms (IQR 0, 20), p<0.0001. In the athletic group the index of left ventricular stiffness was lower then the normals and HCMS patients. 1.2 (0.93, 1.4) compared with the normal median 1.5 (1.3, 1.6) and the HCM, median 2.2 (2.0, 2.3) p < 0.0001.

Conclusions
The timing application between peak tissue velocity Ea and peak mitral opening (by M-Mode) and the new novel index of diastolic stiffening can be used together or separately to differentiate hypertrophic cardiomyopathy from athletic physiologic left ventricular hypertrophy in the "grey zone"

Introduction

Sudden death in athletes is one of the great catastrophes in sport[1]. Identifying athletes at risk of sudden death remains a great challenge. The athlete's heart undergoes adaptive changes in response to physical exercise that can mask some pathological abnormalities[2]. The more important question that needs to be resolved once an athlete is identified as having LVH is whether it is a normal physiological response or a pathological phenomena, with hypertrophic cardiomyopathy being the important differential in the equation. Many methods are currently employed to diagnose whether athletes have physiological or pathological left ventricular hypertrophy (LVH)[3], but they are not comprehensive or practical for large populations. Genetic studies in the past have revealed that a substantial minority of patients with HCM have wall thicknessess in the same range as athletes but genetic testing is not a practical option[3]. Traditional echocardiographic and electrocardiographic features may not be able to distinguish individuals that fall into the " Maron[1] grey zone" between what is physiological and what is pathological.

Doppler tissue imaging (DTI) is an ultrasound modality that can be used to record systolic and diastolic velocities within the myocardium[4, 5]. Studies have recorded mitral annular displacement and velocity both in systole and diastole as indicators of overall cardiac performance[6, 7, 8]. The objective was to evaluate the timing difference between the peak early diastolic tissue E velocity and the peak opening of the mitral valve by M-mode in distinguishing hypertrophic cardiomyopathy (HCM) from athletic physiological left ventricular hypertrophy in the "Maron[1] grey zone" using a novel application of Doppler tissue imaging in conjunction with a novel index of myocardial stiffening.

Methods

Subjects

Between 2002 and 2004 ongoing research of 27 patients diagnosed with hypertrophic cardiomyopathy (HCM) led to the identification of 11(30%) adults with characteristics of mild HCM without left ventricular outflow tract obstruction. They were identified to have HCM based on a combination of clinical presentation, family history of HCM, absence of hypertension and of training that would induce LVH and exclusion of other conditions that could cause cardiac infiltration. Resting Doppler and tissue Doppler indices of diastolic dysfunction were also recorded and each patient had a left ventricular wall thickness of > 13mm.

The physiological LVH group were identified among thirty four highly trained international rowers who had trained intensively 15 to 20 hours /week for more then 5 years who underwent two –dimensional echocardiography and Doppler evaluation. None had a family history of HCM or premature sudden cardiac death and all were normotensive. Of the 34 rowers 17(50%) had a left ventricular wall thickness (LVWT) $\geq$ 12mm. A control group of 30 sedentary normal subjects recruited from hospital personnel which included young hospital doctors and medical students. The study and its protocol were approved by the local research ethics committee and each subject gave informed consent.

Images were obtained with the Philips 5500 and Philips 4500 cardiac ultrasound systems. Standard apical views made it possible to record the DTI at four sites, medial, lateral, inferior and anterior, around the mitral annulus. The characteristic

velocity profile of diastole was obtained in all patients. In each case, peak early (E) and late (A) diastolic mitral annular velocities were recorded, as well as the E/A ratio, deceleration time, isovolumic relaxation time and left ventricular filling pressures were estimated using E/Ea. Recordings at a sweep speed of 100 mm/s allowed for correct temporal observations. Measurements were performed from these recordings off-line by an independent observer with no knowledge of the M-mode timings, Doppler or DTI findings. At least three measurements of each parameter were taken.

Calibration

The time delay between peak tissue annular velocity Ea and peak mitral opening was measured by taking simultaneous DTI and M-mode measurements with the two machines. (Fig 1) A sharply defined time reference pulse was introduced into unused ECG channels on both machines by pressing a footswitch activated circuit. The time intervals from this pulse edge to Ea on one machine and to peak mitral opening on the other were measured using the machines' electronic callipers as in Fig 1.

Accuracy of Temporal Measurements

The temporal resolution of the on-screen callipers varies with the scan sweep velocity setting. With a scan sweep velocity setting of 100ms/s, the callipers gives an on-screen resolution of 5ms. A time difference between any two events on the screen of one machine can therefore be measured to within ±2.5ms. When looking at temporal differences between events on both machines, the calliper resolution will result in a theoretical accuracy of ±5ms.

Echo data analysis

Echo data analysis was performed off-line for calculation of left ventricular volume, ejection fraction and left ventricular mass. Left ventricular mass was estimated by the method of Devereux[9] by applying the Penn convention.

Long axis function by DTI

The four-site mean velocity was calculated thus, mean = $(M+L+I+A)/4$, where M, L, I and A are the peak velocities of the medial, lateral, inferior, and anterior points on the mitral annulus respectively. With the sample volume (gate 6 mm) placed over each point on the mitral annulus, the cursor was aligned to ensure an angle of incidence as close as possible to $0°$.

New non-invasive index of passive diastolic stiffness

Diastolic stiffness was assessed with the use of three indices E, Ea , and the left ventricular end diastolic diameter in diastole (LVEDd). E/Ea represents an index of left ventricular filling pressure[8] and LVEDd was used as an index of volume i.e. pressure volume index. We reasoned that (E/Ea) /LVEDd could provide a novel index of diastolic stiffness. This new and novel index of myocardial stiffness was measured on each patient.

Statistical analysis

Results are presented as means and standard deviations (SD) where the data are normally distributed and medians with inter-quartile ranges (IQR) where the data are non-normally distributed. For comparisons between athletes and HCMs, a student's t-test or non-parametric Wilcoxon rank sum test was used where appropriate. Box and

whisker plots are used for displaying the data. Sensitivity, specificity and accuracy were assessed using standard methods. Inter-observer variability was examined for Ea average and time difference using a non-parametric correlation of association between the measurements[10]. A p<0.05 for a 2-tailed test was considered statistically significant. All statistical analyses were performed using the JMP statistical analysis package (SAS Inst. Inc). One-way analysis of the new index of diastolic stiffness was assessed by the Kruskall-Wallis test between groups.

Reproducibility

Using the method of Bland and Altman[12], the correlation r = 0.0097 (p=0.622), for reproducibility for each four-site average, and r = 0.061 (p=0.758) for the time difference. This suggests that there is negligible inter-observer bias in the measurements.

Results

The general characteristics of the study groups are presented in Table 1. Summary echocardiographic data obtained are listed in Table 2.

The mean age between the HCM, athletes and controls was not statistically significant. Body surface area (BSA) in m^2 in the athlete group was slightly higher than in the control and HCM groups, 2.0 (1.95 , 1.98) vs. 1.84 (1.6,1.98) m^2 and 1.93 (1.90,1.9). As might be expected heart rate (per minute) was lower in the athletes compared with the control and HCM group (65 ± 11 vs. 70.0 ± 5.0 and 67.0 ± 5.0), (Table 1).

Patients with HCM had lower long axis systolic and early diastolic velocities compared with the athletic and normal groups at all four sites of the mitral annulus (Table 2). They had a higher calculated left ventricular filling pressure E/Ea index (mean=10.1±2.78) than the normal (mean 7.1 ± 1.10) and athletic group (mean 6.4±1.63), p=0.0001.

Index of left ventricular passive stiffness E/Ea /LVEDd

The pressure index E/Ea was higher and the LVEDd was lower in the HCM group compared with the controls and the athletes. These data alone suggest the presence of increased chamber stiffness in patients with HCM (Table 2). Also the E/Ea was lower and the LVEDd was higher in athletes compared with normals and HCM. This suggests reduced chamber stiffness in athletes compared to normals and HCMs (Table 2). The athletes have a lower index of left ventricular stiffness than the normals and HCM patients 1.2 (0.93, 1.4) compared with the normal medium 1.5 (1.3, 1.6) and the HCM, medium 2.2(2.0,2.3) p < 0.0001.

Timing of the early diastolic mechanism

In the athlete and control group the peak annular early diastolic tissue velocity preceded the peak mitral E of the M -mode on average by a median of 20 ms (IQR 10, 20) and 10ms (IQR 30,7.5) compared with the HCM group where the peak mitral E of the M-mode preceded the peak annular early diastolic tissue velocity by a median of 10ms (IQR 0, 20), p<0.0001.

Differentiating between pathological and physiological hypertrophy

As shown in Figure 2, a mean diastolic velocity <10 cm/s differentiated pathological
from physiological hypertrophy. Also the time delay from early diastolic tissue
velocity peak Ea to the early M-mode peak E provided a strong differentiation
between HCM and athletic heart in the "grey zone". All patients with hypertrophic
cardiomyopathy had values > or = to 0 for the four site average time difference ,and
all athletes had values < 0, therefore there was complete discrimination between the
groups.

Testing all seven criteria listed in Table 3A, the best differentiation was provided by
(1) a cut of index of myocardial stiffness of < 1.7 and (2) the association of the time
delay between the early mitral M-mode E and the early diastolic tissue velocity of 0.0
ms (i.e. both occurring at the same time or are possibly reversed). Based on standard
statistical methods to calculate sensitivity and specificity[11], Tables 3A show a range
of echocardiographic criteria for differentiating between patients with pathological
LVH and athletes with LVH.

Pseudo-normalisation

Of particular interest, patients in the pathological LVH group who demonstrated
pseudo-normalisation and stage II diastolic dysfunction showed the appropriate
timing reversal directly, even though the isovolumic relaxation time was pseudo-
normal (median = 20 (10, 30)) in the pseudo-normal group compared with median =
10 (0, 13) in the remainder, with p = 0.059.

Discussion

We report on two non-invasive measurements using Doppler tissue imaging which can help to differentiate pathological LVH from athletic physiological hypertrophy in the "grey zone". One is a novel method of assessing diastolic stiffness by applying a ratio based on the pressure/volume relationship (E/Ea) / LVEDd and the other is an novel application of a timing measurement which, along with measurement of early tissue velocity E, is effective in detecting changes of diastolic dysfunction in individuals with HCM. From our study several echo features that permitted demarcation from pathological LVH are identified (Table 2). For example, left ventricular cavity dimension exceeded the upper limits of 5.5 cm ± 0.5. In contrast the HCM group showed small or normal-sized left ventricular cavities of 4.7 cm ± 0.6. However cardiac alterations associated with training differ somewhat depending on the particular sport in which the individual participates[13]. Cavity dimension would not resolve this differential diagnosis.

Early diastolic tissue velocity (E)

Studies by Ho[14] and Nagueh[15] suggest that DTI can be used to identify a group of individuals without hypertrophy as well as individuals with pathological hypertrophy. Our study groups included patients with left ventricular hypertrophy due to disease and exercise and we have shown an Ea < 10 cm/s had a sensitivity of 73% and specificity 100% for differentiating between athletic (physiological) hypertrophy and pathological hypertrophy in the "grey zone" (Table 3A). We found a similar result

between the normal group and the pathological with the same sensitivity and specificity but with slightly increased accuracy (Table 3B).

Index of myocardial stiffness

Our novel index of myocardial stiffness $(E/E_A)/LVEDd)$ showed an increase in myocardial stiffness in the HCM group compared with the normal and athletes (fig. 4). We have also shown that E/Ea/ LVEDD has a sensitivity of 86% and specificity 94% for differentiating between athletic (physiological) hypertrophy and pathological hypertrophy in the "grey zone" similar to the early diastolic tissue (Ea) but slightly better in sensitivity and accuracy.

Timing of the early diastolic interval

We have previously demonstrated that mitral diastolic peak annular tissue velocity occurs earlier then the peak of the early mitral inflow velocity in normal human hearts[17]. Our findings of altered timing between peak tissue velocity (Ea) and peak mitral (E) valve opening on M-mode are similar to those reported by Rodriguez et al.[18] (Table 2). Rodriguez et al[18] also compared DTI with M-mode of the annulus and mitral inflow Doppler velocities in patients with LVH[18]. Patients with LVH showed a delay in peak early diastolic mitral annular velocity (21 ms ± 5.5 ms, p = 0.002, after the E wave). In Rodriguez's study M-Mode and DTI measurements were measured on different heartbeats, with times of the peak velocities referred to the ECG R-wave. In the current study M-Mode and DTI measurements were taken simultaneously and

time differences measured are actual time differences between events in a single heartbeat.

The canine experiments of Rivas-Gotz et al[19] showed a strong relationship between the time interval of the onset of mitral inflow (Tea) in comparison with the time onset of early diastolic velocity of the mitral annulus by DTI (E). However it has been demonstrated that a variation in passive myocardial tension exists in different mammalian species[20]. This discovery raises reasonable doubt as to the validity of simple extrapolation of related experimental data from animal studies to humans. Rodriguez et al[18] also found that in a group with no heart disease the onsets of mitral flow and diastolic annular motion were simultaneous, but the peak annular velocity preceded the peak mitral M-mode E by an average of 20 ms. This was in contrast to patients with LVH where the timing was reversed. These findings and ours support the notion of elastic recoil, but differ in principle from those reported by Rivas-Gotz[19] where a definite time delay between the onsets was reported Table 2. In patients with LVH and HCM we found that peak mitral opening preceded early diastolic annular tissue velocity by approximately 20 ms (Figure 3). Our patients with mild HCM showed abnormal diastolic indices of left ventricular filling. However we have shown that measuring the diastolic mechanism has a sensitivity of 100% and specificity 100% for differentiating between athletic (physiological) hypertrophy and pathological hypertrophy in the " grey zone" far exceeding the sensitivity and accuracy of other techniques to detect diastolic dysfunction in our HCM group (Table 3A). Another perhaps future advantage other then its sensitivity and accuracy is the ability of simultaneous overlay to follow the effects of medication and intervention directly irrespective of preload variables. Our ability to visualise this timing interval

in milliseconds will also enhance our understanding of the coordinated sequence of diastolic dysfunction in HCM.

Cardiac time intervals such as the early diastolic mechanism will become more precise and practical for clinical use when Doppler technology improves to allow automatic simultaneous overlay. This would allow the direct assessment of the early diastolic mechanism, automatic calculation of the index of myocardial stiffness' and left ventricular filling pressures even in patients with atrial fibrillation[21] which cannot be assessed by conventional Doppler. Conventional transmitral flow and pulmonary venous flow velocity patterns are affected by multiple factors that alter preload. Tissue Ea alone although diagnostic may be inconclusive as a lone indice where its peak compared to blood inflow would yield finer diagnostic information. This new timing application and index has several other advantages over conventional Doppler parameters. They were obtained in all subjects included in the study. In previous reports by Masuyama et al[22] and Nagueh et al[23] adequate pulmonary venous flow signals, for example could not be obtained in up to 18% of normals and up to 84% of patients in intensive care units. It is essential that all important diagnostic parameters or alternatives be obtained in all patients especially for the critical diagnosis of what is physiological and what is pathological left ventricular hypertrophy.

The timing method is not clinically practical as it requires two echo machines, but future technological innovation to allow the simultaneous overlay of M-mode or conventional Doppler with DTI spectra using the one ultrasound system will improve the ease and reliability of the timing technique.

Limitations

The number of elite athletes with LVH were small due to the low prevalence of LVH in this group. Individuals with clinically proven mild HCM studied was also small due also to the low prevalence of patients with LVH in the range associated with physiological hypertrophy. The HCM patients in the study were somewhat older although not significantly. Patients subjects aged > then 55 were excluded to avoid any confusing effects of aging. However, in most cases, the differences between the two groups were large enough to have sufficient (>80%) statistical power to detect such a difference. For example, the comparison in Ea 4 site average between HCMS and athletes with n = 11 and n = 17 in each group respectively, would have over 90% power. The Canadian consensus guidelines[24] were not followed exactly because the pulmonary venous flow velocity patterns were omitted but conventional blood flow Doppler indices and LV annular Doppler tissue imaging were obtained on each patient.

The technical limitations with regard to time resolution of the ultrasound systems did not allow us to measure time differences below 5 ms. With further technical advances we would expect to see an improvement in this time resolution in ultrasound systems and hence finer diagnostic differentiation.

Conclusions

The timing application between peak tissue velocity Ea and peak mitral opening (by M-Mode) and the new novel index of diastolic stiffening can be used together or separately to differentiate hypertrophic cardiomyopathy from athletic physiologic left ventricular hypertrophy in the "grey zone".

References

(1) Maron BJ, Sharini J, Poliac LC et al. Sudden death in young competitive athletes. Clinical, demographic, and pathological profiles. JAMA 1996: 276: 199-204

(2) Spirito P, Felicia A, Proschan M et al. Morphology of the "athlete's heart" assessed by echocardiography in 947 elite athletes representing 27 sports. Am J Cardiol 1994: 74: 802-06

(3) Fananapazir L, Epstein ND et al. Prevalence of hypertrophic cardiomyopathy and limitations of screening methods. Circulation 1995: 92: 700-04.

(4) McDicken WN, Sutherland GR, Moran M et al. Colour Doppler velocity imaging of the myocardium. Ultrasound in Med Biol 1992: 18: 6/7, 651-54

(5) Erbel R, Wallbridge DR, Zamorano J et al. Tissue Doppler echocardiography (editorial). Heart 1996: 76(3): 193-96

(6) Galiuto L, Ignone G , De Maria AN et al. Contraction and relaxation velocities of the normal left ventricle using pulsed-wave tissue Doppler echocardiography. Am J Cardiol 1998: 81: 609-14

(7) Fukuda K, Oki T, Tabata T, Luchi A, Ito S. Regional left ventricular wall motion abnormalities in myocardial infarction and mitral annular descent velocities studied with pulsed tissue Doppler imaging. J. Am. Soc. Echocardiography 1998; 11(9): 841-848

(8) Nagueh SF, Lakkis NM, Middleton KJ, Spencer III WH, Zoghbi WA, Quinones MA. Doppler estimation of left ventricular filling pressures in patients with hypertrophic cardiomyopathy. Circulation 1999; 99: 254- 261

(9) Devereux RB Detection of left ventricular hypertrophy by M-mode echocardiography: anatomic validation, standardisation, and comparison with other methods. Hypertension 1987: 9: 119-126

(10) Dickhuth HH, Rocker K, Hipp A et al. Echocardiographic findings in endurance athletes with hypertrophic non-obstructive cardiomyopathy (HNCM) compared to non-athletes with HNCM and to physiological hypertrophy (athletes heart). Int J Sports Med 1994:15:273-277.

(11) Bland JM & Altman DG Statistics Notes: Diagnostic tests 1: Sensitivity and specificity. BMJ 1994; 308:1552 (June)

(12) Bland JM & Altman DG Statistical methods for assessing agreement between two methods of clinical measurement. Lancet 1986: 1: 307-310.

(13) Fisher AG, Adams TD, Yanowitz FG et al. Non-invasive evaluation of world class athletes engaged in different modes of training. Am J Cardiol.1989; 63:337-341.

(14) Ho CY, Sweitzer NK, McDonough B et al. Assessment of diastolic function with Doppler tissue imaging to predict genotype in preclinical hypertrophic cardiomyopathy. Circulation 2002:

(15) Nagueh SF, Bachinski LL, Meyer D et al. Tissue Doppler imaging consistently detects myocardial abnormalities in patients with hypertrophic cardiomyopathy and provides a novel means for an early diagnosis before and independently of hypertrophy. Circulation 2001: 104: 128-130

(16) Vinereanu D, Florescu N, Sculthorpe N et al. Differentiation between pathologic and physiologic left ventricular hypertrophy by tissue Doppler assessment of long axis function in patients with hypertrophic cardiomyopathy or systemic hypertension and in athletes. Am J Cardiol 2001: 88: 53-58.

(17) King GJ, Foley JB, Almane F et al. Early diastolic filling dynamics in diastolic dysfunction. Cardiovasc Ultrasound 2003, 1: 9.

(18) Rodriguez L, Garcia M, Ares MA et al. Assessment of mitral annular dynamics during diastole by Doppler tissue imaging: comparison with mitral Doppler inflow in subjects without heart disease and in patients with left ventricular hypertrophy. Am Heart J 1996: 131: 982-87

(19) Rivas-Goetz, KD, Manolios M, Rao L et al. Time interval between onset of mitral inflow and onset of early diastolic velocity by tissue Doppler: A novel index of left ventricular relaxation. J Am Coll Cardiol 2003;42:1463-70

(20) Greaser H, Berri M, Warren CM et al. Species variations in cDNA sequence and exon splicing patterns in the extensible I-band region of cardiac titin: relation to passive tension. J Muscle Res cell Motil 2002: 23(5-6): 473-482

(21) Sohn DW, Song JM , ZO JH ,et al. Mitral Annular Velocity in the evaluation of left ventricular diastolic function in atrial fibrillation. J Am. Soc echocardiogr 1999,12. 927-31.

(22) Masuyama T, Lee JM, Tamai M, et al. Pulmonary venous flow pattern as assessed with transthoracic pulsed Doppler echocardiography in subjects without cardiac disease . Am J Cardiol 1991 ; 18: 65-71

(23) Nagueh SF, Kopelen HA, Zoghbi WA . Feasibility and accuracy of Doppler echocardiographic estimation of pulmonary artery occlusion pressure in the intensive care unit Am J Cardiol 1995 ; 75: 1256-62.

(24) Rakowski H ,Appleton CP, Chan KL, Dumesnil JG, Honos G, Jue, et al Canadian consensus recommendations for the measurement and reporting of diastolic dysfunction by echocardiography: from the investigators on consenus on

diastolic dysfunction by echocardiography. J Am Soc Echocardiogr 1996;9:736-
60

Fig 1   A time reference pulse was introduced into the displays of both machines

simultaneously. The time from pulse edge to Ea (DTI) on one machine and to

peak mitral (M-mode) opening were measured simultaneously.

Fig 2   Box and whisker plots of 4-site mean early diastolic tissue (mitral annulus)

velocity in a control and athletic group and in patients with HCM

Fig 3   Box and whisker plots for the early diastolic mechanism (ms) in a control and

athletic group and in patients with HCM

Fig 4 Box and whisker plots of an novel index of myocardial stiffness E/A/LVlDd in

a control and athletic and in patients with HCM

Table 1 General characteristics of the study groups

	HC (N = 11)	Athletes (N = 17)	Controls (N =30)	p-value
Age (yrs)$^&$	31 (13,40)	28 (24,30.5)	26 (24,28)	NS
Men /Woman	9/2	14/3	25/5	NS
Heart Rate*	67.4±5.1	65±10.7	70.0±5.1	NS
Body surface area (m²)$^&$	1.93 (1.91,1.98)	2.01(1.95,2.01)	1.84(1.62,1.9)	NS

$^&$median and IQR presented for non-normal data; * mean±SD

Table 2   Standard Echocardiographic data in the study groups

	HCM	Athletes	Controls	p-value
Aortic root diameter (mm)*	3.5±0.37	3.75±0.36	3.24±0.41	0.003
Left atrial Diameter (mm). &	3.99±0.42	3.84±0.42	3.49±0.41	0.002
Septal thickness&	1.32 (1.3,1.47)	1.3 (1.28,1.33)	0.86(0.78,1.02)	<0.0001
Posterior wall thickness*	1.31±0.06	1.3±0.079	0.95±0.17	<0.0001
LVEDD (mm)*	4.6±0.15	5.64±0.12	4.84±0.40	<0.0001
LVESD (mm)*	3.0±0.48	3.63±0.55	3.14±0.48	0.0151
Ejection Fraction %*	67.3±5.08	63.7±4.5	63.9±5.23	0.164
Left ventricular mass index (g/m²)*	167.0±22.4	187.9±24.3	101.96±27.0	<0.0001
E wave (cm/sec)*	59.75±17.5	70.66±15.31	74.39±14.47	0.09
A wave (cm/sec) &	40.5 (21.75,70.3)	36.5 (32.8,47.9)	40(34.5,48.7)	0.94
E/A ratio *	1.09±0.48	1.78±0.4	1.77±0.38	0.0012
IVRT. *	92.7±15.6	82.0±11.6	75.3±9.8	0.014
Dec	223 ± 69	185 ± 40	169 ± 39	< 0.01
Ea averaged four site Velocity (cm/sec) &	9.2(7.05,10.0)	19 (17.3,21.7)	18.4(15.3,19.8)	<0.0001
E/Ea*	10.1±2.78	6.4±1.63	7.1±1.10	0.0014
Systolic Wave Velocity. (cm/sec) *	8.7±2.5	12.2±1.57	10.28±1.40	<0.0001
New index of myocardial stiffness E/Ea/LVEDd &	2.19 (1.92, 2.3)	1.2 (0.93,1.4)	1.5(1.3,1.6)	p< 0.0001

&median and IQR presented for non-normal data; * mean±SD # adjusted for age and gender.

Table 3A Performance of possible echocardiographic criteria for discriminating between patients with HCM and athletes

	Sensitivity	Specificity	Accuracy
4 Site average Ea <9cm/sec	27.3%	100%	71.4%
4 Site average Ea <10cm/sec	72.7%	100%	89.3%
Systolic P velocity<9cm/sec	63.6%	100%	85.7%
(IVS+LVPW)/(LVEDd)>0.6	36.4%	100%	75%
E/A ratio<1.0	36.4%	100%	75%
Flow propagation velocity <50cm	27.3%	100%	71.4%
*4 Site average Time difference between Ea and E M-mode > =0	100%	100%	100%
E/Ea /LVEDd < 1.7	85.7%	94.1%	91.7%

*All patients with hypertrophic cardiomyopathy had values > or = to 0 for the four site average time difference ,and all athletes had values < 0, therefore there was complete discrimination between the groups.

Table 3B Performance of possible echocardiographic criteria for discriminating between patients with HCMs and normals

	Sensitivity	Specificity	Accuracy
4 Site average Ea <9cm/sec	27.3%	100%	80.5%
4 Site average Ea <10cm/sec	72.7%	100%	92.7%
Systolic P velocity<9cm/sec	36.4%	93.3%	78%
(IVS+LVPW)/(LVEDd)>0.6	36.6%	100%	82.9%
E/A ratio<1.0	36.6%	100%	82.9%
Flow propagation velocity <50cm	27.3%	96.7%	78%
4 Site average Time difference between Ea and E M-mode > =0	100%	76.7%	83%
E/Ea/ LVEDd < 1.7	85.5%	86.7%	85.7%
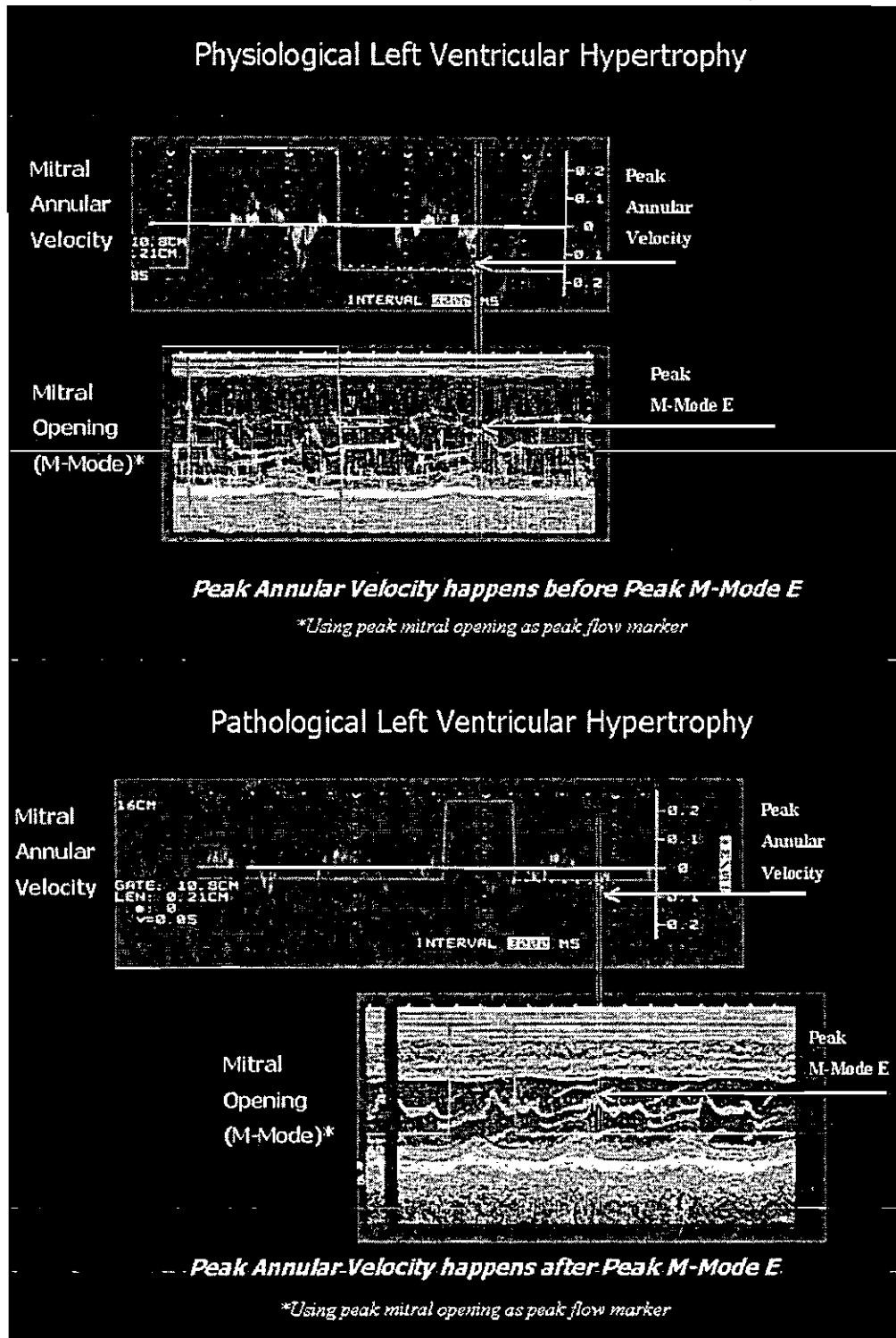
Figure 1
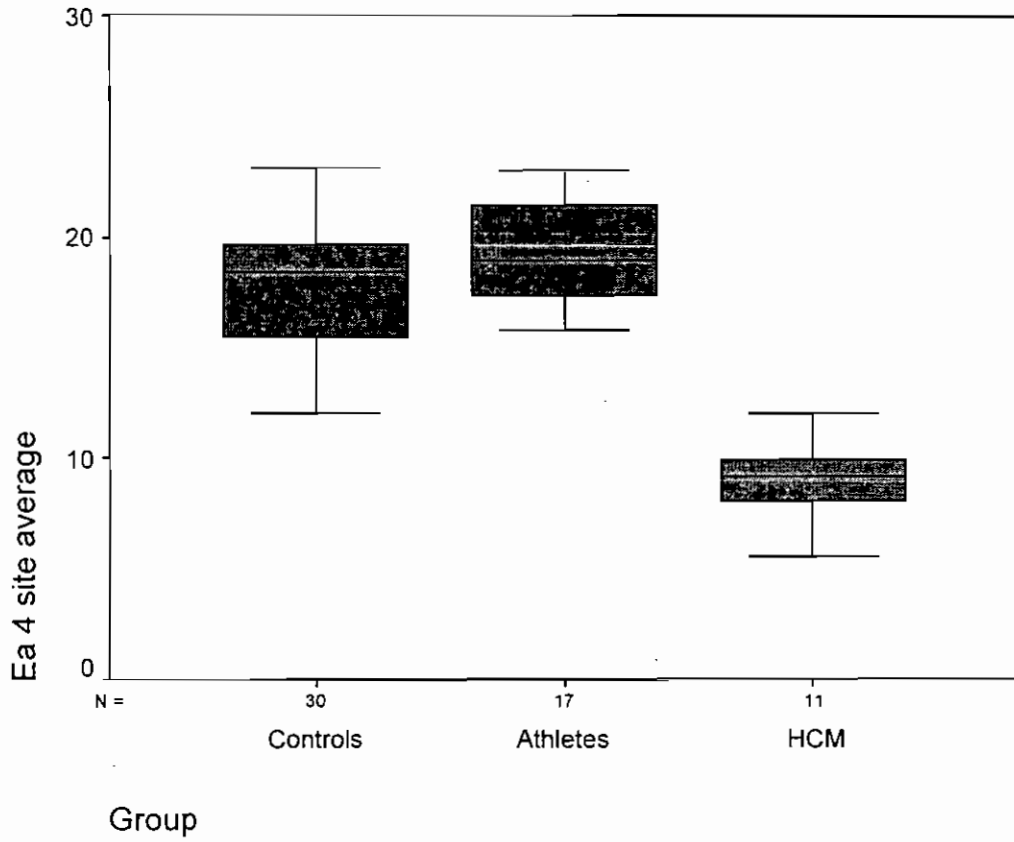
Figure 2
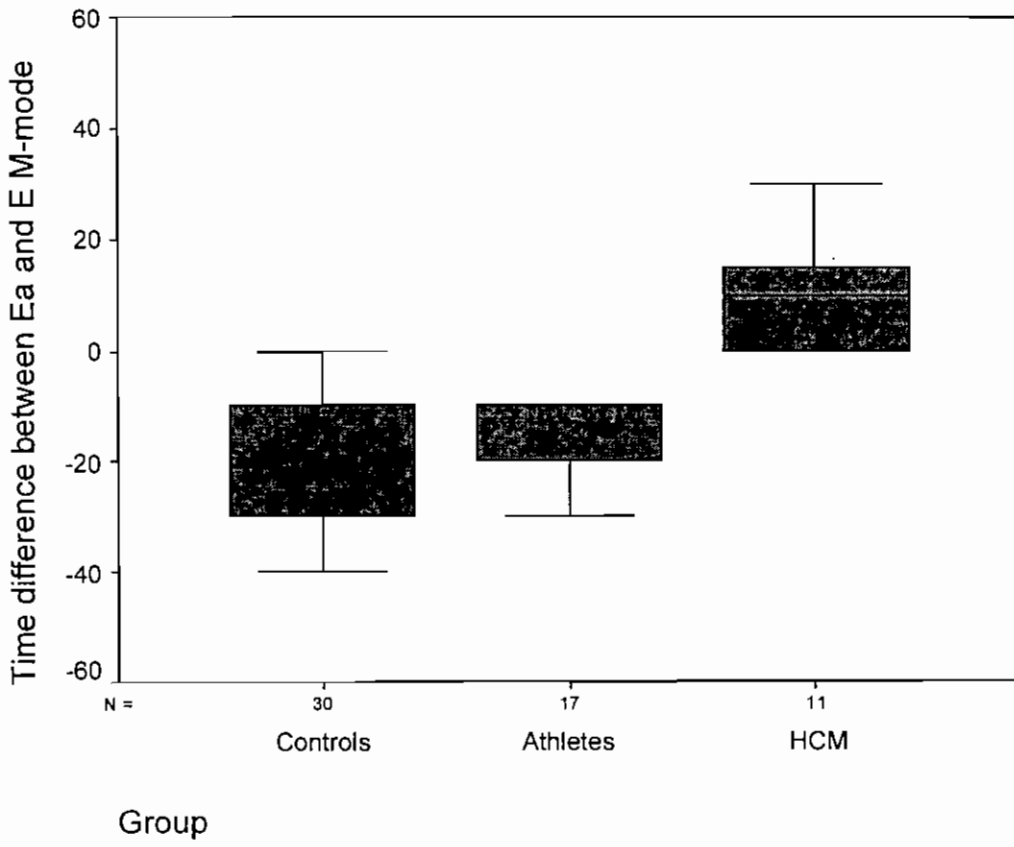
Figure 3
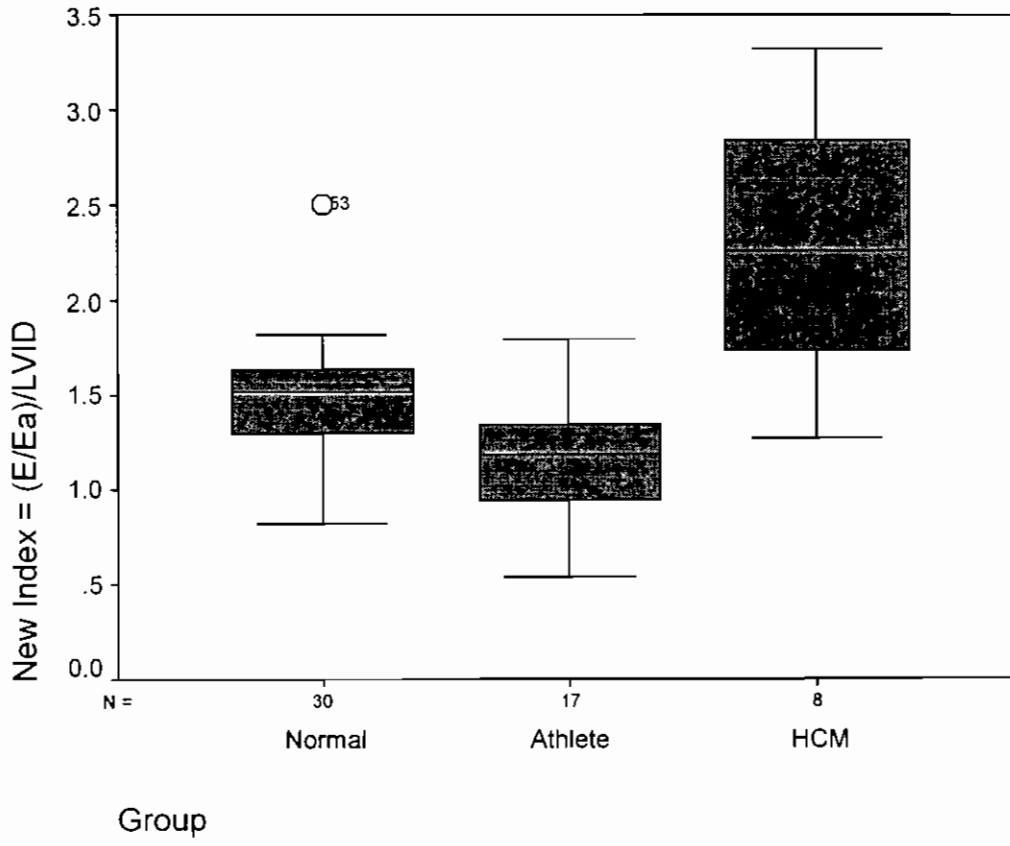
Figure 4

Appendix G

Tables of raw measured data for the study described in Chapter 7

Name	age yrs	sex	HR min⁻¹	LVIDd cm	LVIDs cm	STHICK cm	PWTHICK cm	EF %	E VEL cm/s	Q- ME ms	A Vel cm/s	E/A rat	IVRT ms
DC	58	1	75	5.1	3.3	1.2	1.4	75	35	500	49	0.6	100
AB	53	1	70	5.2	3.8	1.4	1.4	68	45	580	32	1.1	100
EM	61	2	80	3.9	2.8	1.5	1.4	66	43	500	96	0.5	110
AM	40	1	70	5.0	2.9	1.5	1.2	62	60	420	95	.0.6	100
HB	38	2	71	4.5	2.6	1.5	1.3	57	80	510	25	1.5	90
KH	65	2	75	4.5	2.7	1.3	1.3	72	96	370		1.5	90
LC	12	2	68	3.5	2.0	1.3	1.3	68	59	280	59	1.3	90
GC	24	1	69	4.5	3.2	1.3	1.3	72	51	510	26	1.2	110
NK	41	1	61	5.3	2.9	1.3	1.3	65	55		62	0.5	100
ID	12	1	65	4.3	3.2	1.3	1.3	70	72	470	10	1.8	60
AD	13	2	70	4.5	3.3	1.3	1.3	65	62		12	1.5	70
TT	28	1	60	5.6	2.8	1.1	1.2	55	60	550	48	1.2	70
FG	32	1	68	5.6	4.0	1.3	1.3	62	54	600	36	1.5	80
AC	28	1	40	5.6	4.1	1.3	1.3	63	64	550	30	2.2	100
KL	31	1	54	6.3	4.4	1.4	1.4	66	51	530	30	1.8	90
KB	24	1	52	5.4	3.9	1.3	1.3	75	66	550	34	1.9	100
KD	30	1	84	6.3	4.5	1.3	1.3	62	105	520	79	1.3	100
DB	27	1	56	5.9	3.5	1.4	1.5	66	75	530	39	1.9	90
RP	25	2	65	4.2	3.0	1.2	1.2	65	75	500	32	2.3	80
SJ	30	1	54	5.8	4.1	1.3	1.3	64	58	590	37	1.6	80
SW	28	1	59	5.3	3.0	1.3	1.3	58	56	540	41	1.4	80
DB	35	1	65	5.5	3.7	1.3	1.4	67	80	500	48	1.6	80
AS	24	1	40	5.6	3.2	1.3	1.3	64	63	580	31	2.0	70
TH	21	1	49	5.6	3.8	1.3	1.3	62	95	530	34	2.8	74
ST	18	1	51	5.7	2.7	1.3	1.3	65	82	500	48	1.7	60
AD	24	1	65	5.8	3.4	1.3	1.3	62	63	470	40	1.6	70
JB	23	1	54	6.0	4.1	1.2	1.2	58	89	500	53	1.7	80
HW	51	1	65	5.6	3.6	1.3	1.2	68	66	500	35	1.8	90
AB	29	2	74	4.9	2.5	1.0	1.1	67	50	500	35	1.8	80
GO	23	1	62	4.9	2.7	1.1	1.1	62	75	570	40	1.5	80
KF	30	1	65	5.0	2.5	1.1	0.9	55	90	510	40	1.5	90

Name	Age yrs	sex	HR min⁻¹	LVIDd cm	LVIDs cm	STHICK cm	PWTHICK cm	EF %	E VEL cm/s	Q- ME ms	A Vel cm/s	E/A rat	IVRT ms
SO	25	1	65	4.8	2.3	1.0	0.8	58	85	520	30	1.6	85
HD	20	1	68	4.5	2.3	0.7	0.8	62	62	530	25	1.8	80
PS	24	1	85	5.0	3.6	1.1	1.1	67	98	450	60	1.6	90
TA	26	1	68	5.2	3.2	0.8	0.9	60	66	510	40	1.7	80
KB	26	1	71	4.7	3.6	0.9	0.7	62	57	480	35	1.6	80
SL	24	1	70	4.7	3.2	0.7	0.7	64	99	500	60	1.6	80
PK	31	1	65	4.2	3.1	0.9	1.0	63	70	510	37	1.9	75
DM	31	2	94	4.2	3.2	0.8	0.8	68	73	480	59	1.2	70
NM	29	1	80	5.7	3.6	1.0	1.0	70	80	500	60	1.3	80
KH	26	2	90	4.2	2.8	0.8	0.6	64	64	480	52	1.3	80
CD	28	1	68	4.8	3.2	1.0	1.2	58	69	520	29	2.4	80
HB	28	1	65	4.8	3.7	0.8	1.2	72	61	500	36	1.7	70
FC	25	2	62	5.0	3.1	0.5	1.0	65	98	520	58	1.6	70
DR	26	1	60	4.6	3.5	0.8	1.2	72	76	540	27	2.8	60
CC	24	1	75	5.4	3.9	1.0	0.9	64	73	470	32	2.3	80
BD	27	1	85	5.4	3.9	1.2	1.1	70	50	530	33	1.5	60
DG	28	1	66	5.0	3.2	1.2	1.1	68	81	520	42	1.9	80
SH	26	2	64	5.0	3.4	0.7	0.9	64	62	520	29	2.1	70
CW	25	2	65	4.6	2.7	0.8	0.7	53	91	470	36	2.5	60
VA	22	2	70	4.5	2.5	0.7	0.7	68	67	490	43	1.6	80
CR	22	2	60	4.8	2.9	0.9	0.8	54	90	510	46	2.0	80
CC	26	2	75	4.2	2.7	0.7	1.1	55	99	460	53	1.8	50
BL	28	1	82	5.3	3.6	0.8	1.1	67	60	470	48	1.3	80
JH	30	1	71	5.0	3.2	1.0	1.0	63	80	420	40	2.0	70
IH	20	1	45	5.6	4.0	0.8	1.2	68	80	510	40	2.0	70
AG	21	1	65	4.2	3.0	0.8	0.9	68	70	390	37	1.9	60
CM	27	1	65	5.0	3.5	1.1	0.9	65	58	530	44	1.4	90

Name	Age yrs	Ea 4site avg cm/s	Q-Tea ms	Ea/Aa	SysP Vel cm/s	Hcmgroup 1 normal 2 athlete 4 HCM	Ao Size cm	E/Ea	newindex	La size cm
DC	58	7.1	500	0.6	6.1	4	3.5	7.9	1.6	
AB	53	9.3	580	1.0	6.5	4		6.6	1.3	4.0
EM	61	5.5	540	0.5	9.3	4	3.3	10.8	2.8	4.2
AM	40	9.1	440	0.7	8.0	4	3.6	9.6	1.9	4.5
HB	38	6.7	530	1.3	5.0	4	3.2	14.9	3.3	4.2
KH	65	9.2	370	0.9	8.0	4	3.3	13.0	2.9	4.7
LC	12	10.0	710	1.2	8.7	4	2.7	8.0	2.3	3.5
GC	24	9.8	510	1.0	8.0	4	3.8	10.0	2.2	4.0
NK	41	9.0		0.5	11.0	4	3.7			3.5
ID	12	10.0		1.0	12.0	4	3.8			3.7
AD	13	12.0		1.3	13.0	4	4.0			3.6
TT	28	21.4	510	2.0	12.3	2	3.5	5.8	1.0	3.7
FG	32	19.0	560	1.8	14.0	2	3.6	7.6	1.4	3.6
AC	28	18.8	540	2.0	10.2	2	3.6	7.4	1.3	3.7
KL	31	22.0	510	2.2	14.0	2	3.9	7.0	1.1	3.7
KB	24	22.0	540	1.5	13.5	2	3.3	6.6	1.2	3.6
KD	30	20.0	510	2.0	12.5	2	4.0	9.2	1.5	3.9
DB	27	16.9	510	3.8	12.5	2	3.9	7.4	1.3	4.0
RP	25	18.2	480	2.7	9.5	2	3.0	7.6	1.8	3.5
SJ	30	19.0	560	2.8	14.6	2	4.0	6.6	1.1	4.2
SW	28	23.0	520	1.8	12.5	2	4.2	7.5	1.4	4.3
DB	35	22.3	480	1.5	12.0	2	3.8	3.6	0.7	3.8
AS	24	17.2	560	2.1	13.0	2	4.0	6.6	1.2	3.0
TH	21	18.1	520	1.6	14.0	2	3.5	5.3	0.9	4.1
ST	18	17.4	510	0.6	11.2	2	3.8	7.7	1.4	3.2
AD	24	20.5	450	2.0	11.0	2	4.4	3.1	0.5	4.4
JB	23	15.8	480	2.0	11.7	2	3.4	5.6	0.9	4.7
HW	51	15.8	490	1.1	9.5	2	4.1	4.1	0.7	4.0
AB	29	14.1	470	1.7	10.5	1	3.5	7.6	1.6	3.7
GO	23	20.7	540	2.2	9.8	1	3.6	7.6	1.6	3.7
KF	30	18.4	470	2.0	10.0	1	3.6	5.6	1.1	3.7

Name	Age yrs	Ea 4site avg cm/s	Q-Tea ms	Ea/Aa	SysP Vel cm/s	hcmgroup	Ao Size cm	E/Ea	newindex	La size cm
SO	25	19.0	510	1.8	9.5	1	3.0	7.9	1.6	2.9
HD	20	22.3	510	1.9	11.2	1	3.6	5.8	1.3	3.8
PS	24	23.1	420	1.2	12.0	1	3.3	6.6	1.3	3.8
TA	26	12.0	490	1.5	9.5	1	3.7	8.5	1.6	3.8
KB	26	18.6	470	1.9	10.2	1	2.6	6.0	1.3	3.7
SL	24	18.5	460	1.9	10.2	1	3.5	8.3	1.8	3.8
PK	31	18.5	490	1.8	10.2	1	3.4	6.7	1.6	3.8
DM	31	15.7	460	1.2	13.5	1	3.0	7.7	1.8	3.8
NM	29	15.4	490	1.4	13.8	1	3.8	8.1	1.4	3.9
KH	26	14.8	470	1.2	10.9	1	3.4	7.4	1.8	3.6
CD	28	13.9	510	1.8	7.6	1	3.1	8.0	1.7	3.8
HB	28	16.8	490	2.4	10.2	1	3.1	6.6	1.4	3.5
FC	25	21.8	490	1.5	10.3	1	2.5	7.4	1.5	3.6
DR	26	18.0	520	2.7	6.2	1	3.0	7.2	1.6	3.8
CC	24	19.6	450	1.9	10.2	1	3.5	6.7	1.2	3.8
BD	27	15.0	530	1.6	11.0	1	3.7	6.3	1.2	3.8
DG	28	19.7	490	3.1	10.1	1	3.5	7.1	1.4	3.7
SH	26	19.6	520	1.9	9.0	1	3.3	6.2	1.2	3.5
CW	25	20.1	460	2.0	10.6	1	2.8	7.4	1.6	3.2
VA	22	16.2	490	2.2	11.0	1	2.4	7.1	1.6	2.8
CR	22	18.8	510	2.1	10.0	1	2.4	7.8	1.6	2.7
CC	26	13.0	460	1.4	9.6	1	2.5	10.5	2.5	2.7
BL	28	14.6	460	1.5	10.0	1	3.4	7.1	1.3	2.6
JH	30	21.8	390	2.1	10.0	1	2.7	6.7	1.4	2.8
IH	20	17.3	510	1.9	10.0	1	4.5	4.6	0.8	3.8
AG	21	16.3	380	2.9	11.0	1	3.2	7.0	1.7	3.4
CM	27	22.1	490	1.8	10.2	1	3.7	5.6	1.1	3.7

Name	Age yrs	WT kg	Ht Cm	E+E-No1	E+E-N02	Ea avg 1 cm/s	Ea avg 2 cm/s	Bmi kg/m^2	LVMI Kg/m^2
DC	58	79	177	0	0	7.0	7.1	2.5	167
AB	53	80	188	0	0	9.3	9.3	2.3	179
EM	61	78	168	40	40	5.5	5.5	2.8	131
AM	40	90	172	20	20	9.2	9.0	3.0	166
HB	38	64	175	30	30	6.7	6.7	2.1	166
KH	65	52	167	0	0	9.2	9.2	1.9	168
LC	12	40	131	0	0	10.0	10.0	2.3	147
GC	24	70	168	0	0	9.8	10.0	2.5	150
NK	41	85	160	10	10	9.0	9.0	3.3	183
ID	12	43	125	10	10	7.0	7.0	2.8	213
AD	13			10	10	7.0	8.0		
TT	28	76	168	-40	-40	21.3	21.5		173
FG	32	80	190	-40	-40	18.8	19.1		179
AC	28	78	192	-10	-10	18.8	18.8		182
KL	31	82	194	-20	-20	22.0	22.0		239
KB	24	80	186	-10	-10	22.0	22.0		174
KD	30	82	190	-10	-10	20.0	20.0		224
DB	27	85	195	-20	-20	16.9	16.9		223
RP	25	58	165	-20	-20	18.3	18.2		133
SJ	30	90	195	-30	-30	19.0	19.0		181
SW	28	78	190	-20	-20	22.0	24.0		167
DB	35	75	180	-20	-20	22.3	22.3		196
AS	24	75	178	-20	-20	17.2	17.2		191
TH	21	80	183.3	-10	-10	18.0	18.1		190
ST	18	96	185	-20	-20	17.6	17.2		183
AD	24	89	179	-20	-20	20.4	20.6		193
JB	23	77	183	-20	-20	15.8	15.8		190
HW	51	77	180	-10	0	15.8	15.9		177
AB	29	50	160	-30	-30	14.0	14.2		114
GO	23	72	175	-30	-30	20.7	20.7		147
KF	30	72	170	-40	-40	18.3	18.4		126

Name	age yrs	WT kg	Ht cm	E+E-No1	E+E-N02	Ea avg 1 m/s	Ea avg 2 m/s	Bmi kg/m^2	LVMI Kg/m^2
SO	25	55	161	-10	0	18.9	19.0		116
HD	20	77	178	-20	-20	22.5	22.0		108
PS	24	72	177.5	-30	-30	23.2	22.9		60
TA	26	70	177	-20	-20	12.0	12.0		129
KB	26	68	173	-10	-10	18.6	18.5		97
SL	24	70	175	-40	-40	18.5	18.5		78
PK	31	71	176	-20	-20	18.5	18.5		60
DM	31	60	178	-20	-20	15.8	15.6		80
NM	29	79	182	-10	-10	15.4	15.5		62
KH	26	56	169	-10	-20	14.8	14.8		129
CD	28	68	178	-10	-10	14.0	13.7		58
HB	28	55	168	-10	-10	16.7	16.8		125
FC	25	59	165	-30	-30	21.8	21.8		121
DR	26	70	180	-20	-20	18.0	18.0		86
CC	24	70	180	-20	-20	19.6	19.6		97
BD	27	72	181	0	0	14.9	15.0		122
DG	28	74	175	-30	-30	19.6	19.7		153
SH	26	58	165	0	0	19.6	19.6		133
CW	25	52	160	-10	-10	20.1	20.1		98
VA	22	51	175	0	0	16.1	16.2		86
CR	22	53	170	0	0	18.9	18.7		65
CC	26	55	168	0	0	13.0	13.0		95
BL	28	68	177	-10	-10	14.6	14.6		83
JH	30	72	178	30	30	22.0	21.6		121
IH	20	83	183	0	0	17.5	17.1		105
AG	21	65	140	-10	-10	16.0	17.0		123
CM	27	73	175	-40	-40	22.1	22.0		80

Name	Age yrs	bsa m^2	ratio
DC	58	2.0	0.5
AB	53	2.1	0.5
EM	61	1.9	0.7
AM	40	2.0	0.5
HB	38	1.8	0.6
KH	65	1.6	0.6
LC	12	1.2	0.7
GC	24	1.8	0.6
NK	41	1.9	0.5
ID	12	1.2	0.6
AD	13		0.6
TT	28	1.9	0.4
FG	32	2.1	0.5
AC	28	2.1	0.5
KL	31	2.1	0.5
KB	24	2.0	0.5
KD	30	2.1	0.4
DB	27	2.2	0.5
RP	25	1.6	0.6
SJ	30	2.2	0.5
SW	28	2.1	0.5
DB	35	1.9	0.5
AS	24	1.9	0.5
TH	21	2.0	0.5
ST	18	2.2	0.5
AD	24	2.1	0.5
JB	23	2.0	0.4
HW	51	2.0	0.4
AB	29	1.9	0.4
GO	23	1.5	0.5
KF	30	1.9	0.4

Name	Age yrs	bsa m²	ratio
SO	25	1.8	0.4
HD	20	1.6	0.3
PS	24	2.0	0.4
TA	26	1.9	0.3
KB	26	1.9	0.4
SL	24	1.8	0.3
PK	31	1.9	0.5
DM	31	1.9	0.4
NM	29	1.8	0.4
KH	26	2.0	0.3
CD	28	1.6	0.5
HB	28	1.9	0.4
FC	25	1.6	0.3
DR	26	1.7	0.4
CC	24	1.9	0.4
BD	27	1.9	0.4
DG	28	1.9	0.5
SH	26	1.9	0.3
CW	25	1.6	0.3
VA	22	1.5	0.3
CR	22	1.6	0.4
CC	26	1.6	0.4
BL	28	1.6	0.4
JH	30	1.8	0.4
IH	20	1.9	0.4
AG	21	2.1	0.4
CM	27	1.5	0.4

Appendix H

List of publications of the author relating to the work of this thesis, including copies of two posters and their abstracts published in the European Journal of Echocardiography
[Note that the first poster was chosen for its 'outstanding quality' at the 7th Annual Meeting of the European Society of Echocardiograph at Barcelona, December 2003.]

Publications

Barry M, King G & Walsh MW
Assessment of mitral annular descent velocity using pulse tissue Doppler imaging as a quantitative index of left ventricular function
Irish J Med Sci, 2001

Boyle G, Meier H & King G
Integration of blood flow velocity and tissue Doppler information
IPEM Biennial Meeting 2003 (The Physics and Technology of Medical Ultrasound)

Boyle G & King G
A novel method of employing Doppler ultrasound in a cardiac investigation
IPEM Annual Scientific Meeting 2003

King G, Foley BF, Almaine F, Crean P & Walsh M
Early diastolic filling dynamics in diastolic dysfunction
J Cardiovasc Ultrasound, 2003 (1); 9

King G, Foley BF, Crean P & Walsh M
Doppler tissue imaging of early diastolic filling dynamics in diastolic dysfunction
European Society of Echocardiography, Moderated poster No 664, Barcelona, December 2003

King GJ, Foley JB, Crean PC, Hussey M, Walsh MJ
Differentiation between pathological and physiological left ventricular hypertrophy by timeing of the early diastolic mechanism: a novel approach
European Society of Echocardiography, Athens, December 2004

King G, Foley JB, Cosgrave J, Boyle G, Hussey M, Bennett K, Crean P & Walsh M
Novel approaches for distinguishing hypertrophic cardiomyopathy from physiological left ventricular hypertrophy in the "gray zone" using Doppler tissue imaging
Submitted to Heart, February 2005

King G, Hussey M & Walsh M
The molecular 'spring' and echocardiography: the 'slack myocardium', a new concept
Submitted to Irish Journal of Medical Science, February 2005

Early Diastolic Filling Dynamics in Diastolic Dysfunction

King GJ, Foley JB, Crean PC, Walsh MJ.
Trinity Cardiology St James hospital Dublin.

Introduction.

A number of studies have shown that early diastolic Tissue Velocity (Ea) is reflective of events at the very early diastolic stage in the cardiac cycle, including recoiling of the ventricle

Aim

To determine the relationship between Ea(reflective of recoil) and early transmitral flow in Patients with diastolic dysfunction and to compare them to a normal population

Methodology

• 22 controls of mean age 38.4 ± 16 and 25 patients of mean age 61.3 ± 13.2 with clinical Echo and Doppler evidence of diastolic dysfunction without pseudonormalisation were studied

• All patients had normal systolic function

• From the apical view Doppler tissue imaging was performed by placing a sample volume at the lateral mitral annulus

• Doppler blood flow velocities were also recorded across the mitral valve from the apical view, and the acceleration rate of early diastolic flow was measured using a sweep speed of 100mm/sec
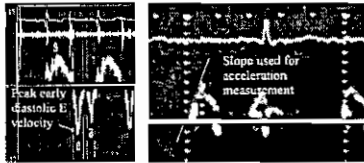

Fig1 (a) Fig1 (b)

Fig 1(a) Pulsed-wave tissue Doppler pattern with diastolic Ea velocity recorded as a surrogate for recoil
Fig 1(b) Slope used for the acceleration measurement on the blood velocity spectrum.

Results:

Means in table adjusted for age.

Parameters.	Diastolic dysfunction	Normal	P Value
E/A ratio	0.7 ± 0.2	1.9 ± 0.5	0.001
TVI atrial.	11.7 ± 3.2 cm	5.5 ± 2.1cm	0.0001
IVRT.	73.0 ± 12 ms	94 ± 6 ms	0.01
Rate of Acceleration	549.2 ± 151.9 cm/sec²	871 ± 128 cm/sec²	0.001
Ea (reflective of recoil)	6.08 ± 1.6 cm/sec	10.3 ± 2.9 cm/sec	0.001

There was a positive correlation between the mitral annular tissue velocity (Ea) and the acceleration of mitral inflow blood velocity in the diastolic dysfunction group (r = + 0.66) ; p= 0.0002, which was not present in the control group (r = + 0.18) ; p = 0.22.
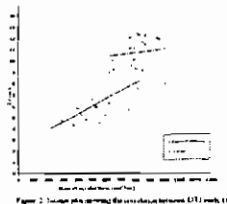

Conclusions

1. Recoil as reflected by Ea is

* An important mechanism for rapid early diastolic filling

• Dissociated from preload dependent diastolic filling in normal

• Strongly associated with early diastolic filling without the influence of preload in patients with diastolic dysfunction

2. This study supports the existence of an early diastolic mechanism in normal and its absence in patients with diastolic dysfunction

REF. 1 Nagueh SF, Sun H, Kopelen H et al, Haemodynamic determinants of the mitral annulus diastolic velocities by tissue Doppler. J Am Coll Cardiology 2001:37; 278-285

Differentiation between pathological and physiological left ventricular hypertrophy by timing of the early diastolic mechanism. A novel approach.

King GJ, Foley JB, Crean PC, Hussey M, Walsh MJ
Trinity Cardiology St. James's Hospital, Dublin, Ireland
Dublin Institute of Technology, Dublin

Introduction

Current echocardiographic methods of differentiating pathological from physiological hypertrophy are limited

Aim

To evaluate a novel application of Doppler tissue imaging in distinguishing athletic physiological hypertrophy from pathological left ventricular hypertrophy.

Methodology

We compared 63 subjects with different types of LV hypertrophy.

- Group 1: 13 patients with mild HCM
- Group 2: 14 patients with systemic hypertension
- Group 3: 36 healthy elite athletes (rowers)
- Group 4: 30 controls

The patients with HCM and systemic hypertension were grouped together to constitute the pathological LVH group

Each subject underwent echocardiography where the time interval between Ea (by Doppler tissue imaging) and the peak mitral opening (by M-mode) were measured simultaneously on the same heart beat. A sharply defined time reference pulse was introduced into unused ECG channels on both machines by pressing a footswitch activated circuit.

Results
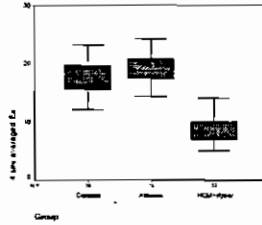
- Patient groups, a lower four site Ea, median 9.0 cm (IQR6 7,10)Athletes group median, 18.7cm (17.3, 20.9)Control group : median, 18.4 (15.3, 19.8). p<0.0001.
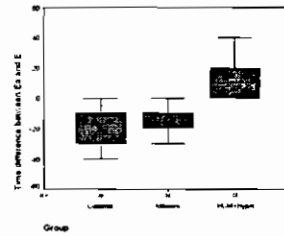
In the athletic group the peak early diastolic annular tissue velocity preceded the peak mitral E of the M-mode by median 20 ms (IQR 10, 20), and in the control group by a median 15 ms (0, 20), compared with the patient groups where the peak early diastolic annular tissue velocity reversed relative to the peak mitral inflow by a median 10 ms (0, 20), p<0.0001.
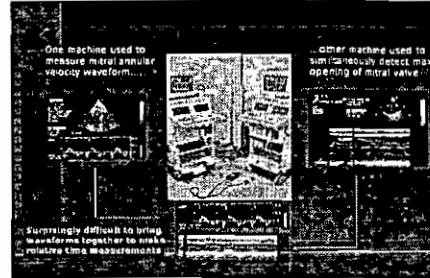
	Sensitivity	Specificity	Accuracy
4 Site average Ea <9cm	44%	100%	76%
4 Site average Ea <10cm	67%	100%	80%
Systolic P velocity<9cm	37%	97.0%	71.4%
(IVS+LVPW)/(LVEDD)	30%	100%	70.0%
EA ratio <1.0	37.0%	100%	73.0%
Flow propagation velocity <50cm	22.2%	100%	60.7%
4 Site average Time difference between Ea and E M-mode ≥≤50	100%	86.1%	92.1%

(Performance of a range of echocardiographic criteria for differentiating between patients with pathological LVH and athletes with physiological LVH)

Conclusions Along with the four site average early diastolic tissue relaxation velocity (Ea) ,this new simple measurement of the time interval between peak early diastolic tissue E and mitral valve opening is useful in differentiating pathological from physiological left ventricular hypertrophy. Reversal of the early diastolic mechanism is a strong predictor of pathological hypertrophy.

Appendix I

Copy of a draft review paper relating to the work of this thesis and submitted to the Irish J Med Sci in February 2005

The molecular 'spring' and Echocardiography:
the 'slack myocardium', a new concept

King G, Hussey M & Walsh M, Cardiology Department, St James's Hospital, Dublin 8 and Faculty of Science, Dublin Institute of Technology, Dublin 8

Heart failure is common and costly, and it primarily affects the elderly. As the elderly population expands, there will be marked increases in the number of persons with heart failure. Epidemiological studies have established that 40 percent to 50 percent of patients with heart failure have a normal ejection fraction ($\geq$50 percent) without primary valve disease, a clinical syndrome that is commonly referred to as "diastolic" heart failure. It was this realization that the heart can only pump out the blood it receives during diastole (regardless of the contractile state) that led researchers and clinicians to concentrate more on the diastolic function of the heart and the ability of the ventricle to fill with blood. Despite great progress in our understanding of and therapeutic approach to heart failure associated with systolic dysfunction, or systolic heart failure, we are now realizing that basic research and clinical investigations have shown us that our understanding of the role of diastole in heart failure is limited.

Recent echocardiographic research using Doppler tissue imaging investigating the early diastolic phase of the cardiac cycle combined with advances in the understanding of myocardial molecular structure and physiology has led us to explore the potential role of what we called the "slack" period of the cardiac cycle that appears to be mediated by the unique properties of titin. This we believe has important implications for heart failure.

Titin is the largest protein in man and is present in striated muscles of the

myocardium. It has multiple cellular functions, the most important being formation of

a "structural skeleton" that also acts as a "molecular spring."[1]

There are two major types of isoforms of full-length titins in human myocardium:

N2B and N2BA. N2B isomers are shorter and stiffer, while N2BA are longer and

more elastic.[2] Different expression of isomers of titin has been linked to the variety of

physiological responses as well as certain myocardial pathologies.[3,4,5,6] For example

dynamic structural switching in expression of isomers has particular importance in

human ischaemic heart disease.[7] A unique N2B sequence exists only in cardiac titin

and allows maximum physiological stretch of sarcomeres. Each of the above

stretched segments expresses recoil forces in response to extension. These forces are

non-lineally proportionate to the length of titin distention or compression.[1]

The "slack sarcomere" concept is an extension of titin research. Such a condition

occurs when titin molecules are neither stretched, nor compressed. At this stage the

"molecular spring" is "at rest" and does not exhibit entropic activity as shown in

Figure 1. The practical clinical importance of this concept is in the ability to expand

the existing concept from a single molecule to the level of the myocardial cell and

then to the myocardium as a whole organ.

Current concepts of cardiac mechanics are limited to the myocardial transition from

the end-diastolic to end-systolic state and back again repetitively. Though such an

approach appears logical, recent advances in the understanding of a cellular state of

"slack sarcomere" presents new opportunities to define an intermediate "slack

myocardium" state for the heart as a whole especially in relation to cardiac heart failure, increasingly recognized as a multifactorial evolving process.[8]

The in-vivo understanding of cardiac mechanics has been greatly enhanced with the development of echocardiography. This resulted in a massive amount of data on cardiac performance and function. Multiple echocardiographic parameters most often derived from 2D assessments were developed for the assessment of left ventricular systolic and diastolic functions. These parameters also include Doppler mitral inflow and aortic outflow profiles and Doppler assessment of myocardial tissue motion with derived parameters, such as tissue strain and its propagation. They are used to describe the normal state and to quantify and stage the degree of cardiovascular pathology. Such parameters helped to differentiate between the interactive forces within the myocardium that are responsible for blood flow within the heart and the great vessels.[9]

No "slack myocardium" status however has been correlated echocardiographically. In fact, no references to a "slack myocardium" could be identified in the literature. End-diastolic ventricular stretch largely depends on the filling pressure difference between the atrium and ventricle. The extent to which titin is stretched plays a paramount role in the systolic Frank-Starling mechanism via several pathways, but primarily via recoil-dependent forces and alteration of actin-myosin coupling.[10] Coupling is altered by a complex process which brings actin and myosin closer together.

The myocardium consists of millions of sarcomeres. Sarcomeres cannot exhibit an absolute synchronicity in mechanics. Even within a few millimeters of myocardial tissue, each sarcomere would reach end-systolic and end-diastolic phases in slightly different millisecond time frames. Such differences would greatly increase within the whole organ, especially in the presence of intraventricular conduction defects. The development of the "slack" state in systole and diastole would only occur during relative synchronicity of a mass of sarcomeres. The implication from this is that if we attempt to define by echocardiographic parameters the "slack" stage for the entire myocardium, we should accept that such phase would not be instantaneous across all sarcomeres.

A number of studies by us indicated that mitral annular diastolic peak tissue velocity (Ea) used as a surrogate for recoil occured earlier than the peak of early mitral inflow blood velocity (E) in normal human hearts.[11,12] These studies also demonstrated that such a relationship was altered in the presence of diastolic dysfunction and elevated atrial pressure. The maintenance of normal cardiac time intervals is related to normal cardiac physiology, mechanics, and hemodynamics. When these are disturbed, cardiac time intervals are altered and they become shortened or delayed. Our findings of altered timing between peak tissue velocity (Ea) at the mitral annulus which we used as a surrogate for recoil and peak mitral early diastolic (E) valve opening on M-mode were similar to those reported by other investigators[13,14]. In other studies M-Mode and DTI measurements were measured on different heart beats, with times of the peak velocities referred to the ECG R-wave[13]. We used M-Mode and DTI measurements which were taken simultaneously and the time differences measured were actual time differences between events in a single heartbeat [12].

In this respect, our technique with a reference time-point imposed on the cardiac cycle independently of intracardiac processes would seem to be the better option and it removed any potential mistakes for absolute measurements. We postulate, that the flow across the mitral valve exhibits decelerating qualities once the stretch of the multitude of molecular springs begins. It therefore seems logical to postulate that the 'slack myocardium' status occurs within a period between the peak myocardial tissue velocity measured at the mitral valve annulus and the peak of the E wave of ventricular inflow via the mitral valve. This timing interval between peaks represents an index of relaxation. But more importantly the positive value seen in the normal can be considered positive for the presence of the early diastolic mechanism i.e. the interval which allows the 'slack myocardium' time to exist which is essential for normal cardiac filling.

As we are aware preload is the force that extends the ventricle in diastole or the force acting to stretch the ventricular fibres at end diastole[10]. Therefore even though the filling pressures are normal preload will affect the rate of blood velocity across the mitral valve depending on the degree of stretch of the left ventricular cavity in diastole. Taking into account the physiological changes that effect preload there should be a varying degree of acceleration of blood flow across the mitral valve, which is dissociated from left ventricular peak recoil (Ea) in the normal. In another of our studies of patients with diastolic dysfunction there was a better relationship between mitral peak annular relaxation recorded by Doppler Tissue Imaging and the rate of acceleration of early diastolic flow recorded by conventional Doppler which was not present in the control group[11]. This provided a new insight into diastolic

filling events in patients with diastolic dysfunction while supporting the existence of an early diastolic mechanism in normal. (Figure 2)

An ability to measure 'slack' myocardial volume could become valuable in the development of meaningful indices related to the relationships with end-diastolic and end-systolic volumes. This would help to establish parameters for quantitative assessment of a whole range of cardiac pathologies associated with heart failure such as diastolic dysfunction, congestive heart failure and ischemic heart disease, which has been shown to have close relationship with changes in titin isoforms and function.[15]

Analysis of pressure loops inside the ventricle and the atrium obtained with high-fidelity catheters, along with synchronized assessment of Doppler mitral inflow profiles and myocardial strain measurements in different regions of the ventricle, are needed to challenge this hypothesis.

In conclusion, we believe that incorporation of recently collected data from molecular and cellular research into cardiac physiology warrants the introduction of the 'slack myocardium' phase of myocardial dynamics. This concept may also facilitate a unique means to diagnose diastolic cardiac heart failure with novel applications of echocardiography.

REFERENCES

1. Granzier H, Labeit S: Cardiac titin: an adjustable multi-functional spring. J Physiol 541(2):335-342, 2002.

2. Cazorla O, Freiburg A, Helmes M, Centner T, et al: Differential expression of cardiac titin isoforms and modulation of cellular stiffness. Circ Res 86(1):59-67, 2000.

3. Hunter RJ, Neagoe C, Jarvelainen HA, Martin CR, et al: Alcohol affects the skeletal muscle proteins, titin and nebulin in male and female rats. J Nutr 133(4):1154-1157, 2003.

4. Hein S, Schaper J: Weakness of a giant: mutations of the sarcomeric protein titin. Trends Mol Med 8(7):311-313, 2002.

5. Itoh-Satoh M, Hayashi T, Nishi H, Koga Y, et al: Titin mutations as the molecular basis for dilated cardiomyopathy. Biochem Biophys Res Commun 291(2):385-393, 2002.

6. Gotthardt M, Hammer RE, Hubner N, Monti J, et al: Conditional expression of mutant M-line titins results in cardiomyopathy with altered sarcomere structure. J Biol Chem 278(8):6059-6065, 2003.

7. Neagoe C, Kulke M, del Monte F, Gwanthmey JK, et al: Titin isoform switch in ischaemic human heart disease. Circulation 106(11):1333-1341, 2002.

8. Jessup M, Brozena S: Heart Failure. N Engl J Med 348:2007-2018, 2003.

9. Rakowski H, Appleton C, Chan KL, Dumesnil JG, et al: Canadian consensus recommendations for the measurement and reporting of diastolic dysfunction in echocardiography. J Am Soc Echocardiogr 9(5):736-760, 1996.

10. Helmes M, Lim CC, Liao R, Bharti A, et al: Titin determines the Frank-Starling relation in early diastole. J Gen Physiol 121(2):97-110, 2003.

11. King GJ, Foley JB, Almane F, Crean PA, et al: Early diastolic filling dynamics in diastolic dysfunction. Cardiovasc Ultrasound 1:9, 2003.

12. King GJ, Foley JB , Cosgrave J , Boyle G , Hussey M , Bennett K , Crean P, Walsh M : Novel approaches for distinguishing Hypertrophic Cardiomyopathy from Physiologic left ventricular hypertrophy in the "Gray Zone" using Doppler tissue imaging. Submitted for consideration to the Journal of the American College of Cardiology Jan 2005.

13. Rodriguez L, Garcia M, Ares MA et al. Assessment of mitral annular dynamics during diastole by Doppler tissue imaging: comparison with mitral Doppler inflow in subjects without heart disease and in patients with left ventricular hypertrophy. Am Heart J 1996: 131: 982-87

14. Rivas-Goetz, KD, Manolios M, Rao L et al. Time interval between onset of mitral inflow and onset of early diastolic velocity by tissue Doppler: A novel index of left ventricular relaxation. J Am Coll Cardiol 2003;42:1463-70

15. Baliga RR: Apoptosis in myocardial Iscemia, Infarction and Altered Myocardial States. Cardiol Clin 19(1):91-112, 2001.
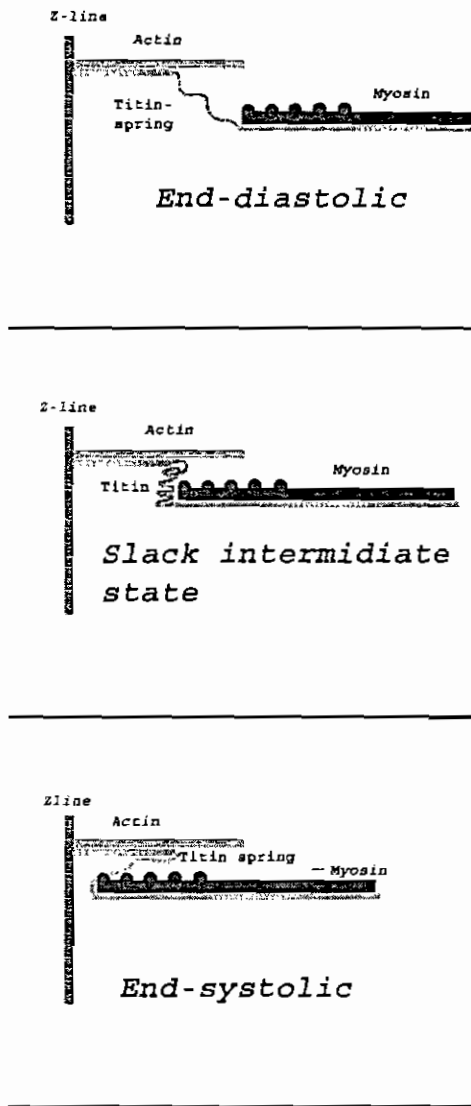
Figure 1. Movement from end-diastolic to end-systolic state of the sarcomere involves major changes in structural status of cardiac titin. End-diastolic stretch requires uncoiling of Ig-like segments, PEVK sequence and N2B/N2BA regions. As the contraction starts with actin-myosin interaction, the recoil spring forces of stretched titin molecules supports shortening of the sarcomere, until the titin has no more stretched segments. At this moment "molecular spring" is inactive and "slack sarcomere" status is acheved. Continuation of active contraction beyond this point requires Ig-like segments of titin to be stretched inwards, creating spring forces ready to initiate the diastole when active actin-myosin interaction will cease. [Permission obtained from Konstantin Yastrebov, MD, PhD]
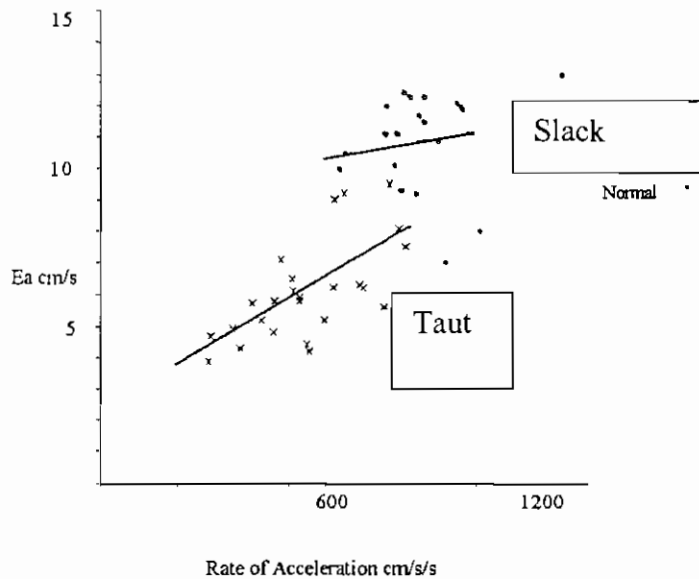
Figure 2. In patients with diastolic dysfunction there was a better relationship between mitral annular relaxation recorded by Doppler Tissue Imaging and the acceleration of early diastolic flow recorded by conventional Doppler (taut myocardium in diastolic dysfunction) which was not present in the control group (slack myocardium in normal). This provides a new insight into diastolic filling events in patients with diastolic dysfunction. [2003 King *et al*; licensee BioMed Central Ltd. This is an Open Access article: verbatim copying and redistribution of this article are permitted in all media for any purpose, provided this notice is preserved along with the article's original URL.]